STUDIES ON HEAT TRANSFER AND PRESSURE DROP CHARACTERISTICS OF NANOFLUIDS IN MICROCHANNELS

A thesis submitted in the partial fulfilment of the requirements for the Degree of

DOCTOR OF PHILOSOPHY

By

HARKIRAT

Registration Number: 901001002

Under the supervision of

Dr. D. GANGACHARYULU
Professor
Department of Chemical Engineering
Thapar University

DEPARTMENT OF CHEMICAL ENGINEERING

THAPAR UNIVERSITY
PATIALA 147004, INDIA.

August 2017

THESIS CERTIFICATE

This is to certify that the thesis entitled "**Studies on Heat Transfer and Pressure Drop Characteristics of Nanofluids in Microchannels"** submitted by **Ms. Harkirat,** in the partial fulfillment of the requirements for the award of the Degree of **Doctor of Philosophy** in the Department of Chemical Engineering, **Thapar University, Patiala (INDIA)** is a bonafide record of research work carried out by her under my supervision and guidance. The contents of this thesis, in full or in parts, have not been submitted to any other Institute or University for the award of any degree or diploma.

(D. Gangacharyulu)
Professor
Department of Chemical Engineering
Thapar University, Patiala,
Punjab, INDIA

(Supervisor)

DECLARATION

I, **Harkirat,** hereby declare that the thesis, entitled, **"Studies on Heat Transfer and Pressure Drop Characteristics of Nanofluids in Microchannels"**, submitted to the **Thapar University**, in partial fulfillment of the requirements for the award of the Degree of Doctor of Philosophy in Chemical Engineering is a record of original and independent research work done by me during the period 2011-2017, under the supervision and guidance of **Dr. D. Gangacharyulu**, Professor, Department of Chemical Engineering, Thapar University. The work contained in this thesis has not been previously submitted to meet the requirements for a degree or diploma at this or any other higher education institution.

(Harkirat)

Registration No: 901001002

ACKNOWLEDGEMENTS

Words are often less to revels anyone's deep regards. With an understanding that work like this can never be the outcome of a single person. I take this opportunity to express my profound sense of gratitude and respect to all those who helped me through the duration of this work.

This work would not have been possible without the encouragement and able guidance of the supervisor Dr. D. Gangacharyulu. Their enthusiasm and optimism made this experience both rewarding and enjoyable. Most of the novel ideas and solutions in this work are the result of our numerous stimulating discussions. Their feedback and editorial comments were also invaluable for the writing of this thesis. I would like to express my gratitude to my supervisor Dr. D. Gangacharyulu for their useful comments, remarks and engagement through the learning stages of this doctorate work. Throughout the long journey of Ph.D. with lot of ups and down during the research, supervisor thought of taking up the research activity with an inspiration and motivation helped me to stay focused on this particular subject. The trust made by supervisor helps me to stand in difficult conditions also.

I am extremely thankful to the Head of the department, Director and Dean Research & Sponsored Projects, Thapar University for extending the opportunity to undertake this doctoral research. I would like to express my appreciation and thanks to the Dr. H. Bhunia, Ph.D. program coordinator, and my Doctoral committee members, Dr. B. Chudasama, Dr. R.K. Gupta and Dr. S.K. Singh for their useful comments and suggestions showered during the interim research evaluations and presentations. I would like to acknowledge the financial support from University Grants Commission (UGC), Government of India for Maulana Azad National Fellowship to carry out the doctoral studies.

As the nanofluids use in microchannels is a challenging area which is not possible without the help of M/s S.R Engineers Limited, Chandigarh. Their help during fabrication of microchannels is so appreciable which cannot be expressed in words. I am very much thankful to SAI Labs, Thapar University Patiala, NIPER Mohali, Punjab and Indian Institute of Technology, Roorkee, Uttarakhand, India for providing the facilities of characterization.

I am kind enough to Dr. V.P. Agrawal, who had given me innovative ideas to pursue my research. His multidimensional approach in solving a particular problem is worth mentioning. I am very thankful to Dr. V.K. Sangal and Dr. Parag Nijhawan for their endless help to complete my research work within confined timelines.

I am also thankful to Mr. Sarthak Sharma and Mr. Manjeet Singh Virk who helps me for the analytical model development. Grateful acknowledgement is made to my friends Ms. Shivani, Ms. Ruchika Thakur, and Ms. Arshdeep Kaur. I am also thankful to all the teaching staff members of the department for their invaluable cooperation and help during the entire tenure of my studies in the department. I would also like to thank Mr. Amit, Mr. Munish, Mr. Shubham, Mr. Krishan and Mr. Rana for their constant help throughout this doctoral research.

This research was never finished without the affection and co-operation of my daughter Mehreen Kaur Sarao. As I was not give her time during their toddlerhood but she understands me at every point without any complaining. During the research work, I had spent days, weeks and months for complete the objectives. This was only possible due to the support of my husband and other family members. Words cannot express how grateful I am to my husband Mr. Mani Kanwar Singh Sarao and in-laws Sardarni Malkeet Kaur and Sardar Satinder Singh Sarao. I desire to express my deep appreciation to my parents. As I am far apart from them but my parents Sardarni Rajveer Kaur and Sardar Raghuvir Singh Sandhu blessings are always with me. It is power of their blessings, which has given me the resolution, self-confidence and enthusiasm for hard work.

Last but not least, I would like to thank God for all good deeds. Without the blessings of God, nothing would be possible.

(Harkirat)

ABSTRACT

High heat fluxes devices in an electronic industry pose a thermal challenge to the researchers of this area. Over the past decade, the use of microchannel heat sink to remove the high heat load from the active heat source has been studied. But as the amount of heat generated is quite high, so, an efficient fluid is required to enhance the cooling performance of microchannel heat sink. The suspensions of nanoparticles in the base fluids term as "nanofluids" proves an efficient fluid for the microchannels.

This present work focuses to compare the different types of nanofluids flowing through the microchannels and find the nanofluids with high heat removal capacity. In the present work, nanoparticles such as alumina, copper oxide (CuO) and multiwalled carbon nanotubes (MWCNT) are extensively used with different types of base fluids such as water (W) or water/ethylene glycol (W/EG) mixtures (90:10, 80:20, 70:30, 60:40 and 50:50). Nanoparticles are dispersed at different concentration ranges from 0.1 vol % to 5 vol % in the base fluids by using two step method. Alumina nanofluids are stable without the use of any kind of surfactant while CuO nanofluids get stabilized by using 0.2 wt % sodium dodecyl sulphate and MWCNT are stabilized with 0.25 wt % of Gum arabic. Further, sonication can be done by using ultrasonicator water bath at a fixed frequency to make more stable nanofluids. As there is no fixed time for sonication has been reported, so optimization of sonication can be done on the basis of thermal conductivity measurements at 40 min, 60 min, 80 min and 100 min. For 80 min of sonication, maximum enhancement in thermal conductivity is observed.

The stability of nanofluids can be determined by measuring the absorbance, thermal conductivity and zeta potential of nanofluids in terms of days without disturbing or shaking the samples. The results showed that CuO nanofluids are least stable nanofluids with stability of 2-4 days while MWCNT nanofluids shows a maximum stability of 24-36 days and alumina nanofluids remain stable for 19-28 days. Stability of nanofluids is affected by changing the base fluids and it increases with increase the ethylene glycol ratio in water. Maximum stability of nanofluids is achieved with W/EG (50:50) base fluids either any type of nanoparticles used. So, ethylene glycol itself acts as a stabilizer in water to enhance the nanofluids stability.

Thermophysical properties of nanofluids are important to determine to know the exact performance of nanofluids in microchannels. The objective of thesis is to determine the thermal conductivity, specific heat, viscosity and density of nanofluids at various temperatures ranges from 20 °C to 80 °C. The thermal conductivity is measured by KD2 Pro, viscosity is measured by Brookfield viscometer and density is measured by Pycnometer. Specific heat measurements of few samples of nanofluids can be done by Differential scanning calorimeter and compare with the theoretical mixture model. The experimental results show a ± 1 % deviation with the model data so further all the predictions of specific heat are done with mixture model.

The thermophysical properties of nanofluids are influenced by various factors such as type of nanoparticles and its concentration, type of base fluids and temperature. An appreciable amount of enhancement is observed in thermal conductivity of nanofluids and it increases with increase in temperature and nanoparticle concentration. MWCNT nanofluids show maximum thermal conductivity in comparison with alumina and CuO nanofluids. Thermal conductivity enhancement increases with increase in the ethylene glycol ratio in water and highest increasement observed with W/EG (50:50) base fluid. Viscosity and density are also an important property which decided the thermal performance of nanofluids while using in thermal systems. There is an insignificant rise in viscosity and density observed after the addition of nanoparticles in the base fluids. This result makes no adverse effect on thermal systems as the thermal conductivity rise is more in comparison with viscosity and density enhancement which gives overall better thermal performance.

Thermal performance of nanofluids are further determined for aluminium microchannel heat sink (MCHS). Rectangular shaped microchannels are fabricated with width, depth and length of 250×2000×40000 μm. There are 21 number of parallel microchannels fabricated on a single unit of aluminium block with a fin spacing of 200 μm. Nanofluids are used to extract the extra amount of heat generated by the heat sink. Overall convective heat transfer is improved by using nanofluids in microchannels with an insignificant rise in pressure drop.

Experiments are performed at various flow rates such 0.2 ml/min to 2 ml/min and at different heat inputs of 2 W, 4 W and 6 W. At very low flow rates, no significant rise in convective heat transfer is observed with nanofluids. Above 0.8 ml/min, flow is fully developed in microchannels with a maximum heat transfer enhancement of 80.49 % at 2 ml/min with 1 vol % nanoparticle concentration of MWCNT-W/EG (50:50) nanofluids. Friction factor

and thermal resistance are quite low at high flow rates which show the improved thermal and hydraulic performance of nanofluids. An analytical model is developed by using Turbo C++ to analyze the heat transfer and fluid flow behavior of nanofluids in microchannels. The predicted model data have a good agreement with experimental data with a deviation of ± 10 % with Reynolds number and friction factor and ± 15 % with Nusselt number. Nanofluids extract upto 70 % heat from the heat sink which makes it a promising heat transfer fluids for thermal systems.

Further, a new MADM-TOPSIS approach is introduced for the evaluation, comparison and selection of best suitable nanofluids for any thermal systems. Actual performance of nanofluids is affected by the various parameters and it's important to identify parametric quantities which concurrently improve the performance of nanofluids. A three stage evaluation scheme is proposed for evaluation, comparison, and optimum selection of a nanofluid known as MADM-TOPSIS approach. The method ensures that the selected nanofluid is closest to hypothetical best nanofluid and farthest from hypothetical worst nanofluids. Selection of nanofluids is done by considering the government rules as well as cost factor requires for a particular application. An example is considered by selecting few nanofluids used in the present work. All the performance attributes are considered to evaluate the best suitable nanofluids for MCHS. This scheme proves very user friendly as simple mathematical procedure is followed for the evaluation. This will be very helpful for the different researchers or people working in the different organizations or industries so that they will know the exactly performance and stability of nanofluids before use it any application.

TABLE OF CONTENTS

LIST OF FIGURES

LIST OF TABLES

NOMENCLATURE

English Symbol	Description	Unit
A	Relative important matrix	Dimensionless
A^*	Positive ideal solution	Dimensionless
A^-	Negative ideal solution	Dimensionless
A_c	Cross sectional area	m^2
A_{eff}	Wetted surface area	m^2
B	Eigen value	Dimensionless
C	Nanoparticle volume concentration	Dimensionless
C^*	Suitability index	Dimensionless
c_p	Specific heat	J/(kg. ^oC)
D	Decision matrix	Dimensionless
D_h	Hydraulic diameter	m
d_p	Particle diameter	m
f	Friction factor	Dimensionless
H	Channel height	m
h	Heat transfer coefficient	$W/(m^2.°C)$
k	Thermal conductivity	W/(m.°C)
k_m	Thermal conductivity of liquid medium	W/(m.°C)
L	Channel length	m
m	Mass	kg
N	Total number of channels	Dimensionless
N	Normalized decision matrix	Dimensionless
n	Shape factor	Dimensionless
P	Pressure	Pa
Pe	Peclet number	Dimensionless
Pr	Prandtl number	Dimensionless
Q	Given heat	Watts
q	Heat absorbed	Watts

English Symbol	Description	Unit
Re	Reynolds number	Dimensionless
R_{th}	Thermal resistance	°C/W
S	Separation measures	Dimensionless
T	Temperature	°C
T_m	Bulk mean temperature	°C
u_f	Fluid velocity	m/sec
u_i	Order no. of attributes	Dimensionless
$\dot{V}$	Volumetric flow rate	m^3/sec
v_i	Code given to particular attribute	Dimensionless
vol %	Volume percent	Dimensionless
W	Double distilled water	Dimensionless
W'	Weight matrix	Dimensionless
W_{ch}	Width	m
WEG	Ethylene glycol percent in water	Dimensionless
W/EG	Water-ethylene glycol mixtures	Dimensionless
wt %	Weight percent	Dimensionless
Z	Weighted normalized decision matrix	Dimensionless

Greek Symbol	Description	Unit
ϕ	Particle volume fraction	Dimensionless
μ_r	Relative viscosity	Dimensionless
η	Efficiency	Dimensionless
μ	Viscosity	Pa.s
ρ	Density	kg/m^3
α	Thermal diffusivity	m^2/sec

Subscript	Description
ch	Microchannel
f	Fin
in	Inlet
out	Outlet
b	Base
bf	Base fluid
nf	Nanofluid
p	Particle
eff	Effective
m	Manometric fluid
std	Standard

Metal/Compound name	Description
Ag	Silver
Al_2O_3	Alumina or aluminium oxide
Cu	Copper
CuO	Copper oxide
H_2O	Water
SiC	Silicon carbide
TiO_2	Titanium oxide

LIST OF ABBREVIATIONS

Abbreviations	Description
ASHRAE	American Society of Heating, Refrigerating and Air Conditioning Engineers
CHF	Critical heat flux
GA	Gum Arabic
EDM	Electrical discharge machine
EDS	Energy dispersive spectroscopy
EO	Ethylene oxide
IEP	Iso electric point
MADM	Multiple attribute decision making
MCHS	Microchannel heat sink
MWCNT	Multiwalled carbon nanotubes
PEG	Polyethylene glycol
PO	Propylene oxide
SDBS	Sodium dodecyl benzene sulfonate
SDD	Silicon drift detector
SDS	Sodium dodecyl sulfate
SEM	Scanning electron microscope
TOPSIS	Technique for order preference by similarity to ideal solution
UV-Vis	Ultraviolet-visible

CHAPTER 1
INTRODUCTION

Digital technology faces a lot of thermal management challenges as their focus is to pack more logic in smallest possible hardware. This chapter gives a brief introduction about present scenario of electronics industry and discussed the latest technologies for controlling the high amount of heat dissipation from active source.

1.1 ELECTRONICS THERMAL MANAGEMENT CHALLENGES

Electronics industry is concerned about the fact that active devices dissipate considerable amount of heat while switching because it may result in thermal runaway. This situation leads to a destructive result of active devices by changing the conditions in a way of increase in temperature of device. Gordon Moore [1] who later founded Intel Corporation, opined that processor speeds, or overall processing power for newly trendy technology of computer chips would become double every two years at low cost. Integrated circuits carry binary computational information i.e. high and low on each transistor as shown in Figure 1.1. The faster and complex an electronic device can work, the more switching between high and low states is observed. Present scenario shows that billions of transistors can fit on chips which become more powerful, smaller and cheaper. But beginning of the end of Moore's law started as the size of transistors is less than 28 nm which have set so close to each other results in interfering with one another's functions. Size of transistors is getting too small to manufacture efficiently that further leads to overheating.

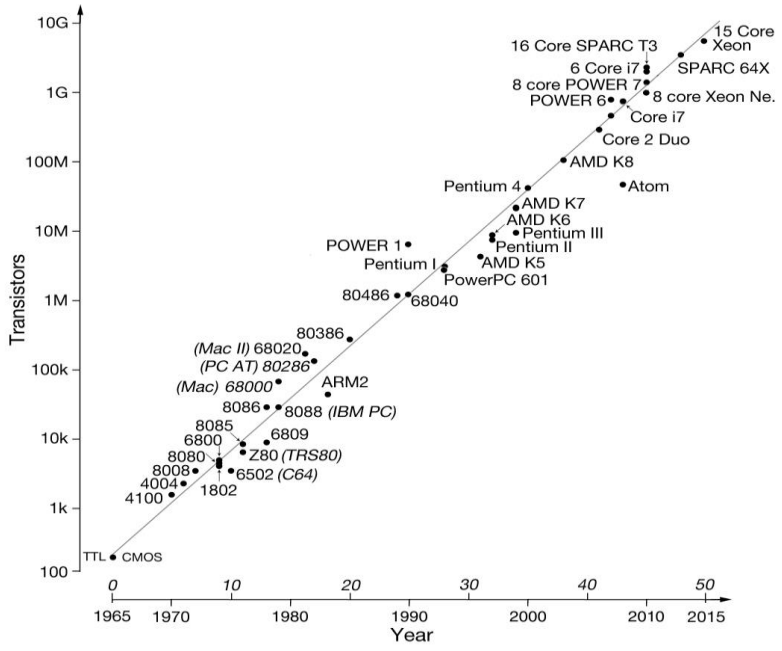

Figure 1.1: Moore' law (No. of transistors per year) [1]

In order to maintain the reliability and performance of the devices, great efforts have been made to maintain an allowable junction temperature by dissipating the heat from active sources to the environment. Typically, heat sink with air cooling technology is preferred to maintain the temperature but nowadays this technology is approaching its limit due to high demand of thermal management. Clearly, a budge from air cooling technology to liquid cooling technology is essential to meet up these confronts in the future.

1.2 FUNDAMENTALS OF MICROCHANNELS

Miniaturization of heat sink is a great technique to enhance the thermal efficiency of cooling systems [2]. Tuckerman and Pease [3] pioneered the microchannels in electronic applications by employing the water through channels fabricated on silicon chips. The microchannel heat sink (MCHS) with a potential to disperse huge extent of heat from a small cross section has been studied extensively over the last two decades. The exceptional features of microchannel heat sinks facilitate these elements to minimize the thermal resistance by carrying a heat source and a heat sink in a very close thermal immediacy.

This heat sink is used for cooling the active source by dissipating large amount of heat and then transferred to the outside environment by passing a coolant through these channels. The unique feature of microchannel heat sinks is their size which is fabricated by the same microfabrication techniques which can be used for electronic devices. With the help of these techniques, fabrication of high precision channels with channel width, W_{ch} and fin width, W_f as minimum as 50 μm and the height and length of channels as per the source requirement is possible.

This is a complex job to decide a channel category like microchannels or minichannels on the basis of their size. So, Kandlikar and Grande [4] presented a modified scheme based on smallest channel dimensions as given in Table 1.1.

For the manufacturing of different shapes and size of microchannels, various techniques are developed such as wire electric discharge machining, vapor depositing, etching, etc. In addition to this, different materials like silicon, glass substrates, metals such as aluminium, copper, titanium, etc. can used for their fabrication [5].

A microchannel heat sink consists of number of channels and fins as displayed in Figure 1.2 [6]. As these micro dimensions channels might be of non-circular cross-section, so a term

hydraulic diameter, $D_{h,}$ is used to analyze the performance of heat sink. Miniaturization technology provides high surface to volume ratio with a small process volume [4, 5]. Among these excellent features, the microchannel heat sink becomes an effective heat removal system used in various applications with numerous benefits and some limitations also.

Table 1.1: Modified channel classification scheme [4]

S. No	Size of channels	Types of channels
1	0.1 μm ≥ D_h	Nanochannels
2	1 μm ≥ D_h > 0.1 μm	Transitional nanochannels
3	10 μm ≥ D_h > 1 μm	Transitional microchannels
4	200 μm ≥ D_h > 10 μm	Microchannels
5	3 mm ≥ D_h > 200 μm	Minichannels
6	D_h > 3mm	Conventional channels

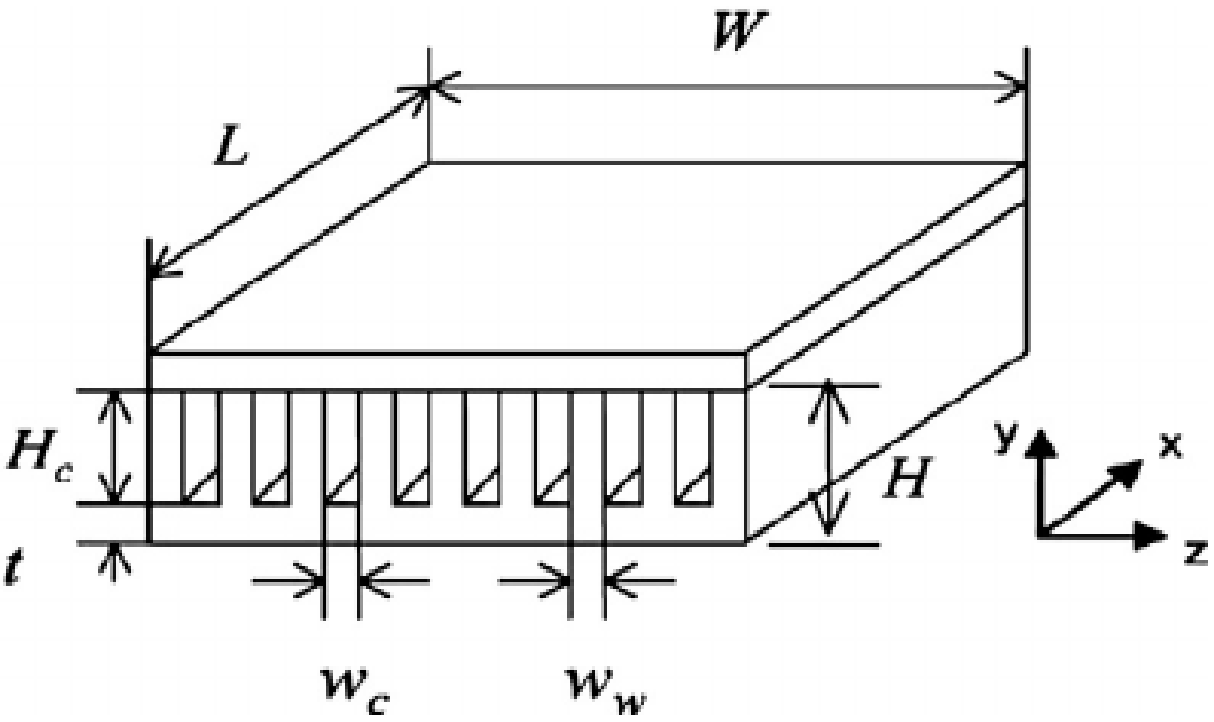

Figure 1.2: Cross-sectional view of microchannel [6]

1.2.1 Benefits of microchannels

a) Better heat removal efficiency due to high surface to volume ratio.

b) As size is small so it can be used for electronic applications.

c) Thermal resistance is very low as the microchannels can be directly incorporated to the heat source.
d) Very small amount of coolant required.
e) Unexceptionally good to produce better heat transfer coefficient when compared with all other conventional channels as well as minichannels.

1.2.2 Limitations of microchannels

a) High precision methods are required for the fabrication of microchannels.
b) Highly viscous liquids are not preferable.
c) Comparatively high pressure drop as flow passage is very small.
d) Fouling problem occur when liquid is used as a coolant.

1.2.3 Applications of microchannels

There are number of various applications where microchannels can be used:

a) Biomedical applications
    1. Drug discovery
    2. Cell analysis (screening, counting, sorting)
    3. Diagnostic tools
    4. Therapeutic tools
    5. Implantable drug delivery systems
    6. Genomics/proteomics (amplification, separation, hybridisation & sequencing)
b) Electronic applications
    1. High performance microprocessors
    2. Laser diode arrays
    3. Electronic cooling
    4. High intensity X-rays
    5. Power systems
c) Chemical engineering applications
    1. Micromixers
    2. Microdispensers
    3. Heat exchangers
    4. Microreactor
    5. Biochemical monitoring of food, soil, water, air, pesticides

d) Industrial applications
    1. Industrial automation
    2. Industrial dispensers
    3. Ink-jet print heads
    4. High throughput screening

1.3 TYPES OF COOLANTS USED IN MICROCHANNELS

Different types of coolants are enforced to flow over these channels to enhance cooling performance of the active source. These coolants might be air, water or any kind of heat transfer fluid. Beside this, immense studies have been restricted to suspensions of micrometer or millimeter sized particles in base fluids [7]. Because these particles have tendency to settle quickly and further suffer from stability and rheological problems. Recent studies are focused mainly on advanced fluids such as nanofluids with a good stability to improve the overall system efficiency.

Choi [8] proposed a term 'Nanofluid' at Argonne National Laboratory in 1995. It can be defined as a dispersion of nano sized particles in the heat transfer fluids such as water, water-ethylene glycol mixtures, pure ethylene glycol, oil, etc. or any kind of heat transfer fluids. Due to nanofluids high thermal conductivity, they receive a lot of attention in the area of heat transfer technology [9]. Further, an appreciable enhancement in heat transfer is also observed in comparison with their respective base fluid [10]. The unique characteristics of nanofluids with minimal clogging and settling of nanoparticles during flow, high thermal conductivity, improved heat transfer coefficient and superior critical heat flux (CHF) have been motivated many researchers to investigate the thermal and hydraulic performance of nanofluids at micro scale level [11].

Most of the studies are focused on thermal conductivity of nanofluids but the fluid properties such as viscosity and density of nanofluids have given least concern by researchers. Since, these properties are equally significant as thermal conductivity to estimate the heat transfer and fluid flow behavior. The viscosity and density of nanofluids are higher than base fluids which in turn increase the frictional pressure drop for single phase flow and pumping power.

Till date, nanofluids had proven as efficient or next generation coolant for dissipating very high heat fluxes for various engineering applications. Some of the applications are listed in Figure 1.3.

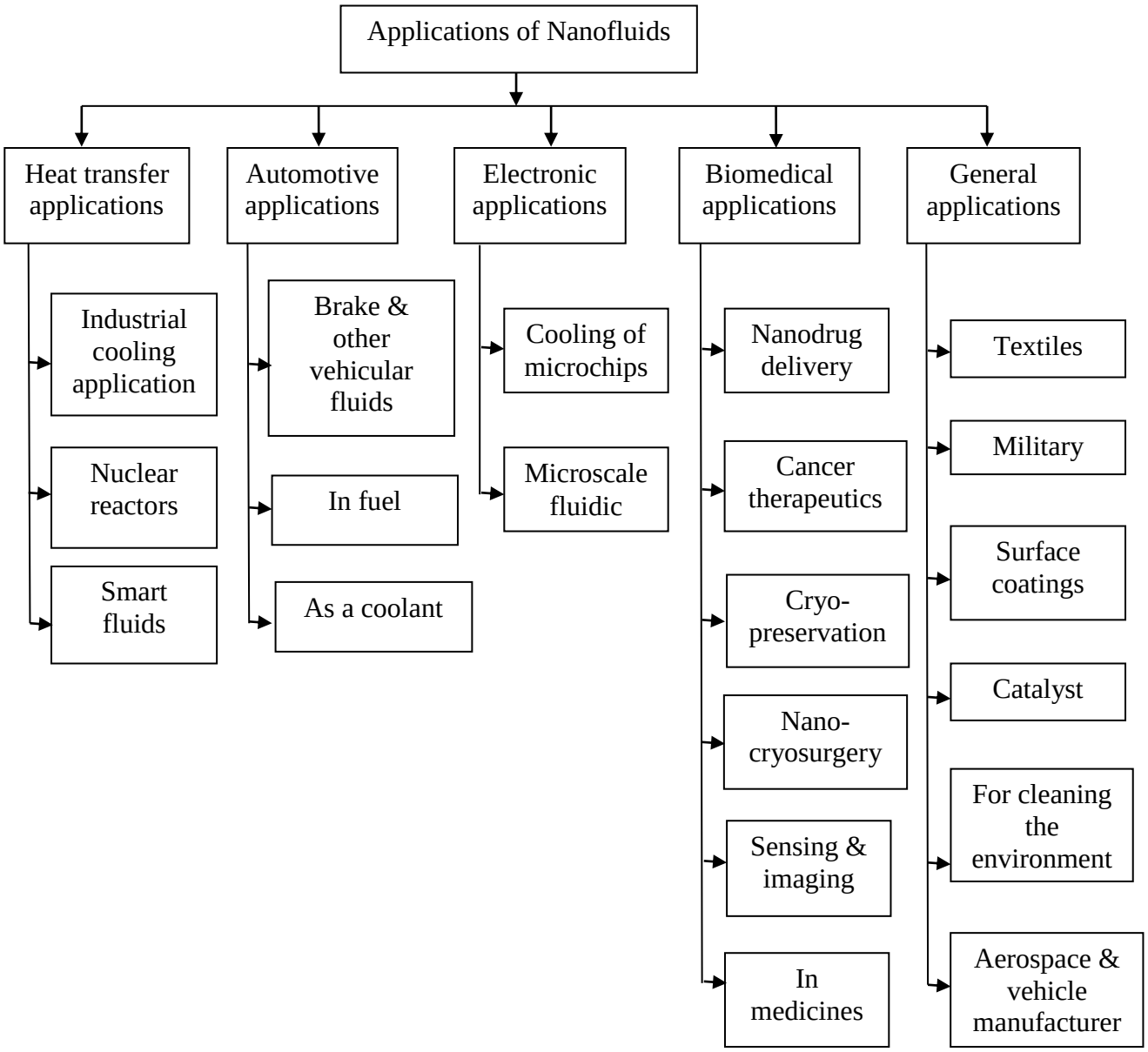

Figure 1.3: Applications of Nanofluids [12]

1.4 CLOSURE

Multi-functional and high performance electronic devices have directed to huge challenges in thermal management. The greedy need of miniaturization technology by electronic industry with the innovative cooling solutions has challenged the thermal engineers. In addition to this, the contradictory requirements of enhanced heat transfer mechanisms with low temperature rise were implemented either by increasing the surface to volume ratio of active source or by introducing advanced heat transfer fluids.

Advanced heat transfer fluids such as nanofluids exhibits excellent performance in microchannels by dissipating large amount of heat. Various experimental and theoretical

studies on the preparation of nanofluids and their thermal properties of different types of nanofluids are available in the literature (Chapter 2). But it is difficult to identify the best and suitable nanoparticles and base fluids for a particular application. Moreover, stability of nanofluids is an important concern for their further use in industrial applications.

This research is primarily focused on the three types of nanoparticles such as Al_2O_3, CuO and MWCNT with the combination of different kind of base fluids such as double distilled water (W) and double distilled water/ethylene glycol (W/EG) mixtures in the ratios of 90:10, 80:20, 70:30, 60:40 and 50:50. Detailed studies are carried out in Chapter 3 for the preparation of nanofluids at different concentrations and their stability analysis with time. In chapter 4, thermophysical properties for nanofluids at different temperatures have identified for their further use in applications. Further, the applications of nanofluids for microchannel cooling devices are still in its infancy. Moreover, improvements of thermal performance in cooling devices with the above mentioned different nanofluids are rarely reported. Chapter 5 emphasizes on the designing of microchannel heat sink test up and developing an analytical model using Turbo C++.

Chapter 6 discussed the outcomes obtained from experiments in terms of heat transfer coefficient, Nusselt number, thermal resistance and friction factor with Reynolds number to evaluate the overall performance of microchannel heat sink. Correlation of experimental data and model development will also carry out. Furthermore, a MADM-TOPSIS approach introduced to identify suitable nanofluids for this particular application by considering numerous factors such as nanoparticles concentration, type of base fluids, stability, thermophysical properties, fluid flow characteristics, heat transfer behavior, etc. presented in Chapter 7. The final conclusion and future scope of work is described in Chapter 8. This research is a promising gateway for industry as well as researchers to classify the suitable nanofluid for cooling application.

CHAPTER 2
LITERATURE REVIEW

This chapter assembles the significant information obtained from the literature on the preparation of nanofluids, their stability parameters and thermophysical properties and usage of nanofluids in microchannels to improve the overall performance of the thermal system. The literature has been systematically studied and presented in the most comprehensible way to construe the research findings as per the following manner:

a) Preparation of nanofluids and the stability methods used to avoid the agglomeration of nanoparticles in the base fluids.
b) Thermophysical properties of nanofluids discussed with their influencing factors.
c) Fluid flow and heat transfer study in conventional channels followed by minichannels. Further, microchannel heat sink using nanofluids are discussed to enhance the overall efficiency of thermal systems.
d) A new MADM-TOPSIS approach is introduced to select the suitable nanoparticles and heat transfer fluids for cooling applications.

The detail survey of literature is as follows:

2.1 PREPARATION OF NANOFLUIDS

Preparation of stable nanofluids is important concern before starting any research or experimentation. This procedure is quite different from micro suspensions as the microparticles have tendency to settle down but nanoparticles can be suspended for long time due to their small size. Although there is a possibility of agglomeration of nanoparticles in fluids and further behaves like micro suspensions. This leads to study the various preparation methods and stability parameters which affect the overall stability of nanofluids. There are two ways for preparing the nanofluids either single step method or two step method.

In single step method, nanoparticles synthesis and dispersion in fluid take place concurrently while in two step method nanoparticles in dry powder form dispersed in the base fluid. During one step process, nanoparticles size can go up to very small extent i.e. less than 10 nm and directly dispersed in base fluids so that process of drying, storage transportation are diminished which in turns improve the stability of nanofluids. But the main difficulty is that only low vapor pressure fluid is used in the process [13]. Whereas, in two step process, any

kind of heat transfer fluids is used for the preparation of nanofluids. There are different techniques follow under one step methods to make a fully stable nanofluids as shown in Figure 2.1.

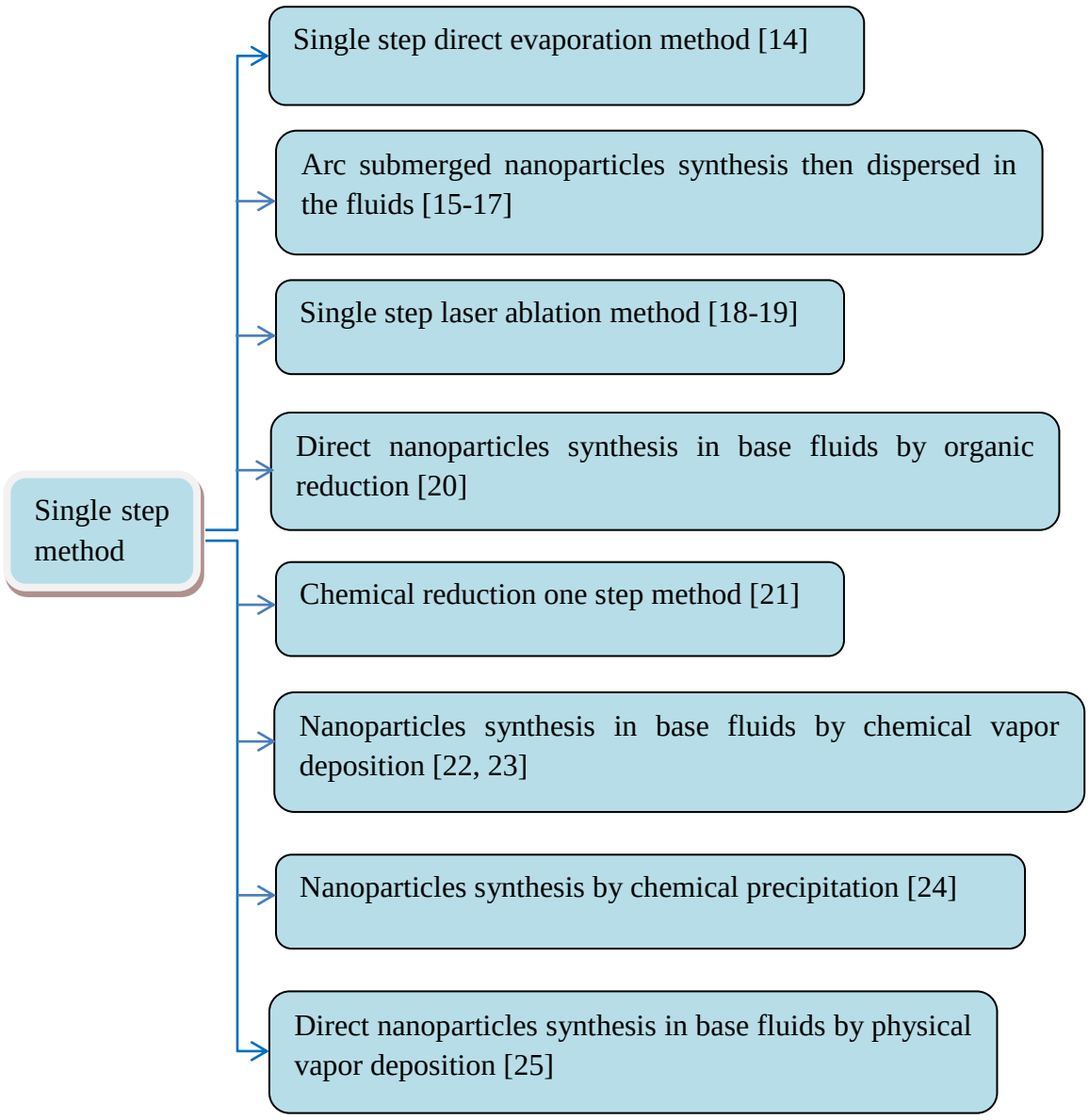

Figure 2.1: Preparation of nanofluids with one step method

Most research in the expanse of heat transfer with nanofluids is carried out by using two step method for preparing the nanosuspensions. Granqvist and Buhrman [26] found the two step process for the preparation of nanofluids. In this method, nanoparticles or nanotubes are procured from manufacturers or synthesis in the laboratory by chemical vapor deposition, mechanical alloying or other suitable techniques and then dispersed in any kind of heat transfer fluids. Nanoparticles handling, storage and transportation leads to agglomeration of nanoparticles in the fluid during dispersion which affect the stability of nanofluids. If the

stability of nanofluids declined, it influenced the thermophysical properties of nanofluids. Therefore, stabilization of nanosuspensions can be done by physical, chemical or electrostatic methods.

2.1.1 Physical methods

Nanofluids can be stabilized through physical methods by breaking the agglomeration of nanoparticles via various techniques such as:

a. Ball milling
b. High pressure homogenizer
c. High shear mixing
d. Magnetic stirrer
e. Ultrasonic disruptor
f. Ultrasonic vibration

Out of all above, ultrasonic vibration is found to be better technique for breaking the agglomeration of nanoparticles. It can be done either by water bath or by probe. Both of these techniques work same without making any difference in stability. But the duration of sonication is a significant constraint for improving the stability of nanofluids. Das et al. [27] noticed the proper dispersion of nanoparticles in fluid after 4 hour of ultrasonic vibration by intense ultrasonication at 200 W. Kole and Dey [28] studied the optimum time of sonication for ZnO nanoparticles in ethylene glycol. They found that ZnO nanoparticles size reduces to 91 nm from 459 nm during sonication of four hour to sixty hour. Further than sixty hour, cluster size increases to 220 nm for 100 hour sonication depicted from Figure 2.2.

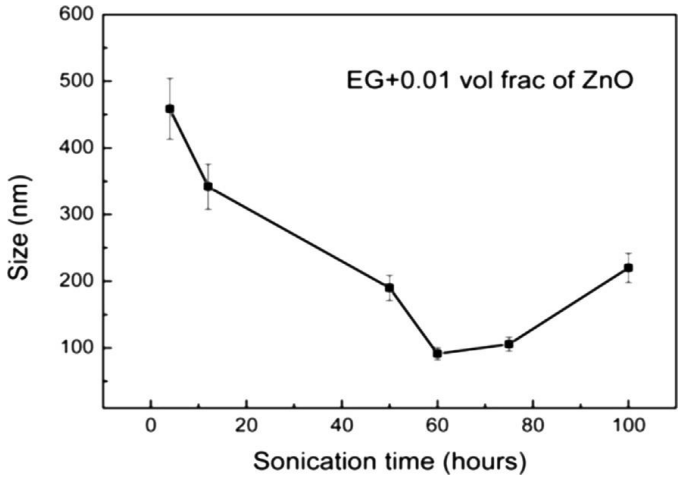

Figure 2.2: Effect of sonication time on ZnO cluster size [28]

Table 2.1: Summary of nanofluids sonication time

Authors	Nanoparticles	Base fluids	Sonication technique	Time
Suresh et al. [29]	CuO	Water	Ultrasonic vibrator (100 W, 36 ± 3 kHz)	6 h
Yang and Liu [30]	CuO	Deionised water	Ultrasonic bath	12 h
Kannadasan et al. [31]	CuO	Water	Ultrasonic bath (100 W, 36 ± 3 kHz)	4 h
Byrne et al. [32]	CuO	Water	Ultrasonic processor (100 W)	7-8 h
Namburu et al. [33]	CuO	Water	Ultrasonic agitator	30 min
Zeinali Heris [34]	CuO	Water	Ultrasonication	2 h
Suresh et al. [35]	Al_2O_3	Water	Ultrasonic vibrator (100 W, 36 ± 3 kHz)	6 h
Gharagozloo and Goodson	Al_2O_3	Deionised water	Ultrasonication (130 W, 60 Hz)	4 h
Raveshi et al. [37]	Al_2O_3	W/EG (50:50)	Ultrasonic bath	2 h
Hung et al. [38]	Al_2O_3	Water	Ultrasonic vibrator operating (400 W)	60 min
Heyhat et al. [39]	Al_2O_3	Water	Ultrasonication (400W, 24 kHz)	60 min
Lee et al. [40]	Al_2O_3	Water	Ultrasonication (30-40 kHz)	5 h
Sundar et al. [41]	Al_2O_3	Water	Ultrasonic bath	2 h
Kumaresan and Velraj [22]	MWCNT	W/EG mixture	Ultrasonication	90 min
Lamas et al.[42]	MWCNT	Water	Ultrasonication	60 min
Yousefi et al. [43]	MWCNT	Double distilled water	Ultrasonication	30 min
Phuoc et al. [44]	MWCNT	Deionised water	Ultrasonic processor (130 W, 20 kHz)	10 min

Sonication time was not fixed for nanofluids as it depends upon the type of nanoparticles, base fluids, any surfactants used or preparation method of nanofluids. Few literatures are reported in the Table 2.1 with no clear vision of best sonication time which makes nanofluids stable for long time. Sonication time varies with type of nanoparticles and base fluids. From the literature, it can be concluded that less sonication time (less than 2 h) is required to produce stable nanofluids if stirring and agitation can be done before sonication of nanofluids.

2.1.2 Electrostatic Methods

Electrostatic methods are preferred to make stable nanofluids for longer time. This can be done by controlling the pH of fluid or by adding suitable surfactants. Various researchers adjusting the pH value of nanofluids for their stabilizing by keeping it away from Iso electric point (IEP) so that nanofluids have higher zeta potential value [45, 46]. Sundar et al. [47] prepared the stable Al_2O_3 and CuO nanofluids by adjusting the pH value with no surfactant added. It was observed that zeta potential of Al_2O_3 nanofluids was higher than 20 mV at pH 1 and 5 while for CuO nanofluid, better dispersion was observed at pH 1 and 11. At pH 1, nanofluids were in acidic nature which sequentially damages the thermal conductivity measurements.

Fedel et al. [48] investigated the stability of TiO_2-H_2O nanofluids with acidic as well as non-ionic dispersant by maintaining the pH value. They concluded that nonionic dispersant such as PEG 600 turned out to be effective dispersant if used as 2:1 ratio (PEG: TiO_2). Further, Gowda et al. [49] studied the pH effect on alumina and CuO nanofluids and concluded that nanofluids with similar concentrations and low pH value or high surface charge have a higher thermal conductivity. Mondragon et al. [50] achieved the best dispersion state with high zeta potential value by fixed the pH value away from IEP and results obtained as pH= 9 for silica nanofluids and pH = 4 for alumina nanofluids.

Controlling the pH value for all the nanofluids are not in good practice. If pH cannot be controlled then some surfactants can be added to make stable nanofluids. In the literature, various surfactants were listed such as sodium dodecyl benzene sulfonate (SDBS), sodium dodecyl sulfate (SDS), oleic acid, salt, dodecyltrimethyl-ammonium bromide, gum arabic, sodium octanoate, cetyltrimethyl-ammonium bromide etc. which can be used for various nanoparticles [51]. For example, Mondragon et al. [50] and Naraki et al. [52] stabilized the carbon nanotubes and CuO nanofluids by using SDS. Wen and Ding [53] used SDBS for

stabilizing alumina-water nanofluids. But by changing the pH or adding the surfactant, thermal properties of nanofluids have changed. So, researchers were doubter to use these stabilization methods [11, 54]. It can be more suitable to use ultrasonication technique as it is a best way to break the particle agglomeration by keeping the same thermal properties of nanofluids for longer time.

2.1.3 Chemical Method

This method is a surfactant free method as the surface modification of nanoparticles or activator addition can be done to increase the stability of nanofluid for longer time before their dispersion in the base fluid. There are different nanoparticles which are undergone through functionalization results into stable nanofluids. Most of the researchers preferred to functionalize the carbon nanotubes (CNTs) before using in any kind of application. Singh et al. [54] suspended the CNTs in a mixture of nitric acid and sulfuric acid for chemical treatment and further washed the nanotubes with deionized water. By this process, carboxyl acid group attached to the surface of CNTs with hydrophilic behavior results into good dispersion in base fluids without using any surfactant. Hwang et al. [55] stabilized the CNTs by mechanochemical reaction through which hydrophilic functional groups attached to the surface of nanotubes with no contamination in fluid and high thermal conductivity. Plasma treatment was also one of the techniques to alter the surface characteristics of diamond nanoparticles by imparting the several polar groups present on the surface which can improve their stability in water [56]. A detailed study on surface modifications technique was reported by Yu and Xie [57] in 2011.

2.2 THERMOPHYSICAL PROPERTIES OF NANOFLUIDS

Thermophysical properties of nanofluids such as thermal conductivity, specific heat, viscosity and density are important to determine for estimating the actual performance of nanofluid in any thermal system. Lot of research was carried out for estimating the thermophysical properties of nanofluids with different nanoparticles, basefluids, nanoparticles concentration, nanoparticles size and shape and temperature and still the research is going on. But no consistency or same value was observed by researchers by using the same type of nanoparticles with same type of basefluids. This is due to the various factors which affecting the thermophysical properties of nanofluids listed as:

a. Type of base fluids
b. Type of nanoparticles
c. Shape and size of nanoparticles

d. Nanoparticles concentration
e. Preparation method
f. Additives or surfactants used
g. pH value
h. Sonication time
i. Stability
j. Temperature
k. Measurement techniques of thermophysical properties

By changing any above factors during experimentation or theoretically prediction, a modified value of thermophysical properties was observed. Few literature studies of thermophysical properties of nanofluids are reported as:

2.2.1 Thermal conductivity of nanofluids

The thermal conductivity enhancement of nanofluids makes it more appropriate instead of traditional heat transfer fluids used in heat transfer applications. Thermal conductivity can also determine from various theoretical models and compared with the experimental predictions. The first model proposed by Maxwell [58] in 1881 and it was further improved by Hamilton and Crosser [59] in 1962 by comprising the effect of particle shape.

Maxwell model

$$\frac{k_{eff}}{k_m} = 1 + \frac{3*(\alpha - 1)*\phi}{(\alpha + 2) - (\alpha - 1)*\phi} \tag{2.1}$$

Hamilton and Crosser model

$$\frac{k_{eff}}{k_m} = \frac{\alpha + (n-1) - (n-1)(1-\alpha)*\phi}{\alpha + (n-1) + (1-\alpha)*\phi} \tag{2.2}$$

where, $\alpha = \frac{k_p}{k_m}$

k_p = Thermal conductivity of solid particles

k_m = Thermal conductivity of liquid medium

k_{eff} = Effective thermal conductivity of slurry

ϕ = Particle volume fraction

n = Shape factor [for sphere = 3, for cylinder = 6]

Experimentally measurement of thermal conductivity are carried out with different techniques such as transient plane source, steady state method, temperature oscillation method, transient hot wire method or KD2 Pro. Present section covers the discussion on experimentally observed thermal conductivity with the consideration of various parameters which affect it. As the present thesis uses alumina, CuO and CNTs based nanofluids, therefore, studies are limited to alumina, CuO and carbon nanotubes based nanofluids in literature discussion.

From the Table 2.2, it is found that nanofluids thermal conductivity depend on the various factors such as type of base fluids, temperature, type and size of nanoparticles, volume fraction of nanoparticles and dispersion method of nanoparticles into base fluids. Thermal conductivity of nanofluids enhances with increase in temperature as well as with increase in volume fraction of nanoparticles by exhibiting linear relationship. Enhancement in thermal conductivity rises with nanoparticles of higher thermal conductivity. But few exceptions revealed nonlinear relationship for thermal conductivity with rise in nanoparticle volume concentration. These discussions give details of thermal conductivity values affecting by various parameters which are listed in the literature by different researchers. But till date no fixed value or enhancement in thermal conductivity was found due to various influencing factors.

Table 2.2: List of influencing factors and thermal conductivity enhancement of nanofluids

Type of Base fluids	Type of nanoparticles	Size of nanoparticles	Influencing factor	Observation (Thermal conductivity enhancement)	Authors
Water, HE-200 oil	CuO/Al_2O_3/Cu	36/33/18 (nm)	Particle size, Base fluid	60 % improvement for 5 vol % CuO particles in water	Eastman et al. [60]
Water, EG	CuO/Al_2O_3	18.6,23.6/24.4,38.4 (nm)	Particle size, volume fraction (linear relationship), Base fluid	20 % improvement for 4 vol % CuO/EG mixture while 10 % enhancement for 4 vol % of Al_2O_3/water nanofluid.	Lee et al. [61]
Water, EG, PO, EO	CuO/Al_2O_3	23/28 (nm)	Particle size, volume fraction (linear relationship), Dispersion method and base fluid	12 % improvement for 3 vol % Al_2O_3/water nanofluids while 25 % enhancement at 5 vol % Al_2O_3/EG nanofluid	Wang et al. [62]
Water	CuO/Al_2O_3	28.6/38.4 (nm)	Particle size, volume fraction (linear relationship), Temperature	2-4 times increase with temperature ranges from 21 ºC to 52 ºC	Das et al. [27]
Water, EG, PO	Al_2O_3	12.2-302 (nm)	Particle size (SSA), pH value, base fluid	20 % enhancement for 5 vol % Al_2O_3/water while 29 % improvement for 5 vol % Al_2O_3/EG and maximum enhancement for 5 vol % Al_2O_3/PO i.e. 38 %	Xie et al. [45]
Water	CuO/Al_2O_3	29/36 (nm)	Volume fraction and temperature	Appreciable enhancement with temperature and nanoparticle concentration	Li and Peterson [63]

Type of Base fluids	Type of nanoparticles	Size and concentration of nanoparticles	Influencing factor	Observation (Thermal conductivity enhancement)	Authors
Oil	MWNTs	25×50 μm	Volume fraction (nonlinear relationship)	160 % at 1 vol %	Choi et al. [8]
Water	CNTs	20–60×~10μm	Temperature	23.7 % and 31 % enhancement for 0.84 % CNT volume fraction for 20 ºC and 45 ºC	Wen and Ding [64]
Water	MWNTs, DWNTs	130×10 μm	Volume fraction, Temperature	34 % improvement for 0.6 vol % suspension	Assael et al. [65-67]
Water	Al_2O_3	13 nm	Particle size, type of base fluids and nanoparticles	30 % enhancement for 4.3 vol % Al_2O_3/water nanofluid	Masuda et al. [68]
Water	CuO	50 nm	Volume fraction	17 % for 0.4 vol % CuO/water nanofluid	Zhou and Wang [69]
Water	CuO	shuttle-like 20×100 nm	Particle shape, volume fraction (nonlinear relationship)	28 % enhancement for 3 vol %	Zhu et al. [70]
Water/EG/ DE	CNTs	15 nm×30 μm	Volume fraction (linear relationship) and type of base fluids	7.0 % enhancement for 1.0 vol % of CNTs/water while 12.7 % enhancement with EG based CNTs nanofluid. Moreover, maximum improvement of 19.6 % observed at 1.0 vol % of CNTs/DE nanofluid	Xie et al. [71]

Type of Base fluids	Type of nanoparticles	Size and concentration of nanoparticles	Influencing factor	Observation (Thermal conductivity enhancement)	Authors
EG /EO	CNTs	20-30 nm	Volume fraction (linear relationship) and type base fluids	12.4 % improvement at 1 vol % volume fraction of CNTs with EG base fluids and 30 % enhancement at 2 vol % of CNTs with EO base fluid	Liu et al. [72]
Water	Al_2O_3	30 ± 5 nm	Volume fraction	Maximum enhancement of 1.44 % observed at the concentration of 0.3 vol %	Lee et al. [40]
Water /EG	Al_2O_3	8-282 nm	Temperature, Volume fraction, Particle size and type of base fluids	Thermal conductivity enhancement decreases when the particle size decreases below 50 nm	Beck et al. [73]
Water	$Al_2O_{3/}$ CuO	36, 47/29 nm	Temperature, Volume fraction, Particle size	Approximately 16 % enhancement in thermal conductivity for each type of nanofluids at temperature between 20 ºC and 40 ºC	Mintsa et al. [74]
Water	Al_2O_3	20, 50, and 100 nm	Temperature, Volume fraction and Particle size	Maximum 14.7 % enhancement observed for 20 nm size nanoparticles and 2 wt % concentration at 50 ºC	Teng et al. [75]
EG	Al_2O_3	40-50 nm	Temperature, nanoparticles concentration	Maximum 19 % enhancement observed for 8.6 vol %	Pastoriza-Gallego et al. [76]
Water	MWCNT	10-15 nm	Temperature, nanoparticles concentration	At low as 0.001 vol % concentration, appreciable enhancement was observed	Kim et al. [77]
EG	CuO	10 nm	Temperature, Volume fraction and Particle size	For better thermal properties, nanoparticles surface functionalization done for improved stability	Shima et al. [78]

2.2.2 Viscosity of nanofluids

After thermal conductivity, the next important thermo-physical property is viscosity for determining the thermal performance of nanofluids. Very few literature studies [40, 76-83] discussed the rheological measurements of nanofluids. Viscosity of nanofluids was also influenced by the same factors which affecting the thermal conductivity. Those influencing factors are type and concentration of solid content, particle shape and size, temperature, pH and the ionic strength of the medium and the sonication time applied during the dispersion method. Some theoretical models were also developed to validate the experimental data. The first classical model of first order was developed by Einstein [84] with an assumption of particle volume fraction less than 1 %.

$$\mu_r = (1 + 2.5\phi) \tag{2.3}$$

Afterward, Einstein model was modified by Brinkman [85] for the nanosuspensions of less than 4 % volume fraction of nanoparticles.

$$\mu_r = \frac{1}{(1-\phi)^{2.5}} \tag{2.4}$$

where, μ_r is the relative viscosity which is the ratio of the nanofluids viscosity μ_n to the base fluid viscosity μ_{bf} and ϕ is the volume fraction of nanoparticles in base fluid.

But viscosity values derived from these models are not comparable with the experimental results obtained by various researchers as shown in Figure 2.3. Most of the research showed that nanofluids viscosity was greater than their respective base fluid and further rises with rise in concentration. Liu et al. [86] determined the viscosity of CuO - ethylene glycol nanofluids with change in particle volume fraction. They found 10.7 % to 83.4 % increase in viscosity for 1 to 5 vol % nanoparticles volume concentration. Ding et al. [79] observed the influence of shear rate on the viscosity of CNT nanofluids. Their results suggest that at low shear rate, CNT viscosity was not affected by gum arabic as the gum arabic solutions is very low viscosity than CNT nanofluids. At particular shear rate, nanofluids viscosity increases with decrease in temperature and increase in concentration same as observed by Liu et al [86].

In addition to this, Kumaresan and Velraj [22] also found that surfactant effect was almost abolished at temperatures more than 25 ºC. The nonlinear behavior of viscosity was observed with increase in nanoparticles concentration and negligible rise in viscosity was noticed for low multiwalled carbon nanotubes (MWCNT) concentration such as 0.15 vol %.

Chen et al. [87] prepared surfactant free CNTs and found that nanofluids have lower viscosity than base fluids due to their lubricative effect at low particle volume concentrations such as less than 0.4 vol %. For higher particle volume fraction (> 0.4 vol %), viscosity increased with increase in concentration as well as increased with temperature above the 55 ºC. Garg et al. [88] observed the effect of ultrasonication on the viscosity of MWCNT nanofluids. It was found that sonication time is first associated with declustering of MWCNT tubes and with increase in sonication time, breakage of nanotubes in shorter sizes results in decrease in viscosity. Furthermore, Gowada et al. [49] declared that Brownian velocity of nanoparticles reduced by viscosity of nanofluids to decrease the agglomeration of nanoparticles in base fluids.

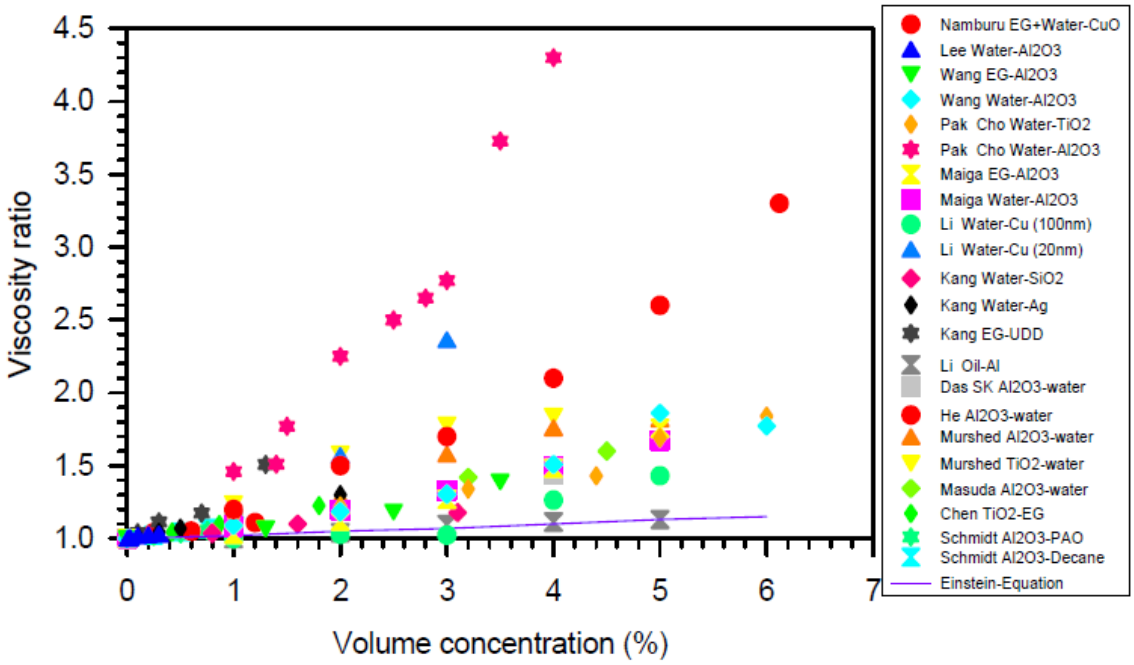

Figure 2.3: Viscosity studies of nanofluids from literature [18]

Sridhara and Satapathy [89] reviewed in detail for the viscosity of alumina nanofluids and reported that decrease in temperature and rise in particle concentration increased the viscosity of nanofluids. But hysteresis phenomenon observed at higher temperature which makes the nanofluid more viscous by altering the nanofluids rheological properties.

As viscosity is an important parameter for any thermal engineering systems which decided the cost of pumping power and also affected the thermal conductivity. From Liu et al. [90] and Khedkar et al. [91] studies, it was concluded that increase of viscosity increase the cost of pumping power as well as counteract the advantage of enhanced thermal conductivity.

From above discussions, it was interpreted that nanofluids viscosity increases with rise in nanoparticle volume concentration and fall in temperature. Beyond critical temperature, nanofluids viscosity increases with temperature by changing the nanofluids rheological properties.

2.2.3 Density of nanofluids

The third thermophysical property i.e. density is very important property for determining the thermal capacity of nanofluids. Very few investigations were found on the experimental and theoretical based density of nanofluids and some of them were discussed. The mixture model was used to estimate theoretically density of nanofluids.

$$\rho_{nf} = \rho_p \phi + \rho_{bf}(1-\phi) \tag{2.5}$$

where, ρ_{nf} is the density of nanofluids, ρ_{bf} is the density of base fluids, ρ_p is the density of nanoparticles used, and ϕ is the volumetric concentration of nanoparticles.

Density of alumina-EG/water (60:40) nanofluids for a temperature range of 0 ºC to 50 ºC was measured experimentally by Vajjha et al. [92] and good conformity occurred with theoretical model. Harkirat and Gangacharyulu [93] was measured the density of alumina-water nanofluids affecting by temperature and nanoparticles concentration. They observed that density of nanofluids increases with increase in nanoparticles concentration and decrease in temperature.

Kumaresan and Velraj [22] compared the experimentally observed density values and theoretically predicted value from Pak and Cho relation of CNT-water/EG (70:30) nanofluids. They observed that nanofluids density was higher than base fluids and enhances with the concentration and these experimental values showed large deviations with theoretical values which were increased with increase in concentration. Recent studies performed by Shoghl et al. [94] showed that density is an important parameter to determine the pressure drop and pumping power. They measured the density of nanofluids with temperature and concentration and compared with the predicted values by mixing rule. The comparison showed that mixing rule is precisely measured the density values and it can be further used in the studies.

2.2.4 Specific heat of nanofluids

Specific heat is an imperative thermophysical property that decides the nanofluids heat capacity and further helpful in heat transfer studies. Very few experimental studies were carried out to calculate the specific heat of nanofluids. Most of the researchers preferred mixture model based on volume average basis and mass fraction basis. Mixture model on volume average basis used by [Pak and Cho [95], Maiga et al. [96] and Jang and Choi [97] represented by

$$c_{nf} = c_p \phi + c_{bf}(1-\phi) \tag{2.6}$$

where, c_{nf} is the nanofluids specific heat, c_{bf} is the base fluids specific heat, c_p is the particle specific heat, and ϕ is the volumetric concentration of nanoparticles.

Most of the researchers [98-102] preferred to use mixture model based on mass fraction basis to calculate specific heat of nanofluids which can be represented as

$$c_{nf} = \frac{\phi(\rho c_p)_p + (1-\phi)(\rho c_p)_{bf}}{\rho_{nf}} \tag{2.7}$$

where, ρ_{nf} values obtained from above equation no. 2.5 and the subscripts *p*, *bf* and *nf* represent the nanoparticle, basefluid and the nanofluid respectively.

Namburu et al. [98] and Zhou and Ni [100] performed the experiments to analyze the specific heat of nanofluids and showed that nanofluids specific heat decreases with rise in nanoparticles volume fraction. There was a good agreement between predicted model values and experimental data. Further, Bergman [99] did a theoretical study on internal forced convection by taking the effect of specific heat. Specific heat of nanofluids was calculated by both equation (2.6) and (2.7) and model based on mass fraction basis was given the accurate values for the specific heat of nanofluids.

2.3 FLUID FLOW AND HEAT TRANSFER IN MINICHANNELS

Nanofluids with appreciable thermal conductivity enhancement and very small rise in density and viscosity give a new direction for researchers to use in thermal applications. Researchers from different areas such as biological, electrical, mechanical have shown their interest in nanofluids. They can use the nanofluids in different applications. Most of the research is carried out as a nanofluids coolant flowing through any conventional, minichannels and

microchannels. Present section discusses the experimental and numerical studies on heat transfer and fluid flow characteristics of nanofluids for diverse systems.

Since the pioneer work by Pak and Cho [95], convective flow and thermal performance of nanofluids was extensively studied over the past two decades. Convective heat transfer in the turbulent flow system examined inside a 10 mm diameter tube using water-Al_2O_3 [d_p = 13 nm] and water-TiO_2 [d_p = 27 nm] nanofluids. At same average velocity of nanofluid, drop of 3-12 % in heat transfer coefficient was observed in comparison with water, which was due to huge increase in viscosity which might be reduced the heat transfer while Xuan and Li [103] found the 40 % enhancement for Cu-water nanofluid at same velocity in the turbulent regime. The same behavior of increase in Nusselt number was observed by Li et al. [25] in the transition flow regime [Re = 1000 to 4000] with Cu-water nanofluids.

Nguyen et al. [104] inspected the thermal performance of Al_2O_3-H_2O nanofluid experimentally and found 40 % rise in the heat transfer coefficient for 6.8 vol % of nanoparticles concentration when compared with pure water. They also observed that smaller the nanoparticles, better the thermal performance. Experiments for both laminar and turbulent flow regimes using CuO-water and Al_2O_3-water nanofluids with 1 m length and 6 mm diameter tube were conducted by Heris et al. [82]. Maximum enhancement of 40 % was observed for 3 vol % nanoparticles concentration of Al_2O_3-water nanofluids in comparison with CuO nanofluid. Rea et al. [105] and Williams et al. [106] experimentally observed the heat transfer and viscous pressure loss features in turbulent and laminar flow regime for zirconia-water and alumina-water nanofluids. They claimed that due to the change in thermophysical properties of the nanofluids with reference to water, abnormally rise in heat transfer coefficient was observed since the nanofluids act as homogeneous mixtures.

Inspired by nanofluids enhancement in conventional channels, various researchers worked for nanofluids flow in minichannels with an appreciable results. Ho and Chen [107] studied the forced convective heat transfer performance for minichannel heat sink using nanofluids and water as a coolant and observed that nanofluids cooled heat sink having better thermal performance in comparison with water. Ijam et al. [108, 109] also carried out experiments in minichannel heat sink by using different nanoparticles such as alumina, TiO_2 and SiC with water as a base fluid. They found that maximum improvement of cooling was 17.32 % i.e. for alumina nanofluids. Naphon and Nakharintr [110] studied the pressure drop and thermal characteristics of nanofluid in minichannel heat sink with small sized rectangular shaped fins.

It was found that no extra pressure drop rise with nanofluids instead of water whereas significant enhancement in heat transfer was observed with nanofluids. Sohel et al. [111] conducted experiments for Al_2O_3-H_2O nanofluids at various concentrations ranging from 0.10 to 0.25 vol % to estimate the thermal performance of a copper minichannel heat sink at the flow rates ranging from 0.50 to 1.25 L/min and Reynolds no. from 395 to 989. Maximum 18 % enhancement in heat transfer coefficient and 15.72 % reduction in thermal resistance were observed for nanofluids when compared with water.

Aliabadi and Sahamiyan [112] recently investigated the flow of Al_2O_3-water nanofluids in corrugated minichannels heat sink by considering the effect of flow rate, nanoparticles weight fraction and geometrical parameters. The results show that heat transfer performance was improved although with an augment in pressure drop at constant heat flux with the straight minichannel heat sink. By increasing the wave amplitude and decreasing the wave length, decrease in thermal resistance was observed for the different geometries of channels. Numerous numerical studies on the nanofluids fluid flow and thermal characteristics by using two phase or single phase models were performed by different research groups and some outcomes were compared with experimental data. Moraveji and Ardehali [113] worked on homogeneous or single phase model as well as three diverse two-phase models such as Eulerian, mixture and volume of fluid to study the forced convection during the nanofluid flow in a minichannel heat sink at constant heat flux. Numerically obtained findings were relate with the experimental results of Ho and Chen [107] and found that two phase mixture model have good correlation with the data obtained experimentally in comparison to single phase model which was also concluded by Khoshvaght-Aliabadi et al. [114].

2.4 FLUID FLOW AND HEAT TRANSFER IN MICROCHANNELS

Several researchers worked for conventional and minichannels but microchannel heat sink (MCHS) seek an attention especially from electronic industry to enhance the cooling efficiency of active devices. The MCHS with the efficient coolant such as nanofluids proves the best combination for cooling in electronic industry. In this section, as per the literature studies, all the relevant information in this area are tried to reveal.

In one of early studies of nanofluids in MCHS, Koo and Kleinstreuer [115] numerically examined the CuO-water/EG based nanofluid flowing through microchannels. They observed the better heat transfer performance of the carrier fluids with high Prandtl numbers flowing

through large aspect ratios microchannels. They recommended that channel walls should be treated to avoid the accumulation of nanoparticles.

Chein and Huang [116] analyzed the friction coefficients and heat transfer coefficients for silicon MCHS using Cu-water nanofluids from theoretical models and experimental correlations. Nanofluids was considered as single phase fluid and from experimental correlation, it was found that nanofluids enhanced the MCHS cooling performance when compared with water due to its high thermal conductivity. There was no extra pressure drop generated in MCHS by nanofluids as the nanoparticles are small in size and particle volume concentration was too low. Further, the thermal performance of a microchannel heat sink was evaluated numerically by Jang and Choi [117] with 2 nm diamond-water and 6 nm Cu-water nanofluids. They found that at a fixed pumping power of 2.25 W, nanofluids reduced the thermal resistance by enhanced the cooling performance of MCHS about 10 % with 1 vol % diamond based nanofluids. Nanofluids also reduce the temperature difference among coolant and microchannel wall which further remove high heat flux of 1350 W/cm^2.

At the same time, another numerical study carried out by adopting thermal dispersion model for improving the cooling performance of single phase MCHS using Cu nanofluids by Abbassi and Aghanajafi [118]. For thermal dispersion model, Nusselt number was assumed to be function of channel aspect ratio. They depicted from the results that with nanofluids, an appreciable amount of heat transfer enhancement observed and it escalates with the augmentation of particle volume concentration and Reynolds number. The results also showed that Nusselt number increases further by flow conditions changes to turbulent regime by increasing the Reynolds number.

Lajvardi et al. [119] developed a correlation of Nusselt number for nanofluid flow through silicon microchannels and correlate with the experimental measurements of Li and Xuan. For low Reynolds no. or laminar flows, Nusselt number decreases with increasement of nanolayer thickness by increasing the nanoparticles concentration in fluids. They achieved the maximum reduction of 15 % in thermal resistance with a volume fraction of 2 % and power input of 3 W. Chein and Chuang [120] theoretically and experimentally studied the silicon based microchannel heat sink (MCHS) performance using CuO-H_2O nanofluids as coolants. From theoretical analysis, it was clear that MCHS cooling performance with nanofluid flow absorb more heat and attaining lower wall temperature than MCHS with their respective pure fluid. Then, experimentally verify these theoretical predictions by varying nanoparticles

volume concentration i.e. 0.2 to 0.4 %. At low flow rates, nanofluids absorb more heat than water whereas for high flow rates, nanoparticles contribution for extra heat absorption was negligible. Therefore, theoretical predictions agreed with experimental results for low flow rates while theoretical and experimental results did not match for high flow rates. As nanofluids viscosity was high but merely a small increase in pressure drop was observed. The findings also showed that agglomeration of nanoparticles could be reduced by increasing the nanofluid bulk temperature.

Tsai and Chein [121] used CNT-water and Cu-water nanofluids for investigated the MCHS performance by using nanofluids. They contradicted the Koo and Kleinstreuer [115] recommendations of low porosity and low aspect ratio. It was also observed that nanofluids with higher concentration reduced more the temperature difference between bulk fluids and microchannel heat sink bottom wall as compared to base fluids. Lu and Nanna [122] investigated for outlet/inlet manifold designs and location and length of outlets and inlet for better performance of MCHS. Results showed that trapezoidal shaped manifold with circular outlet and inlet yield the best flow distribution. The heat transfer enhancement in microchannels featured to microconvection within the channel, fluid channel wall interaction, laminar flow and conductive heat transfer through the microchannels wall.

Li and Kleinstreuer [123] developed a new KKL (Koo-Kleinstreuer-Li) model for nanofluids which was completely in agreement with the experimental data sets. They explored the heat transfer performance of nanofluids in a trapezoidal microchannel by using user-supplied pre and post processing software and Navier Stokes solver CFX-10. Results showed that nanofluids such as CuO-water enhanced the overall thermal performance and the enhancement is directly proportional to the nanoparticles volume fraction but with concentration, slightly extra pressure drop was observed which will rather reduce the beneficial effects.

Shokouhmand et al. [124] investigated the thermal performance of silicon based MCHS using Cu-water nanofluids and found that nanofluids did not contribute to the extra pressure drop and almost same pressure drop was observed for all the concentration of nanofluids as well as water. It was also observed that laminar flow ($Re < 2000$) is under power 3 W and for higher powers, flow becomes turbulent. Jung et al. [125] experimentally determined the nanofluid flow and heat transfer characteristics of nanofluids in silicon single rectangular microchannel. Alumina of size 170 nm with water and water/EG mixture (50:50) was used in the

experiments. Nanofluids were flow in different dimensions of microchannels such as 50×50 μm, 50×100 μm and 100×100 μm with 15 mm length. They found that ethylene glycol based nanofluids was not suitable for smaller dimensions of microchannels as the ethylene glycol is four times more viscous than water. They observed the 32 % enhancement in heat transfer coefficient without any major losses for 1.8 vol % nanofluid. It was also confirmed that Nusselt number did not much vary with the nanoparticle concentration as shown in Figure 2.4. They also developed correlation same as of Dittus–Boelter correlation.

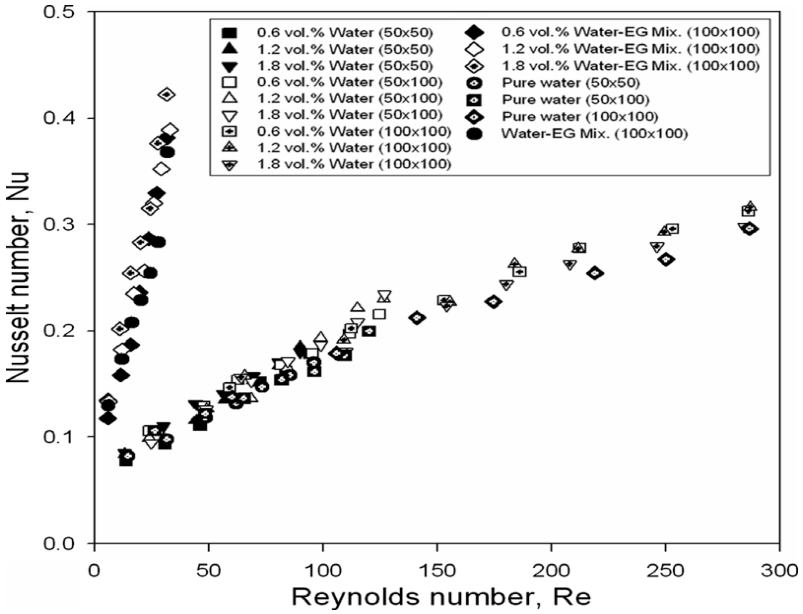

Figure 2.4: Variation of Nusselt number with Reynolds number for different nanofluids flow through different dimensions of microchannels [125]

Bhattacharya et al. [126] numerically investigate the heat transfer coefficient (HTC) of alumina-water nanofluid through silicon based rectangular shaped MCHS with conjugate heat transfer approach. Simulation results showed that if Reynolds number increases from 250 to 700, thermal resistance reduced by 7.8 % as by using nanoparticle concentration of 2 vol %. Further, wall temperature reduces with increase in Reynolds number which was responsible for enhancement in HTC and decreasing overall conductive thermal resistance. After Bhattacharya et al. [126] numerical studies, Wu et al. [127] investigated experimentally single phase flow and heat transfer characteristics of alumina-water nanofluids in silicon based trapezoidal microchannels (D_h=194.5 μm). They studied the effect of nanoparticles concentration, Reynolds number and Prandtl number on pressure drop and heat transfer of nanofluids flowing through microchannels. It was found that heat transfer coefficient increased by 4.2-5.7 % and 10.2-15.8 % for 0.15 vol % and 0.26 vol % nanoparticles

concentration which was significant enhancement in comparison with the pressure drop rise of nanofluids i.e. 3-4.2 % and 3.4-5.5 % at 0.15 vol % and 0.26 vol % concentration at the flow rate ranges from 5×10^{-8} m^3/s to 26.5×10^{-8} m^3/s. With increase of wall temperature of channels, boiling heat transfer doubtful in microchannels as nanoparticles deposition on the inner wall was observed.

Harirchian and Garimella [128] conducted various set of experiments to investigate the effect of cross sectional area of channel, aspect ratio of channel, channel width and channel depth on boiling heat transfer in microchannels using Fluorinert FC-77 and perfluorinated dielectric fluid. Results showed that cross sectional area of channel is a significant factor to establish heat transfer and boiling mechanisms in microchannels. Nucleate boiling was dominant in the channels of cross section area larger than specific value i.e. 0.089 mm^2 and below this value of cross sectional area, heat transfer coefficient was not dependent. For single and two phase regions, pressure drop and heat transfer coefficient rises at constant heat flux with decrease in the microchannel cross sectional area.

Chein and Chen [129] also studied the effect of geometry in terms of inlet and outlet arrangements to analyze the heat transfer performance of MCHS. They numerically investigated the heat sinks with different inlet-outlet arrangements by changing the locations. It was found that better heat transfer performance observed for a heat sink in which coolant was supplied and collected vertically when compared with the horizontal inlet outlet arrangement. As the geometry of MCHS shows a vital role for achieving the better thermal performance therefore further numerical investigation was carried out for different shapes of MCHS such as triangular, trapezoidal and rectangular by Gunnasegaran et al. [130]. They numerically observed the effect of friction factor and pressure drop of fluid flow in microchannels by using finite volume method. It was found that MCHS with smallest hydraulic diameter having better performance and Poiseuille number and friction factor values strongly vary with the change in shape and size of MCHS.

In additional to this, Mohammed et al. [131] also numerically examined the thermal performance of rectangular shaped MCHS by using finite volume method to solve the heat transfer equations for Reynolds number in the range of 100-1000. They used Al_2O_3-H_2O nanofluids for nanoparticles volume concentration ranging from 1 % to 5 %. It was observed that wall shear stress and heat transfer coefficient increases while thermal resistance decreases with increase in nanoparticles concentration. Although, nanofluids with higher

concentration such as 5 % did not contribute for extra heat absorption and performance was approximately same as of water. Further, slightly rise in pressure drop was observed in MCHS with nanofluids in comparison with water.

Escher et al. [132] experimentally observed the MCHS performance by using silica nanofluids (particle volume fraction upto 31 %). All the thermophysical properties were measured experimentally used for evaluating the performance of heat sink. Nusselt number was evaluated for different channel width of MCHS as a function of volumetric flow rate. Experimentally observed data shows a deviation of not more than 10 % with the theoretical predictions. They reveal that the thermal conductivity enhancement must be more than viscosity enhancement for achieving the better thermal performance of nanofluids cooled MCHS.

Mohammed et al. [133] numerically examined the influence of different water based nanofluids such as SiO_2, diamond, CuO, Ag, $Al_2O_3$and TiO_2 (2 vol % nanoparticle concentration) on heat transfer performance of aluminium based MCHS using finite volume method. Results showed that overall heat transfer and fluid flow performance in MCHS were maximum improved by using Ag-H_2O and diamond-H_2O nanofluids. As diamond-H_2O nanofluids have the highest heat transfer coefficient with lowest temperature and Ag-H_2O nanofluids had the lowest pressure drop and wall shear stress. While Al_2O_3-H_2O nanofluids were the lowest heat transfer coefficient and SiO_2-H_2O nanofluids generate the highest pressure drop in microchannels so less preferable as coolants in microchannels.

Solovitz and Mainka [134] derived the optimized power law for observing the flow regime in multi micro channel heat sink. This model was valid for laminar flow under fully developed conditions performed by computational simulations. This power law design helps to maintain uniform speed in parallel arrangement at low Reynolds number with a deviation less than 3 % of overall channel speed. They observed some maldistribution at higher Reynolds number but this was not significant with untapered designs.

Seyf and Mohammadian [135] studied the fluid flow and heat transfer characteristics of a counter flow microchannel heat exchanger with alumina-water and CuO-water nanofluids. Numerical heat transfer simulations were carried out by using finite volume method to assess the effects of volume fraction of nanoparticles, Reynolds number and Brownian motion on pumping power, effectiveness and performance index of heat exchanger. Results showed that

Al_2O_3-water nanofluid was lower effectiveness and pumping power as compared with CuO water nanofluid. With increase in particle volume fraction, effectiveness and pumping power increases while performance index decreases and with decrease in Reynolds number vice versa behavior observed. It was also inferred that performance index and pumping power were not responsive to higher nanoparticles concentration and lower Reynolds number.

In the same manner, Farsad et al. [136] also performed a numerical simulation by developing a 3D model using FLUENT software for estimating thermal and hydraulic performance of copper based MCHS sink using alumina nanofluids. They found an enhancement of 4.5 % in cooling performance by using alumina nanofluids at 8 vol % concentration in microchannels compared with pure water. It was also concluded that metal based nanofluids showed better performance when compared with that of oxide metal nanofluid. After so many numerical studies, Singh et al. [137] investigated the heat transfer performance of water and ethylene glycol based alumina nanofluids in microchannel experimentally as well as numerically. Different size of microchannels with 218 and 303 μm hydraulic diameters was fabricated to flow alumina nanofluids with different particle volume fraction of 0.25 vol %, 0.5 vol %, and 1 vol %. They found an appreciable enhancement in heat transfer characteristics with low viscosity base fluids, higher Reynolds number and concentration of nanofluids. It was concluded from numerical simulation that nanoparticles concentration was irregular at the outlet of channel due to particle relocation.

Anoop et al. [138] performed experiments to estimate forced convective heat transfer inside the microchannels by using silica nanofluids as a coolant. Experimental findings showed that heat removal by nanofluids from MCHS was good up to critical value of flow rate i.e. below 10^{-4} kg/sec. It was also found that effectiveness of nanofluids start declined at higher Reynolds number so heat removal appears to be superior at lower Reynolds number. Furthermore, higher Reynolds number was also responsible for fouling in microchannels hence high flow rates were not recommended. Hung et al. [139] examined the thermal performance of alumina nanofluids numerically in 3-D MCHS. They suggested that microchannels heat sink substrate materials with higher thermal conductivity and coolant fluid with lower viscosity enhanced the overall thermal performance of MCHS. They obtained the 21.6 % enhancement in heat transfer performance by using nanofluids instead of water. Furthermore, thermal resistance decrease up to a critical value of nanoparticles concentration and beyond that thermal resistance starts increasing. Therefore, to obtain a

lower thermal resistance, proper adjustment of volume fraction and pumping power was required.

Kamali [140] et al. investigated the thermal performance of MCHS with alumina - water and MWCNT-water nanofluids. They observed the mean reduction in thermal resistance was higher as 18 % for MWCNT nanofluids in comparison with 1 % reduction for alumina nanofluids. Mirzaei and Dehghan [141] also numerically studied the fluid flow and heat transfer behavior in microchannels at constant heat flux using alumina water based nanofluids. An appreciable heat transfer enhancement and slightly increase in friction factor was observed while using nanofluids instead of pure water. Furthermore, Ramiar and Ranjbarn [142] numerically explored the effect of size and type of nanoparticles on the performance of horizontal microchannel. Results showed that nanoparticles with smaller diameter and higher thermal conductivity gave more enhancements in Nusselt number.

In the recent study, Rimbault et al [143] performed experiments to evaluate the thermal and hydraulic performance of CuO nanofluids flowing through rectangular MCHS in laminar and turbulent conditions. It was found that pressure drop shoots by increasing the particle volume fraction and enhanced up to 58 % for 4.5 % volume fraction under heating condition compared with water. Furthermore, heat transfer coefficient and energetic performance coefficient showed worst performance at higher concentration. So, best heat transfer performance was given by nanoparticles volume concentration of 1.03 % over water.

Recently one more study by Duursma et al. [144] for evaluating the heat transfer and fluid flow behavior using alumina-ethanol based nanofluids within the microchannels. Single phase nanofluids did not contribute to the extra pressure drop even by varying particle volume concentration. Infrared camera was used to capture boiling two phase flow through microchannel wall. It was observed that pressure drop was fluctuating and unstable when flow boiling happened. Maximum heat transfer enhancement i.e. 5 fold enhancement over ethanol was observed at 0.05 % nanoparticles volume concentration.

After extensive discussion on nanofluids fluid flow and heat transfer characteristics over microchannels, a brief summary of alumina, CuO and CNTs base nanofluids flowing through different shape and size of microchannels are tabulated in Table 2.3. This shows that nanofluids are promising fluid for microchannels as it enhances the overall thermal efficiency at a low cost of pumping power.

Table 2.3: Summary of thermal and hydraulic characteristics of alumina, CuO and CNTs based nanofluids in microchannels

AUTHOR	TYPE OF MCHS	STUDIES	NANO FLUIDS USED	BASE FLUIDS	SIZE OF CHANNEL	OBSERVATIONS
Koo and Kleinstreuer [115]	Rectangular shape	Numerical	CuO	Water/EG	W_{ch} = 50 μm	High heat performance with high Prandtl number carrier fluids
Chein and Chuang [120]	Silicon trapezoidal shape	Theoretical and experimental	CuO	Water	W_t = 500μm, W_b = 500μm H = 100 μm	For high flow rates, no extra heat absorbed by nanoparticles
Li and Kleinstreuer [123]	Silicon trapezoidal shape	Numerical correlation	CuO	Water	W_t = 500μm, W_b = 358.4 μm H = 100 μm	Thermal performances enhances with small increase in pumping power
Jung et al. [125]	Silicon single rectangular microchannel	Experimentally	Alumina	Water and Water/EG (50:50)	a. 50×50 μm b. 50×100 μm c. 100×100 μm L= 15 mm	Smaller dimensions of channels not fit for EG based nanofluids. 32 % enhancement in heat transfer coefficient. No appreciable effect of concentration on Nusselt no.
Bhattacharya et al. [126]	Silicon rectangular microchannel	Numerically	Alumina	Water	57 μm×180 μm, L= 10 mm	Thermal resistance reduced by 7.8 % with 2 vol % as Re increases from 250 to 700
Wu et al. [127]	Silicon trapezoidal shape	Experimentally	Alumina	Water	W_t = 447.1 μm, W_b = 219.6 μm H = 152.8 μm	Heat transfer enhancement goes upto 15.8 % for 0.26 vol % at 26.5×10^{-8} m^3/s flow rate

AUTHOR	TYPE OF MCHS	STUDIES	NANO FLUIDS USED	BASE FLUIDS	SIZE OF CHANNEL	OBSERVATIONS
Mohammed et al. [131]	Aluminium rectangular microchannel	Numerically	Alumina	Water	280×430 μm L= 10 mm	Higher concentrations (≥ 5 %) of nanofluids do not contribute extra heat absorption and performance.
Mohammed et al. [133]	Aluminium triangular microchannel	Numerically	Al_2O_3, Ag, CuO, diamond, SiO_2, and TiO_2	Water	280×430×452 μm, L= 10 mm	Diamond nanofluids have highest and alumina nanofluids have lowest heat transfer coefficient.
Seyf and Mohammadian [135]	Silicon counter flow heat exchanger	Numerically	Alumina	Water	40×40 (μm), L= 10 mm	Alumina nanofluids have lower effectiveness and pumping power compared with CuO nanofluids. Higher particle concentrations do not for extra performance.
Farsad et al. [136]	Copper zig zag channels	Numerically	Alumina, CuO, Cu	Water	27×11 (μm), With 2 mm thickness	4.5 % enhancement in cooling performance by using alumina nanofluids at 8 vol %. Metal based nanofluids showed better performance.
Singh et al. [137]	Silicon trapezoidal shape	Numerically and experimentally	Alumina	Water and EG	W_t = 740 μm, W_b = 500 μm H = 220 μm	Maximum enhancement observed for higher concentrations and low viscosity base fluids.
Hung et al. [139]	Silicon, aluminium, copper, steel	Numerically	Al_2O_3, Ag, CuO, diamond, SiO_2, and Cu	Water	W_t , W_c and H = a. 56×44×320 μm b. 55×45×287 μm c. 50×50×302 μm	Substrate material with higher thermal conductivity and base fluid with lower viscosity shows better performance. 21.6% enhancement in heat transfer coefficient observed.

AUTHOR	TYPE OF MCHS	STUDIES	NANO FLUIDS USED	BASE FLUIDS	SIZE OF CHANNEL	OBSERVATIONS
Kamali et al. [140]	Rectangular shape	Numerically	Alumina, MWCNT	Water	280×430 (μm)	Thermal resistance reduced by 18 % for MWCNT nanofluids
Mirzaei and Dehghan [141]	Rectangular shaped	Numerically	Alumina	Water	W_c = 0.4 mm, H = 1 mm, L= 12 mm	Heat transfer coefficient increases and friction factor increase by using nanofluids.
Rimbault et al. [143]	Aluminium rectangular shaped	Experimentally	CuO	Water	W_c = 25.22 mm, L= 106.81 mm.	Best heat transfer performance with low pressure drop rise was obtained at 1.03 vol % concentration and worst performance at higher concentrations with 58 % enhancement in pressure drop at 4.5 vol %.
Duursma et al. [144]	Rectangular shaped	Experimentally	Alumina	Ethanol	W_{in} = 8 mm, d_{in} = 0.8 mm d_{wall} = 0.54 mm	Maximum heat transfer enhancement i.e. fivefold enhancement over ethanol was observed at 0.05 % nanoparticles volume concentration.

2.5 MADM-TOPSIS APPROACH FOR THE SELECTION OF SUITABLE NANOPARTICLES FOR THERMAL SYSTEMS

The ability to choose the most suitable nanofluids for a particular application is the primary concern for design engineer. The core objective of nanofluids selection is to identify best suitable nanoparticles and base fluids with the combination of different parameters which influence the preparation of nanofluids.

During selection process of stable nanofluids, various sets of attributes have to be considered to get optimal results. Concurrent engineering considers all aspects of life cycle right from the concepts, design, development, fabrication, applications and finally disposal of the product i.e. nanofluids. It encourages collaborations and team work and results in reduction of product development time and cost saving, time to market and customer satisfactions. As per the customer's needs, manufacturers consider all the attributes concurrently and developed the desired product in minimal time. From the past studies it is clear that authors have not considered all the factors concurrently for the preparation of nanofluids. For example, Yang et al. [145] used trimethyoxysilane as a surfactant for the preparation of silicon dioxide (SiO_2) nanofluids with water as a base fluid while Qu et al. [146] and Anoop et al. [138] prepared SiO_2 nanofluids by varying the pH 9.7, 4.9 or 4.5.

Most of the researchers [89] worked on alumina (Al_2O_3) nanofluids as these are the stable nanofluids and no surfactant is required for its preparation. Masuda et al. [68] observed an enhancement of 1.324 times in thermal conductivity of alumina nanofluids with water while Lee et al. [61] measured 1.10 times enhancement in conductivity. This difference in enhancement ratio is due to the size of nanoparticles. Phuoc et al. [44] conducted the experiment for multi walled carbon nanotubes (MWCNT) which get stabilized for months by 0.2 wt % cationic chitosan as it is a biocompatible while it can also experimentally concluded by Garg et al. [88] that the MWCNT samples were stable for over 1 month by the use of gum arabic in de-ionized water. Haddad et al. [147] reported the performance characteristics of zinc oxide (ZnO), copper oxide (CuO) and titanium dioxide (TiO_2) nanofluids varies with the shape and size of nanoparticles, base fluids, preparation method, surfactants used and sonication time.

Attributes can be of any quantitative or qualitative in nature but are quantified on interval scales. Any kind of material or system selection for a particular application can be done by using fuzzy decision making or by using multi attribute decision making methods [148, 149].

MADM methodology is used for the selection of mechatronic system [150], selection of plant layout [151], selection of a robot [152] and in selection of supplier [153]. This approach is very user friendly and used in various applications.

In actual numerous attributes control the selection process of nanoparticles and base fluids for the preparation of stable nanofluids. An exhaustive list which contains attributes and design parameters relevant for the preparation and stability of nanofluids is not accessible in the literature. The objective of this study is to propose a MADM approach to deal with the decision making problems of both qualitative and quantitative attributes for the ranking and optimum selection of nanofluids. A ranked value judgment on a TOPSIS scale or on a graphical scale for the nanofluids is introduced. The literature review does not show any contribution in the area of selection of best suitable nanofluids for a particular application. TOPSIS is one of the many approaches under the umbrella of MADM. It is most suitable for design related problems [149-153]. TOPSIS permits to consider large number of parameters/attributes simultaneously while other methods not. No special mathematical techniques or tools are required to learn for the implementation of this methodology for the selection of best suitable nanofluids. A simple MATLAB can be used which is very user friendly to evaluate the matrix. The attempt made by the authors for the selection of best nanofluids for a particular application does not exist yet before.

2.6 CLOSURE

Preparation of nanofluids can be done either by one step method in which nanoparticles synthesis and dispersion concurrently occur in the base fluids or two step method such as dispersion of purchased nanoparticles directly into the base fluids. After dispersion of nanoparticles in base fluids, stability of nanofluids is an important concern for researchers. Various methods are available to make stable nanofluids such as adding surfactant or activator, by controlling the pH of fluids, agitating, stirring or sonication. These stability methods help the nanoparticles to remain suspended in the base fluids for longer time.

The thermal properties of nanofluids have significant role to evaluate the thermal characteristics of nanofluids. Various factors such as type of nanoparticles, base fluids, stability methods, pH, temperature, nanoparticles concentration, etc., affecting the thermophysical properties are listed in the literature. An appreciable enhancement in thermal conductivity is reported which makes the nanofluids suitable for use in any kind of heat transfer applications. Viscosity of nanofluids is slightly higher for nanofluids which decrease

with increase in temperature and decrease in nanoparticles concentration. But at higher temperatures, hysteresis phenomenon observed which makes the nanofluid more viscous by altering the nanofluids rheological properties. Density of nanofluids can be predicted either by mixture model or experimental techniques as predicted values is almost same as of experimental values. Further, specific heat of nanofluids used to calculate the heat capacity of nanofluid which was accurately calculated by mixture model on mass fraction basis.

There are number of studies reported in the area of nanofluids heat transfer and hydraulic performance through minichannels. As an electronic industry need a miniature device such as microchannel heat sink with an efficient coolant. So, microchannel heat sink with nanofluids proves a best way to enhance the overall efficiency of thermal system. Most of the numerical studies are carried out for determining the heat transfer and fluid flow characteristics of nanofluids in microchannels. Very few experimental studies are reported which shows limitation of use of higher nanoparticles concentrations and less than 100 μm hydraulic diameter of microchannels. This lead to leakage, sedimentation and clogging of nanoparticles, more pressure drop in microchannels. So, it will be better to perform more experiments to analyze the real picture of nanofluids flow in microchannels.

An MADM-TOPSIS approach is introduced which helps to select the best suitable nanoparticles and base fluids for any kind of thermal system. This approach deals with the decision making problems of both qualitative and quantitative attributes for the ranking and optimum selection of nanofluids and further with the help of MATLAB, matrix can be solved. The attempt made for the selection of best nanofluids for a particular application does not exist yet before.

2.7 SCOPE OF PRESENT WORK

From the above literature studies, scope of the present study is as follows.

1. Nanofluids used in this study are prepared by two step methods by procuring the nanoparticles and base fluids commercially. Optimization of sonication time can be done as in literature no fixed sonication time was given for nanofluids. Before measuring the thermophysical properties of nanofluids, stability of nanofluids with days will be carried out with the help of zeta potential measurement, absorbance value, thermal conductivity measurement and visual observation.
2. Thermophysical properties such as thermal conductivity, viscosity, density and specific heat of nanofluids are measured at different temperature ranges from 20 ºC to 80 ºC.

Mathematical equations for nanofluids are developed in terms of base fluids, concentration and temperature.

3. Rectangular shaped microchannels are fabricated and nanofluids fluid flow and thermal characteristics are measured for different flow rates and heat inputs.
4. Software program is developed to correlate the present experimental data and further for the researchers ease to calculate the heat transfer performance by giving the input conditions.
5. A new MADM-TOPSIS approach is introduced for the selection of suitable nanofluids for any kind of thermal applications. This methodology is useful for the researchers for the selection of nanofluids with better performance and good stability in less time and effort.

Scope of the study is limited to some points following as:

1. Nanoparticles used in this study are alumina, copper oxide and multiwalled carbon nanotubes (MWCNT). There is lot of information available in the literature for alumina nanoparticles. So, alumina is used to verify the results as reported in the literature. To make a comparison with aluminium oxide nanoparticles, copper oxide nanoparticles are used. Further, MWCNT is used because of its high thermal conductivity in comparison with others and also very few investigations are carried out with MWCNT flowing through microchannels.
2. Base fluids such as water and water-ethylene glycol mixtures in the ratio of 90:10, 80:20, 70:30, 60:40 and 50:50 are used. Detailed study of these base fluids with the combination different nanoparticles have not seen yet before.
3. The study is limited to microchannel substrate material aluminium due to less information available in literature related to this. Thermal performance and fluid flow behavior of alumina, copper oxide and MWCNT nanoparticles with different base fluids are examined by flowing nanofluids through aluminium microchannel substrate.
4. Heat transfer and fluid flow performance is limited to laminar flow with a fixed microchannel size (more than 100 μm) and shape (rectangular). As the present study mainly focused on the different type of nanoparticles and base fluids behavior in the microchannels.
5. Nanoparticles concentration does not go beyond 1 vol % in microchannels to avoid the sedimentation and clogging of nanoparticles in channels.

2.8 OBJECTIVES OF THESIS WORK

From the scope of work, the final objectives for thesis work are decided as:

1. To prepare Al_2O_3, CuO and CNT nanofluids by dispersing Al_2O_3, CuO and CNT nanoparticles in base fluid i.e. distilled water and ethylene glycol-water mixture of various concentration ranges from 0.1 % to 5 % by volume.
2. To measure the transport properties of nanofluids in the range of temperature such as 20 °C to 80 °C.
3. To evaluate the heat transfer and pressure drop characteristics of above mentioned nanofluids in aluminium based MCHS at different flow rates and temperatures.
4. Correlation of experimental data and model development.

CHAPTER 3

PREPARATION CHARACTERIZATION AND STABILITY OF NANOFLUIDS

This chapter presents a detailed description of materials used for the preparation of nanofluids and their preparation methodology including the optimization of sonication time and further discussed the stability of nanosuspensions with respect to days to meet the first objective of thesis. Stability of nanofluids is concluded by thermal conductivity values, zeta potential measurement, absorbance measurement and visually analysis. The measurements are carried out till no particle agglomeration observed.

3.1 MATERIALS

Present thesis focussed on three types of nanoparticles such as Alumina (Al_2O_3), Copper oxide (CuO) and Multiwalled carbon nanotubes (MWCNT) which were procured from Nanoshel LLC, USA. Details of nanoparticles are listed in Table 3.1.

Table 3.1: Description of nanoparticles

S. No	Type of nanoparticles	Particle size	Purity (%)	Color	Thermal conductivity (W/m.^{o}C)	Density (kg/m^3)	Specific heat (J/kg.^{o}C)
1	Al_2O_3	20 nm	≥ 99	White	35	3950	880
2	CuO	25-55 nm	≥ 99	Black	32.9	6310	532
3	MWCNT	L=3-8 μm O.D=10-20 nm	≥ 99	Black	2586	2600	740

Different base fluids such as double distilled water (W) and double distilled water/Ethylene glycol(W/EG) mixtures in the ratio of 90:10, 80:20, 70:30, 60:40 and 50:50 by volume were used. Ethylene glycol with 99 % purity was purchased from SDFCL, Mumbai, India whereas double distilled water was available in the laboratory of Chemical Engineering Department in Thapar University, Patiala, Punjab. India. Surfactant such as sodium dodecyl sulphate (SDS) was procured from M/s SDFCL, Mumbai, India whereas Gum Arabic (GA) was procured from M/s Nice Chemicals Pvt. Ltd**,** Cochin, Kerala, India.

3.2 MORPHOLOGY AND STRUCTURE ANALYSIS OF NANOPARTICLES

Nanoparticles were characterized on a scanning electron microscope (JEOL JSM 6510 LV) equipped with integrated silicon drift detector (SDD) technology to carry EDS analysis at

SAI lab, Thapar University, Patiala, Punjab, India. For alumina and CuO nanoparticles, scanning electron microscope (S-3400, Hitachi Ltd., Tokyo, Japan) operated at an excitation voltage of 15 kV at NIPER, Mohali, Punjab, India.

Typical SEM micrograph of Alumina, CuO and MWCNT shows the surface morphology and size of nanoparticles. It is clearly depicted from Figure 3.1 that alumina has spherical structure with nanometer size. The EDS analysis of alumina shows in Figure 3.2 that it contains 61.29 % oxygen and 38.71 % aluminium element by weight.

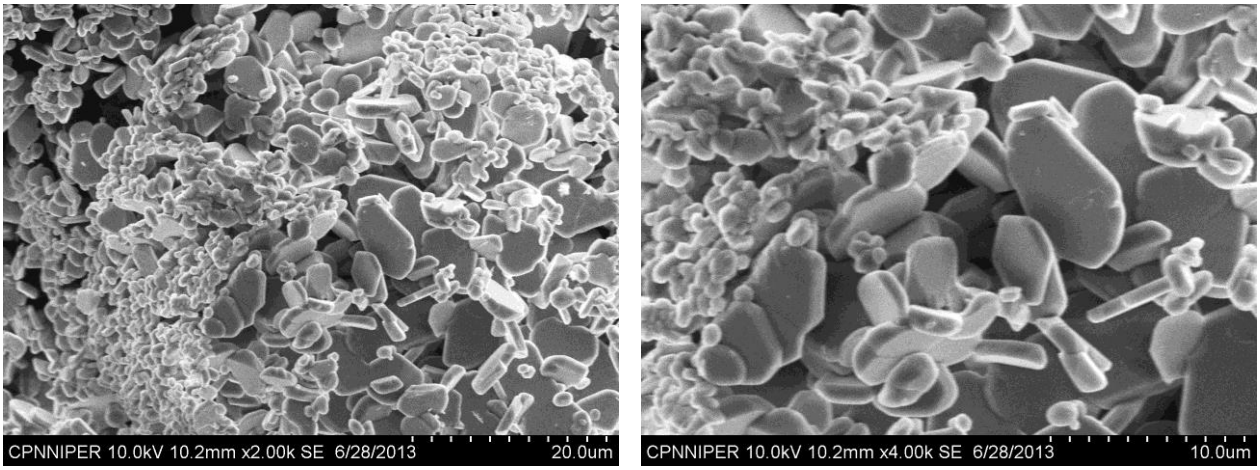

(a) (b)

Figure 3.1: (a& b) SEM image of Alumina

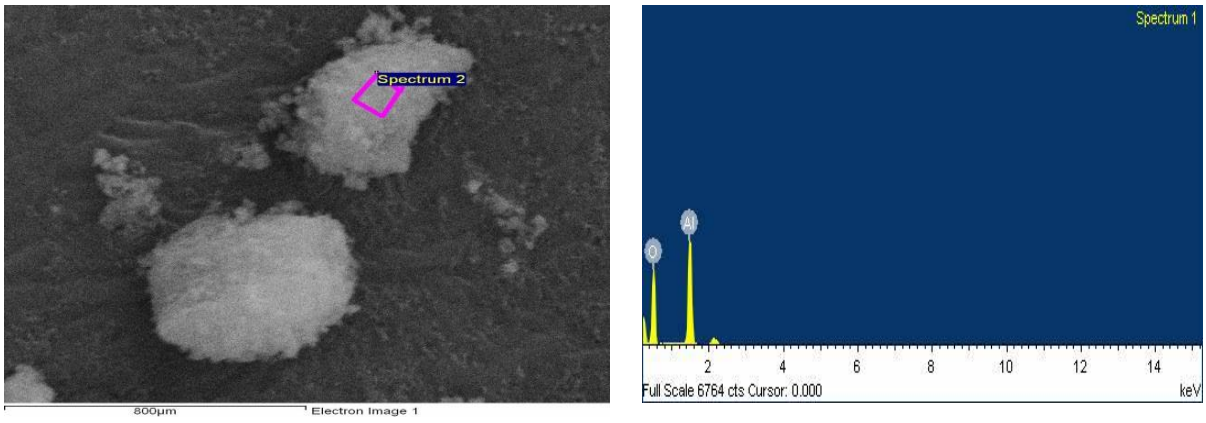

(a) (b)

Figure 3.2: (a & b) EDS spectra of Alumina

From Figure 3.2, it clearly exhibits that CuO has spherical structure with nanometer size. The EDS analysis of CuO shows that it contains 65.50 % copper and 34.50 % oxygen element by weight.

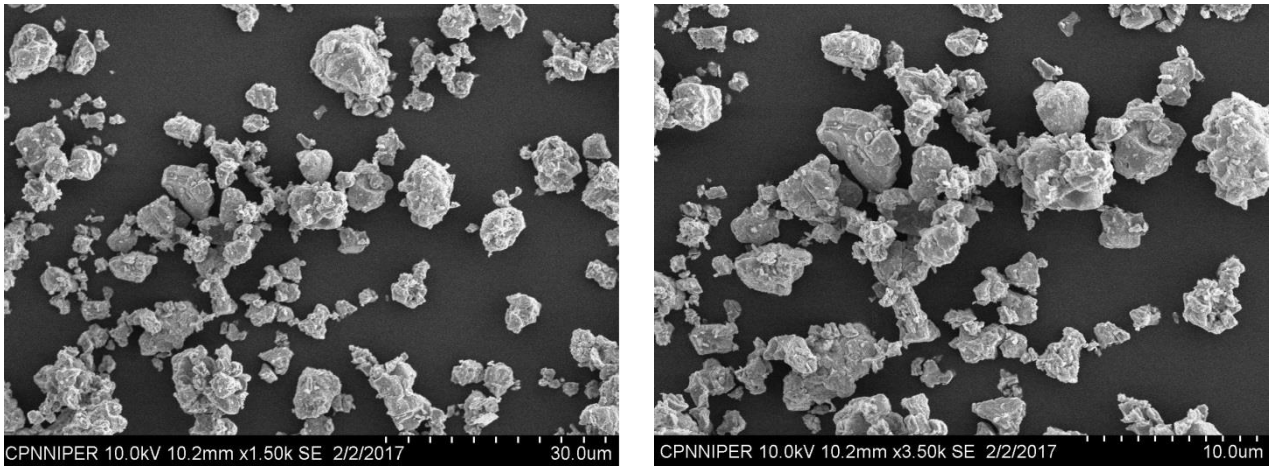

(a) (b)

Figure 3.3: (a& b) SEM image of CuO

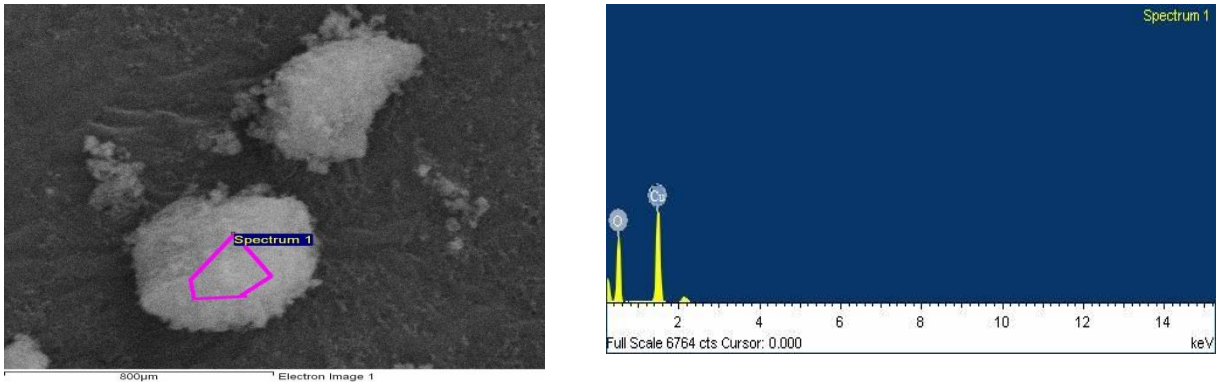

(c) (d)

Figure 3.4: (a& b) EDS spectra of CuO

It clearly exhibits from Figure 3.5 that MWCNT has tube like structure with nanometer size. The EDS analysis of MWCNT shows that it contains 91.50 % carbon and 8.5 % oxygen element depicted from Figure 3.6. The presence of Oxygen element signifies the functionalization improvement of MWCNT for various heat transfer applications (Masipa et al. [154]).

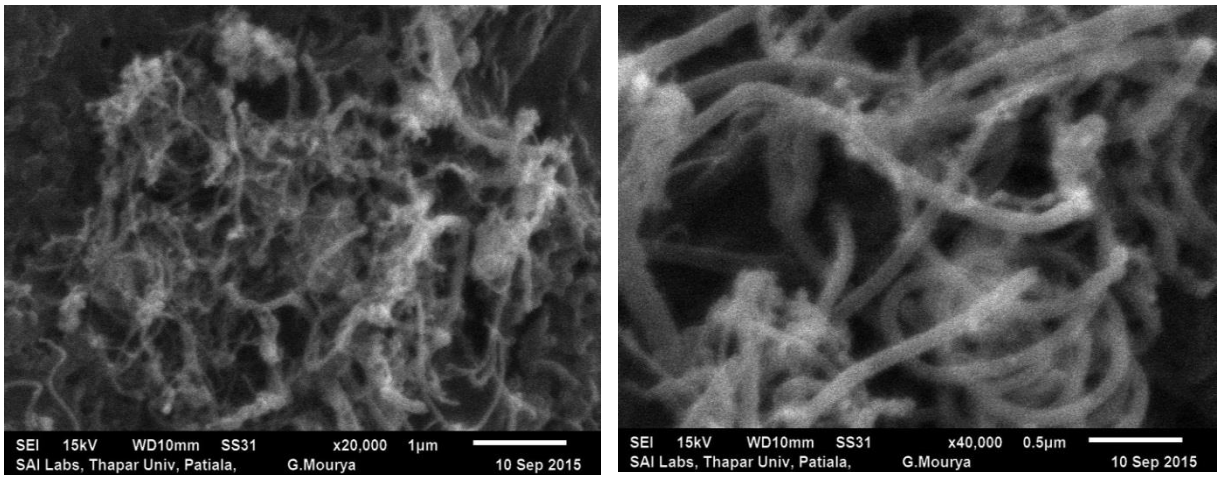

(a) (b)

Figure 3.5: (a& b) SEM image of MWCNT

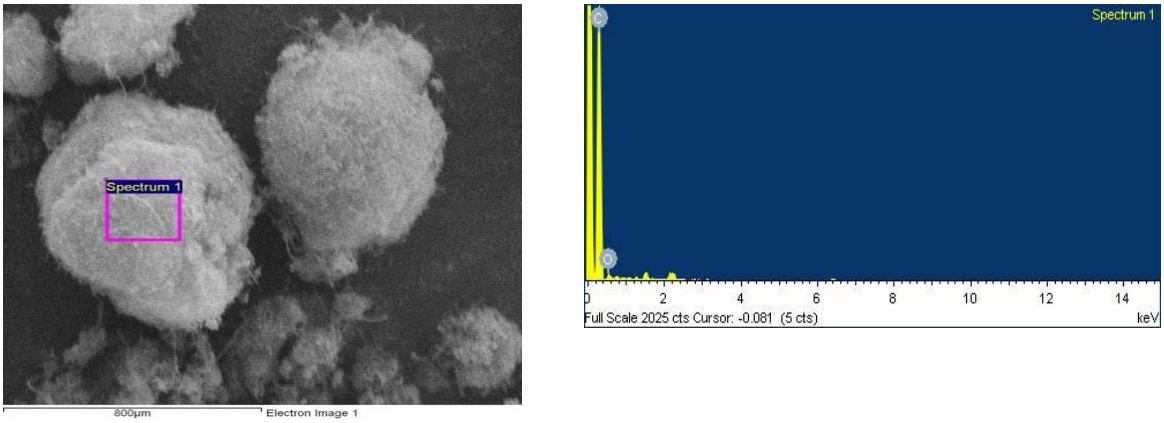

(a) (b)

Figure 3.6: (a& b) EDS spectra of MWCNT

3.3 PREPARATION OF NANOFLUIDS

Nanofluids can be produced either by one step method or two step method as studied in the literature. The main objective of thesis is to prepare the nanofluids of various concentration ranges from 0.1 % to 5 % by volume which can easily achieved by two step method.

Methodology followed for the preparation of nanofluids is as follow:

1. Alumina nanoparticles are directly dispersed in the base fluids without any surfactant added.
2. Stable CuO nanofluids are prepared with the help of surfactant. From the literature, various surfactants are listed but SDS is a more suitable surfactant for CuO nanofluid which helps the CuO nanoparticles to remain suspended in base fluids for longer time.

For uniform and stable dispersion of CuO nanoparticles, 0.2 wt % SDS was added in the base fluids [52].

3. Due to highly hydrophobic nature of MWCNT, these nanoparticles are not suspended in the base fluids directly. To make stable and homogeneous suspensions of MWCNT in base fluids, a shift is required from hydrophobic nature to hydrophilic nature either by functionalization or by adding surfactant. For stable uniform dispersion of MWCNT nanofluids, 0.25 wt % of GA was added in the base fluids as suggested by Bandyopadhyaya et al. [155] and Garg et al. [88].

After dispersion of nanoparticles in the base fluids, proper stirring was carried out through magnetic stirrer for better dispersion. Afterwards, ultrasonication technique is used for the proper dispersion of nanoparticles in base fluids at high frequency which helps in the breaking of highly aggregated nanoparticles in the base fluids. This is done by ultrasonic cleaner (model: 3800) with an amplitude of 40 kHz which was procured from Branson Ultrasonics, USA (Figure 3.7). From the literature, it was clear that there is no fixed time for sonication to make stable nanosuspensions. In the present work, sonication time is optimized on the basis of thermal conductivity values. For this, thermal conductivity measurements of nanofluids were performed after sonication of 40 min, 60 min, 80 min, and 100 min.

Figure 3.7: Ultrasonicator

Thermal conductivity is a main property of fluid as it plays a significant role for predicting the thermal performance of fluids. In the present work, thermal conductivity of nanofluids was measured by KD2 pro Thermal Property Analyzer (Decagon Inc., Pullman, WA, USA.)

using a KS-1 single-needle (60 mm long and 1.3 mm diameter) sensor shown in Figure 3.8. KD2 Pro measured the thermal conductivity in the range of 0.2 to 2.00 W/(m.°C) with an accuracy of ± 5 %. Calibration of equipment was carried out by glycerol provided along with the KD2 pro equipment with an accuracy of ± 1.5% which is under acceptable range to carry out the experiments. This property can be used to observe the stability of nanofluids as well as to optimize the sonication time.

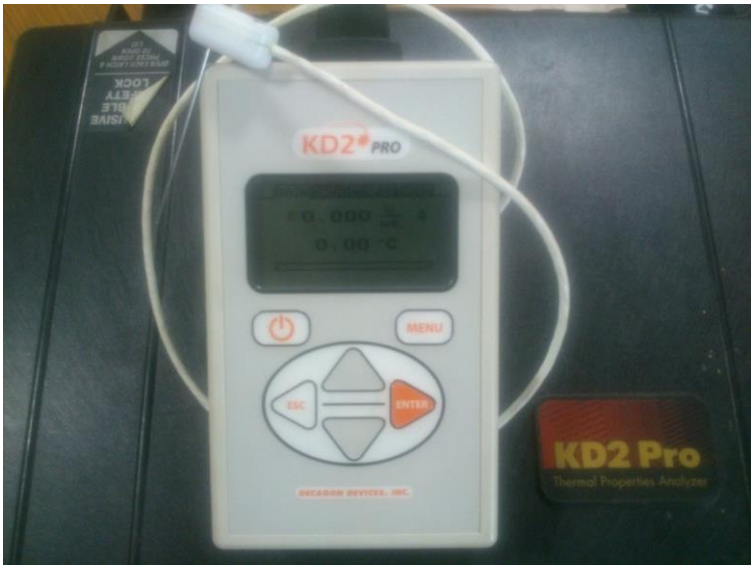

Figure 3.8: Thermal Property analyzer with KS-1 single-needle

It can be clearly observed from Figure 3.9 that there is no appreciable enhancement in the thermal conductivity of the nanofluids after sonication of 40 min because the highly aggregated nanoparticles were not fully dispersed in the base fluids. With increase in sonication time, stability and thermal conductivity of nanosuspensions is improved as it helps in the uniform dispersion of nanoparticles in the fluids. Nanofluids show maximum enhancement in thermal conductivity after sonication of 80 min when compared with the results of 40 min, 60 min and 100 min. So, it can be concluded that full stable dispersion of nanoparticles (Al_2O_3, CuO and MWCNT) in the W or W/EG mixtures takes place with the ultrasonic vibration for 80 min. After 80 min, thermal conductivity of nanofluids start declined. This is due to the high energy sonication for longer time which results into nanoparticles defects [156]. So, in order to make stable nanofluid, sonication time is optimized for 80 min for all nanoparticles and base fluids combination used in present study.

A similar trend has been observed by Khedkar et al. [91] with CuO-water nanofluids. Moreover, Sundar et al. [41] reported two hour sonication time for the preparation of Al_2O_3-

W/EG mixtures nanofluids. The two hour sonication time is a longer time in comparison with present study as well as Khedkar et al. [91] study. More sonication time reduces the stability of nanofluids as it retards the repulsive forces between nanoparticles [41]. So, it is concluded that nanofluids became more stable and give high thermal conductivity enhancement with the sonication of 80 min.

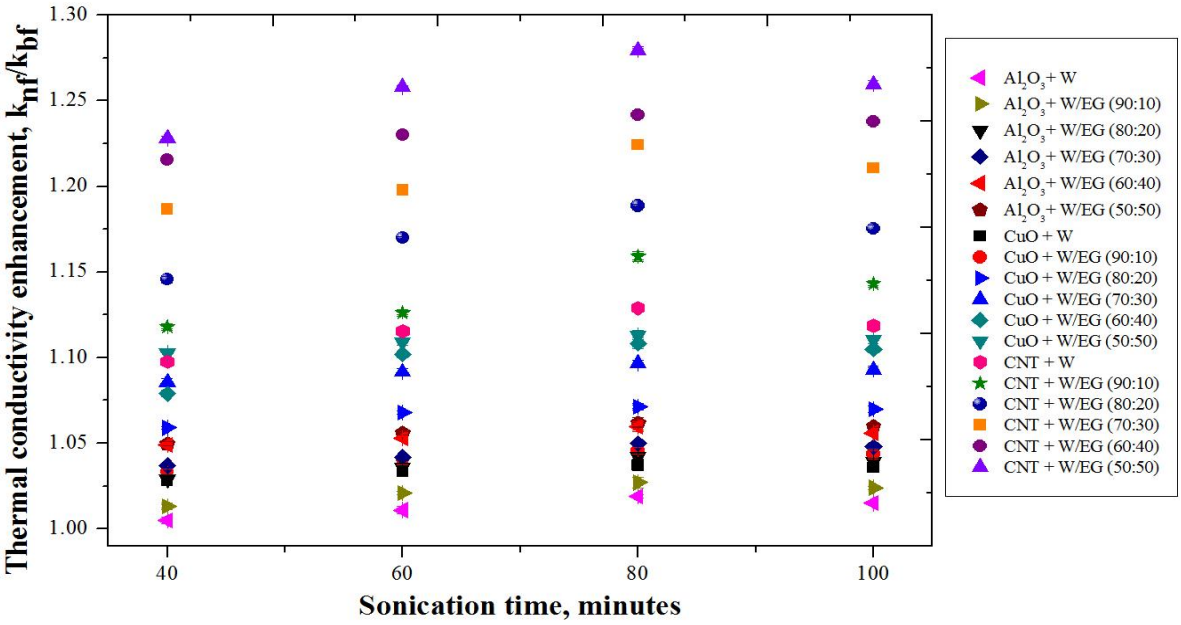

Figure 3.9: Optimization of sonication time

3.4 STABILITY MONITORING METHOD

Stability of nanofluids is extremely important to study so that nanofluids can be used in different applications. In this work, the stability of nanofluids was concluded by absorbance, thermal conductivity and zeta potential measurements as well as by visual observation. For the stability analysis, experiments were carried out for 0.1 vol % of nanoparticles (Al_2O_3, CuO and MWCNT) concentration with different base fluids such as W and W/EG (90:10, 80:20, 70:30, 60:40, and 50:50).

The nanofluids dispersion stability were observed visually and recorded by a camera. This process was repeated till the sedimentation of nanoparticles was observed at the bottom of the glass tube. As stability cannot be concluded on the basis of visual analysis solely; therefore; UV spectrophotometer technique was used to quantitatively measure the dispersion stability of nanofluids by monitoring the absorbance of nanofluids. The absorbency of nanofluids with W or W/EG mixtures was determined by UV-Vis spectrophotometer (Model: DR5000) in ultra-violet region at a wavelength of 238 nm for alumina, 270 nm for CuO nanofluids and

253 nm for MWCNT facility available in the Department of Chemical Engineering, Thapar University, Patiala, Punjab, India. The stability of the prepared nanofluids was monitored till the absorbance value show a relative error of $\geq \pm 0.01$ with reference to initial reading.

Further, thermal conductivity measurements with time were carried out to ensure the stability of the nanofluids. This was done till the thermal conductivity value show a relative error of $\geq \pm 0.02$ w.r.t initial reading. Thermal conductivity of the nanofluids might be decreased due to nanoparticles agglomeration.

At last, Zeta potential measurements were carried out by Brookhaven 90 plus particle size analyzer with PALS zeta potential software in the School of Physics and Material Science, Thapar University, Patiala, Punjab, India. This is related to the stability of colloidal dispersions by indicating the degree of repulsion between adjacent and similarly charged particles in a fluid. Degree of repulsion increases if zeta potential of dispersant is having high value which leads to good stability. Colloids with good stability show zeta potential value of 40 mV to 60 mV while suspensions with zeta potential value in the range of 30 mV to 40 mV are physically stable nanofluids. Moreover, nanofluids with limited stability show zeta potential value of less than 20 mV while those having zeta potential less than 5 mV indicate agglomeration [57, 157]. Further results were compared with these interpretations of Yu and Xie [57] and Mahbubul et al. [157].

3.4.1 Stability of CuO nanofluids

Stability of nanofluids can be concluded on the basis of characterization results shown in Figure 3.10-3.13. It is interpreted that CuO-W nanofluids is a least stable nanofluid and nanoparticles start settle down just after 2 days of their preparation as depicted from Figure 3.10-3.13. Settling of CuO nanoparticles in the base fluids after 4 days of preparation had clearly observed in Figure 3.10. In addition to this, absorbance and thermal conductivity measurements shown that CuO-W/EG (50:50) nanofluids were also not too good in stability. Maximum stability of 4 days i.e. 108 h was observed for CuO-W/EG (50:50) nanofluids. CuO-W/EG (90:10) nanofluids were stable up to 60 h while CuO-W/EG (80:20) was stable for 3 days i.e. 72 h. Moreover, CuO-W/EG (70:30) nanofluids lose their stability after 84 h and CuO-W/EG (60:40) nanofluids remain stable for 96 h (Figure 3.11-3.12). It is clearly analyzed from zeta potential analysis that CuO nanoparticles start settling down after 2-4 days lying with a limited stability.

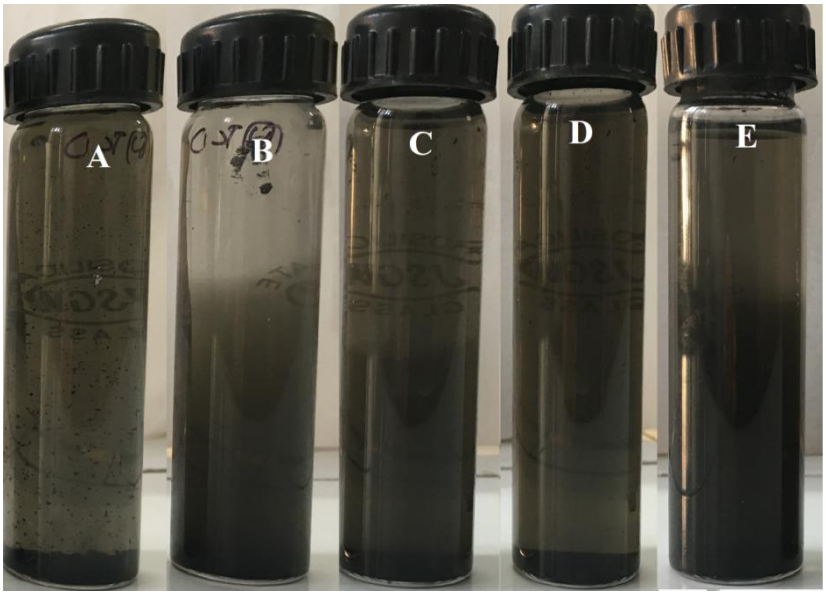

Figure 3.10: Visual observation of CuO nanofluids after 4 days

SAMPLE: A = W, B = W/EG (90:10), C = W/EG (80:20), D = W/EG (70:30), E = W/EG (60:40) and F = W/EG (50:50)

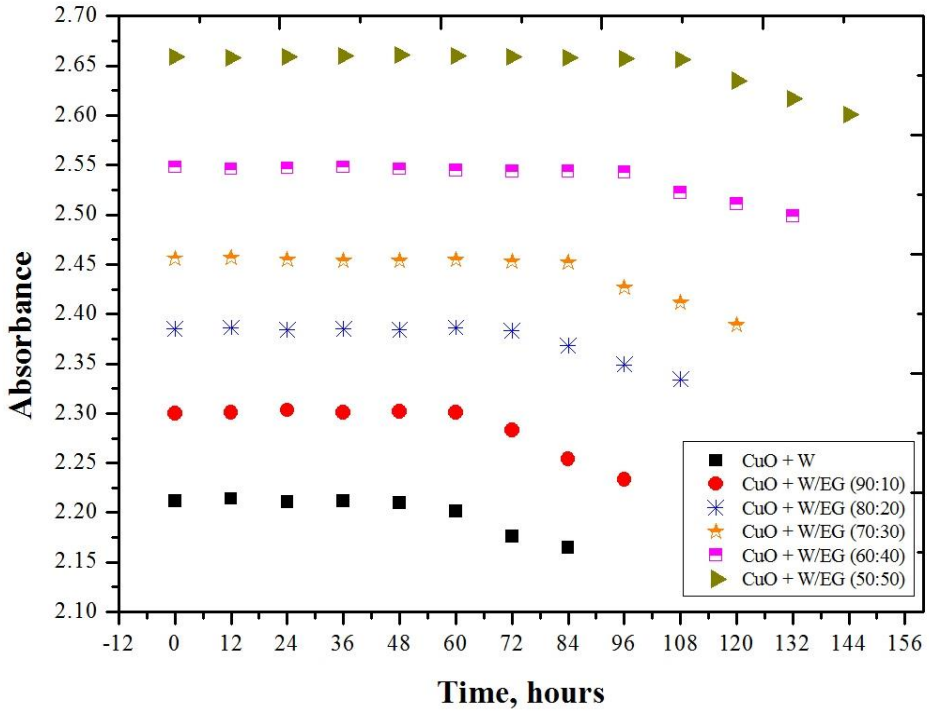

Figure 3.11: Absorbance measurements of CuO nanofluids at λ_{max} 270 nm

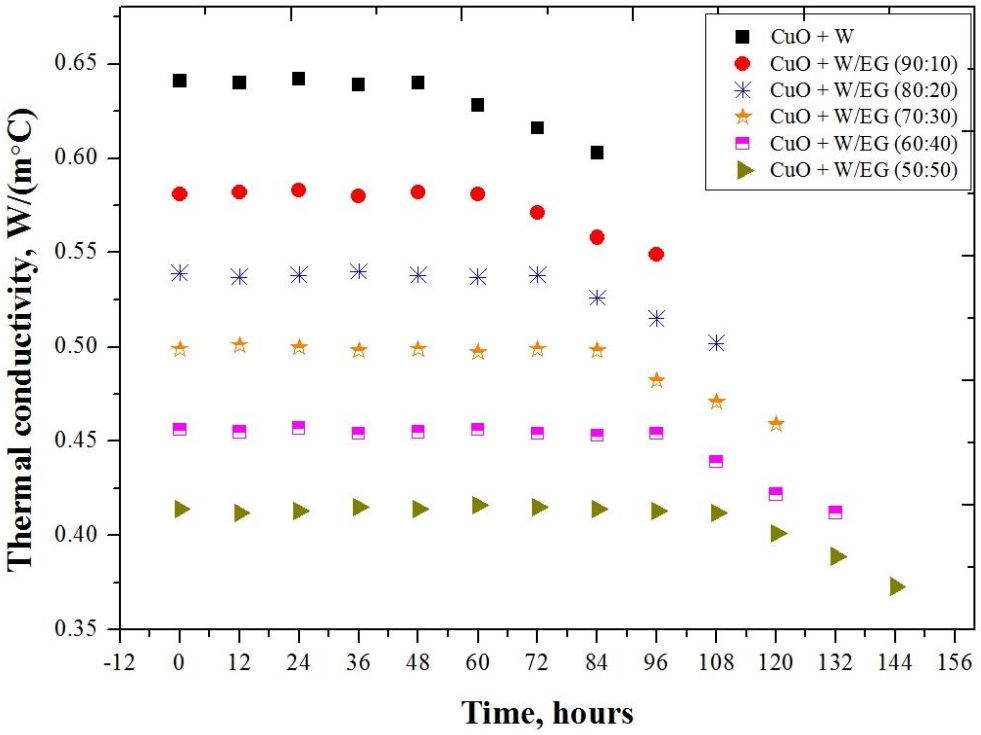

Figure 3.12: Thermal conductivity measurements of CuO nanofluids

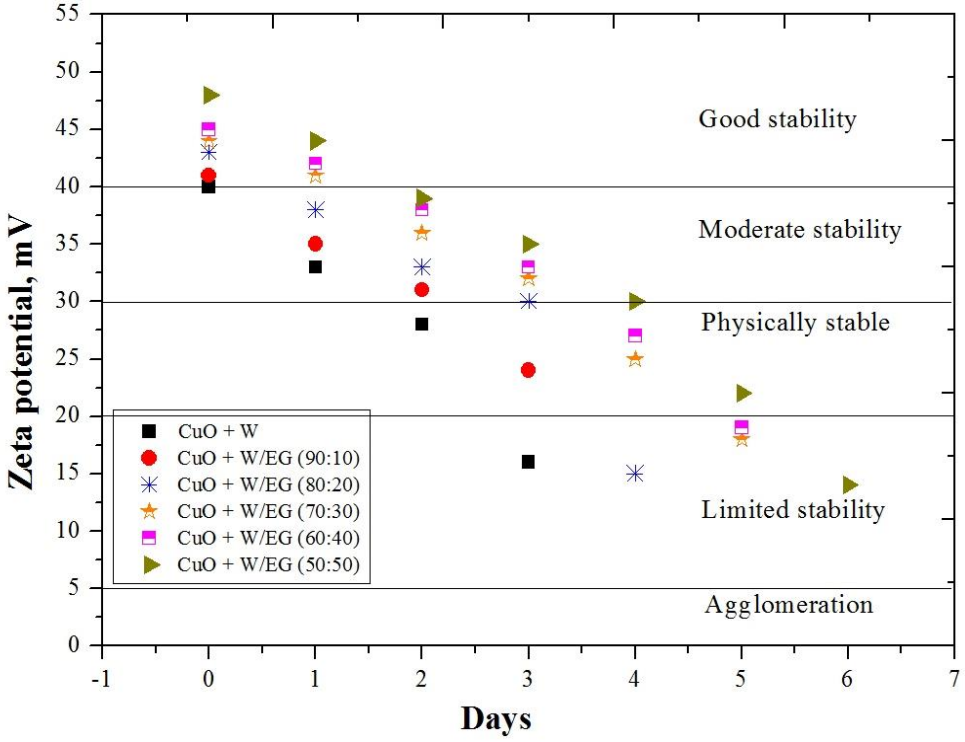

Figure 3.13: Zeta potential measurements of CuO nanofluids

3.4.2 Stability of Alumina nanofluids

Alumina nanofluids are comparatively more stable than CuO nanofluids. From Figure 3.14-3.17, it can be observed that alumina-W nanofluid is stable for 19 days while alumina with W/EG (50:50) base fluid is most stable nanofluid for 28 days without any nanoparticles agglomeration. It can be clearly displayed in Figure 3.15-3.17 that Alumina-W/EG (90:10) nanofluids were stable for 20 days and stability increases to 23 days with Alumina-W/EG (80:20) nanofluids. Moreover, alumina nanoparticles remains uniform suspended for 25 days in W/EG (70:30) base fluids and 26 days with W/EG (60:40) base fluids. From the zeta potential analysis and visual analysis, it is clear that alumina nanofluids are physically stable nanofluids for 28 days without any nanoparticles sedimentation at the bottom (Figure 3.14 and Figure 3.17).

Figure 3.14: Visual observation of Alumina nanofluids after 28 days

SAMPLE: A = W, B = W/EG (90:10), C = W/EG (80:20), D = W/EG (70:30), E = W/EG (60:40) and F = W/EG (50:50)

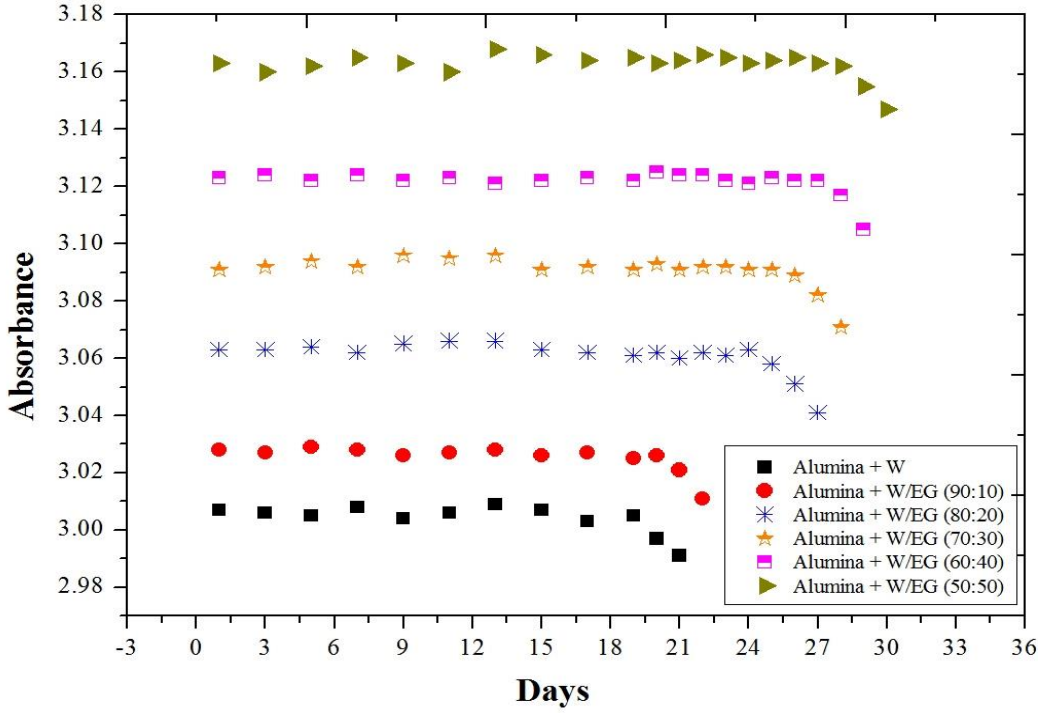

Figure 3.15: Absorbance measurements of alumina nanofluids at λ_{max} 238 nm

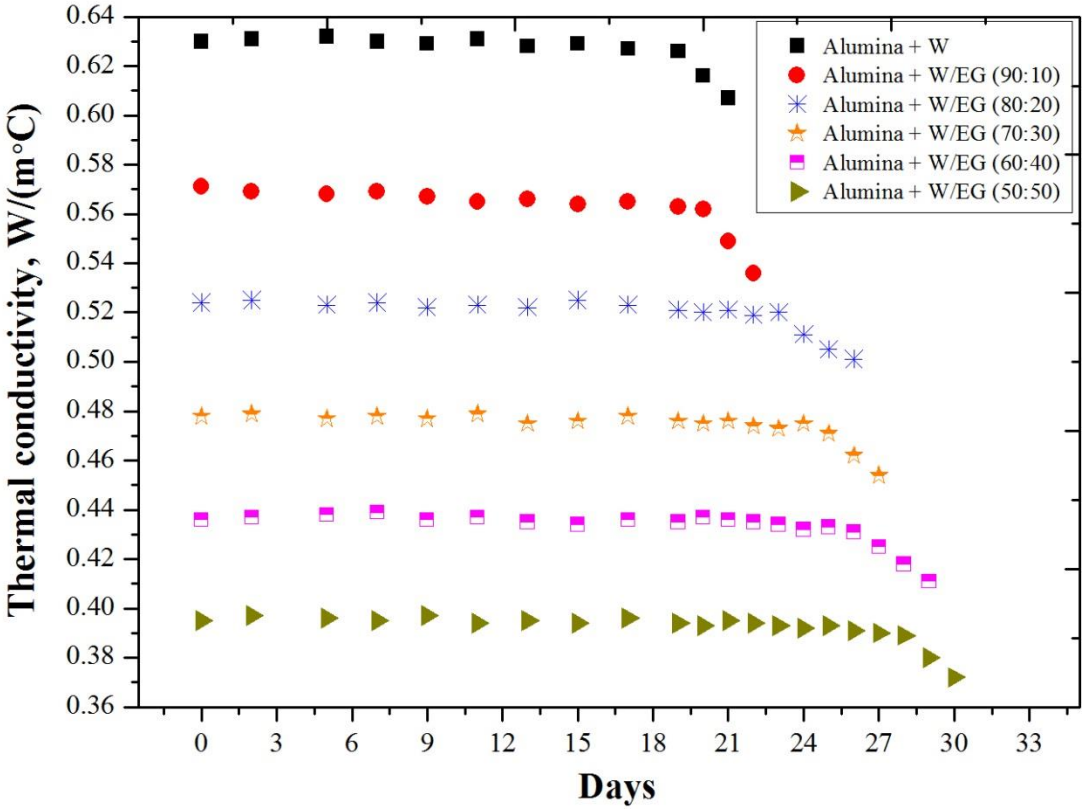

Figure 3.16: Thermal conductivity measurements of alumina nanofluids

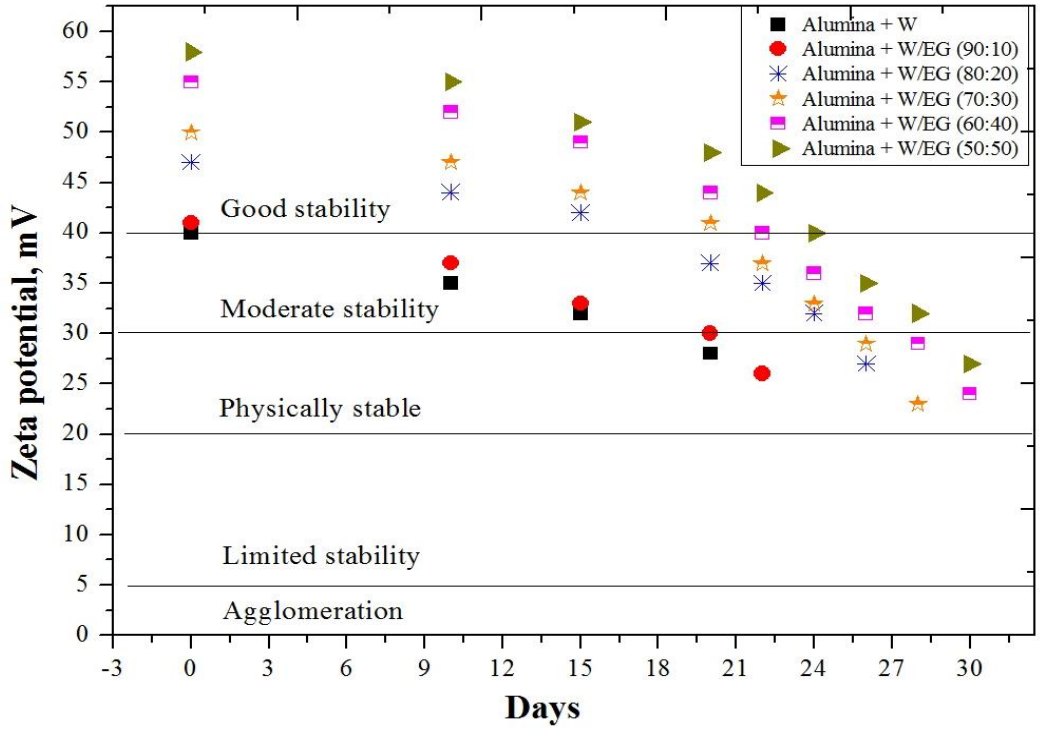

Figure 3.17: Zeta potential measurements of alumina nanofluids

3.4.3 Stability of MWCNT nanofluids

It can be observed that MWCNT nanofluids shows maximum stability in comparison with alumina nanofluids and CuO nanofluids as shown in Figure 3.18-3.21. It is found that MWCNT-W nanofluids show stability for 24 days while MWCNT-W/EG (80:20) nanofluids are stable for 28 days. Moreover, MWCNT-W/EG (70:30) nanofluids are stable for 30 days and with increase in EG ratio in water, the stability of MWCNT-W/EG (60:40) nanofluid increases for 35 days. Maximum stability of 36 days was obtained for MWCNT-W/EG (50:50) nanofluids with no particle sedimentation.

From zeta potential analysis, it can also interpreted that water based MWCNT nanofluid is physically stable till 26 days while MWCNT nanofluid with W/EG (50:50) is physically stable for 39 days. No agglomeration or sedimentation of nanotubes is observed in MWCNT base nanofluid as shown in Figure 3.18 after 36 days of preparation.

Figure 3.18: Visual observation of MWCNT nanofluids after 36 days

SAMPLE: A = W, B = W/EG (90:10), C = W/EG (80:20), D = W/EG (70:30), E = W/EG (60:40) and F = W/EG (50:50)

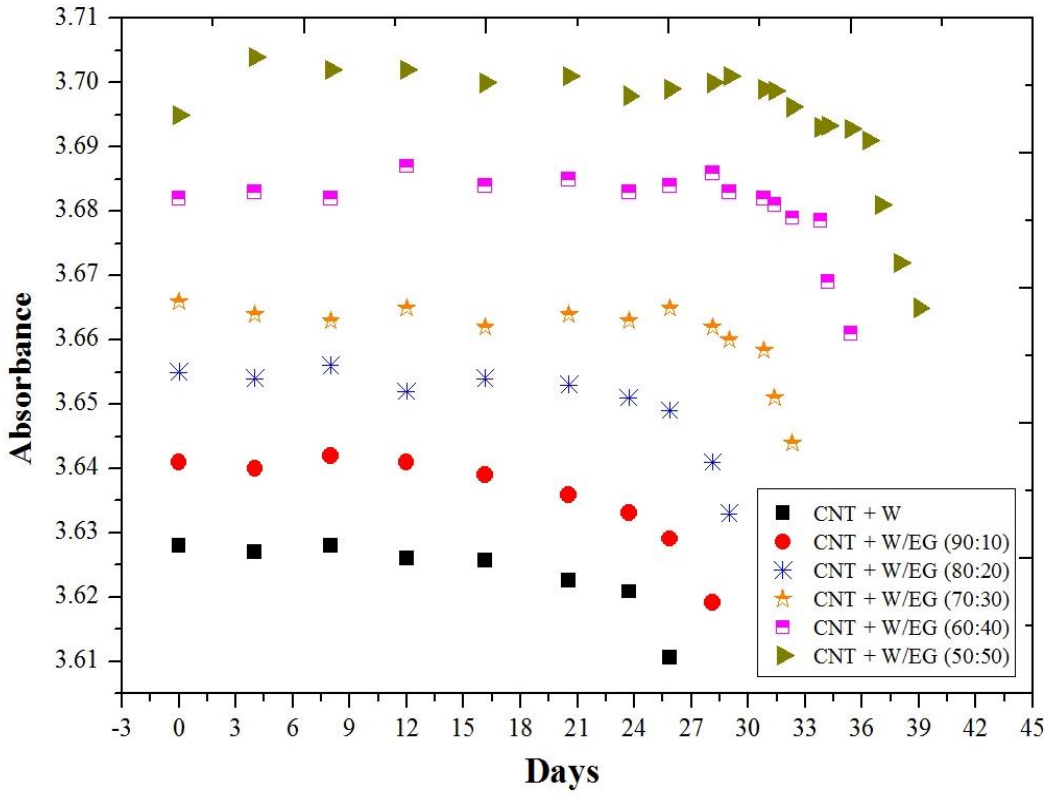

Figure 3.19: Absorbance measurements of MWCNT nanofluids at λ_{max} 253 nm

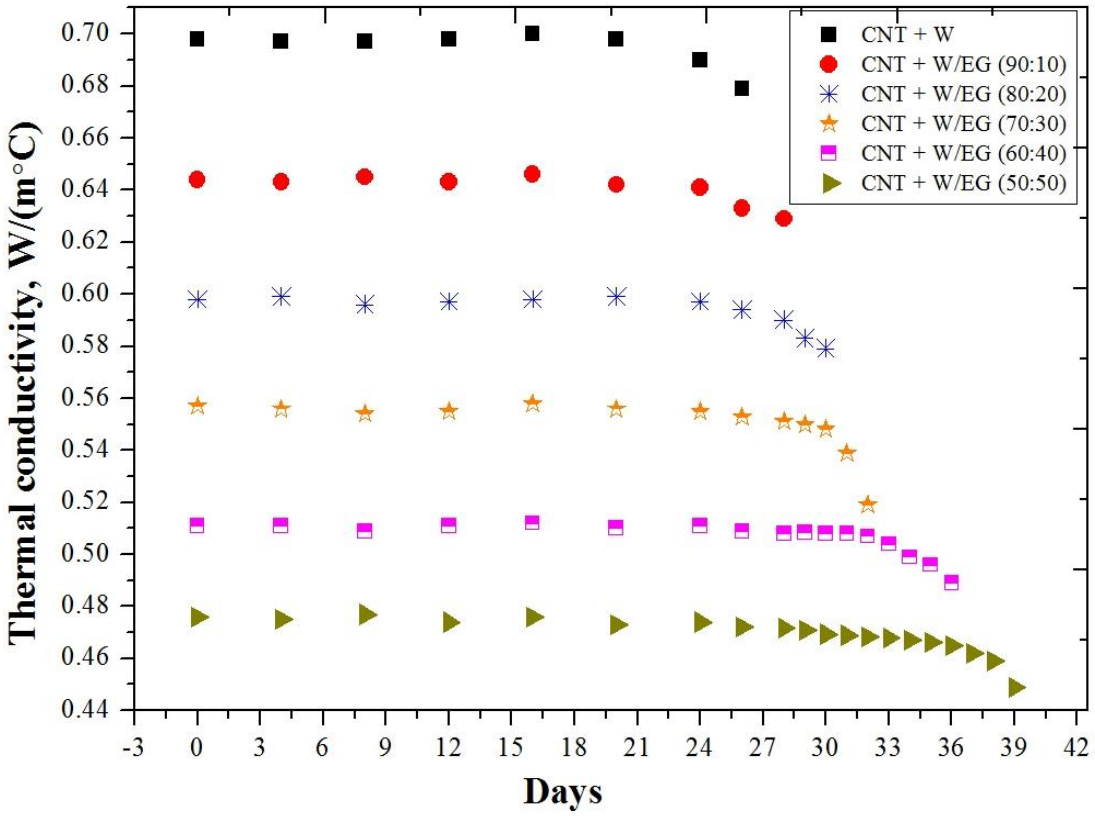

Figure 3.20: Thermal conductivity measurements of MWCNT nanofluids

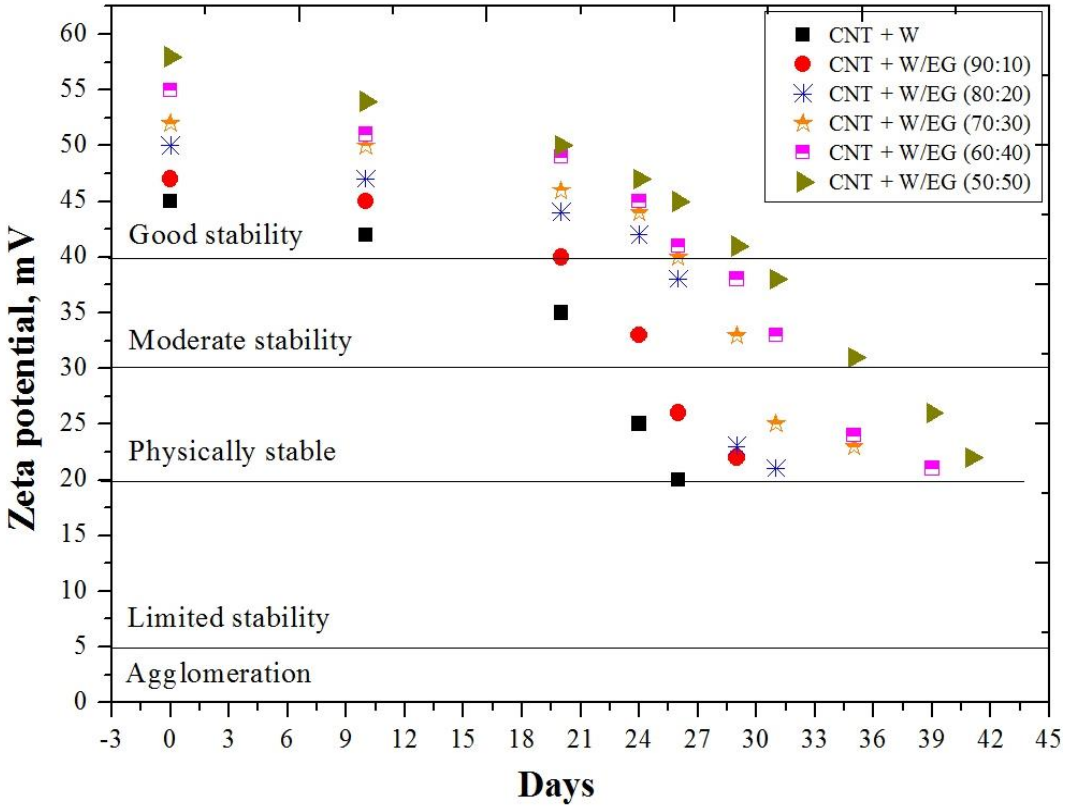

Figure 3.21: Zeta potential measurements of MWCNT nanofluids

From all the analysis (Figure 3.10-3.21), it can be concluded that with increase in the ratio of ethylene glycol in water, nanoparticles disperse more uniformly in their respective base fluids. Nanofluids with higher ratio of ethylene glycol in water such as W/EG (50:50) shows more stability in comparison with water. A MWCNT-W/EG (50:50) nanofluid is the most stable nanofluids for 36 days. As ethylene glycol itself acts as a stabilizer in base fluids which makes the nanofluid more convenient to use in the industrial sectors that require EG as an antifreeze protection for heat transfer applications.

3.5 CLOSURE

In the present work, detailed studies on the preparation of nanofluids are carried out. Alumina nanoparticles are uniformly dispersed in base fluids without surfactant while MWCNT and CuO nanoparticles required SDS and GA surfactant for their uniform dispersion in the base fluids. Further, nanofluids are stabilized by optimizing the sonication time to 80 min. As the stability is an important concern for any nanofluids, so it is determined by measured the thermal conductivity, absorbance and zeta potential of nanofluids with days. Maximum stability was achieved for MWCNT nanofluids. Moreover, stability was also affected with the change in base fluids and the results showed that W/EG (50:50) base fluids enhanced the stability of nanosuspensions either any kind of nanoparticles used. After carrying out the preparation and stability analysis of nanofluids, next step is to carry out the thermophysical properties measurements at different temperatures in the ranges from 20 °C to 80 °C.

CHAPTER-4
THERMOPHYSICAL PROPERTIES OF NANOFLUIDS

After preparation of nanofluids, the next step is to determine the thermophysical properties of the prepared nanosuspensions. All the techniques used for the measurements of these properties are discussed. The thermophysical properties such as viscosity, density and thermal conductivity are measured at different temperatures ranges from 20 ºC to 70 ºC experimentally as above 70 ºC, nanofluids stability declined due to the nanoparticles agglomeration. A general correlation is also developed from the experimental measurements in terms of concentration, base fluids and temperature. The specific heat of nanofluids is calculated from the theoretical model.

4.1 THERMAL CONDUCTIVITY OF NANOFLUIDS

Present work used Thermal property analyzer i.e. KD2 pro equipment for measuring the thermal conductivity. In chapter 3, thermal conductivity of nanofluids was measured to optimize the sonication time as well as to check the stability of nanofluids. The technique used to calculate the thermal conductivity was already discussed. The KS-1 sensor pertain a lesser extent of heat to the single needle that aids to avoid the free convection in fluid. Thermal conductivity was measured for all the samples at different temperature ranges from 20 ºC to 70 ºC with the interval of 10 ºC. This temperature is maintained in water bath in which water circulation is done continuously and then sample is immersed in a water circulating bath as shown in Figure 4.1.

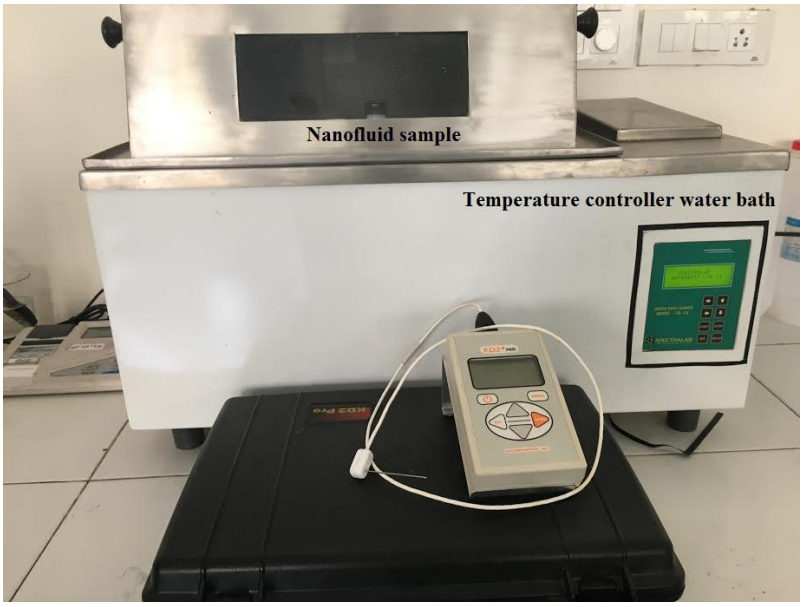

Figure 4.1: Thermal Property analyzer with temperature controller water bath

Firstly, thermal conductivity measurements were carried out for all the base fluids used for the nanofluids preparation such as W and W/EG mixtures. To check the consistency and accuracy of experimental methodology followed for measuring the thermophysical properties of nanofluids, experimentally measured data were compared with American Society of Heating, Refrigerating and Air Conditioning Engineers standards revealed in Table 4.1 (ASHRAE 2006). These experimental measurements confirmed good conformity with the ASHRAE standard values as ± 2 % deviations observed for all measurements of thermal conductivity with reference data (Figure 4.2).

Table 4.1: Thermal conductivity values as per ASHRAE standards, W/(m.°C)

Temperature, °C	W	W/EG (90:10)	W/EG (80:20)	W:EG (70:30)	W/EG (60:40)	W:EG (50:50)
20	0.59	0.542	0.492	0.445	0.404	0.365
30	0.618	0.555	0.503	0.455	0.411	0.372
40	0.635	0.567	0.514	0.463	0.418	0.379
50	0.648	0.578	0.521	0.470	0.424	0.382
60	0.659	0.590	0.526	0.474	0.427	0.386
70	0.668	0.599	0.533	0.479	0.432	0.389

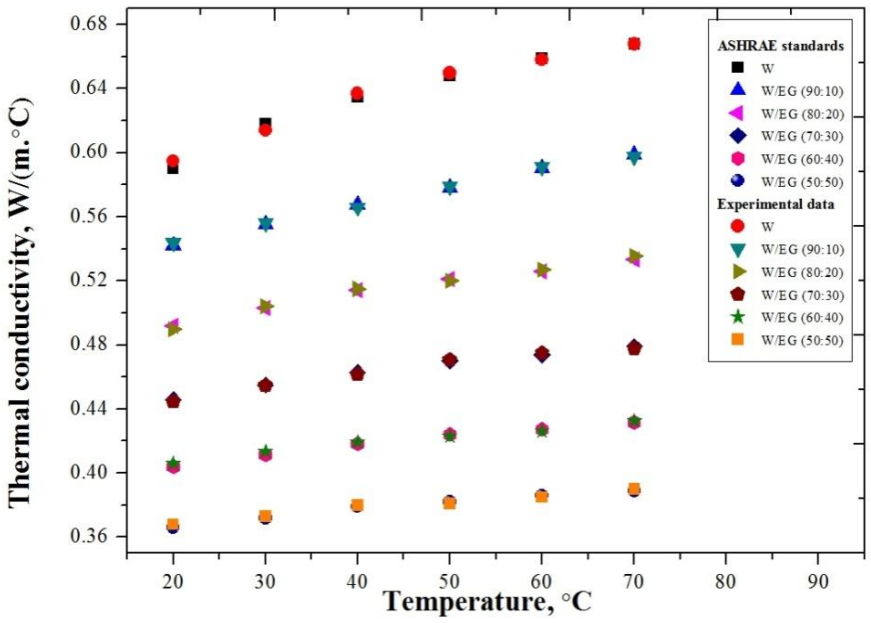

Figure 4.2: Experimental thermal conductivity data comparison with ASHRAE standards

After calibration, introduce the nanofluids sample for measuring the thermal conductivity. According to Figure 4.3-4.6, it can be concluded that enhancement in thermal conductivity influenced by the type of nanoparticles, type of base fluids, nanoparticles concentration as well as temperature which was same as observed by various researchers [61-78]. Thermal conductivity increases by rise in nanoparticle concentration as well as temperature. Table 4.2 shows the percentage enhancement in thermal conductivity of different nanoparticles with different base fluids for temperature ranges from 20 ºC to 70 ºC. It shows that thermal conductivity enhancement increases by rise in nanoparticle concentration, moreover, type of base fluids, type of nanoparticles and temperature play an imperative role in thermal conductivity enhancement.

4.1.1 Effect of different type of nanoparticles

Extreme enhancement in thermal conductivity was observed for MWCNT based nanofluids in comparison with alumina and CuO nanofluids. This enhancement is due to the Brownian motion of nanoparticles as well as due to higher thermal conductivity of nanoparticles (MWCNT = 2000-3000 W/m.K) which get dispersed in low thermal conductivity fluid to improve overall conductivity. Alumina - W nanofluids shows the least enhancement of 10 % while CuO-W nanofluids have 11 % enhancement for 5 vol % nanoparticles at 30 ºC. These results are in agreement with the results of Lee et al. [61] as they also observed that CuO nanofluids have higher enhancement than alumina nanofluids as tabulated in Table 2.2.

4.1.2 Effect of different type of base fluids

Irrespective of this, experimental findings in terms of base fluids comparison confirm that nanoparticles with base fluid W/EG (50:50) contributes maximum enhancement in thermal conductivity while water base fluids shows the least enhancement. The same trend in the thermal conductivity behavior is observed by various researchers [45, 47, 62, 71, 89, 97]. From these studies it can be concluded that the enhancement is due to nanoparticles Brownian motion within the base fluids resulting from the collision of particles. More rapid collision results more Brownian motion which helps to enhance the thermal conductivity. From Chapter 3, it can also interpreted that with increases the EG fraction in water, stability of nanofluids rises. This reason may also contribute for appreciable thermal conductivity enhancement observed with W/EG (50:50) base fluids.

4.1.3 Effect of temperature

Thermal conductivity of any fluids is a function of temperature as it increases with increase in temperature but the thermal conductivity enhancement in nanofluids shows some unusual behavior with temperature. At 50 ºC, maximum enhancement was observed and beyond that enhancement decreases (Figure 4.6). It is also observed that at higher temperatures nanofluids become unstable due to nanoparticles agglomeration. This reason may also decline the percentage enhancement in thermal conductivity of nanofluids at higher temperature. But overall nanofluids thermal conductivity increases appreciably with increase in temperature which makes it seemly important in heat transfer applications.

Mathematical correlation equations are developed in terms of temperature, nanoparticle concentration and type of base fluids which shows a good fit of thermal conductivity data with experimental data with R^2 value is approximately 0.98 or above.

For alumina nanofluids

$$k = 0.6016226 + 0.0008969 \times T + 0.007895 \times C - 0.0051 \times WEG \quad (4.2)$$

For CuO nanofluids

$$k = 0.60568226 + 0.0008918 \times T + 0.0094104 \times C - 0.004801 \times WEG \quad (4.3)$$

For MWCNT nanofluids

$$k = 0.6480765 + 0.00108329 \times T + 0.020423 \times C - 0.0049797 \times WEG \quad (4.4)$$

where, k is the thermal conductivity in W/(m.ºC), T is the temperature in degree Celsius, C is the nanoparticles volume concentration and WEG is the ratio of ethylene glycol in water.

Table 4.2: Percentage enhancement in thermal conductivity for nanofluids

Thermal conductivity enhancement for nanoparticles concentration of 0.1 vol % and 5 vol %												
		Temperature, °C											
Nanoparticles	Base fluids	20		30		40		50		60		70	
		Volume concentration (%)											
		0.1%	5%	0.1%	5%	0.1%	5%	0.1%	5%	0.1%	5%	0.1%	5%
Alumina	W	1.8	10	1.9	10.4	2	9.3	2.6	10.3	2.1	9.1	1.8	8
	W/EG (90:10)	2.2	10.3	2.7	10.1	2.8	9.5	3	10.1	2.3	9.2	1.9	8.2
	W/EG (80:20)	3.4	9.5	4.1	10.5	4.6	10.6	4.7	10.7	4.2	10.2	3.5	9.4
	W/EG (70:30)	3.6	11.2	5	11.3	5.6	11.4	6	11.9	5.7	11.3	5.2	10.6
	W/EG (60:40)	4.7	11.4	6	11.8	6.4	12.1	6.6	12.5	6.2	12.3	5.8	12
	W/EG (50:50)	6	12	6.2	12.1	6.6	12.6	6.8	13.3	6.4	12.9	6.1	12.3
CuO	W	3.5	10.3	3.7	11	3.8	10.9	4	11.3	2.8	9.5	1.8	8.4
	W/EG (90:10)	3.9	11.4	4.6	11.6	4.8	11.8	4.9	11.9	4.1	11.1	3.8	10.7
	W/EG (80:20)	5.9	13.1	7.1	13.2	7.2	13.2	7.3	13.5	6.9	13.3	6	12.6
	W/EG (70:30)	8.5	16.1	9.6	16.7	9.7	17	10	17.2	9.9	16.8	9.3	16.2
	W/EG (60:40)	8.1	17.3	10.8	17.9	10.9	18.1	11	18.3	10.7	17.9	10.2	17.4
	W/EG (50:50)	10.7	18.6	11.2	19	11.3	19.3	11.8	19.6	11.4	19.2	11	18.8
MWCNT	W	9	25.2	12.9	26.4	13	28	13.3	25.6	11.7	24.2	10.5	23.2
	W/EG (90:10)	14.2	28.6	15.9	30.3	16	30.5	16.2	30.9	15	30	15.2	29.5
	W/EG (80:20)	16.7	31.7	18.8	33.1	18.9	33.4	19.2	33.6	19.6	33.3	18.1	32.7
	W/EG (70:30)	20.2	34.3	22.4	35	22.7	35.6	22.6	35.9	22.9	35.8	22.8	35
	W/EG (60:40)	22	36.4	24.2	37	25.6	37.2	27	37.4	26.4	37.1	26.2	36.8
	W/EG (50:50)	26	38.2	26.4	39.5	28	40.1	28.1	40.8	27.2	41.7	26.9	41.6

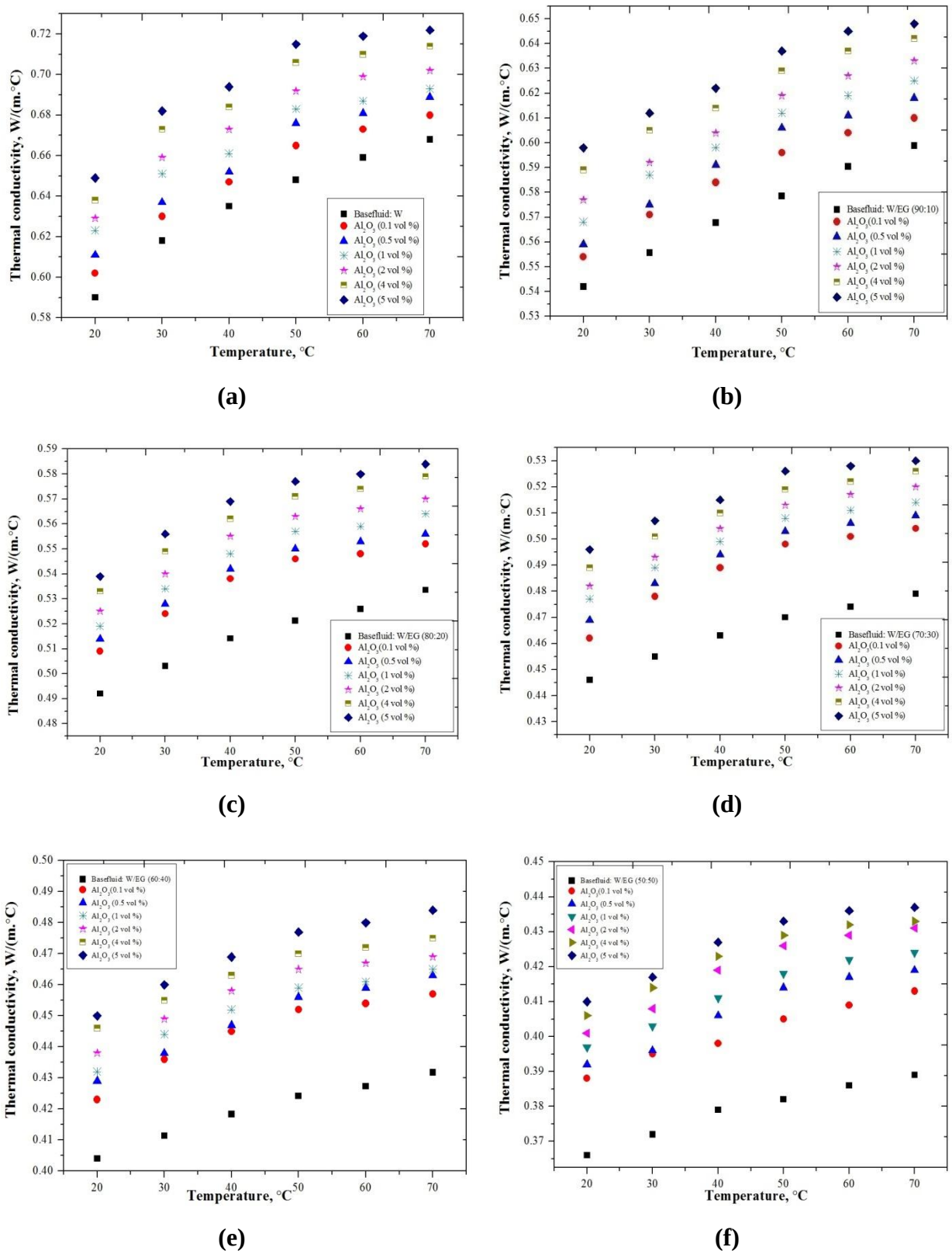

Figure 4.3: Thermal conductivity of alumina nanofluids at different temperature and different Base fluids such as (a) W (b) W/EG (90:10) (c) W/EG (80:20) (d) W/EG (70:30) (e) W/EG (60:40) (f) W/EG (50:50)

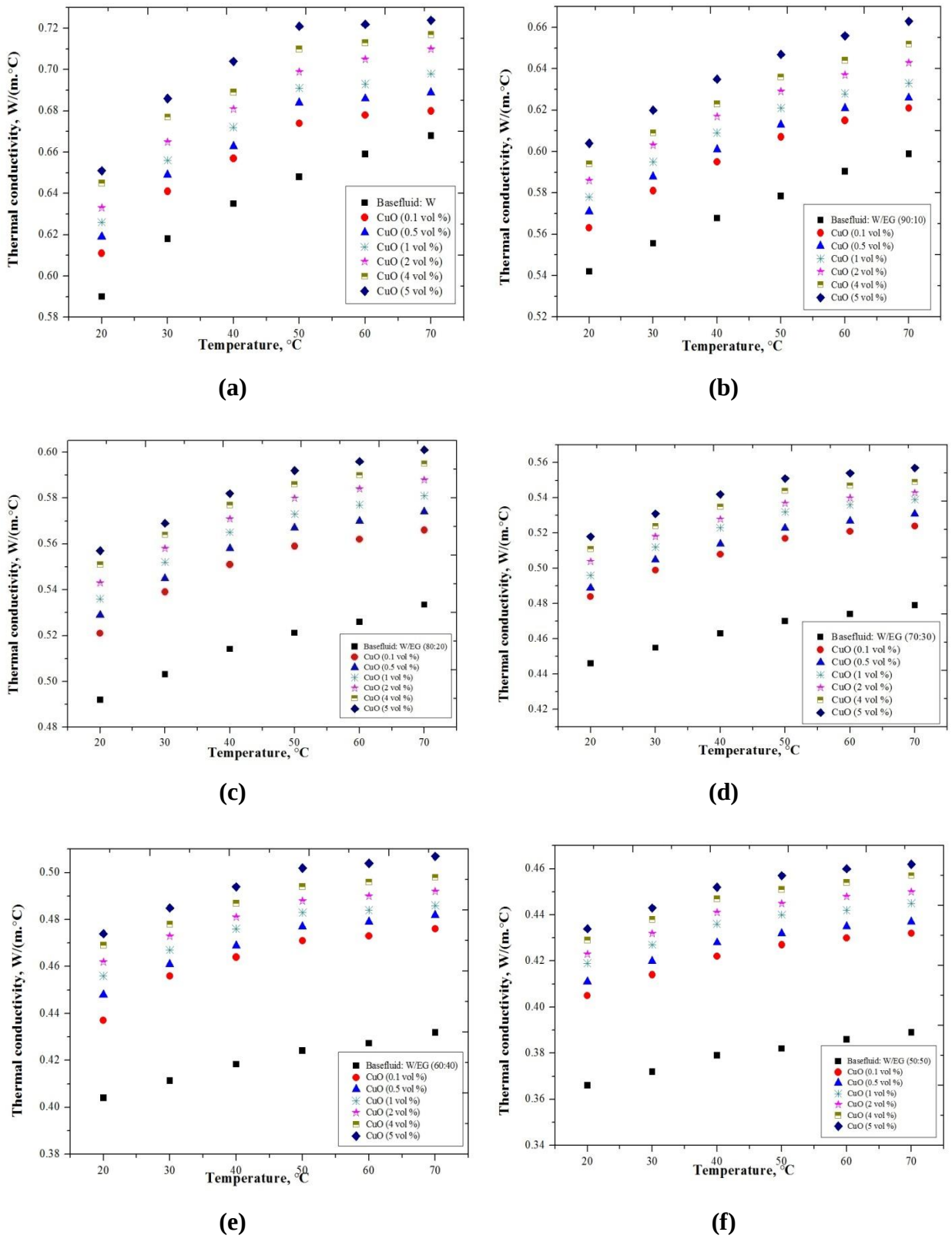

Figure 4.4: Thermal conductivity of CuO nanofluids at different temperature and different base fluids such as (a) W (b) W/EG (90:10) (c) W/EG (80:20) (d) W/EG (70:30) (e) W/EG (60:40) (f) W/EG (50:50)

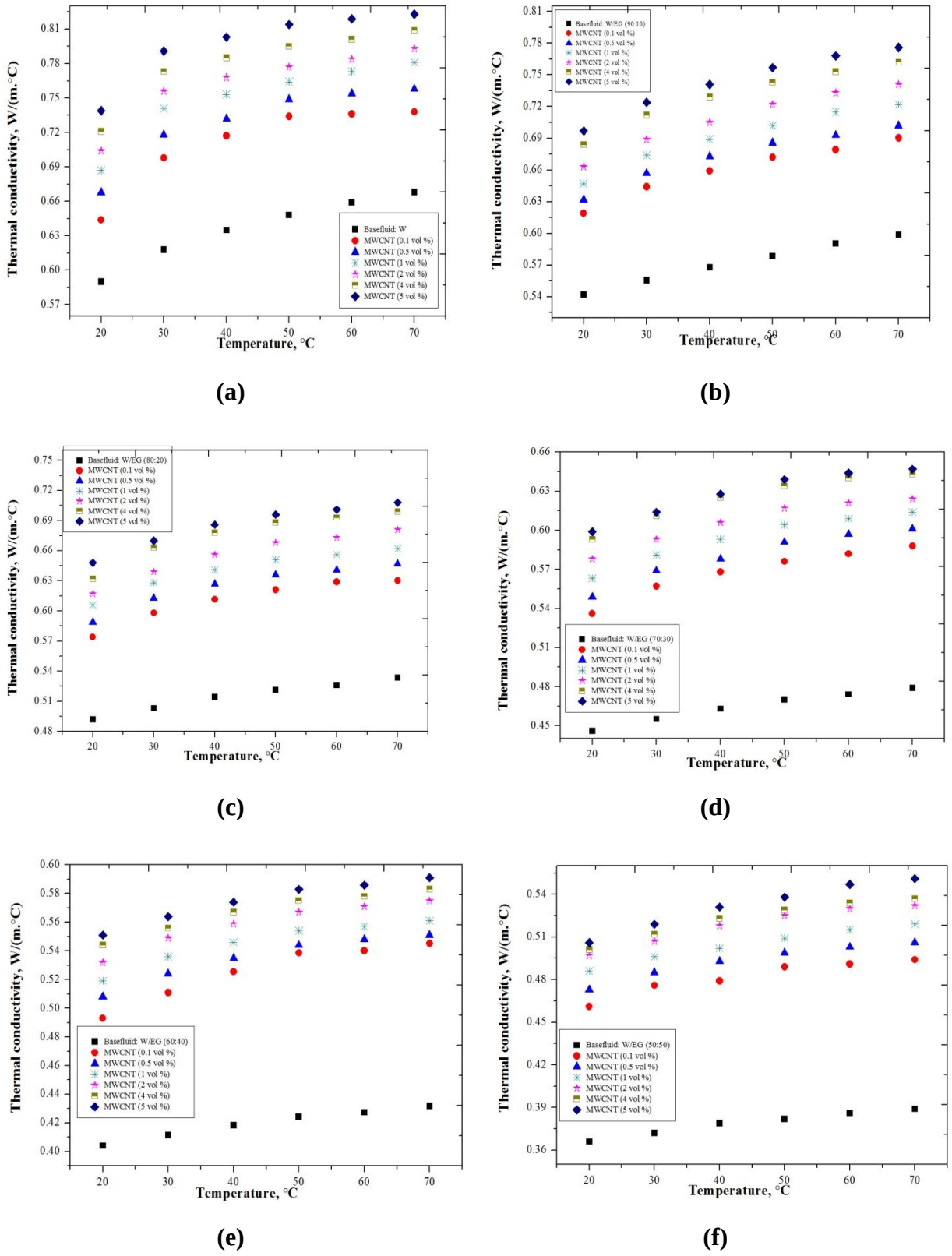

Figure 4.5: Thermal conductivity of MWCNT nanofluids at different temperature and different base fluids such as (a) W (b) W/EG (90:10) (c) W/EG (80:20) (d) W/EG (70:30) (e) W/EG (60:40) (f) W/EG (50:50)

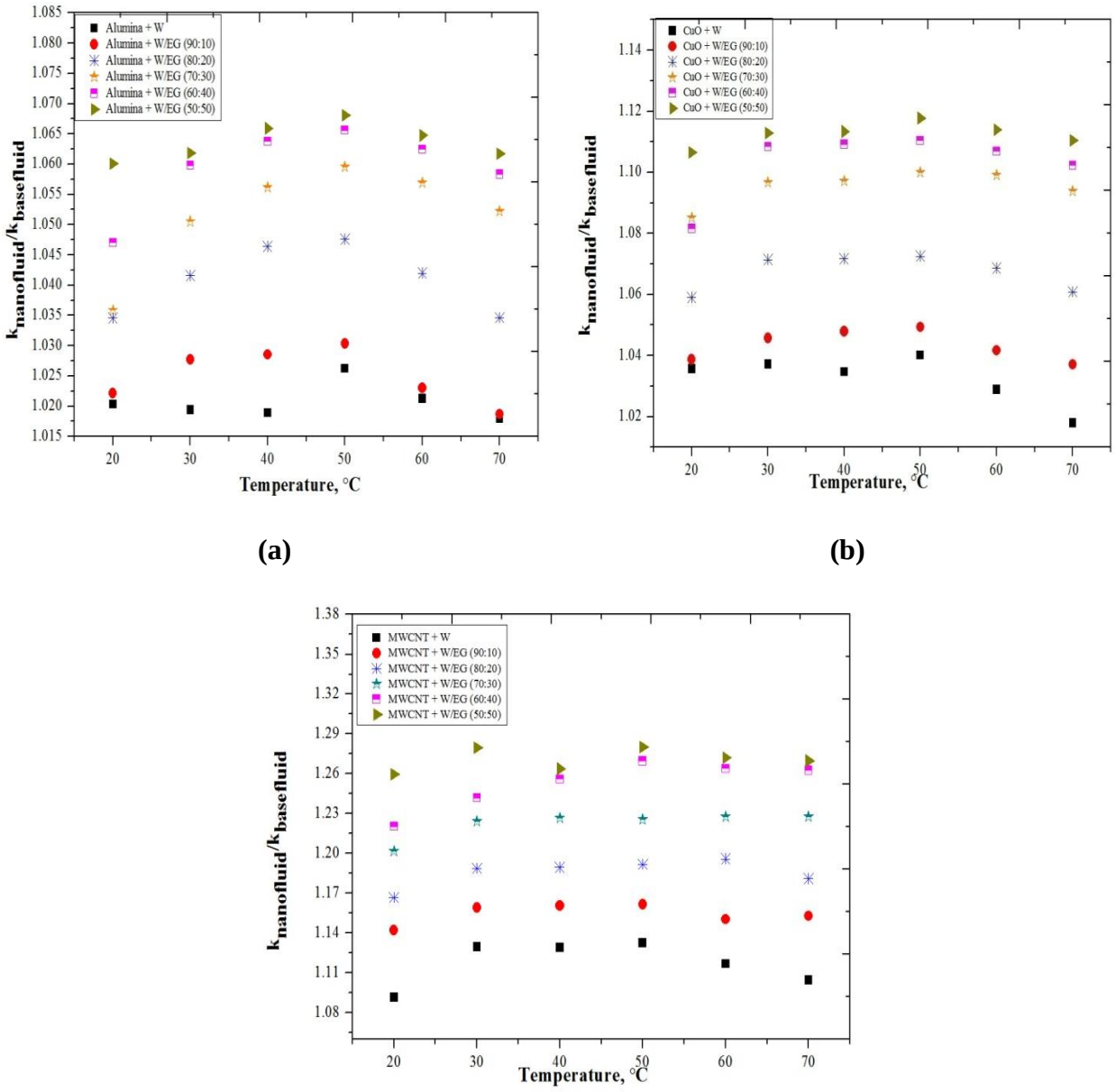

Figure 4.6: Enhancement in thermal conductivity of nanofluids (a) Alumina nanofluids (b) CuO nanofluids (c) MWCNT nanofluids

4.1.4 Comparison of Nanoparticles and Base fluids

From the Figure 4.7, it can be clearly depicted that MWCNT nanofluids have maximum enhancement in thermal conductivity in comparison with their respective base fluid. This is due to the higher thermal conductivity of MWCNT which dispersed in the base fluids. Moreover,

CuO nanofluids also have also shown an appreciable increase in thermal conductivity in comparison with the alumina nanofluids. With increase in the ethylene glycol ratio, the percentage enhancement also increases which is very important in the heat transfer applications.

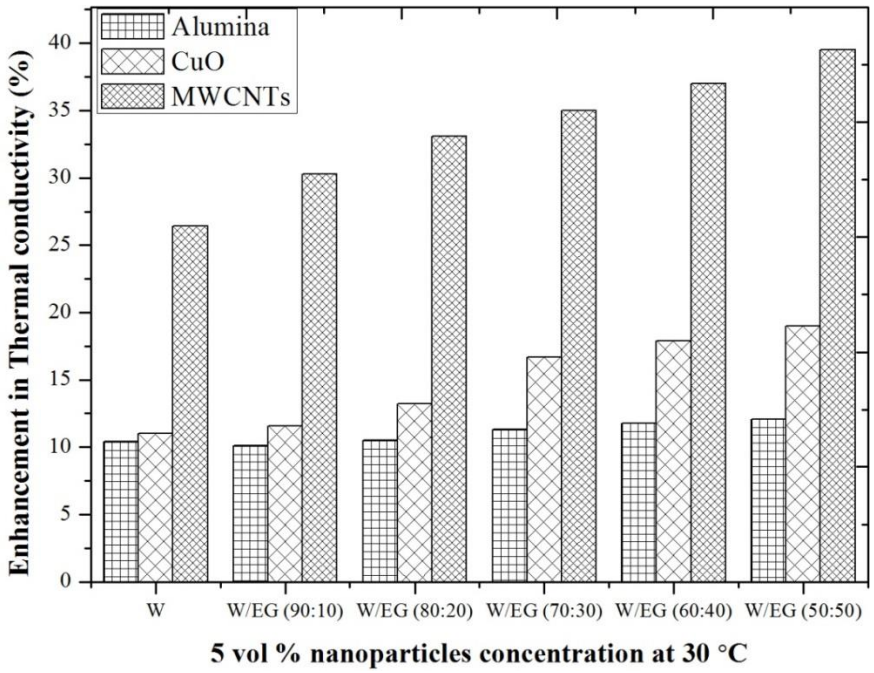

Figure 4.7: Comparison of thermal conductivity enhancement with nanoparticles and base fluids

4.2 VISCOSITY OF NANOFLUIDS

There are various techniques available for the measurement of viscosity but the present work used Brookfield viscometer DV-II + Pro for viscosity measurements. Dynamic viscosity is a quantity of fluid's resistance to flow that was determined by Brookfield viscometer DV-II + Pro at a particular shear stress or shear rate as displayed in Figure 4.8. This viscometer was procured from Brookfield Engineering Laboratories, Inc, MA, USA. The DV-II + Pro are working on a principle of driving a spindle engrossed in the liquid by a calibrated spring. The deflection in spring was determined by a rotary transducer provides the viscous drag of the fluid against the fluid. The measurement units of viscosity are milli-Pascal seconds or centi-Poise. The measured viscosity is depend on the full measure rotation of the calibrated spring, the shape and size of the spindle, the rotating speed of the spindle and the vessel the spindle is rotating in. Viscometer should be auto zero before any measurements. Viscosity is measured at different temperatures

ranges from 20 ºC to 70 ºC and temperature is maintained by water bath attached with the Brookfield viscometer as displayed in Figure 4.8.

Figure 4.8: Brookfield viscometer

Before starting the experiments with nanofluids, viscosity measurements of base fluids were carried out to check reliability of experimental method. So, experimental data were compared with ASHRAE standards tabulated in Table 4.3. Experimental outcomes show the good relation with standard data within a deviation of ± 1 % with reference data (Figure 4.9).

Table 4.3: Dynamic viscosity values as per ASHRAE standards, Pa. s × 10^3

Temperature, °C	W	W/EG (90:10)	W/EG (80:20)	W:EG (70:30)	W/EG (60:40)	W:EG (50:50)
20	1.002	1.182	1.658	2.129	2.971	3.811
30	0.798	0.915	1.308	1.695	2.261	2.948
40	0.654	0.720	1.062	1.345	1.778	2.265
50	0.548	0.620	0.893	1.112	1.445	1.817
60	0.467	0.570	0.810	0.901	1.298	1.430
70	0.405	0.529	0.690	0.748	1.074	1.149

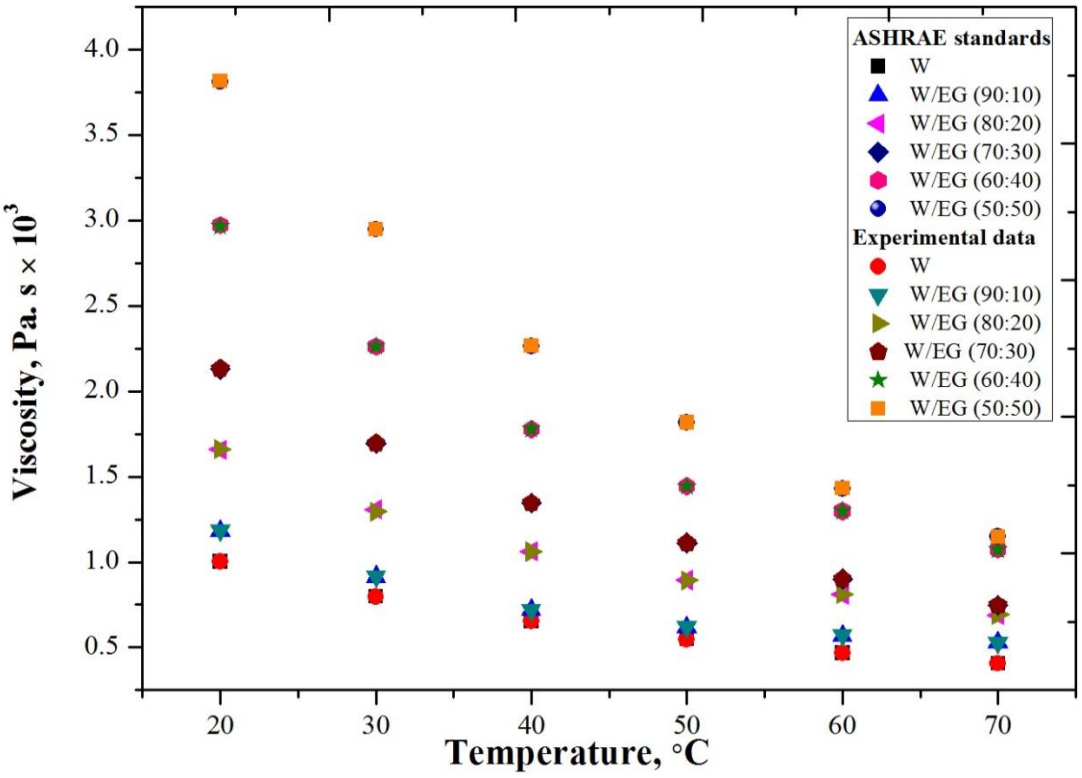

Figure 4.9: Comparison of experimental viscosity data with ASHRAE standards

In this present work, detailed viscosity studies of nanofluids with temperature and various nanoparticle concentrations were investigated. From the literature studies, it has been confirmed that alumina, CuO and MWCNT based nanofluids showing the Newtonian behavior for a particular shear stress range. So, viscosity measurements of nanofluids were carried out at particular shear stress range and different temperatures. Viscosity of nanofluids depends on type of nanoparticles, base fluids, temperature as well as nanoparticles concentration. Viscosity variations with all these factors are clearly depicted in Figure 4.10, 4.11 and 4.12. From these figures, it can be concluded that nanofluids viscosity are higher than the viscosity of their respective base fluids. Moreover, viscosity increases with decrease in temperature and increase in particle concentration. The percentage rises in viscosity of different nanofluids with temperature and nanoparticles concentration are tabulated in Table 4.4.

4.2.1 Effect of different type of nanoparticles

Least enhancement in viscosity was observed for MWCNT nanofluids when compared with alumina and CuO nanofluids while maximum rise in viscosity was monitored for CuO nanofluids. This is due to high density of CuO nanoparticles and very low density of MWCNT.

As alumina nanofluids are surfactant free but MWCNT and CuO nanofluids get stabilized with surfactants. But the surfactants solution was very low viscosity in comparison with nanofluids viscosity so the viscosity of nanofluids was measured without considering the effect of surfactants [79]. Alumina-W nanofluids have 8.65 % rise in viscosity, CuO-W/EG (50:50) nanofluids viscosity increased by 3.39 % while viscosity rise by 2.98 % for MWCNT-W/EG (50:50) at 30 ºC for 5 vol % nanoparticles concentration. These results showed that viscosity rise was very low when compared with results reported by various researchers [22, 62, 86].

4.2.2 Effect of different type of base fluids

Base fluids play a very important role to decide the cooling efficiency of nanofluids. Nanofluids thermal properties changes with the change of base fluids. The rise in viscosity of nanofluids shows immense variation with different base fluids such as W or W/EG mixtures. The rise in viscosity of nanofluids with W/EG base fluids is quite less in comparison with the water based nanofluids. The same behavior of EG based nanofluids was reported by Sridhara and Satapathy [89].

4.2.3 Effect of temperature

Viscosity is a function of temperature and in general for liquids with no suspensions, viscosity increases with decrease in temperature. Nanofluids viscosity also increases with decrease in temperature behaving as liquids due to weaken intermolecular force between nanoparticles and base fluid [158]. But there was least rise in viscosity observed with temperature when compared with their respective base fluids. No consistency observed for percentage rise in viscosity at different temperatures. From the Table 4.4, it was found that percentage rise in viscosity increases with increase in temperature.

Table 4.4: Percentage rise in viscosity for nanofluids

Percentage rise in viscosity for nanoparticles concentration of 0.1 vol % and 5 vol %												
		Temperature, ºC											
Nanoparticles	Base fluids	20		30		40		50		60		70	
		Volume concentration (%)											
		0.1%	5%	0.1%	5%	0.1%	5%	0.1%	5%	0.1%	5%	0.1%	5%
Alumina	W	2.99	8.88	1.63	8.65	8.10	7.95	9.85	15.51	9.64	17.56	9.63	19.01
	W/EG (90:10)	3.09	9.23	1.86	6.23	8.06	11.94	7.90	13.39	7.37	12.63	8.32	12.29
	W/EG (80:20)	1.56	6.71	1.91	4.97	3.55	6.92	6.17	10.20	7.25	10.58	5.30	10.81
	W/EG (70:30)	1.41	5.77	2.01	3.54	3.27	6.17	6.03	9.17	7.33	11.43	7.09	11.36
	W/EG (60:40)	2.46	5.03	1.40	2.91	2.16	4.35	3.83	6.05	3.92	6.39	3.26	6.05
	W/EG (50:50)	1.98	4.10	2.10	3.22	2.08	5.61	3.03	5.06	4.62	7.27	3.66	6.70
CuO	W	4	9.48	2.38	9.15	9.02	8.41	11.13	16.42	10.28	18.42	10.62	19.75
	W/EG (90:10)	6.29	11.77	2.51	6.89	8.89	12.50	8.87	14.35	8.60	13.68	9.07	12.85
	W/EG (80:20)	3.56	8.33	6.27	5.43	5.14	7.39	7.06	10.76	7.99	11.20	6.17	11.39
	W/EG (70:30)	1.69	6.14	2.36	3.89	3.64	6.62	6.56	9.62	7.88	11.99	7.62	12.17
	W/EG (60:40)	3.09	5.40	1.58	3.13	2.50	4.58	4.25	6.46	4.31	6.77	3.72	6.52
	W/EG (50:50)	2.19	4.46	2.34	3.39	2.34	5.87	3.36	5.34	5.03	7.55	4.18	7.14
MWCNT	W	1.89	7.68	1.25	8.02	6.88	12.39	8.39	14.78	7.70	16.92	8.39	18.02
	W/EG (90:10)	2.29	7.88	1.53	5.79	7.08	11.25	7.09	12.90	5.44	11.93	7.37	11.72
	W/EG (80:20)	0.93	5.87	1.67	4.66	3.43	6.55	5.60	9.64	7	10.21	5.01	10.37
	W/EG (70:30)	0.61	3.71	1.29	3.30	3.12	5.80	5.75	8.72	7.10	10.88	6.81	10.83
	W/EG (60:40)	0.89	3.62	1.22	2.59	1.82	3.96	3.62	5.70	3.74	6	2.98	5.58
	W/EG (50:50)	1.09	2.55	1.73	2.98	1.94	5.47	2.81	4.90	4.33	6.85	3.39	6.07

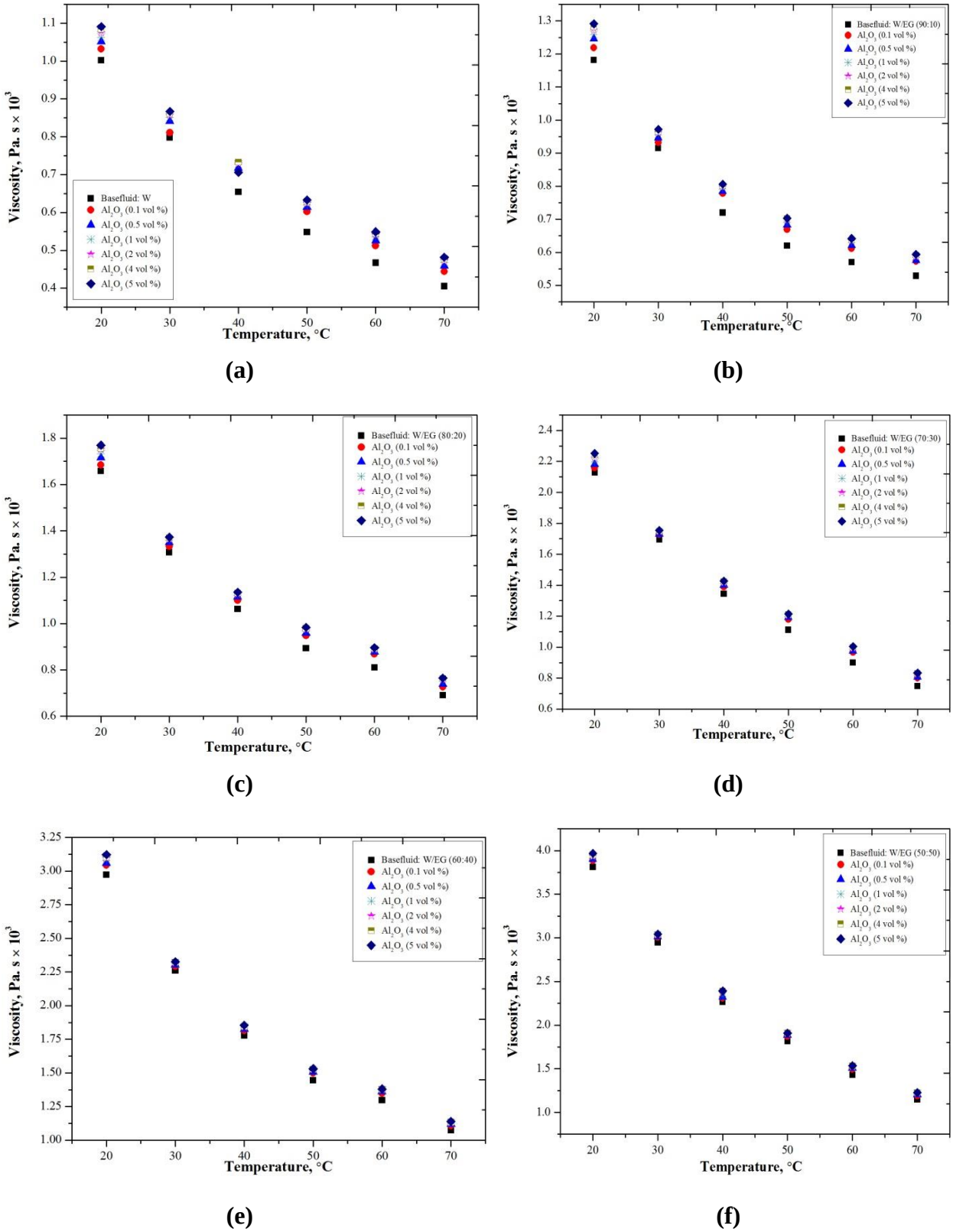

Figure 4.10: Viscosity of alumina nanofluids with temperature and different base fluids such as (a) W (b) W/EG (90:10) (c) W/EG (80:20) (d) W/EG (70:30) (e) W/EG (60:40) (f) W/EG (50:50)

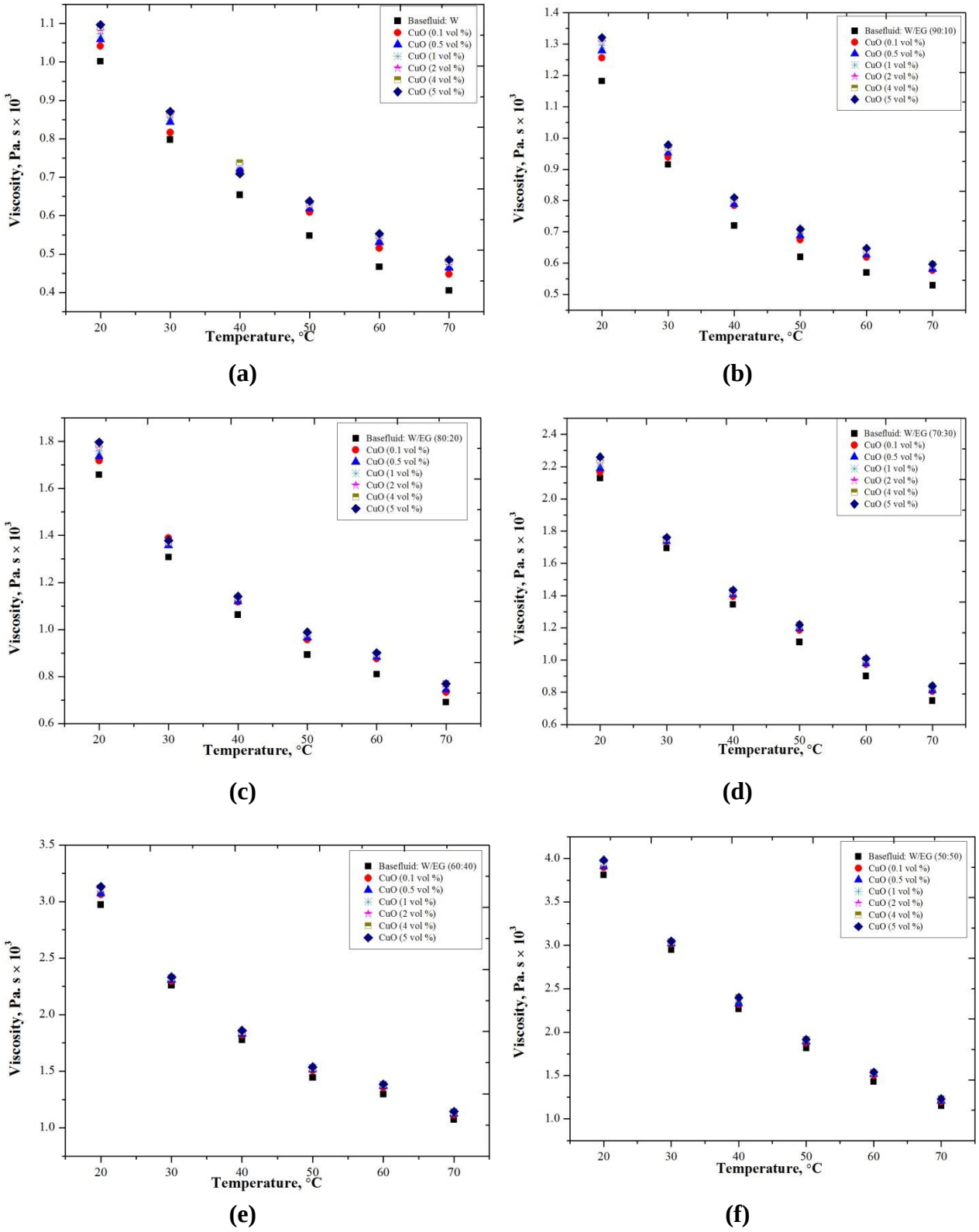

Figure 4.11: Viscosity of CuO nanofluids with temperature and different base fluids such as (a) W (b) W/EG (90:10) (c) W/EG (80:20) (d) W/EG (70:30) (e) W/EG (60:40) (f) W/EG (50:50)

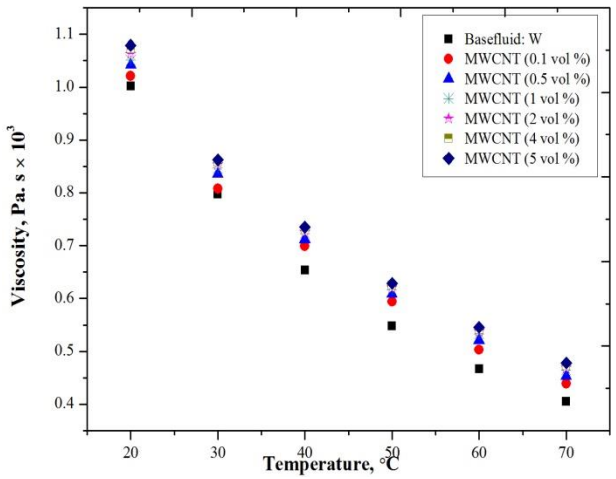

(a)

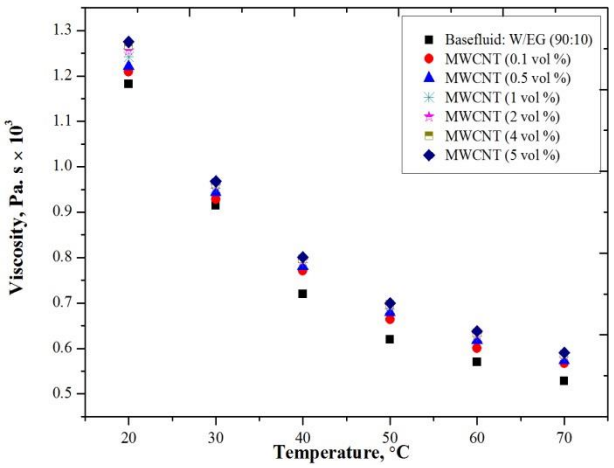

(b)

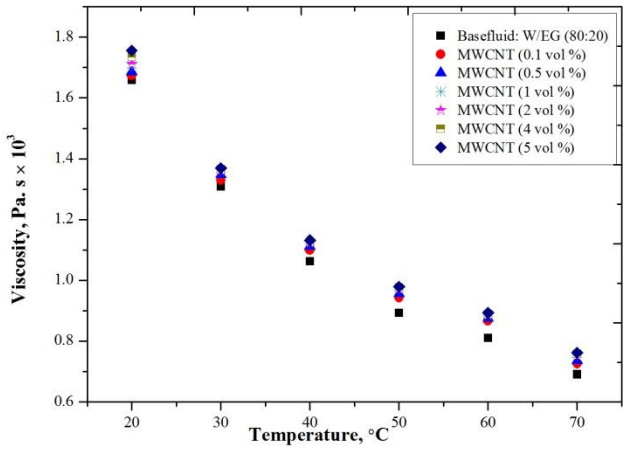

(c)

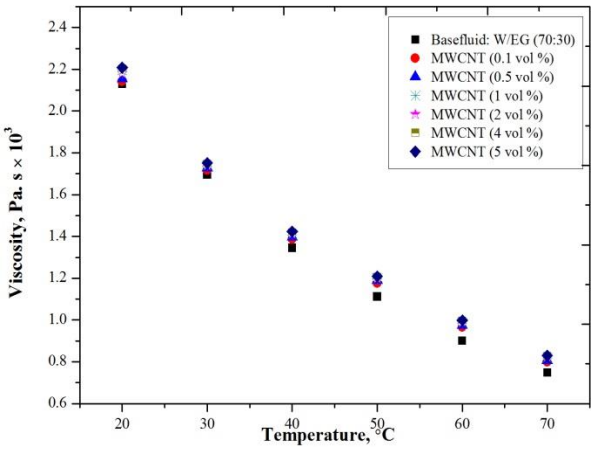

(d)

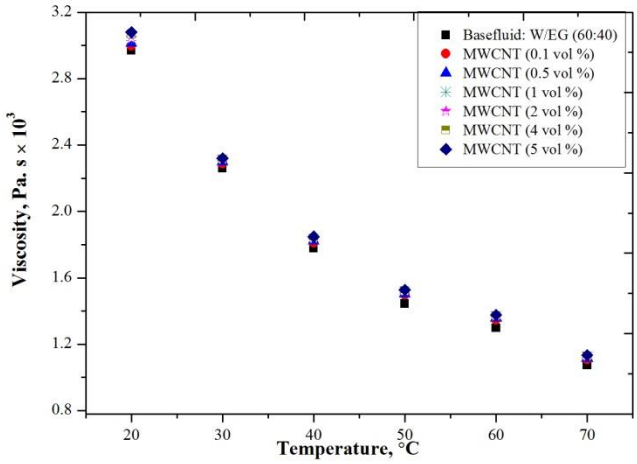

(e)

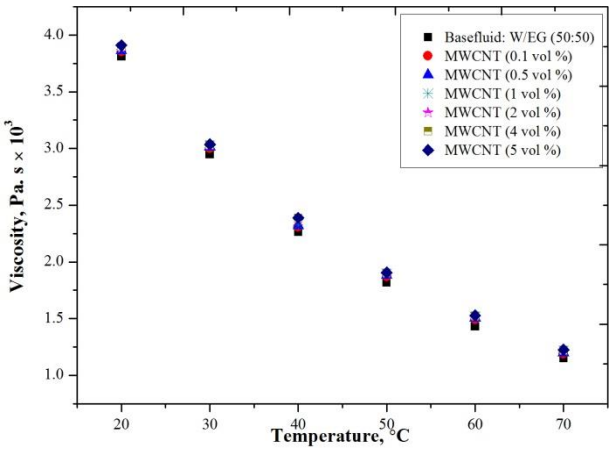

(f)

Figure 4.12: Viscosity of MWCNT nanofluids with temperature and different base fluids such as (a) W (b) W/EG (90:10) (c) W/EG (80:20) (d) W/EG (70:30) (e) W/EG (60:40) (f) W/EG (50:50)

Mathematical correlation equations are developed in terms of temperature, nanoparticle concentration and type of base fluids which shows a good fit of viscosity data with experimental data with R^2 value is approximately 0.98 or above.

For alumina nanofluids

$$\mu = 1.72275603 - 0.0265935 \times T + 0.011464 \times C - 0.032778 \times WEG \quad (4.5)$$

For CuO nanofluids

$$\mu = 1.7363124 - 0.0267501 \times T + 0.0117586 \times C - 0.032747 \times WEG \quad (4.6)$$

For MWCNT nanofluids

$$\mu = 1.706344 - 0.0262813 \times T + 0.010705 \times C + 0.0326505 \times WEG \quad (4.7)$$

where, μ is the viscosity in Pa.s$\times 10^3$, T is the temperature in degree Celsius, C is the nanoparticles volume concentration and WEG is the ratio of ethylene glycol in water.

4.2.4 Comparison of Nanoparticles and Base fluids

Viscosity behaviors of nanofluids can be clearly illustrated in Figure 4.13. This shows that CuO nanoparticles enhancement is maximum and MWCNT nanofluids have least enhancement either any kind of base fluids used. Ethylene glycol based nanofluids are more viscous but viscosity rise is reduced with the addition of ethylene glycol in water.

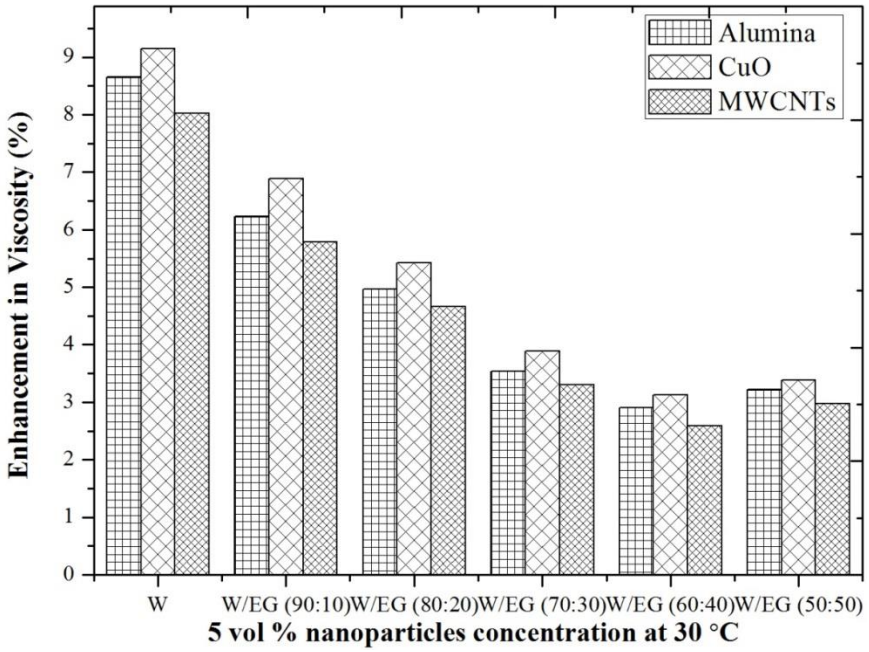

Figure 4.13: Comparison of viscosity enhancement with nanoparticles and base fluids

4.3 DENSITY OF NANOFLUDS

Density could be measured by precision way with the help of pycnometer. The pycnometer is a glass bottle having a tight-fitting glass cork with a capillary hole in it. This hole discharges an unused liquid when closing a top-filled pycnometer and permits for finding a particular volume of working and/or measured liquid by a high precision (Figure 4.14). First weight an empty bottle then a known volume of standard liquid (water) with known density filled in the pycnometer and weighed it. Then, repeat the procedure for the fluid with unknown density. As the volume of both the samples is same so it follows the equation as:

$$\frac{m_{std}}{\rho_{std}} = \frac{m_f}{\rho_f} \tag{4.1}$$

where, m_{std} is the mass of standard fluid such as water having known density of ρ_{std} and m_f is the mass of the fluid with unknown density of ρ_f. The unknown density of fluid is determined from the equation 4.1.

Figure 4.14: Pycnometer

Density measurements were carried out for all the base fluids such as W and W/EG mixtures to verify the precision of Pycnometer by comparing the experimental readings with ASHRAE standards (Table 4.5). This shows the good agreement between experimental data and standard data with a deviation of ± 1 % with reference data (Figure 4.15).

Table 4.5: Density values as per ASHRAE standards, kg/m^3

Temperature, °C	W	W/EG (90:10)	W/EG (80:20)	W:EG (70:30)	W/EG (60:40)	W:EG (50:50)
20	998.2	1014.2	1030	1046	1060	1074
30	995.7	1011	1026	1042	1055	1069
40	992.3	1007	1022	1037	1051	1065
50	988.1	1003	1017	1033	1046	1059
60	983.2	1001	1015	1030	1042.8	1056
70	977.8	995	1010	1025	1037	1050

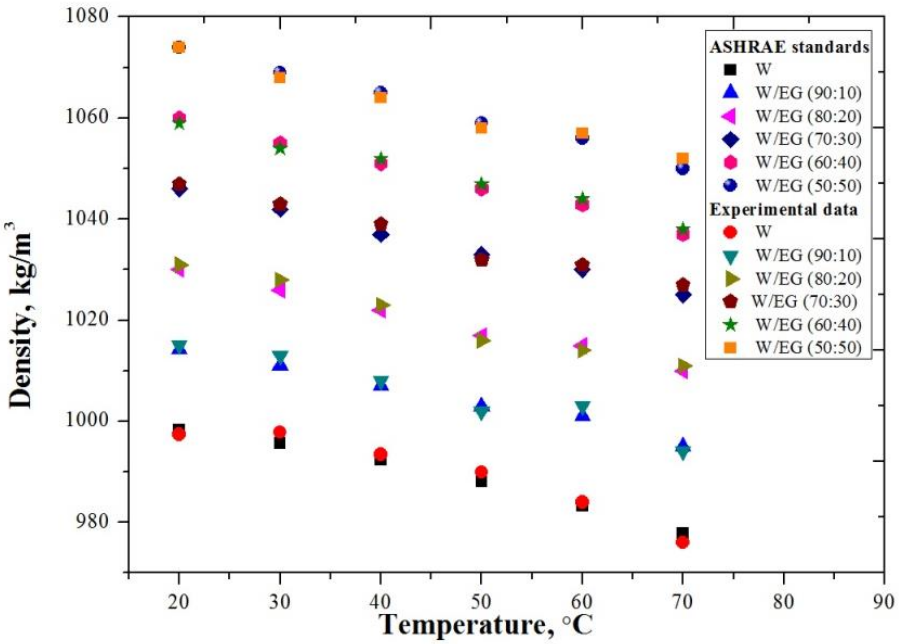

Figure 4.15: Comparison of experimental density data with ASHRAE standards

After determining the nanofluids thermal conductivity and viscosity, density of nanofluids were measured at different temperatures as this is an important property used for estimating the thermal and hydraulic performance of nanofluids. Kumaresan and Velraj [22] reported that theoretical models of density measurement cannot predict the density accurately as it results into higher deviation, so the experiments were carried out.

It can be interpreted from the Figure 4.16, 4.17 and 4.18 that density of nanofluids increases with decrease in temperature as well as increase in nanoparticles concentration. Density of nanofluids

decreases with increase in temperature due to weaken intermolecular forces between nanoparticles and base fluids. It is also observed that by increasing the EG ratio in water, nanofluids density also increases but the percentage enhancement in density of nanofluids with reference to base fluid is very low. From the Table 4.6, it is clearly seen that rise in density of nanofluids was very low when compared with their respective base fluids. There is no such remarkable effect of type of nanoparticles, base fluid and temperature was observed.

Maximum rise of 1-2 % in density was observed if any kind of nanoparticles with different concentrations and base fluids used at any temperature ranges from 20 ºC - 70 ºC. The same trend is followed by the nanofluids as followed by basefluids density with change in temperature. This percentage of rise is very small in comparison with the rise of thermal conductivity and viscosity. From these results, it can be concluded that this enhancement is significant for any type of heat transfer application.

Mathematical correlation equations are developed in terms of temperature, nanoparticle concentration and type of base fluids which shows a good fit of density data with experimental data with R^2 value is approximately 0.98 or above.

For alumina nanofluids

$$\rho = 1014.3351 - 0.42628 \times T + 1.78487 \times C - 1.467506 \times WEG \quad (4.8)$$

For CuO nanofluids

$$\rho = 1015.10982 - 0.431133 \times T + 1.81809 \times C - 1.46761 \times WEG \quad (4.9)$$

For MWCNT nanofluids

$$\rho = 1013.064313 - 0.412946 \times T + 1.736101 \times C + 1.4648252 \times WEG \quad (4.10)$$

where, ρ is the density in kg/m^3, T is the temperature in degree Celsius, C is the nanoparticles volume concentration and WEG is the ratio of ethylene glycol in water.

Table 4.6: Percentage rise in density for nanofluids

Percentage rise in density for nanoparticles concentration of 0.1 vol % and 5 vol %												
		Temperature, ºC											
Nanoparticles	Base fluids	20		30		40		50		60		70	
		Volume concentration (%)											
		0.1 %	5 %	0.1 %	5 %	0.1 %	5 %	0.1 %	5 %	0.1 %	5 %	0.1 %	5 %
Alumina	W	0.39	1.06	0.54	1.23	0.84	1.40	0.46	1.47	0.67	1.25	0.45	1.30
	W/EG (90:10)	0.45	1.33	0.59	1.22	0.37	0.88	0.45	1.22	0.52	1.24	0.59	1.23
	W/EG (80:20)	0.75	1.81	0.76	1.53	0.68	1.43	0.44	1.02	0.56	1.11	0.76	1.33
	W/EG (70:30)	0.41	1.36	0.67	1.18	0.46	1.32	0.55	1.27	0.61	1.29	0.48	1.09
	W/EG (60:40)	0.50	1.02	0.66	0.98	0.46	1.25	0.47	1.12	0.63	1.20	0.38	0.98
	W/EG (50:50)	0.46	1.46	0.75	1.51	0.54	1.23	0.55	1.27	0.48	1.08	0.68	1.38
CuO	W	0.47	1.14	0.62	1.30	0.92	1.47	0.566	1.54	0.77	1.32	0.54	1.38
	W/EG (90:10)	0.54	1.40	0.67	1.26	0.45	0.95	0.50	1.28	0.57	1.30	0.67	1.27
	W/EG (80:20)	0.81	1.87	0.81	1.59	0.74	1.49	0.51	1.07	0.62	1.17	0.81	1.36
	W/EG (70:30)	0.51	1.45	0.74	1.23	0.60	1.39	0.61	1.32	0.66	1.34	0.52	1.15
	W/EG (60:40)	0.64	1.06	1.23	1.03	0.53	1.30	0.52	1.19	0.67	1.25	0.44	1.05
	W/EG (50:50)	0.54	1.52	0.80	1.57	0.63	1.29	0.63	1.34	0.55	1.12	0.75	1.44
MWCNT	W	0.36	0.97	0.53	1.15	0.75	1.35	0.33	1.39	0.58	1.19	0.31	1.21
	W/EG (90:10)	0.32	1.04	0.39	1.15	0.29	0.84	0.35	1.16	0.43	1.17	0.40	1.16
	W/EG (80:20)	0.46	1.46	0.48	1.47	0.58	1.38	0.38	0.97	0.47	1.07	0.67	1.25
	W/EG (70:30)	0.32	0.94	0.47	1.13	0.38	1.24	0.48	1.21	0.54	1.25	0.39	1.04
	W/EG (60:40)	0.33	0.90	0.37	0.92	0.38	1.18	0.38	1.06	0.55	1.15	0.27	0.94
	W/EG (50:50)	0.32	1.15	0.56	1.45	0.44	1.19	0.46	1.21	0.37	1.02	0.60	1.31

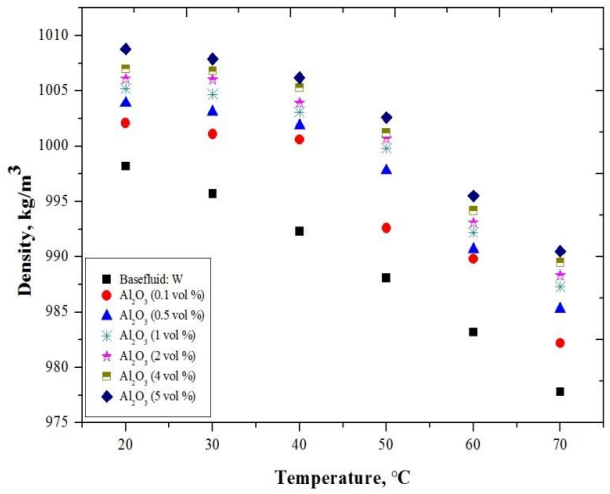

(a)

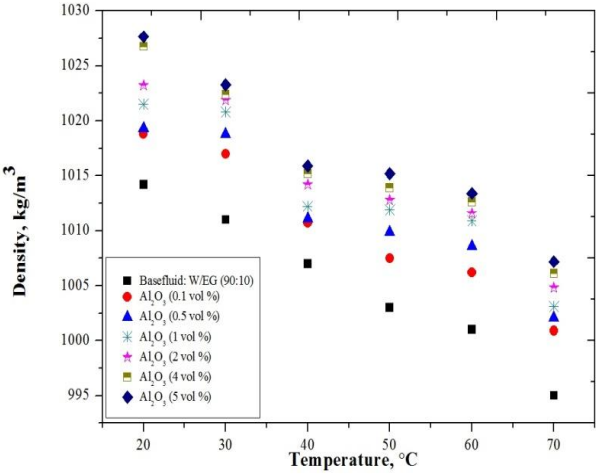

(b)

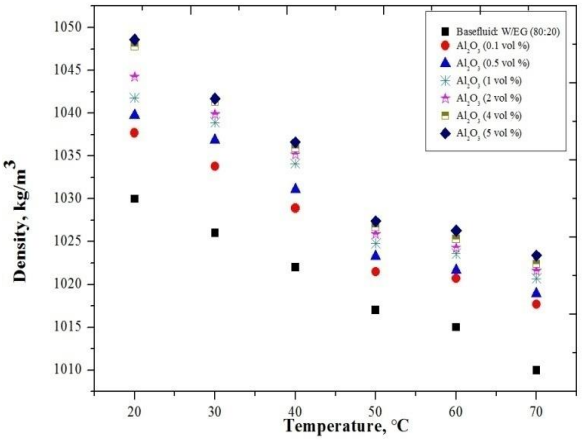

(c)

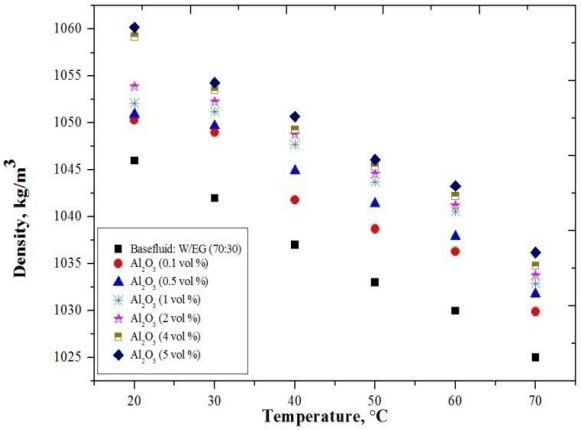

(d)

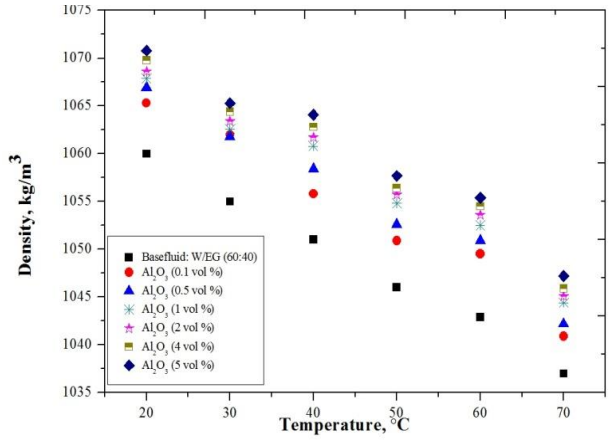

(e)

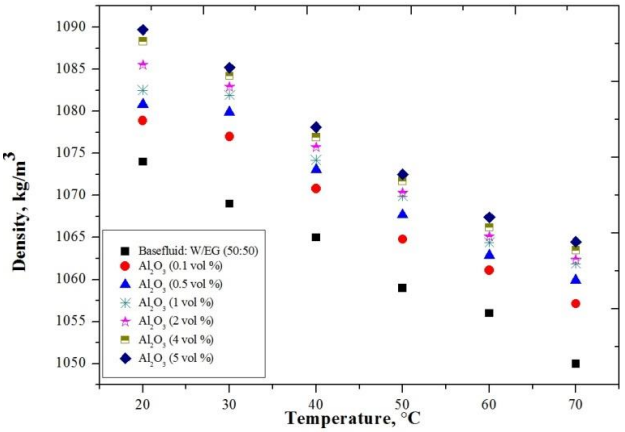

(f)

Figure 4.16: Density of alumina nanofluids with temperature and different base fluids such as (a) W (b) W/EG (90:10) (c) W/EG (80:20) (d) W/EG (70:30) (e) W/EG (60:40) (f) W/EG(50:50)

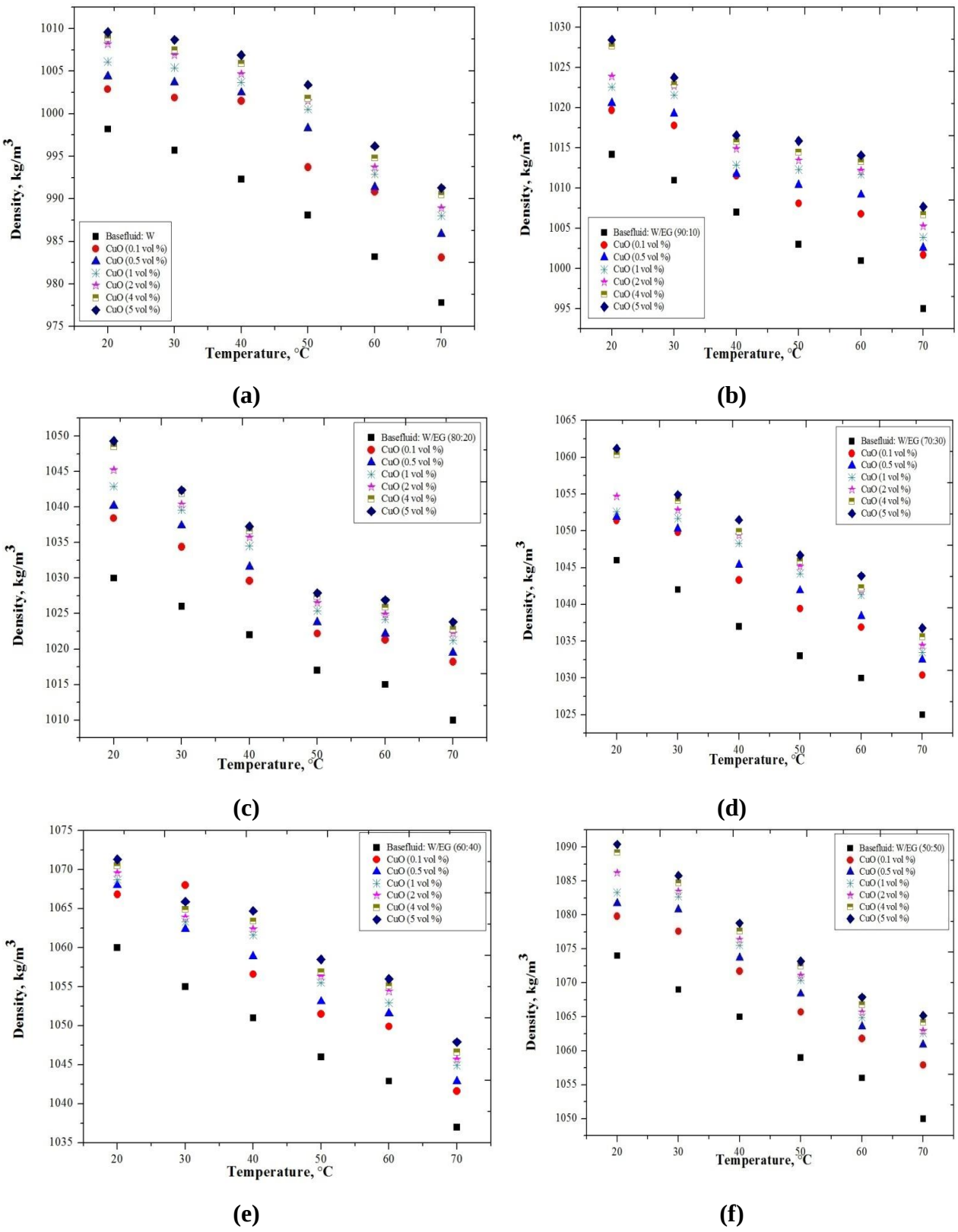

Figure 4.17: Density of CuO nanofluids with temperature and different base fluids such as (a) W (b) W/EG (90:10) (c) W/EG (80:20) (d) W/EG (70:30) (e) W/EG (60:40) (f) W/EG (50:50)

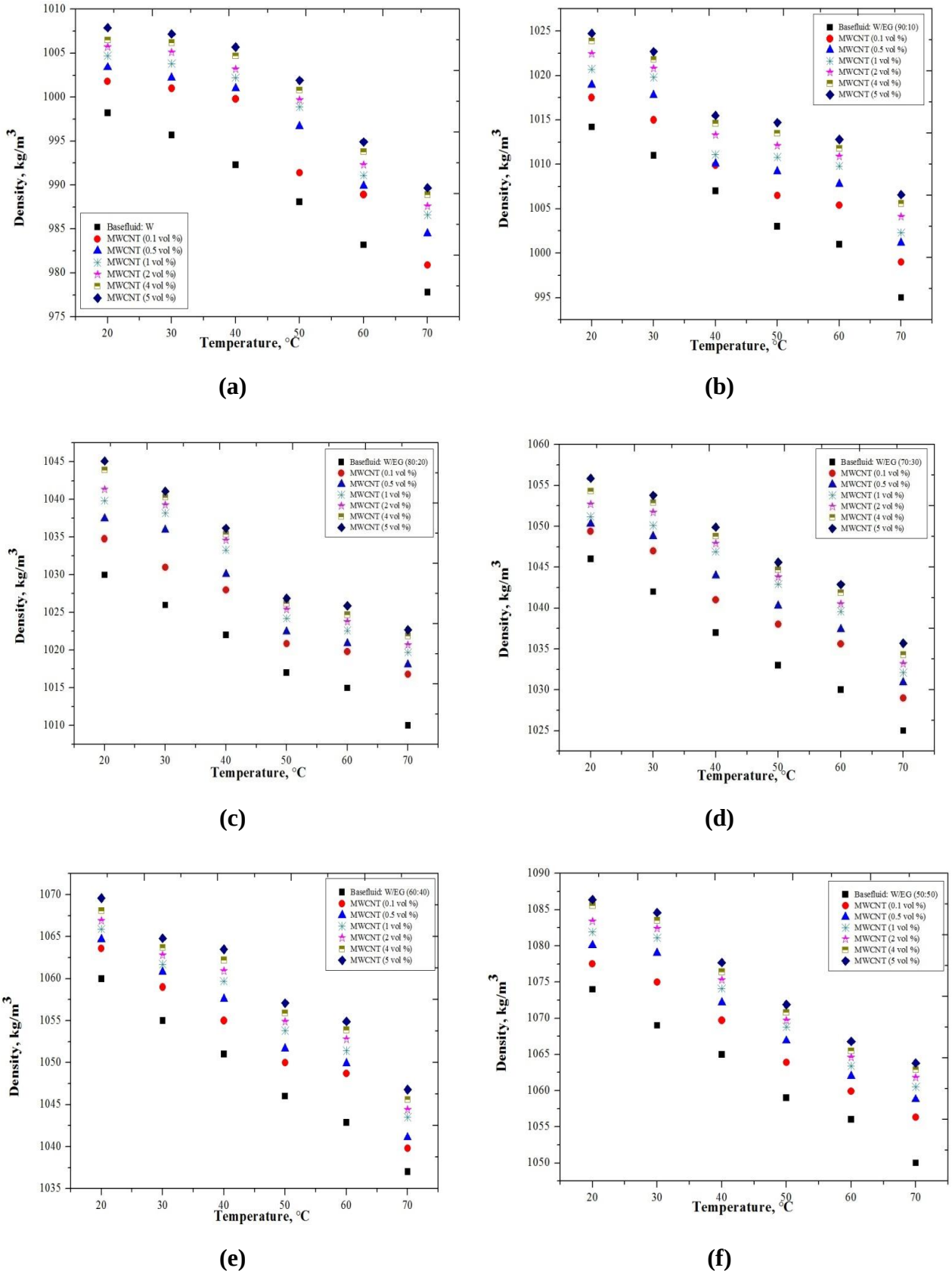

Figure 4.18: Density of MWCNT nanofluids with temperature and different Base fluids such as (a) W (b) W/EG (90:10) (c) W/EG (80:20) (d) W/EG (70:30) (e) W/EG (60:40) (f) W/EG (50:50)

4.4 COMPARISON OF THERMAL CONDUCTIVITY, VISCOSITY AND DENSITY OF NANOFLUIDS

The rise in density and viscosity of nanofluids are quite low when compared with thermal conductivity enhancement (Figure 4.19). These results are very suitable in heat transfer area as industrialist and researchers are attracted for a fluid with low viscosity and density and high thermal conductivity. Due to this pumping power cost for nanofluids approximately remains same as of base fluid but the rate of heat transfer get enhanced which will directly improve the efficiency of thermal system. In addition to this, base fluid such as W/EG (50:50) proves an efficient fluid for nanoparticles in terms of stability as well as thermal conductivity enhancement. So, this characteristics of W/EG mixtures with nanoparticles makes it more suitable to use in high altitude regions as the freezing point of W/EG (50:50) gets dropped upto -36.5 °C from 0 °C i.e. the freezing point of water; with the addition of ethylene glycol in water.

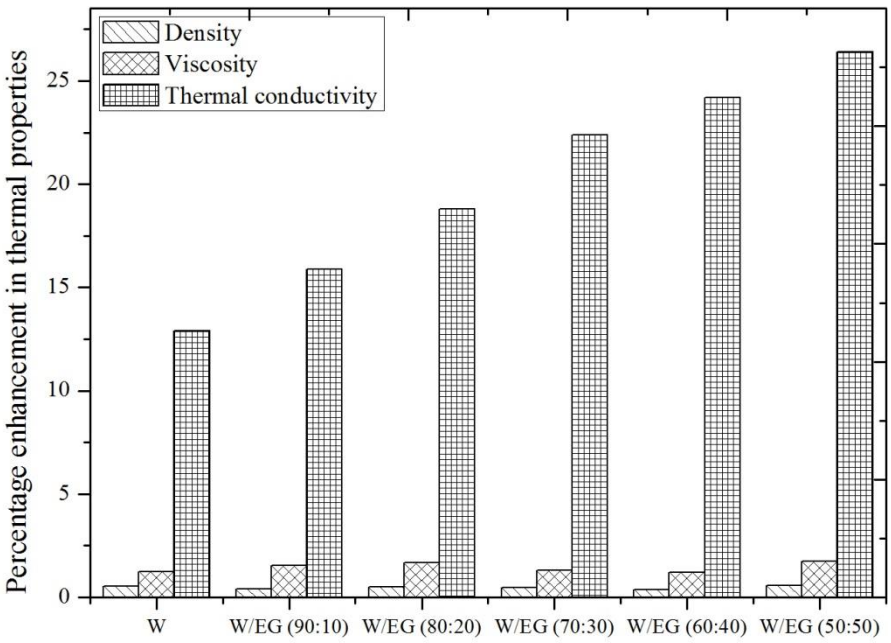

Figure 4.19: Comparison of thermal conductivity, viscosity and density of MWCNT nanofluids at 30 °C (0.1 vol %)

4.5 SPECIFIC HEAT OF NANOFLUIDS

From the literature studies, it was shown that mixture model based on mass fraction basis produce the accurate values for the specific heat of nanofluids. So, specific heat of nanofluids calculated as

$$c_{nf} = \frac{\phi(\rho c_p)_p + (1-\phi)(\rho c_p)_{bf}}{\rho_{nf}} \tag{4.11}$$

where, ρ_{nf} values obtained from equation no. 2.5 and the subscripts *nf*, *bf* and *p* symbolize the nanofluid, basefluid and nanoparticle, respectively.

To verify the model data, few samples were tested by Differential Scanning Calorimetry (Model: DSC131 evo) in IIT Roorkee, Utrakhand, INDIA and data shows a good fit with less than ± 1 % deviation as shown in Figure 4.20. So, further samples readings were obtained directly from the mixture model.

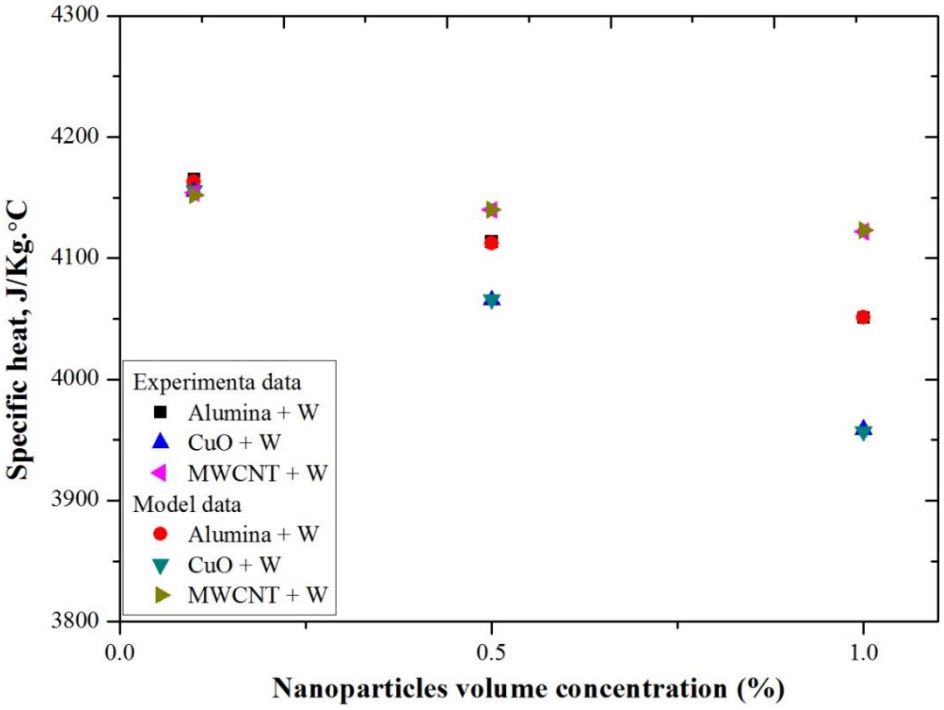

Figure 4.20: Comparison of experimental specific heat of nanofluids with mixture model

4.6 CLOSURE

In the existing chapter, detailed study of thermal conductivity, viscosity and density of prepared nanofluids at different temperature is carried out. These properties of nanofluids depend on the type of nanoparticles and its concentration, base fluids and temperature. Out of alumina, CuO and MWCNT, maximum thermal conductivity enhancement and least rise in viscosity were observed for MWCNT. Furthermore, base fluid such as W/EG (50:50) shows highest thermal conductivity enhancement in comparison with other base fluids. Slightly decrease in thermal conductivity enhancement of nanosuspensions was experimentally determined above 50 ºC due to the agglomeration of nanoparticles at higher temperatures.

CHAPTER 5
PERFORMANCE EVALUATION METHODOLOGY AND EXPERIMENTAL SETUP

In previous chapters, preparation, stability and measurement of thermophysical properties of nanofluids were done. Next step is to synthesize the analytical model for the fluid flow and heat transfer studies of nanofluids in microchannels. This model have been presented in the chapter along with the specific configurations adopted for the system considered, analytical consideration for the analysis, parameters involved in the analysis and the step-wise procedure adopted for the calculations. Further, the simplified flow diagram for the computer programs written in C++ language for carrying out calculations has also been presented in this chapter. This section also deals with the fabrication of microchannels, assemble up the set up for the heat transfer and fluid flow studies of microchannels, experimental procedure with uncertainty analysis in the measurements.

5.1 SPECIFICATIONS OF MICROCHANNELS

Before going for the modeling, microchannels materials, shape and size are important factors to decide the thermal performance of the nanofluids flowing through this system.

5.1.1 Microchannel material

In this present work, substrate material was chosen as aluminium as Hung et al. [139] discussed the fact that substrate with good thermal conductivity shows better thermal performance. Aluminium material (237 W/m.°C) is having much better thermal conductivity than silicon material (148 W/m.°C). As copper is having high thermal conductivity but still aluminium is preferred due to its light weight nature, more easily available and rust free element whereas copper is heavy and expensive elements.

5.1.2 Shape of microchannels

After deciding the substrate material, next step was to choose the shape of microchannels. From the literature studies, it is found that rectangular shape of microchannels having high heat transfer coefficient and low friction factor with lowest thermal resistance in comparison with trapezoidal and triangular shapes [130]. Moreover, the flow area is more in rectangular channels compared with other shapes of channels.

5.1.3 Size of microchannels

Microchannels were fabricated by using electrical discharge machine (EDM) at SR Engineers Ltd. Chandigarh as shown in Figure 5.1. During fabrication of channels on aluminium block by using EDM, the width of channels and fins were not go beyond to certain limit i.e. less than 200 μm. Breakage or bending of aluminium channels occurred if the channel size goes beyond this limit i.e. less than 200 μm as pure aluminium is a soft material. Moreover, to avoid the clogging of nanoparticles in channels and achieving the maximum convective heat transfer, width and depth of channels is not preferred below this range and fixed at W_{ch}= 250 μm and H_{ch} = 2 mm with a fixed aspect ratio of 8 [159]. Microchannels with their 3-D view are shown in Figure 5.2.

5.1.4 Fluid flow inlet and outlet arrangement

For the fluid inlet and outlet, manifolds were created adjoining with the microchannels. The position of inlet and outlet sections is important to decide for better heat transfer rate with low pressure drop and friction factor. Sehgal et al. [160] studied the different flow arrangements within the manifold to find the best one with highest heat transfer performance. They found that P-type flow arrangement provides minimum friction factor with less variation in pressure drop as well as appreciable heat transfer performance of MCHS. So, present work focuses on P-type flow through microchannels by making inlet and outlet holes at the top of the manifolds.

Figure 5.1: EDM machine with aluminium block

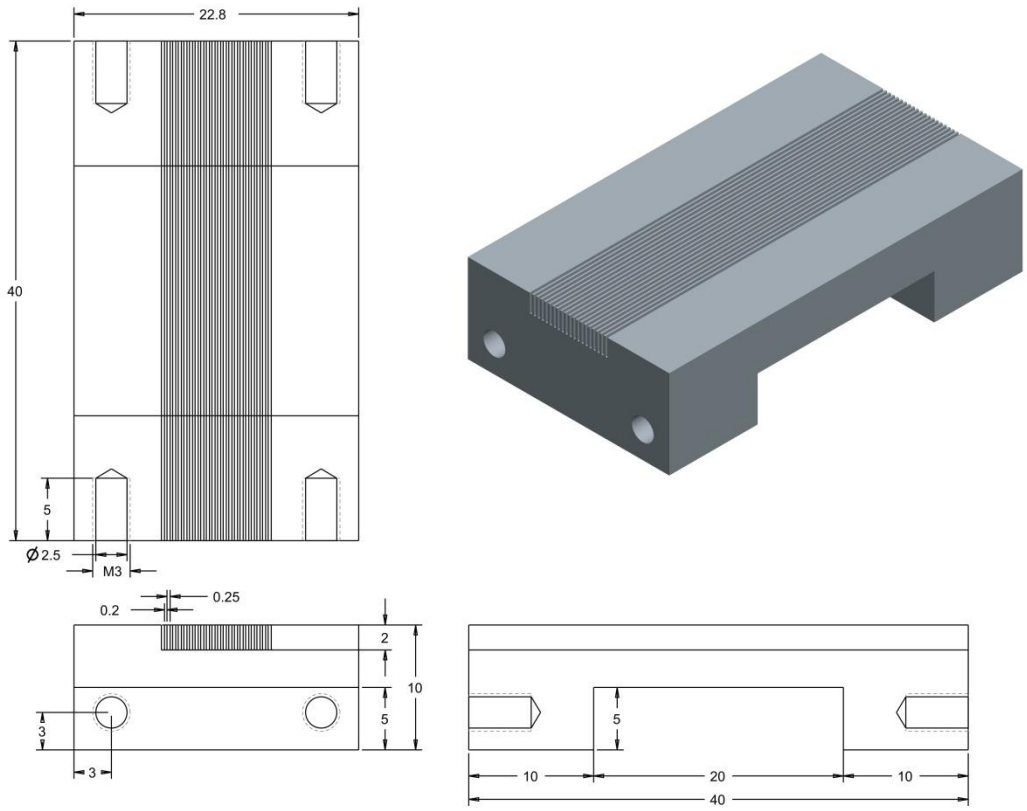

Figure 5.2: Orthographic view of microchannels with all dimensions

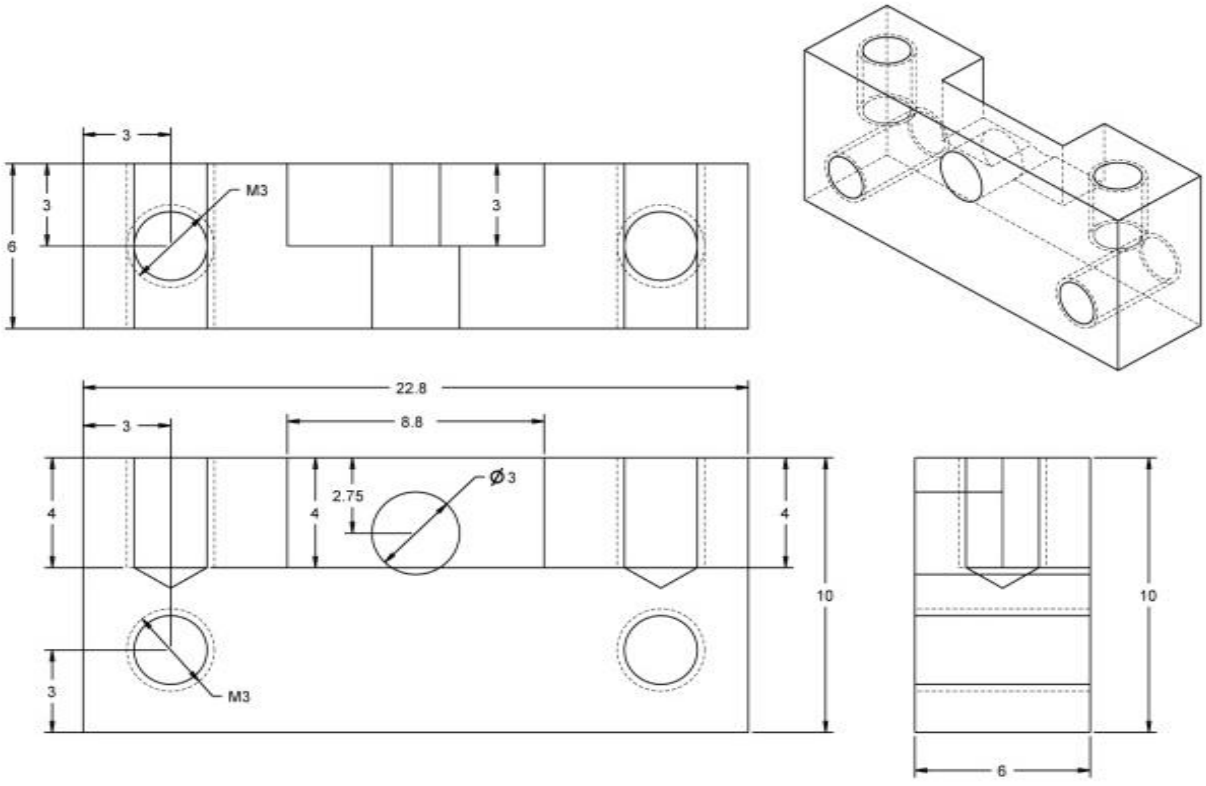

Figure 5.3: Geometric configuration of manifold with dimensions

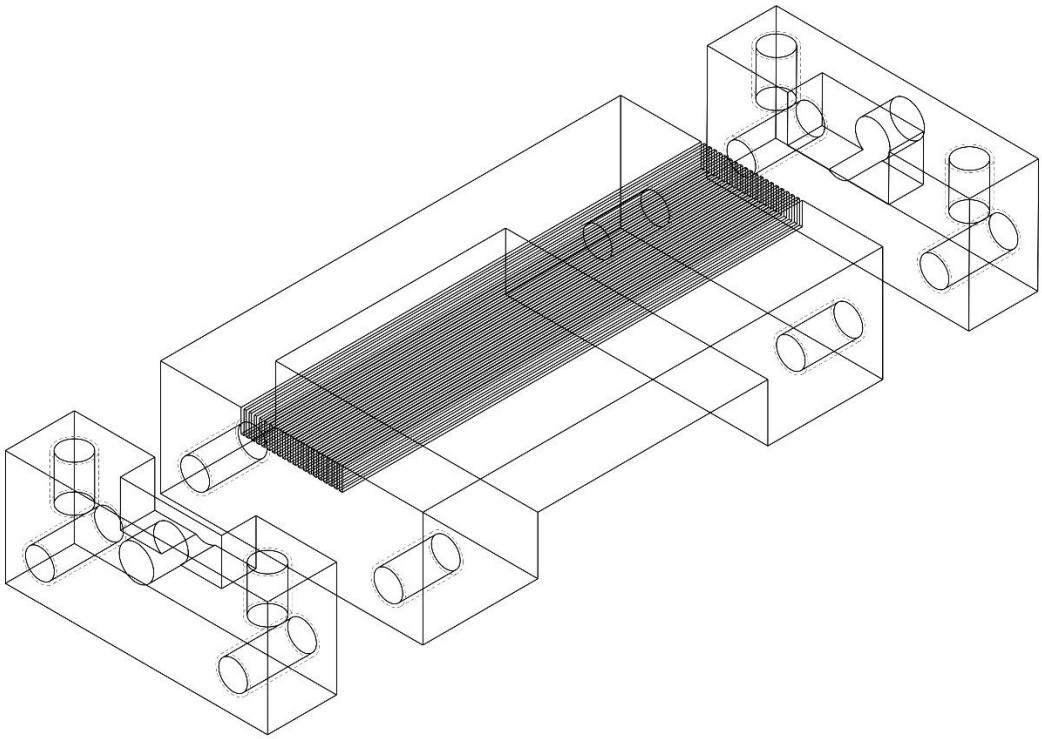

(a)

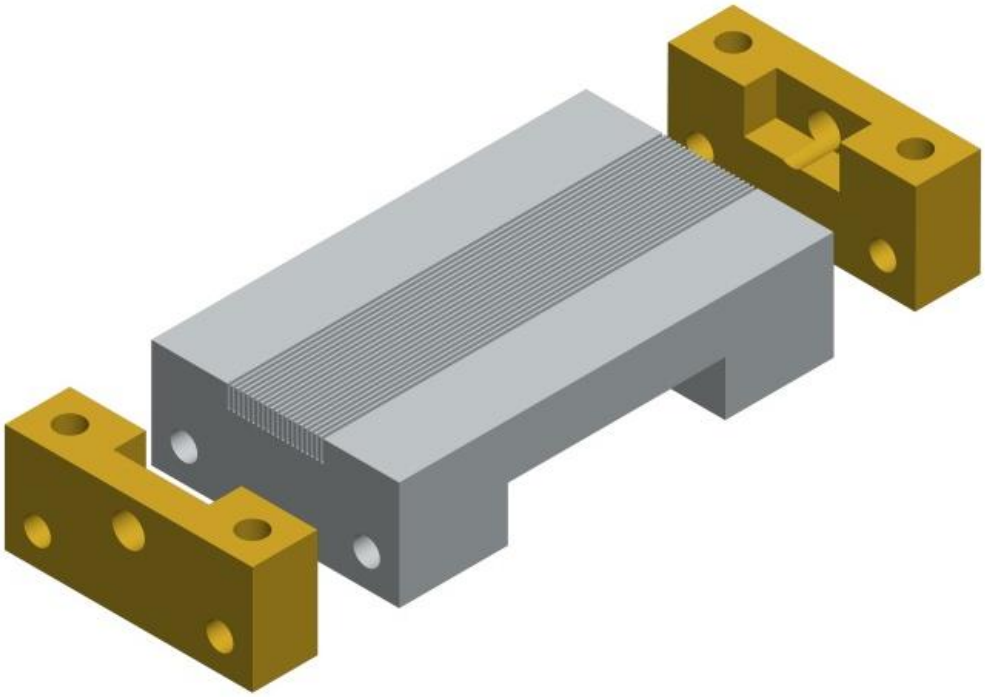

(b)

Figure 5.4 (a&b): Isometric view of Microchannels assembly

There are 21 number of mirochannels fabricated on a single unit of aluminium block of size 22.8×4×40 mm. Manifold units were fabricated separately and then fixed with channels block tightly by nut bolts.The dimensions of maniflod with the description of all the nuts bolts used for the fabrication is shown in Figure 5.3. The isometric view of the microchannels with their manifold are revealed in Figure 5.4.

After the fabrication of aluminium channels, proper cleaning of channels as well as manifold was required. During cutting of channels and manifolds, small dust particles and molecular contamination occurred between the channel spacing. The aluminium block was boiled in acetone for 5 minutes and then continously rinsed with hot double distilled water. After rinsing, drying of channels done by using hot air blower to remove all the water droplets.

5.2 ANALYTICAL CONSDIERATIONS

5.2.1 Basefluid allocation

To decide the cooling performance of a thermal system, it is required to decide an effcient heat transfer fluid. In this present work, base fluids such as water and water-ethylene glycol (W/EG) mixtures (90:10, 80:20, 70:30, 60:40 and 50:50) was used. The W/EG (50:50) mixtures can work upto the temperature of -36.5 ºC which makes them suitable for any kind of applications in colder regions. The general properties of fluids are tabulated in Table 5.1 as per ASHRAE standards.

Table 5.1: Properties of base fluids as per ASHRAE standards

Properties	**W:EG (50:50)**	**W:EG (60:40)**	**W:EG (70:30)**	**W:EG (80:20)**	**W:EG (90:10)**	**W**
Thermal conductivity, W/(m.ºC)	0.372	0.411	0.455	0.503	0.556	0.618
Density, kg/m^3	1069	1055	1042	1026	1011	995.7
Viscosity, Pa. s × 10^3	2.948	2.261	1.695	1.308	0.915	0.798
Specific heat, J/(kg. ºC)	3317.912	3502.008	3675.226	3835.891	3988.189	4178
Freezing point, ºC	-36.5	-24.5	-16	-9	-4	0
Boiling point, ºC	107	106	104	102	100	100

5.2.2 Fluid flow rate

Fluids with higher velocities provide high pressure drop but also higher heat transfer coefficients. The velocity should be large enough to avoid any nanosuspensions settling, but rise to a certain limit as it may cause erosion. The typical design values available from literature shown in Table 2.3 are:

For nanofluids in microchannels
In terms of velocity: 0.01 m/s to 0.1 m/s
In terms of flow rate: 1×10^{-8} m^3/s to 20×10^{-8} m^3/s

5.2.3 Fluid temperature

The maximum temperature (difference between fluid outlet temperature and fluid inlet temperature) difference leads to high heat transfer rate. The optimum value is found by creating an economic analysis of alternative designs and further depends on the application.

5.2.4 Fluid thermophysical properties

The fluid thermophysical properties such as thermal conductivity, specific heat, viscosity and density are required for any type of thermal and hydraulic analysis. These properties are generally estimated at the mean temperature of fluids to calculate the heat transfer coefficient. The general correlations for thermal conductivity, viscosity and density in terms of concentration, temperature and ethylene glycol ratio were developed for alumina, MWCNT and CuO nanoparticles in chapter 4. These properties were calculated from correlations and specific heat was calculated from standard relation as given in equation 2.7.

5.2.5 Assumptions considered

While analyzing the microchannels thermal performance, the following assumptions were made:

a. Equal distribution of temperature drop over the channels.
b. No heat loss to surroundings.
c. The temperature of fluid was considered constant over any cross section of channel.
d. Fluid flow rate was assumed uniform across the channels.
e. Fluid properties were operating at its mean operating temperature.
f. No phase change of fluids was considered.
g. The heat transfer coefficients, flow rates and fluid properties of fluids were considered constant throughout the each channel.

h. The channel wall resistance was neglected.
i. The entrance and exit loss coefficients were not considered.

5.3 METHODOLOGY FOR ANALYTICAL CALCULATIONS [161]

5.3.1 Step wise procedure

a. After given the input conditions, evaluate the surface and core geometry of microchannels including the hydraulic diameter.
b. Based on geometry calculations, fluid velocity is determined.
c. It is required to evaluate the thermophysical properties of fluids at assumed average temperature from the correlations developed from experimental data.
d. Further, Nusselt number is evaluated by determine the Reynolds number, thermal diffusivity, Peclet number and Prandtl number.
e. The fin efficiency calculated with heat transfer coefficient which is evaluated from Nusselt number.
f. Then, the outlet temperature of fluids is calculated by determining the average temperature difference between surface and fluid.
g. Finally, Nusselt number, Reynolds number, friction factor and heat loss is calculated from the model.

5.3.2 System equations

The equations used for analytical calculations in the present work are:

For the surface geometry of microchannels

Hydraulic diameter: $D_h = \frac{2 \times W_{ch} \times H_{ch}}{W_{ch} + H_{ch}}$ (5.1)

Wetted surface area: $A_{eff} = NL_{ch}(W_{ch} + 2\eta_f H_{ch})$ (5.2)

Cross sectional area: $A_c = W_{ch} \times H_{ch}$ (5.3)

where, W_{ch} is the width of channel, H_{ch} is the height of channel, L_{ch} is the total length of channel and N is the total number of channels.

Then, the fluid velocity is calculated from the flow rate and cross-sectional area of microchannels.

Fluid velocity: $u_f = \dot{V} \times A_c$ (5.4)

All the thermophysical properties are calculated at bulk mean temperature from the general correlations developed in Chapter 4 given in equation no. 4.2 to 4.10.

By calculating the thermal conductivity, specific heat, density, viscosity and of nanofluids, Nusselt number can be evaluated from the generalized equation given by Xuan and Li [103],

Nusselt number: $Nu = a(1 + b\phi^x * Pe^y)\,\mathrm{Re}^z \times \mathrm{Pr}^{0.4}$ (5.5)

where, a, b, x, y and z are constants determined from present experimental values. All the parameters used in the equation 5.5 are evaluated as:

Thermal diffusivity $\alpha_{nf} = \dfrac{k_{nf}}{\rho_{nf} \times c_{pnf}}$ (5.6)

Peclet number: $Pe = \dfrac{d_p \times u_f}{\alpha_{nf}}$ (5.7)

Reynolds number: $\mathrm{Re} = \dfrac{D_h \times u_f \times \rho_f}{\mu_{nf}}$ (5.8)

Prandtl number: $\mathrm{Pr} = \dfrac{c_{pnf} \times \mu_f}{k_{nf}}$ (5.9)

where, k_{nf}, μ_{nf}, ρ_{nf}, c_{pnf} are the thermophysical properties of nanofluids, d_p is the nanoparticle diameter, u_f is the fluid velocity and D_h is the hydraulic diameter of microchannels.

From the Nusselt number, heat transfer coefficient (h) can be evaluated in the following manner:

$$h = \frac{(Nu \times k_f)}{D_h} \tag{5.10}$$

The average temperature difference of surface and the fluids from the conductive and convective heat transfer of fluid by assuming fin adiabatic tip condition:

$$\Delta T = \frac{Q}{h(2H_{ch}\eta_f + W_{ch}) \times N \times L_{ch}} \tag{5.11}$$

The fin efficiency is $\eta_f = \frac{\tanh(mH_{ch})}{mH_{ch}}$ (5.12)

and m is calculated as $m = \sqrt{\frac{2h}{k_m \times W_f}}$ (5.13)

where, k_m is the substrate thermal conductivity and W_f is the width of fin.

For determine the flow characteristics, friction factor is determined in terms of Reynolds number:

$$f = C(\mathrm{Re})^x \quad (5.14)$$

where, C and x are constants determined from the experimental values.

5.4 COMPUTER PROGRAM

The input data required for analytical models include nanoparticles size and their properties, surface geometry of channels, fin configuration, fluid flow rates, fluid properties correlation, thermal properties of substrate material, base fluid properties, inlet temperature and maximum base temperature. Using the developed correlations, computer program are developed in Turbo C++ language for carrying out thermal performance analysis for microchannels with nanofluids. The salient features of this program are described in this section. Simplified flow diagrams have also been given as in Figure 5.5. The complete listing of the program is given in Appendix-1.

The program takes input data related to type of nanoparticles and base fluids, fluid operating parameters such as flow rates and inlet temperature of fluid, heater specifications, microchannels geometry, number of channels, nanoparticles and base fluids properties and heat input.

The program computes the surface and core geometry properties such as wetted surface area, cross-sectional area and hydraulic diameter. This programs has started by assuming the outlet temperature of the fluids as same as maximum base temperature. Then, calculate the thermophysical properties of the fluid from developed correlations at average assumed temperature.

FLOW CHART FOR MICROCHANNELS THERMAL PERFORMANCE

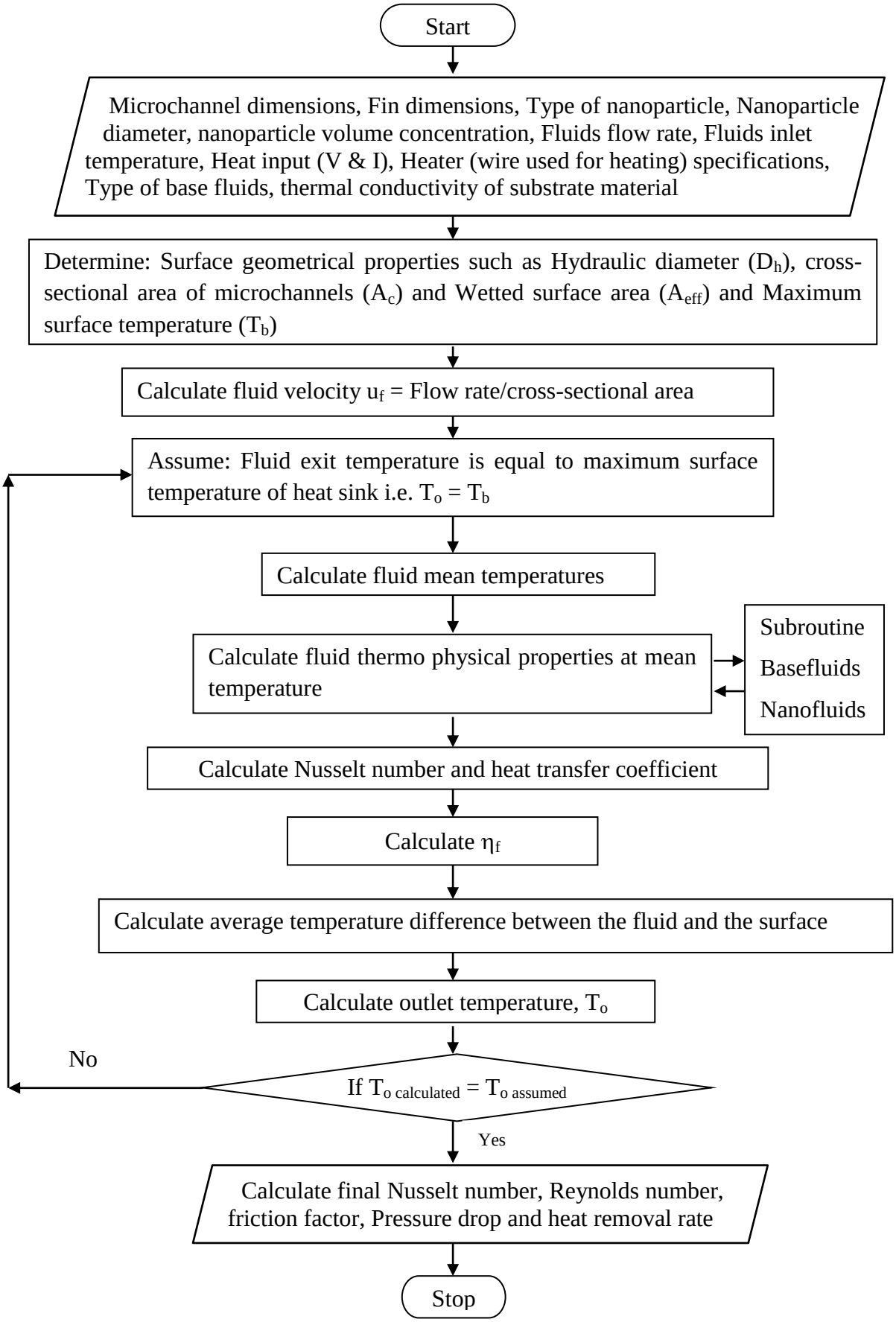

Figure 5.5: Flow diagram for microchannels heat sink system

Afterwards, main program considers for estimating the Nusselt number, heat transfer coefficient, heat transfer area, fin efficiency and final temperature difference between surface and fluid. Further, it computes the final outlet temperature of the fluids from the temperature difference of the fluid and surface. Evaluate the average temperature and compared with the assumed value. If it shows the error less than 0.5 ºC, the final heat transfer coefficient and Nusselt number are evaluated. If the error was more than 0.5 ºC, then repeat the procedure by assuming the new temperature.

With this computer program, thermal performance of microchannels using alumina, CuO and MWCNT nanofluids are evaluated as a function of nanoparticles concentration, ethylene glycol ratio in water (varied from 10 to 50), different temperatures (20 ºC to 60 ºC) and flow rates. In addition to this, this analytical data are compared with the experimental values for the validation.

5.5 DESCRIPTION OF EXPERIMENTAL SETUP

The experimental setup is designed to study the heat transfer and fluid flow characteristics within the MCHS. The setup comprises of heat sink, syringe pump with control software, display unit for temperature, voltage and current, inclined manometer and liquid storage tank. Detailed discussion on main components of set up as follow as:

5.5.1 Test section details (Microchannel heat sink)

The test section consists of heat sink, heaters, thermal insulating layer and pyrex glass sheet for top covering. The 21 rectangular parallel microchannels with a length of 40000 μm was fabricated on aluminium block. The width (W_{ch}) and thickness (W_f) of a microchannel was 250 μm and 200 μm with a depth (H_{ch}) of 2000 μm. The schematic diagram of microchannels is shown in Figure 5.6.

As the major problem in microchannels was leakage between channels and top covering acrylic sheet. So, before fitting of insulation layer and heater, leakage through microchannels was checked. A grease paper was used between the microchannels and pyrex glass sheet and then tighten with screws to avoid the leakage of fluid from channels. To check the leakage of the fluid from the microchannels, an experiment can be done. Test section exposed in Figure 5.7 with top covering was kept under the water and then fluid flow continuously through the channels for 3-4 hours. During this, no bubbles formation observed in the water showing that the system is leakage proof.

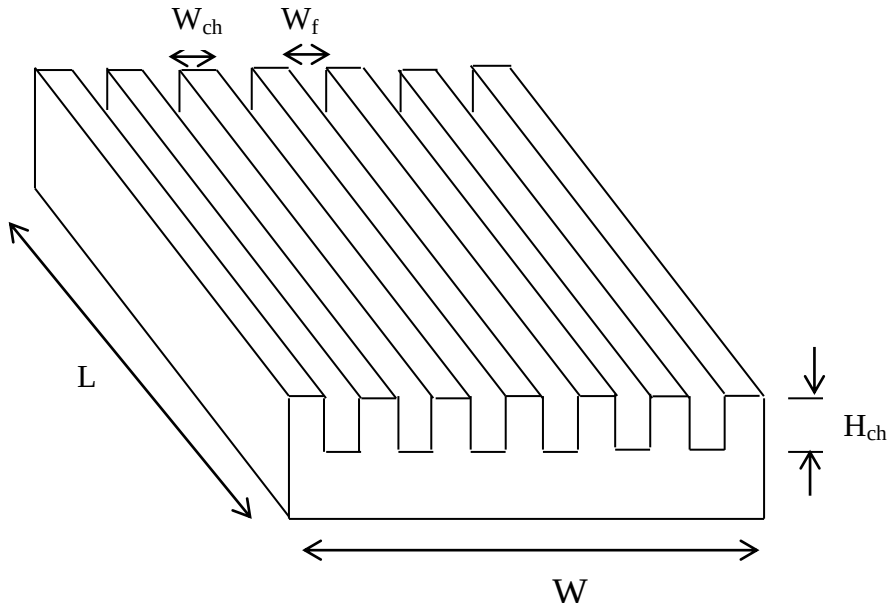

Figure 5.6. Description of aluminium microchannels

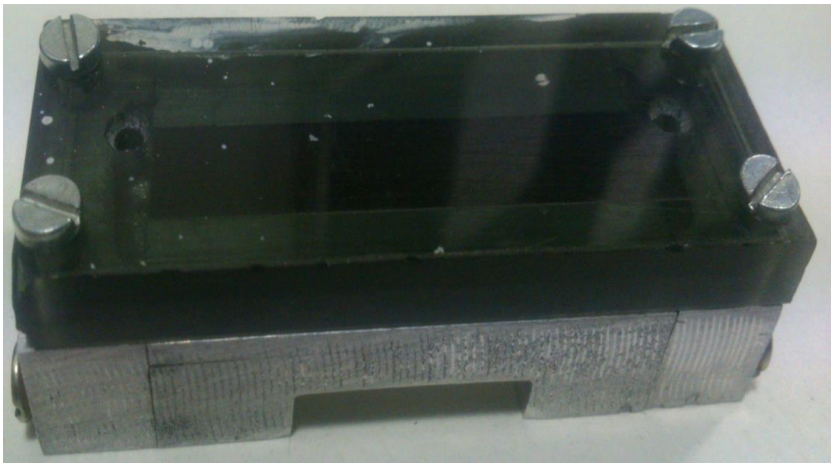

Figure 5.7: Microchannels with top covering

Afterwards, the aluminium heat sink was placed on aluminium base along with nichrome wire heater. The heater with a DC power supply in the range of 0-80 V and 0-2 A was positioned just below the heat sink. Two T-type thermocouples were placed between the heater and heat sink to simulate the heat flux generated by aluminium chip. Figure 5.8 gives the schematic diagram of test section along with heater and top covering acrylic sheet. Two circular holes on the pyrex glass sheet were made just above the manifold for the fluid inlet and outlet shown in Figure 5.8.

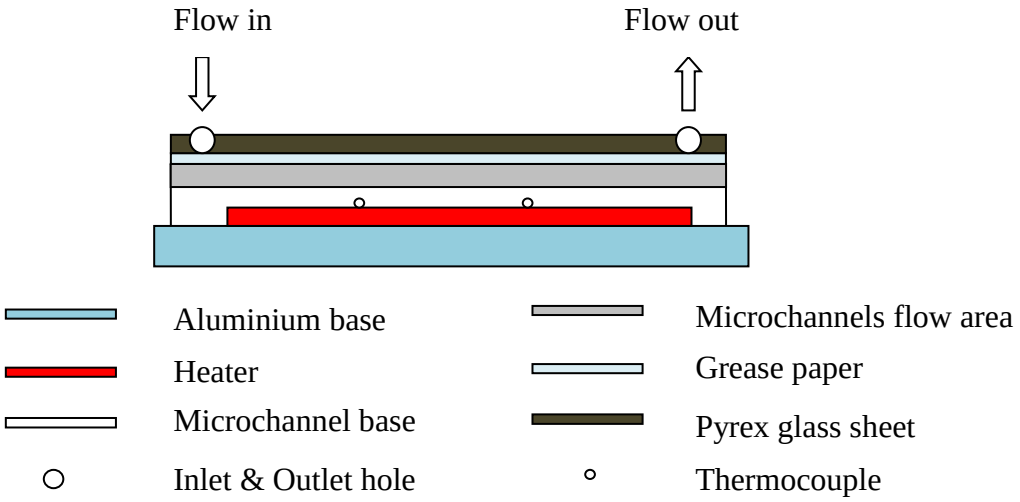

Figure 5.8: Schematic representation of Test section

5.5.2 Syringe pump

A pump is a foremost component for the experimental set up. As experiments were carried out at very low flow rates, so syringe pump was selected for providing the driving force to fluids. A syringe pump (Model no. SP-102) with a control accuracy of ± 5 % programmed by software was procured from E-Spin Nanotech, Kanpur, India. Flow with maximum accuracy was obtained due to their computer controlled drive mechanism. Software was installed in computer as per the guidelines and then made a connection with all the serial cables shown in Figure 5.9 and 5.10. Specifications of syringe pump as follows in Table 5.2.

Table 5.2: Specifications of syringe pump

Syringe pump: Two independent channel with separate drive unit	
Flow rate	1 µl/min to 10 ml/min
Acceptable syringe size	1 ml to 12 ml
Drive mechanism	Computer control
Voltage input	220-240 volt
Control unit	Separated • USB to serial cable • Serial converter • Serial cable (for connecting syringe pump controller to RS-232 converter) • Syringe pump controller • 4 pin connector
Unique characteristics	• Volume and time control • Infusion and withdrawal

Figure 5.9: Syringe pump with serial cables and connector unit

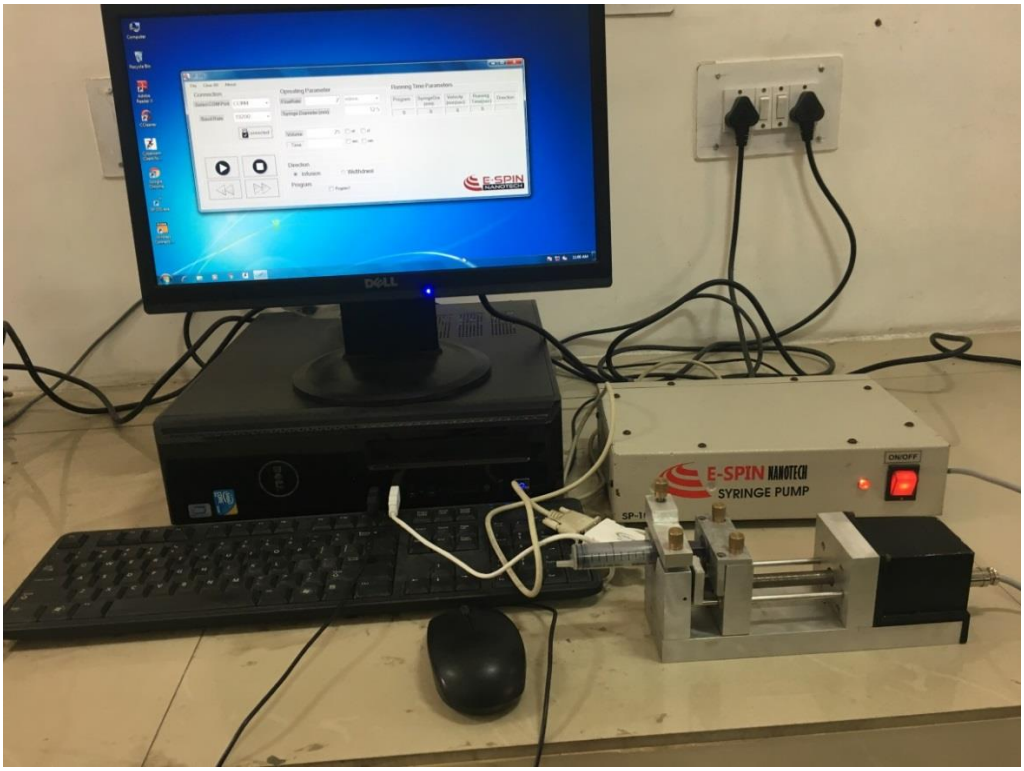

Figure 5.10: Syringe pump with connections and computer program

5.5.3 Pressure measuring device

An inclined manometer at 15º as shown in Figure 5.11 was connected at the inlet and outlet of microchannels for measuring the pressure drop by the fluid when it flows through the

channels. Mercury as a manometric fluid was taken in a manometer to calculate the appreciable pressure drop generated by nanofluid flowing through the channels.

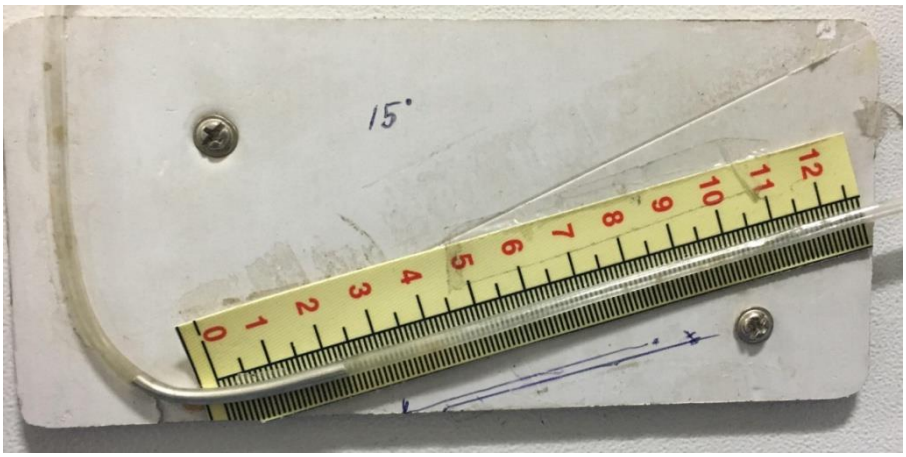

Figure 5.11: Inclined manometer at 15º

5.6 EXPERIMENTAL SET UP

The schematic diagram of experimental setup is shown in Figure 5.12. Base fluids and nanofluids were flowing through the microchannels with the help of syringe pump. Heat was supplied through the heater controlled by variate. Highly sensitive five T-type thermocouples were used to find the fluid and heat sink temperature. Thermocouples were fixed in the storage tank, at inlet and outlet of the channel and bottom of heat sink. The calibration of temperature, voltage and current sensors were done by an ISO accredited laboratory by NABL i.e. NIIRT-Centre for Calibration, Analysis, and Testing, Industrial area, Panchkula, Haryana, India. The uncertainty associated with voltage, current and temperatures are given in Table 5.3. The methodology used for calibration by NABL is SCP-01.TTH for temperature and for voltage and current is SCP-03.ETC and SCP-05.ETC. The inclined manometer is used to measure the pressure drop produced by nanofluids. The clear view of experimental set up with all the connections are shown in Figure 5.12.

Table 5.3: Uncertainty measurements in voltage, current and temperatures

S.No.	Parameters	Uncertainty measurements
1	Voltage	± 1.2 %
2	Current	± 1.2 %
3	Temperature	± 0.3 °C

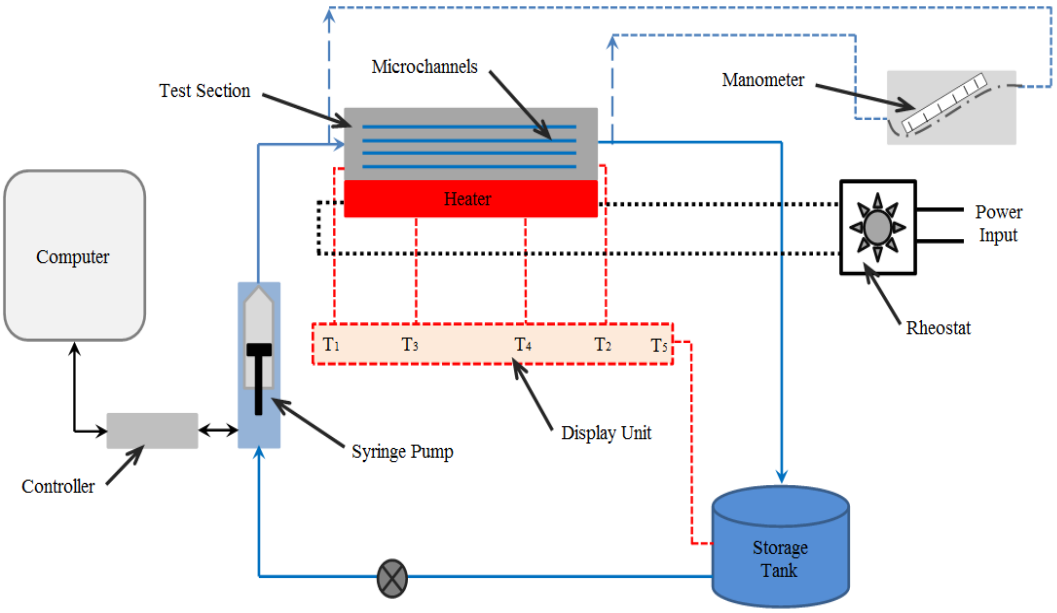

Figure 5.12: Schematic diagram of experimental setup

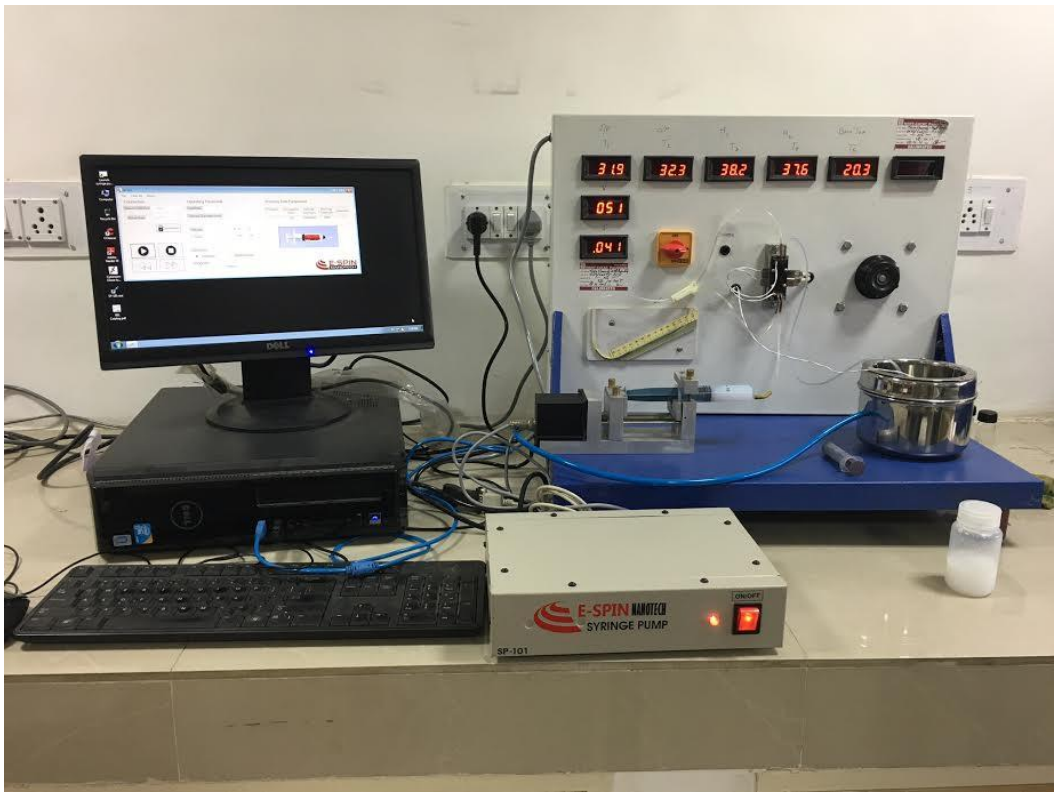

Figure 5.13: Experimental set up

5.7 EXPERIMENTAL PROCEDURE

The thermal and hydraulic performance of MCHS by using nanofluids was investigated at different flow rates of fluids as well as at different heat inputs. Experimentations were carried out at low flow rates of 0.2 ml/min to 2 ml/min as Chein and Chuang [120] studies revealed that nanoparticles did not absorbed extra heat at high flow rates. As no appreciable heat transfer coefficient was observed at 0.2 ml/min so the lowest range was fixed to 0.2 ml/min. And beyond the 2 ml/min, no additional heat transfer was observed for base fluids so maximum limit was fixed to 2 ml/min. Additionally, each test section was tested for different heat inputs such as 2 W, 4 W, and 6 W. More than 6 W heat input, heat sink temperature go beyond 85 °C initiates the boiling of fluids. Thermophysical properties and stability of nanofluids were affected at the high temperatures. So, the experiments were conducted in the range of 2 to 6 W heat loads. For a given heat input and flow rate, readings were measured till the steady state achieved.

First the experiments were conducted for the base fluids i.e. W and W/EG mixtures (90:10, 80:20, 70:30, 60:40 and 50:50). Afterwards, thermal and hydraulic performance of nanofluids was examined by using different nanoparticles such as alumina, CuO and MWCNT at different concentrations and base fluids. Results were compared with the analytical values produce from the analytical model.

The equations used for the experimental calculations are as follows:

Heat absorbed by the coolant during flow in microchannels is

$$q = \dot{m} c_p \Delta T = \dot{V} \rho_f c_p (T_o - T_i) \tag{5.13}$$

To estimate the MCHS efficiency, average heat transfer coefficient of the working fluid through the aluminium microchannels is calculated from heat absorbed by the coolant as

$$h = \frac{\dot{V} \rho_f c_p (T_o - T_i)}{A_{eff} \Delta T} \tag{5.14}$$

$$A_{eff} = N L_{ch} (W_{ch} + 2 \eta_f H_{ch}) \tag{5.15}$$

where, η_f is the fin efficiency assuming as 100 % due to high thermal conductivity aluminium material [2]. $\dot{V}$ is the volumetric flow rate, ρ_f is the density, c_p is the fluid specific heat

flowing in microchannels, N is the total number of microchannels and A_{eff} is the effective heat transfer area of rectangular microchannels. The top wall used for covering the microchannels is excluded in the total area calculations.

The experiments were run till the steady state achieved with the repetition of three consecutive same readings of temperature with time. All the thermophysical properties are calculated at bulk mean temperature. The mean temperature difference such as ΔT is used to estimate the cooling performance of MCHS. This is calculated as

$$\Delta T = T_b - \left(\frac{T_i + T_o}{2} \right) \tag{5.16}$$

where, T_b is the average base temperature of heat sink, T_i and T_o are the fluid temperature at inlet and outlet section.

The heat transfer performance of the nanofluids behaving as a coolant in microchannels in a laminar region of 1< Re <100 is estimated on the basis of dimensionless heat transfer coefficient, Nusselt number, which is defined as,

Nusselt no. $$Nu = \frac{h * D_h}{k_f} \tag{5.17}$$

Prandtl no. $$\mathrm{Pr} = \frac{c_p \mu_f}{k_f} \tag{5.18}$$

Reynolds no. $$\mathrm{Re} = \frac{D_h * u_f * \rho_f}{\mu_f} \tag{5.19}$$

where, ρ_f, μ_f and k_f are the density, dynamic viscosity and thermal conductivity of flowing fluid at bulk mean temperature, D_h is the hydraulic diameter of channel, u_f is the average velocity and h is a heat transfer coefficient calculated from equation 5.2.

The fanning friction factor f is used to determine the flow behavior of nanofluids through aluminium microchannels. It is defined in terms of pressure drop and velocity as

$$f = \frac{D_h \Delta P}{2 \rho_f {u_f}^2 L_c} \tag{5.20}$$

where, u is the average velocity of fluids in aluminium microchannels and L_c is the length of the microchannels. ΔP is the pressure drop calculated from the manometer inclined at an angle θ of 15º giving a differential movement of x of manometric fluid with a density, ρ_m:

$$h_f = \frac{\rho_m x \sin\theta}{\rho_f} \tag{5.21}$$

Thermal resistance is also one of the interpretations to determine the thermal performance of fluid flowing through microchannels. Smaller the thermal resistance shows better thermal performance. It can be evaluated by:

$$Thermal\ resis\tan ce\left(R_{th}\right) = \frac{Mean\ temperature\ difference\left(\Delta T\right)}{Heat\ transfer\ rate\left(q\right)} \tag{5.22}$$

$$\text{or, } R_{th} = \frac{1}{hAe_{ff}} \tag{5.23}$$

5.8 UNCERTAINTY ANALYSIS FOR EXPERIMENTAL MEASUREMENTS

All the experimentally measured properties have some uncertainties which are demonstrated in Table 5.4. Further the final results were also associated with uncertainty which were calculated from the equations 5.25 to 5.30 by using propagation analysis.

$$\frac{\partial A_{eff}}{A_{eff}} = \left[\left(\frac{\partial W_{ch}}{W_{ch}}\right)^2 + \left(\frac{\partial L_{ch}}{L_{ch}}\right)^2 + \left(\frac{\partial H_{ch}}{H_{ch}}\right)^2\right]^{1/2} \tag{5.24}$$

$$\frac{\partial D_h}{D_h} = \left[\left(\frac{\partial W_{ch}}{W_{ch}}\right)^2 + \left(\frac{\partial H_{ch}}{H_{ch}}\right)^2\right]^{1/2} \tag{5.25}$$

$$\frac{\partial q}{q} = \left[\left(\frac{\partial \rho}{\rho}\right)^2 + \left(\frac{\partial c_p}{c_p}\right)^2 + \left(\frac{\partial \dot{V}}{\dot{V}}\right)^2 + \left(\frac{\partial A_{eff}}{A_{eff}}\right)^2 + \left(\frac{\partial T_o}{T_o}\right)^2 + \left(\frac{\partial T_i}{T_i}\right)^2\right]^{1/2} \tag{5.26}$$

$$\frac{\partial h}{h} = \left[\left(\frac{\partial \rho}{\rho}\right)^2 + \left(\frac{\partial c_p}{c_p}\right)^2 + \left(\frac{\partial \dot{V}}{\dot{V}}\right)^2 + \left(\frac{\partial A_{eff}}{A_{eff}}\right)^2 + \left(\frac{\partial T_o}{T_o}\right)^2 + \left(\frac{\partial T_b}{T_b}\right)^2 + \left(\frac{\partial T_i}{T_i}\right)^2\right]^{1/2} \tag{5.27}$$

$$\frac{\partial Nu}{Nu} = \left[\left(\frac{\partial k}{k}\right)^2 + \left(\frac{\partial D_h}{D_h}\right)^2 + \left(\frac{\partial h}{h}\right)^2\right]^{1/2} \tag{5.28}$$

$$\frac{\partial R_{th}}{R_{th}} = \left[\left(\frac{\partial q}{q}\right)^2 + \left(\frac{\partial T_o}{T_o}\right)^2 + \left(\frac{\partial T_b}{T_b}\right)^2 + \left(\frac{\partial T_i}{T_i}\right)^2\right]^{1/2} \tag{5.29}$$

Table 5.4: Uncertainties associated with experimental measured values

S.No.	Parameters (units)	Uncertainty (%)
1	Thermal conductivity, k (W/m.°C)	± 2
2	Density, ρ (kg/m^3)	± 1
3	Viscosity, μ (Pa.sec)	± 1
4	Specific heat, c_p (J/kg.°C)	± 1
5	Flow rate, $\dot{V}$ (ml/min)	± 5
6	Temperature inlet, T_i (°C)	± 1
7	Temperature outlet, T_o (°C)	± 1
8	Temperature base, T_b (°C)	± 1
9	Width of channel, W_{ch} (m)	± 2
10	Height of channel, H_{ch} (m)	± 2
11	Length of channel, L_{ch} (m)	± 2

Above equations are used to calculate the uncertainty of the effective area and hydraulic diameter of microchannels, heat received by the coolant, heat transfer coefficient and dimensionless Nusselt number and the thermal resistance of microchannels heat sink system. The maximum uncertainties are calculated and tabulated in Table 5.5.

Table 5.5: Uncertainties measurements for calculated parameters

S.No.	Parameters (units)	Uncertainty (%)
1	Effective area, $A_{eff,}$ (m)	2.01
2	Hydraulic diameter, D_h (m)	2.01
3	Heat received by the coolant, $q_{f,}$ *(W)*	6.58
4	Heat transfer coefficient, h (W/m^2.°C)	6.61
5	Nusselt number	7.21
6	Thermal resistance, R_{th} (°C/W)	6.72

5.9 CLOSURE

The present chapter discusses in detail about the fabrication of microchannels and further setup design for the heat transfer and fluid flow studies. The setup consists of test section, syringe pump, manometer device and temperature, voltage and current display unit. An analytical model is developed by using Turbo C++ language to correlate the data with

experimental values. All the equations used for the analytical and experimental calculations are discussed. A simplified flow diagram is given which shows the step used to develop a C++ program. The uncertainties in the experimental measurements are also considered with the consideration of uncertainties in all the parameters used for the calculation. The results obtained from experimental setup and analytical model are discussed in detail in next chapter.

CHAPTER 6
HEAT TRANSFER AND FLUID FLOW CHARACTERISTICS

In the previous chapter, C++ program was developed which is used to validate the experimental data. Experimental set up with all the equations used to find the Nusselt number, friction factor and thermal resistance was already discussed in detail. Present chapter carries out the detailed study of nanofluids flow and heat transfer characteristics flowing through microchannels. A general correlation was also developed for Nusselt number and friction factor valid for alumina, CuO and MWCNT based nanofluids. These studies will help in understanding the real picture of nanofluids in microchannels so that it can be further used in any cooling applications. A comparison of all the nanoparticles, base fluids, flow rate and heat inputs made and then an attempt is made to correlate the experimental data with analytical model.

Experiments were performed for different nanoparticles, nanoparticles concentration, base fluids, heat inputs and flow rates as given in Table 6.1.

Table 6.1: List of various parameters used in experimentation

1	Type of nanoparticles	Alumina, CuO, MWCNT
2	Nanoparticles concentration	0.1 vol %, 0.5 vol % and 1 vol %
3	Type of base fluids	W, W/EG (90:10), W/EG (80:20), W/EG (70:30) W/EG (60:40) and W/EG (50:50)
4	Heat inputs	2 W, 4 W and 6 W
5	Flow rate	0.2 ml/min to 2 ml/min (0.333×10^{-8} m^3/s to 3.333×10^{-8} m^3/s)

6.1 HEAT TRANSFER PERFORMANCE OF NANOFLUIDS

The unique characteristics of nanoparticles such as very high thermal conductivity make it more attractive in thermal applications. The thermal performance of nanofluids directly depends on the heat transfer coefficient so it is calculated by taking the difference between average base temperature and bulk mean temperature (average of inlet and outlet temperature). This section discussed the effect of flow rate, heat inputs, type of nanoparticles and their concentration and the base fluids on heat transfer performance of MCHS system.

6.1.1 Effect of heat inputs

Experiments for all the base fluids and nanoparticles at various concentrations were conducted at various heat inputs such as 2 W, 4 W and 6 W. Thermal performance of nanofluids for microchannels are greatly affected by change the heat input of sink. From the Figure 6.1-6.3, it was clearly observed that highest heat transfer coefficient at 4 W while the lowest heat transfer coefficient observed at 2 W. For the heat input of 2 W, temperature of heat sink was 30-35 °C and nanofluids inlet temperature was at room temperature so very less mean temperature difference was observed while at 4 W, heat sink temperature reaches near 50 °C which gives more rise in mean temperature difference. Due to this, heat transfer coefficient is highest for 4 W of heat input. At the heat input of 6 W, heat sink temperature was touches 70 °C which makes the nanofluids unstable as discussed in Chapter 4. Slightly decrease in heat transfer coefficient at 6 W was observed due to the nanoparticles sedimentation at higher temperatures. Heat input capacity may vary according to the size and shape of heat sink and size of microchannels. The present work shows the best result at 4 W either any kind of nanoparticles or base fluids used. Beyond 6 W, nanofluids boiling start as the sink temperature reaches at 95 °C.

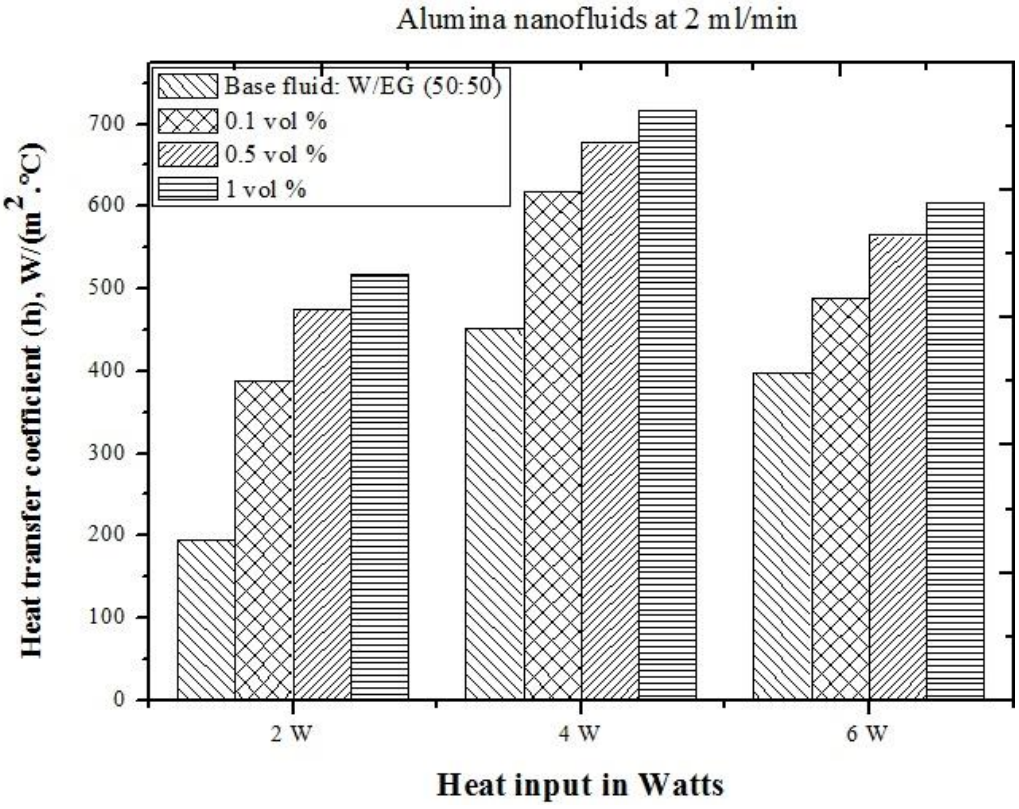

Figure 6.1: Comparison of heat transfer coefficient of alumina nanofluids at different heat inputs

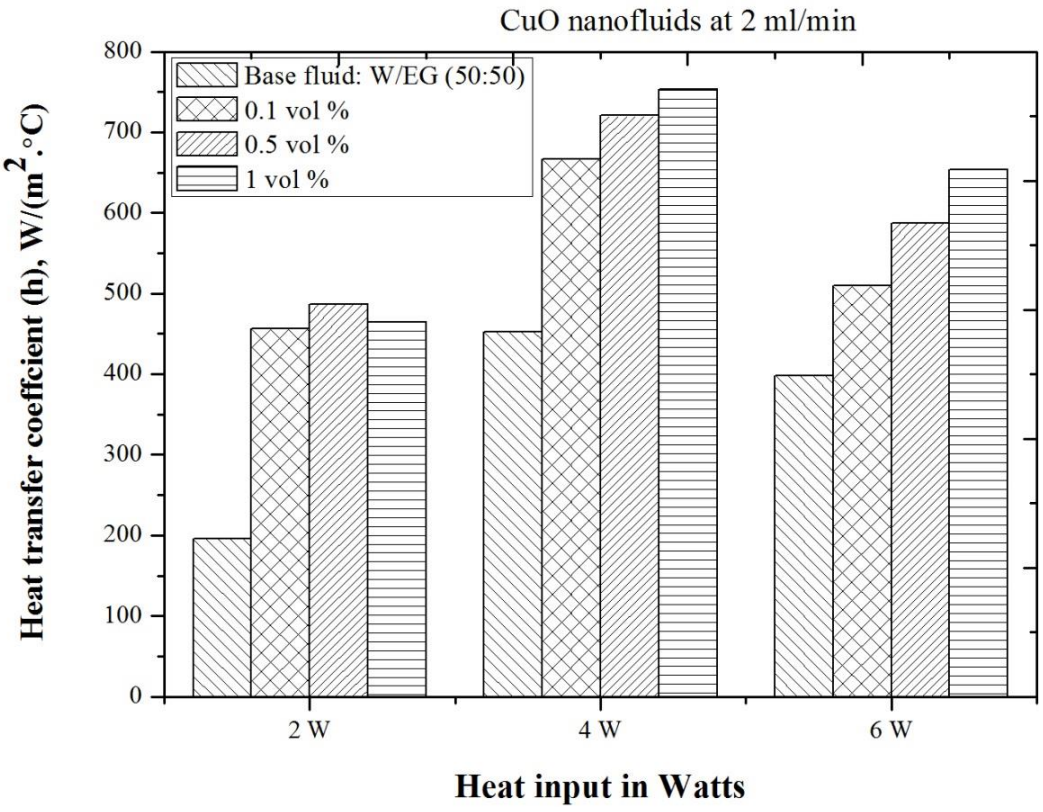

Figure 6.2: Comparison of heat transfer coefficient of CuO nanofluids at different heat inputs

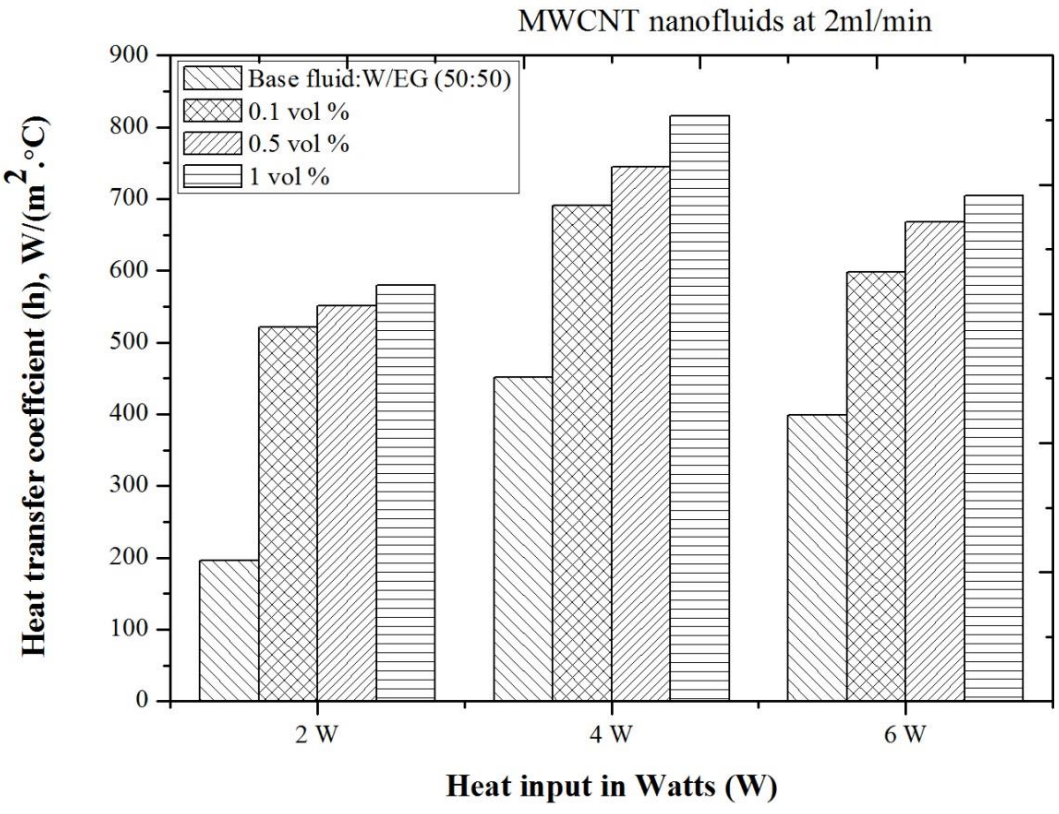

Figure 6.3: Comparison of heat transfer coefficient of MWCNT nanofluids at different heat inputs

6.1.2 Effect of flow rates

The present work carried out for the low flow rates in the range of 0.33×10^{-8} m^3/s to 3.33×10^{-8} m^3/s (0.2 ml/min to 2 ml/min) as most of the literature studies were carried out for the flow rate of 2 ml/min to 20 ml/min [120, 127]. Chein and Chuang [120] found that nanoparticles did not contribute for extra heat absorption at high flow rates i.e. more than 15 ml/min while Wu et al. performed experiments in the range of 2 ml/min to 15 ml/min and observed the appreciable enhancement in heat transfer performance. Very few studies were reported the microchannels heat sink performance at very low flow rates. So, the detailed discussion is carried out with nanofluids flowing through microchannels at low flow rates of less than 2 ml/min.

From the Figure 6.4-6.6, the findings show that at low flow rates such as less than 1.5×10^{-8} m^3/s, very low heat transfer coefficient was observed and moreover, no extra amount of heat absorbed by nanofluids. There was similar trend of heat transfer coefficient observed for all the nanoparticles such as alumina, CuO and MWCNT and the base fluids used for the experimentation. At high flow rates, an appreciable enhancement in heat transfer coefficient was depicted. From the results it was confirmed that better convective heat transfer with nanofluids was obtained at high flow rates i.e. more than 1.5×10^{-8} m^3/s. Maximum enhancement in heat transfer coefficient was observed for 1 vol % of nanoparticles concentration at the flow rate of 3.33×10^{-8} m^3/s reported in Table 6.2.

Table 6.2: Percentage enhancement in Heat transfer coefficient at 3.33×10^{-8} m^3/s

Percentage enhancement in Heat transfer coefficient (At 4 W)									
Type of Base fluids	Nanoparticles volume concentration (%)								
	0.1	**0.5**	**1**	**0.1**	**0.5**	**1**	**0.1**	**0.5**	**1**
	Alumina			CuO			MWCNT		
W	6.20	46	50	23.46	51.9	54.7	37.99	54.65	60.1
W/EG (90:10)	14	45	52.2	26.8	52.4	55.12	41.2	54.8	59.7
W/EG (80:20)	22.3	43	54	32.7	53.5	57.1	43.7	56.7	62.2
W/EG (70:30)	25	46.43	56.45	45.5	56.3	65.91	49.8	60.3	68.4
W/EG (60:40)	36.2	49.3	57.46	46.9	57.9	65.58	51.6	64.4	76.74
W/EG (50:50)	36.5	49.8	58.63	47.4	59.47	66.58	52.8	64.89	80.49

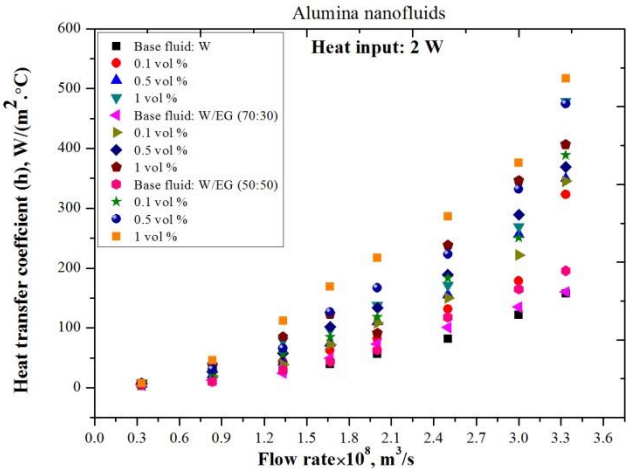

(a)

At heat input of 2 W

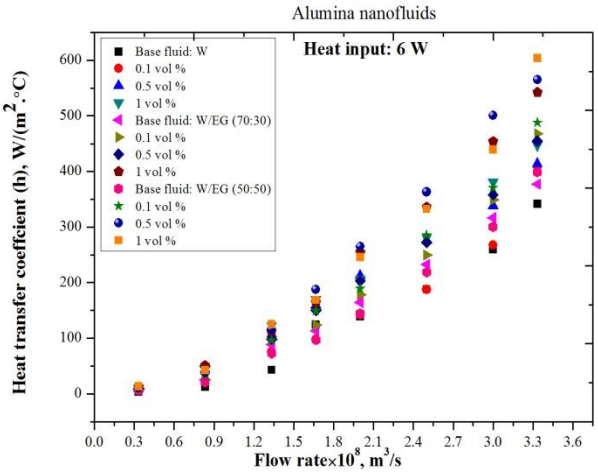

(b)

At heat input of 6 W

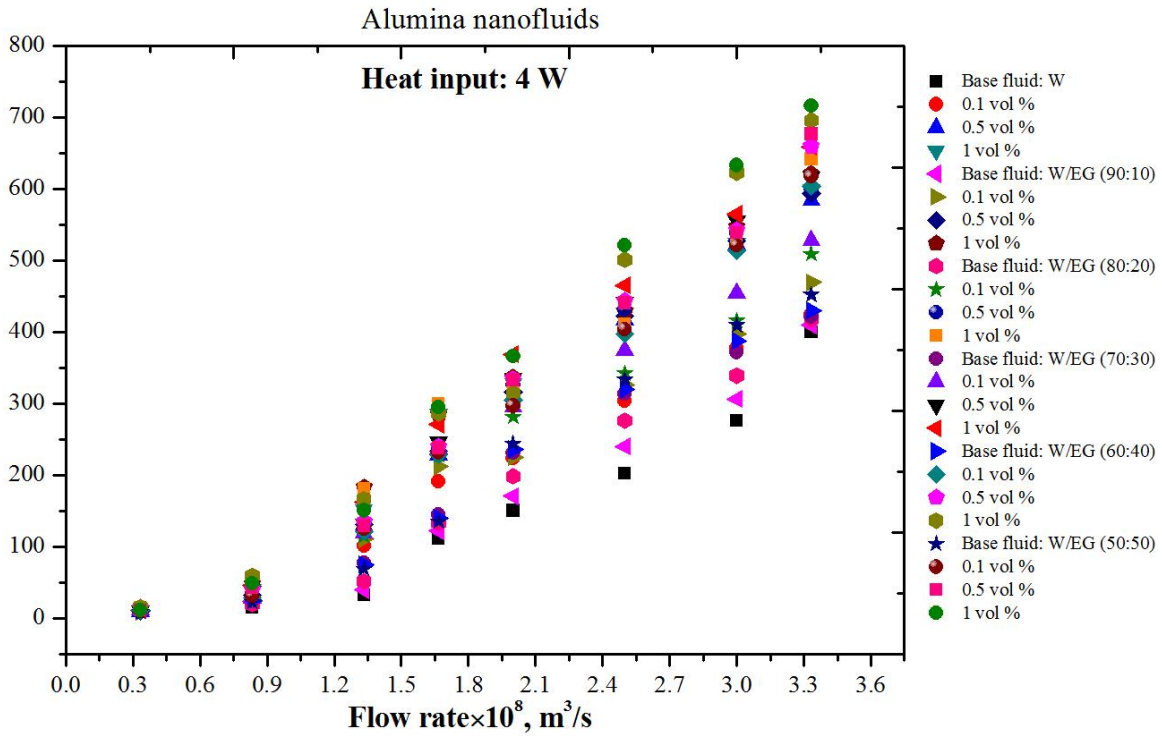

(c)

At heat input of 4 W

Figure 6.4: Heat transfer coefficient of alumina nanofluids in microchannels

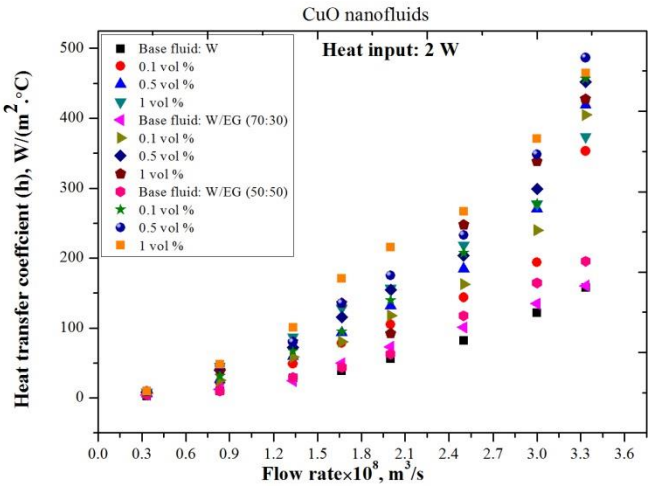

(a)

At heat input of 2 W

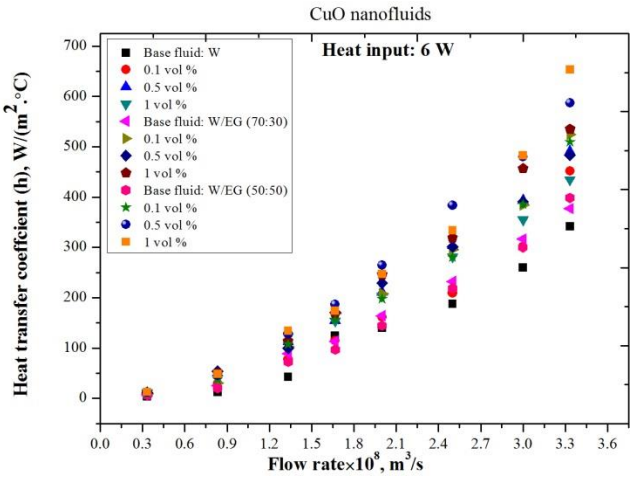

(b)

At heat input of 6 W

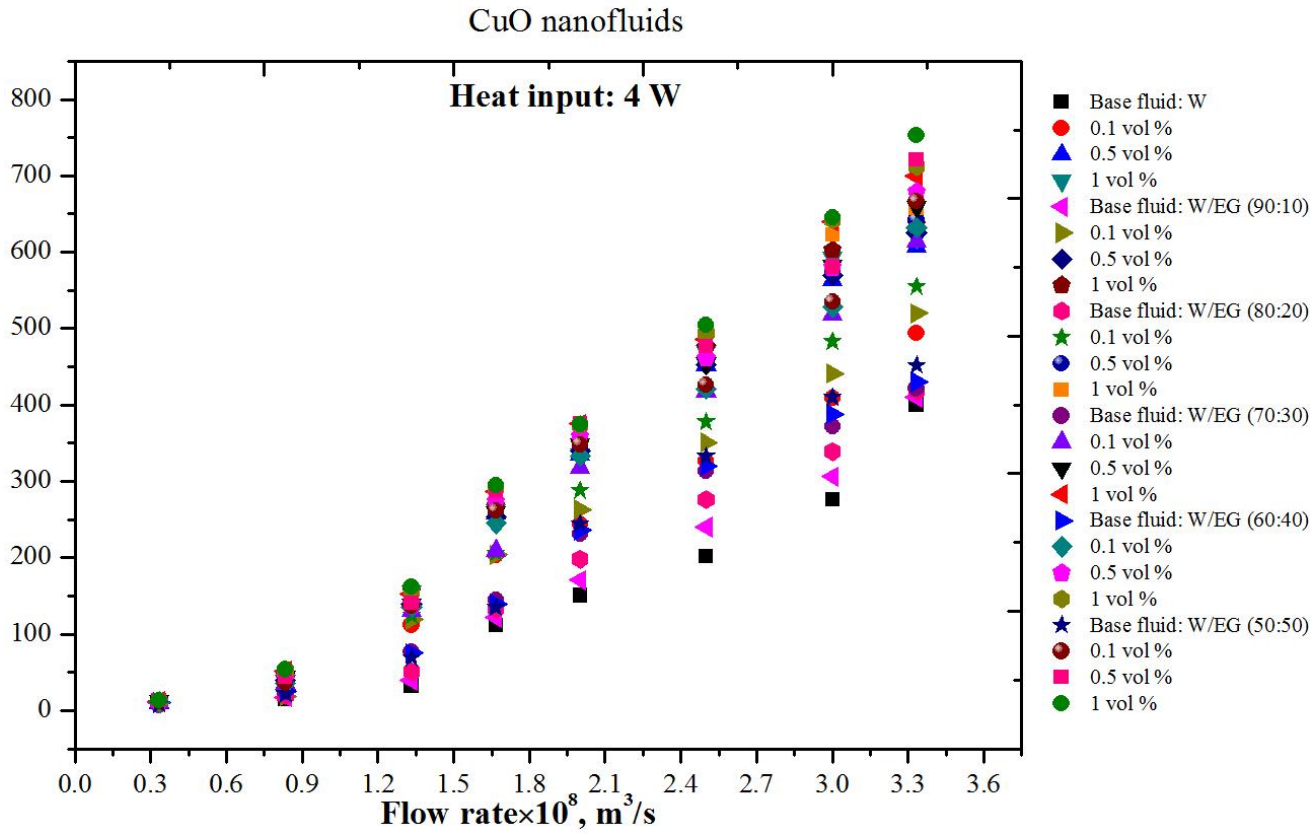

(c)

At heat input of 4 W

Figure 6.5: Heat transfer coefficient of CuO nanofluids in microchannels

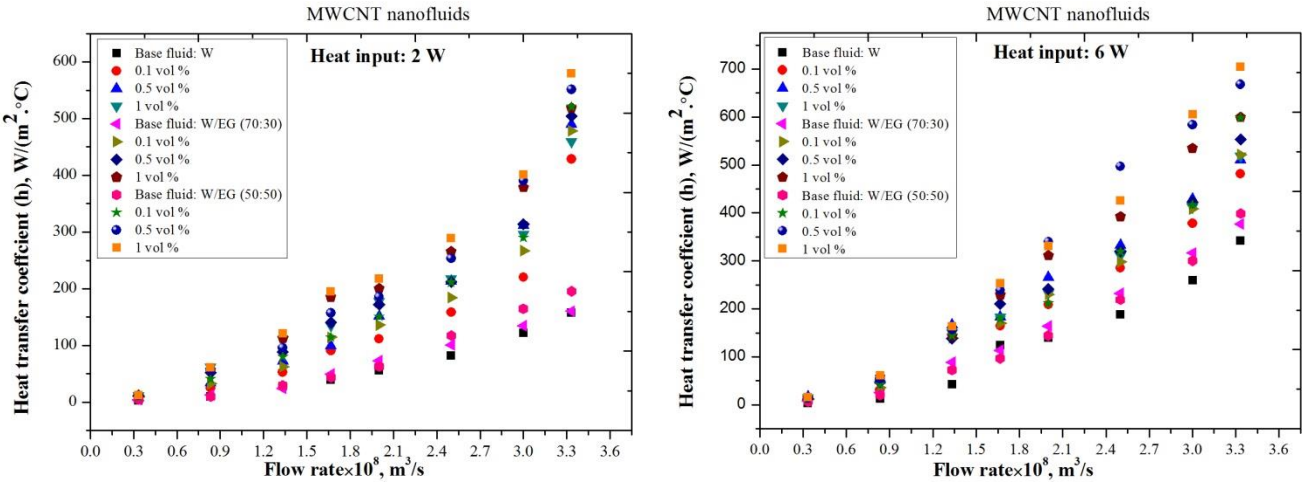

(a) (b)

At heat input of 2 W **At heat input of 6 W**

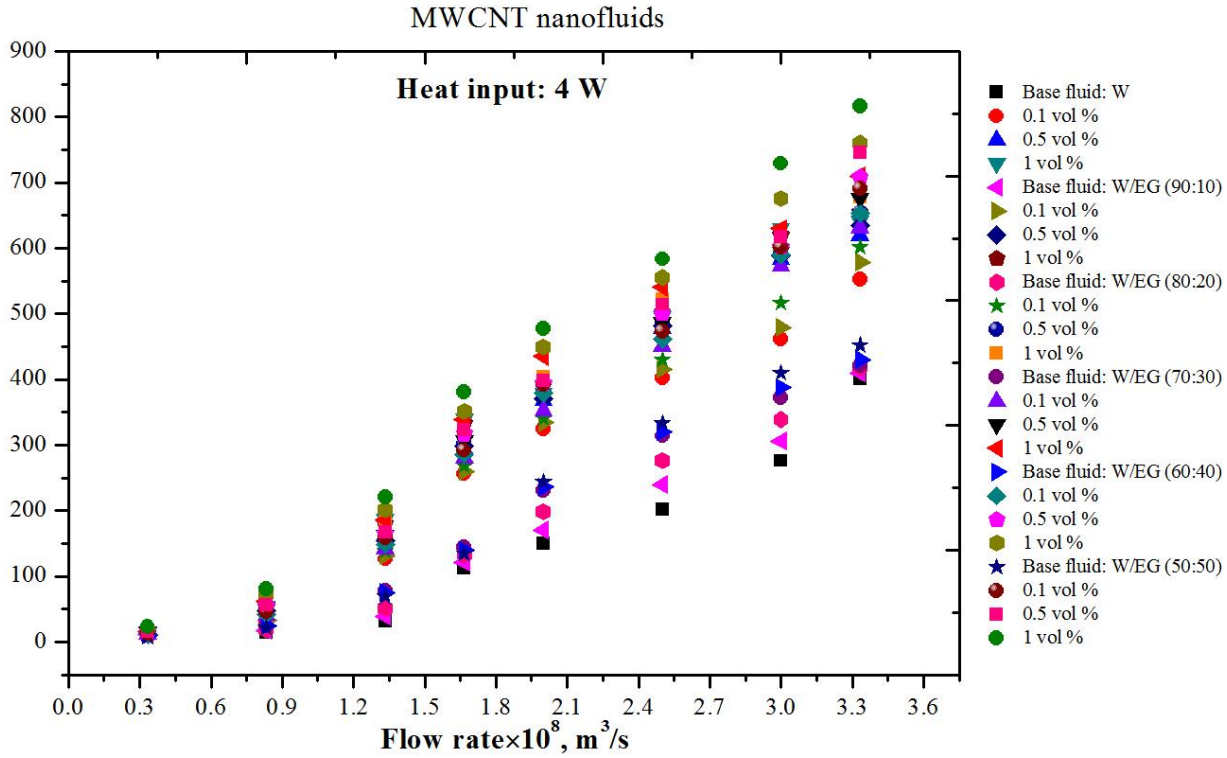

(c)

At heat input of 4 W

Figure 6.6: Heat transfer coefficient of MWCNT nanofluids in microchannels

6.1.3 Effect of base fluids

From the literature it was confirmed that base fluids selection is an equally important as nanoparticles concentration. Experiments were performed with W and W/EG mixtures (90:10, 80:20, 70:30, 60:40 and 50:50) base fluids. With change in base fluids, thermal

performance of nanofluids also varied. It was confirmed in chapter 4 that with increase in ethylene glycol ratio, thermal conductivity enhancement increases and same trend was observed for heat transfer performance of nanofluids as tabulated in Table 6.2. From the Figure 6.7, heat transfer performance of nanofluids with different base fluids has clearly observed.

From the results, it can be depicted that there was less change observed in heat transfer coefficient with the addition of ethylene glycol ratio by 10 in water. The data interpretations is more clear with W, W/EG (70:30) and W/EG (50:50). The heat transfer enhancement for MWCNT-W is 37.99 %, CuO-W is 23.46 %, Alumina-W is 6.2 % and it increased to 52.8 % for MWCNT, 47.4 % for CuO, 36.5 % for alumina nanofluids with W/EG (50:50) base fluids at nanoparticles volume fraction of 0.1 %. Moreover, Figure 6.7 also demonstrates that extremely high heat transfer coefficient was observed for W/EG (50:50) mixtures in comparison with other base fluids either any kind of nanoparticles being used in the system.

6.1.4 Effect of nanoparticles

Heat transfer performance of nanofluids in microchannels heat sink system depends on the type of nanoparticles chosen for preparing the nanofluids. Present work used three types of nanoparticles and compared at same flow rate and heat input condition. From the Figure 6.7, it can be concluded that multiwalled carbon nanotubes have higher heat transfer coefficient while alumina nanofluids show least heat transfer performance. The same behavior of nanoparticles was observed by Mohammed et al. [133] and Kamali et al. [140]. From these studies, it can be concluded that MWCNT-W/EG (50:50) based nanofluids shows higher heat transfer performance of 52.8-80.49 % in comparison with CuO and alumina nanofluids.

6.1.5 Effect of nanoparticles concentration

Nanoparticles volume concentration is an important factor which contributes a lot to enhance the thermal efficiency of system. During experimentation, nanoparticles concentration did not go beyond 1 vol % to avoid the nanoparticles sedimentation and clogging in channels. The increase in thermal conductivity of nanofluids and the Brownian motion with increase in volume concentration is the main reason for enhancing the overall thermal performance of nanofluids with increase in concentration. From the Figure 6.4-6.6, it is clear that thermal performance increases with increase in nanoparticle concentration. Table 6.2 provides the percentage enhancement of heat transfer coefficient at different concentrations.

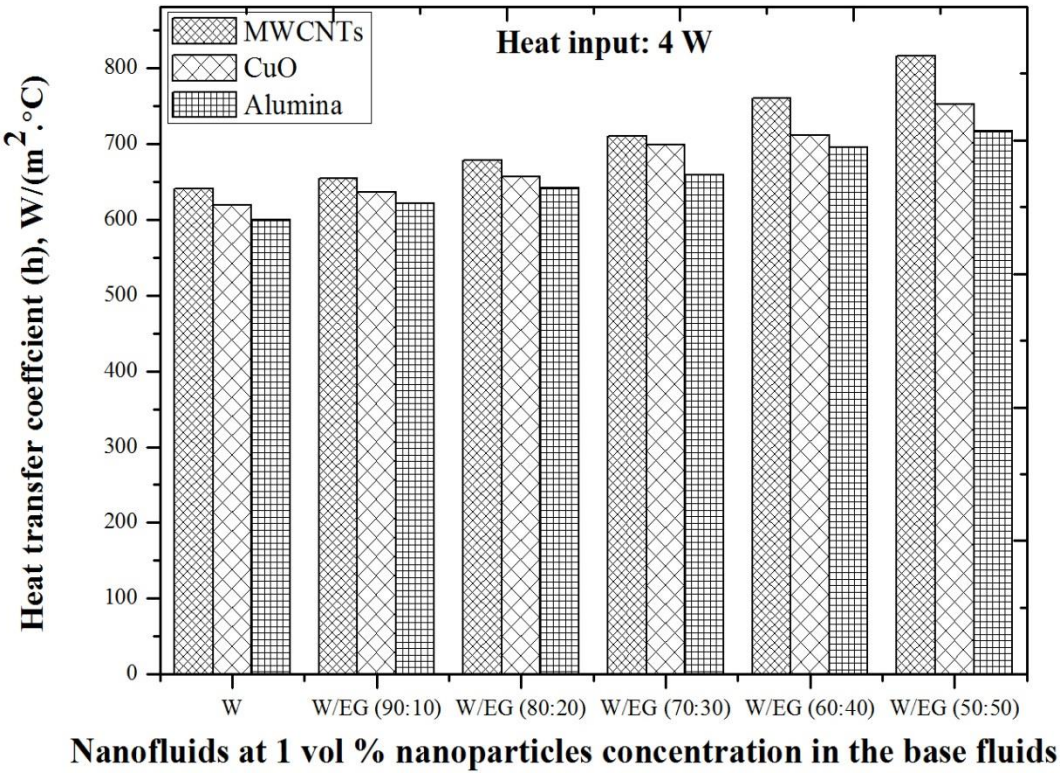

Figure 6.7: Comparison of heat transfer coefficient of Alumina, CuO and MWCNT nanofluids

6.1.6 Nusselt number vs. Reynolds number

Variation of Nusselt number with Reynolds number for alumina, CuO and MWCNT nanofluids are shown in Figure 6.8-6.9. Figure 6.8 makes no clear vision of nanofluids behavior so base fluids with W, W/EG (70:30) and W/EG (50:50) were used for data interpretation. It was shown that Nusselt number variation with Reynolds number followed the similar trend as observed by heat transfer coefficient with the flow rate. Nusselt number increases with increase in nanoparticle concentration as well as with increase in Reynolds number.

The reason for the enhancement of heat transfer in microchannels by using nanoparticles is explained by Wu et al. [127] and Giraldo et al. [162]. They explained the fact that higher enhancement with nanofluids in comparison with the base fluids is due to the nanoparticle interaction with the channel wall and this enhancement is more if the nanoparticles concentration increases. This increases the collision between the nanoparticles and their interaction with the channel walls. Nanoparticles behave as heat carrier which disturbs the boundary layer by colliding with the channels wall. This leads to higher temperature

difference across the wall which results in improved heat transfer rate of nanofluids in comparison with their respective basefluids.

The results also show that EG based nanofluids having higher Nusselt number in comparison with the water based nanofluids. The same trend was observed by Koo and Kleinstreuer [115] and explained the fact that EG based nanofluids had experienced stronger thermal flow developing effects. It can be concluded from the results that even at very low Reynolds number; W/EG (50:50) based nanofluids shows high Nusselt number which was not achieved by water based nanofluids even at higher Reynolds number. The Nusselt number less than 0.7 was observed in our study which was in agreement with the experimental study of Jung et al. [125].

An empirical correlation was developed for dimensionless Nusselt number in terms of dimensionless numbers such as Peclet number (Pe), Reynolds number (Re) and Prandtl number (Pr). This correlation given in equation 6.1 was valid for all the base fluids and nanoparticles used in this work.

$$Nu = 0.1205\,(1 + 4.285\,\phi^{0.854}\,Pe^{0.118})\,Re^{0.133}\,Pr^{0.4} \qquad (6.1)$$

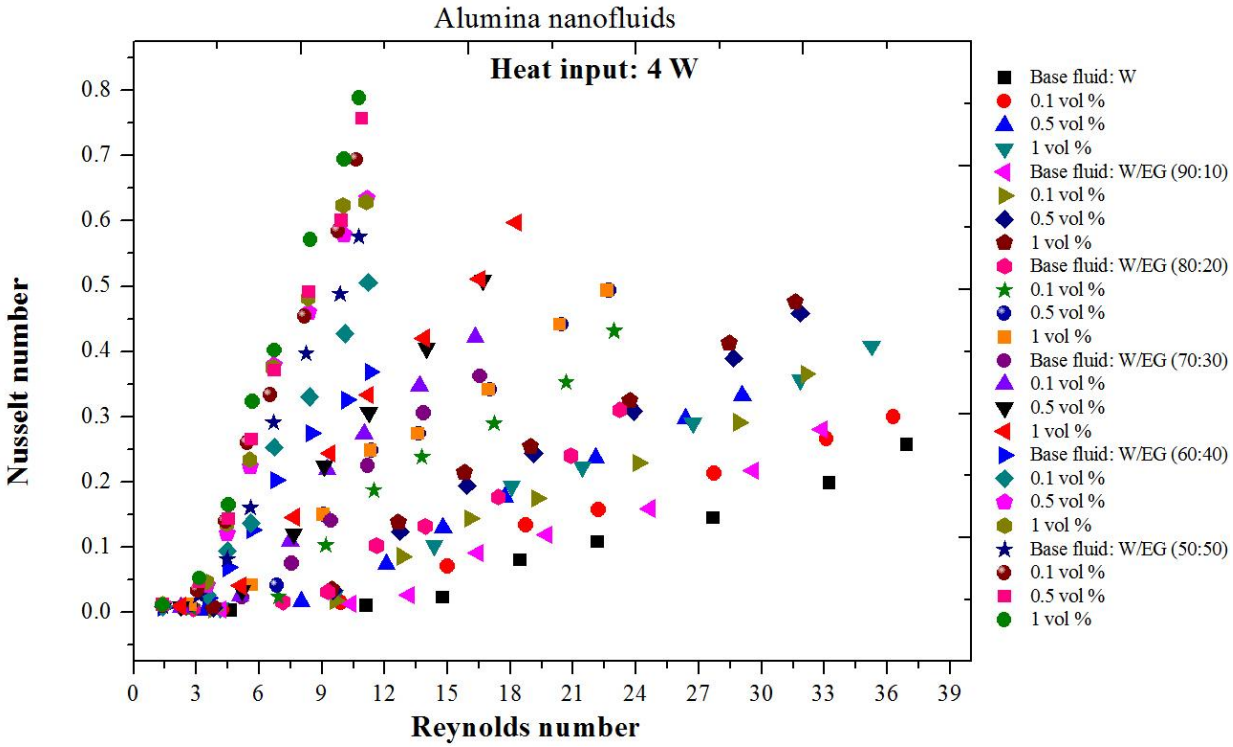

Figure 6.8: Variation of Nusselt number with Reynolds number for alumina nanofluids with all base fluids

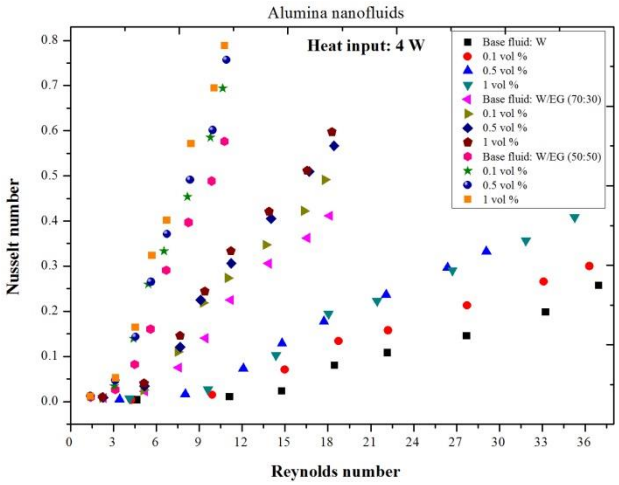

(a)

Alumina nanofluids

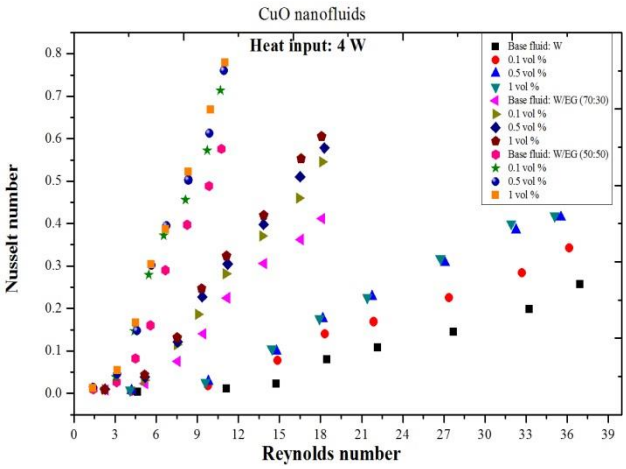

(b)

CuO nanofluids

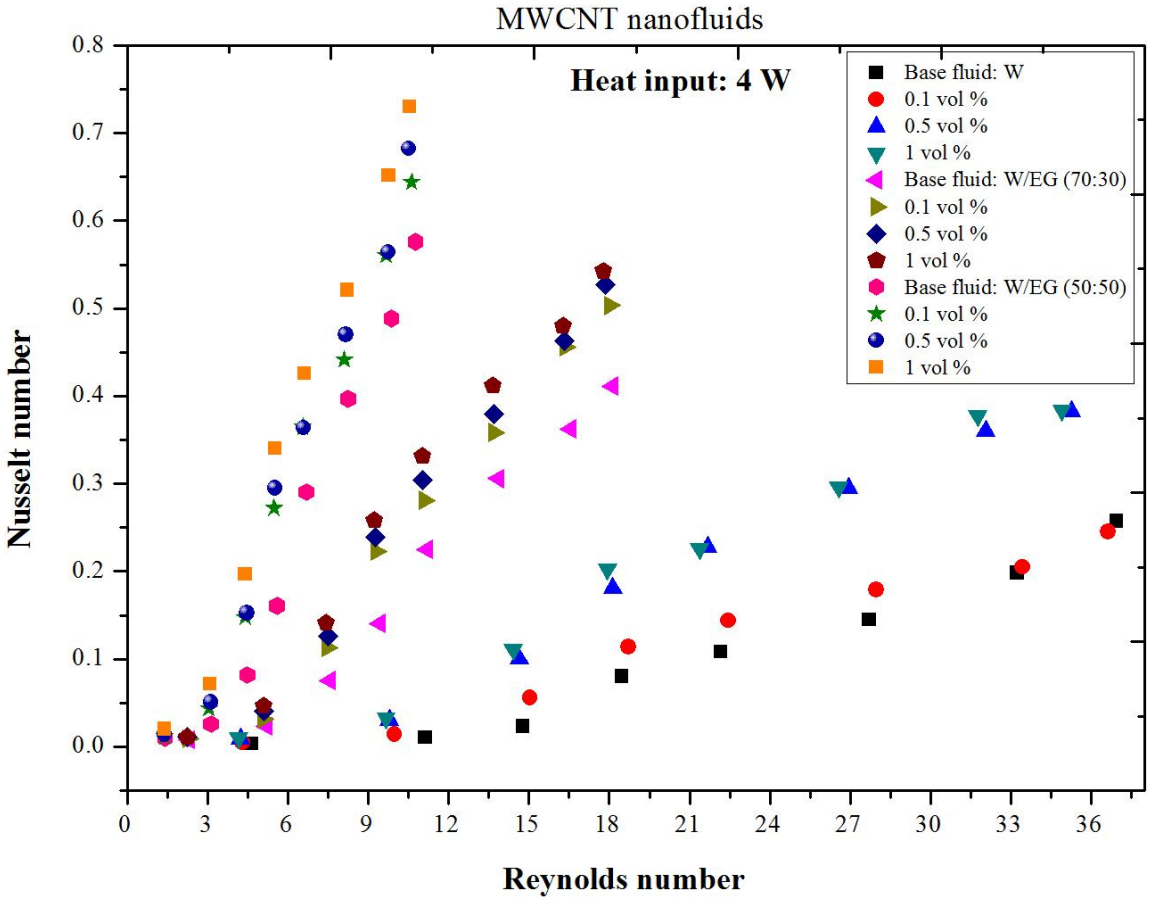

(c)

MWCNT nanofluids

Figure 6.9: Variation of Nusselt number of nanofluids with Reynolds number

6.2 HYDRAULIC PERFORMANCE OF NANOFLUIDS

Experiments were performed at low Reynolds number to know the exact flow behavior of nanofluids in microchannels whether it is fully developed laminar or not. Friction factor for the nanofluids with different base fluids, heat inputs and different type of nanoparticles and their concentration are shown in Figure 6.10-6.12. From the Figures, it can be concluded that at very low Reynolds number, friction factor is quite high which might be a possibility of undeveloped flow. Afterwards, sudden decline in friction factor was observed with increase in the Reynolds number which shows that the fluid flow is fully developed. Friction factor is a function of Reynolds number and it decreases with increase in Reynolds number. The measured values of friction factor are in very low range and even almost same at all the heat inputs. At high Reynolds number, friction factor becomes almost independent of base fluid and nanoparticle concentrations. The change in friction factor with base fluids and concentration was very negligible. At high Reynolds number, the friction factor value for all the nanosuspensions was approximately same. Similar observations for friction factor were made by various researchers [125, 127, 131, 143].

From the results it can be interpreted that there was slightly increase in friction factor of nanofluids was observed when compared with their respective base fluids. For water based nanofluids, friction factor increased for MWCNT, alumina and CuO nanoparticles was 4.9 %, 5.3 % and 6.1% at 1 vol % concentration as compared with the base fluids. As ethylene glycol is more viscous than water, so ethylene glycol based nanofluids have more friction and it increases with increase in ethylene glycol ratio in water. But the increased in friction factor in comparison with their respective base fluids was almost same either any kind of base fluids used. For W/EG (50:50) base fluid, friction factor was increased upto 5.1 %, 5.7 % and 6.6 % for observed for MWCNT, alumina and CuO nanoparticles at 1 vol % concentration. The small rise in friction factor of nanofluids in comparison with their base fluids make it more suitable in any kind of heat transfer applications. Nanofluids flow in microchannels become more appropriate at low flow rates as friction factor rise is very small and heat transfer performance is appreciably worth. From the experimental data, an empirical correlation was developed for friction factor in terms of Reynolds number:

$$f = C\,(Re)^{-2.2196}, \qquad (6.2)$$

where, C is a constant which changes with the type of base fluids are tabulated in Table no. 6.3

Table 6.3: Friction factor constant value for different basefluids

Base fluids	W	W/EG (90:10)	W/EG (80:20)	W/EG (70:30)	W/EG (60:40)	W/EG (50:50)
Constant, C	0.560325	0.2439	0.1989835	0.1540667	0.105942	0.05781667

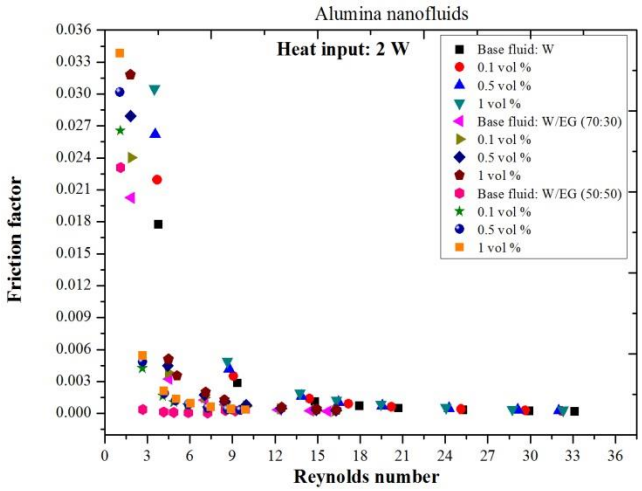

(a)

At heat input of 2 W

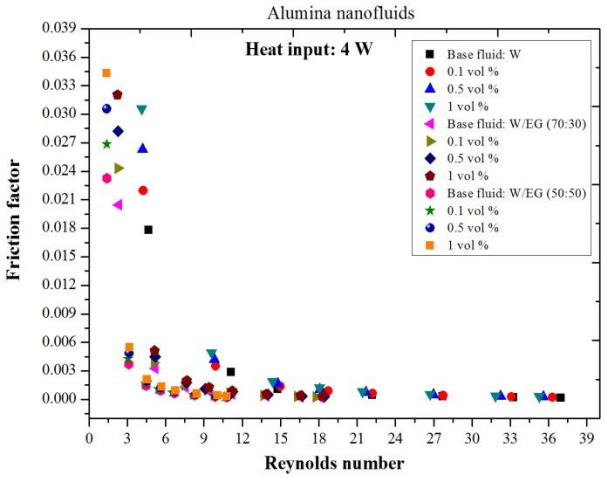

(b)

At heat input of 4 W

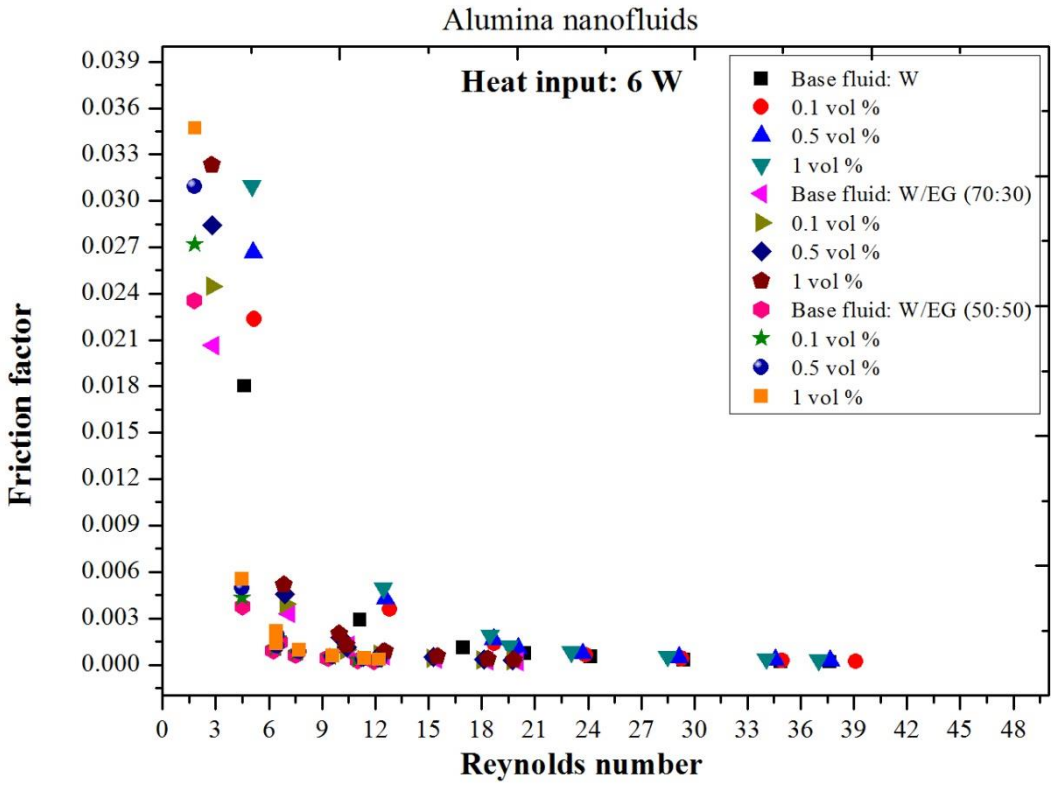

(c)

At heat input of 6 W

Figure 6.10: Variation of friction factor with Reynolds number for alumina nanofluids

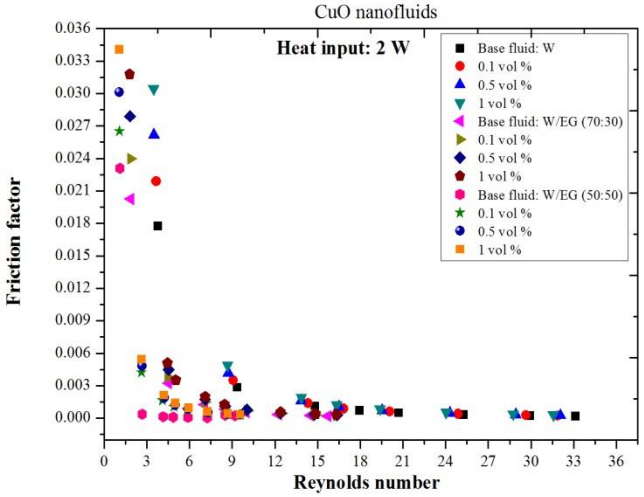

(a)

At heat input of 2 W

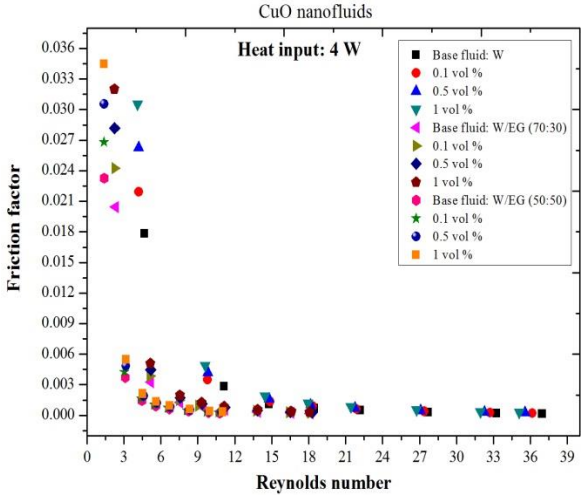

(b)

At heat input of 4 W

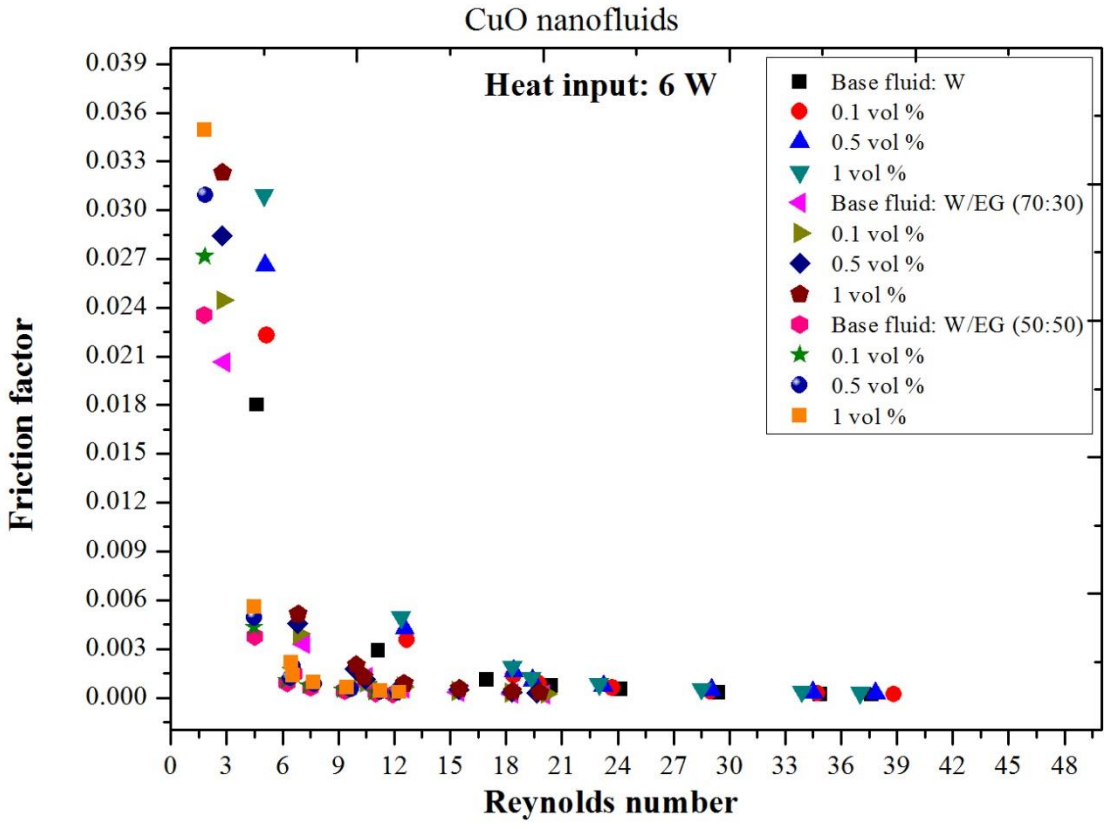

(c)

At heat input of 6 W

Figure 6.11: Variation of friction factor with Reynolds number for CuO nanofluids

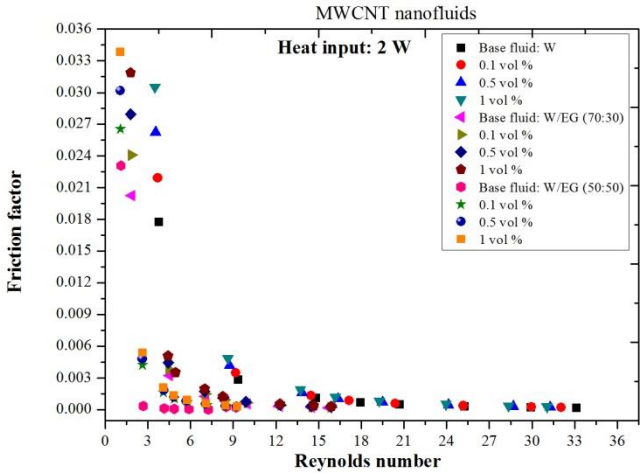

(a)

At heat input of 2 W

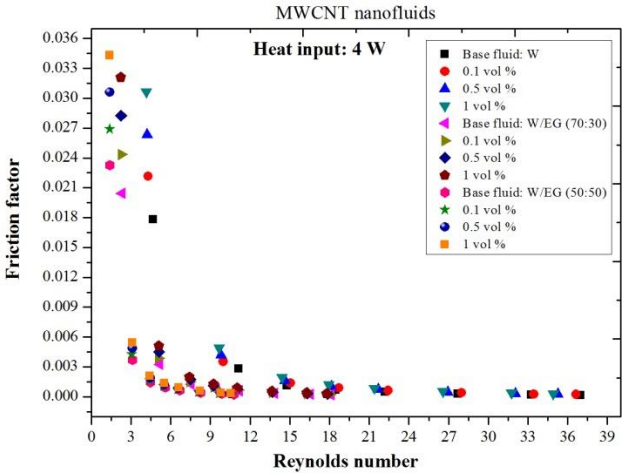

(b)

At heat input of 4 W

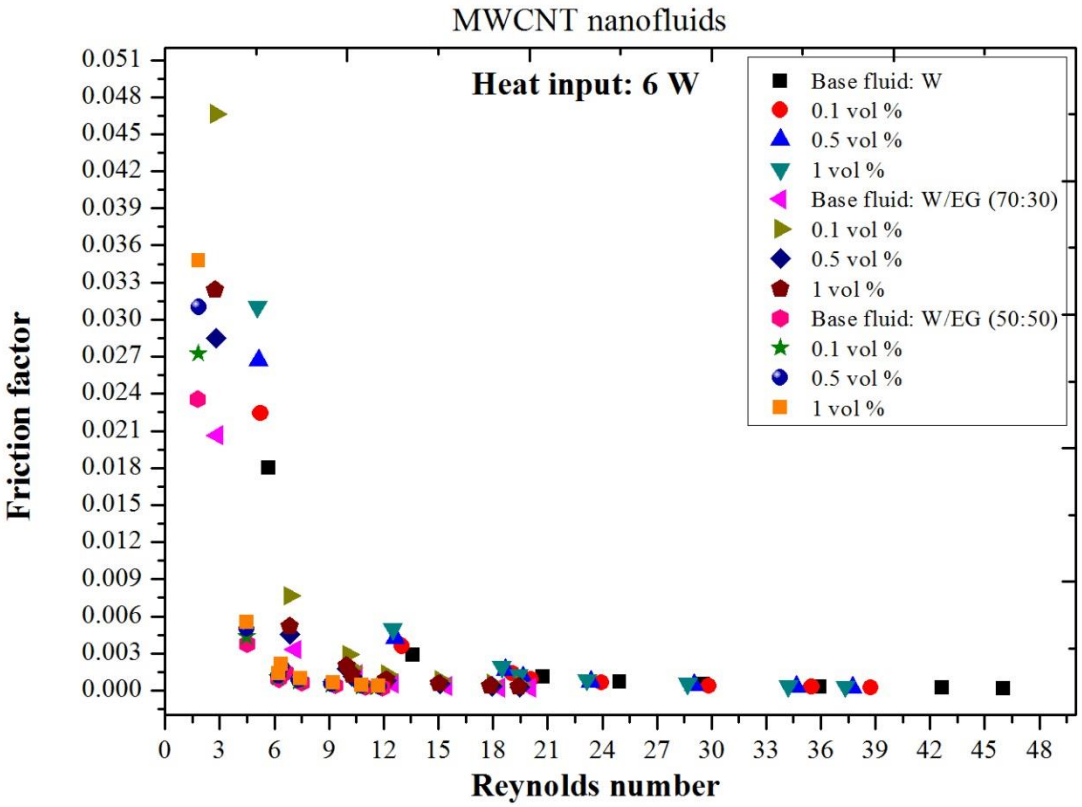

(c)

At heat input of 6 W

Figure 6.12: Variation of friction factor with Reynolds number for MWCNT nanofluids

6.3 THERMAL RESISTANCE

Thermal resistance is one of the most important parameter for deciding the cooling performance of microchannels. Lower the thermal resistance value, better the thermal performance of nanofluids in microchannels. To conclude the thermal performance of nanofluids in microchannels, thermal resistance was calculated. Thermal resistance comparison was made for different heat inputs and Reynolds number as well as for different base fluids and nanoparticles and their volume concentration. The effects of these factors are discussed as follows:

6.3.1 Effect of heat inputs

From the above results, it was clear that better heat transfer in terms of convective heat transfer coefficient achieved at a heat input of 4 W. Thermal resistance variations with Reynolds number at different heat inputs are plotted in the Figure 6.13-6.15. It can be depicted from these figures that nanofluids flow through microchannels at the heat input of 4 W shows less thermal resistance in comparison with 2 W and 6 W heat input. At the heat input of 6 W, nanofluids resistance increases to small extent in comparison with 4 W which might be related with the instability of nanofluids at higher temperatures. Still, thermal resistance at 6 W is less in comparison with thermal resistance at 2 W. At a given heat input of 2 W, temperature of heat sink is not so high, therefore, very low amount of heat get absorbed by the working fluid results into not appreciable outcomes.

6.3.2 Effect of Reynolds number

Experiments were performed at low Reynolds number to observe the exact performance of nanofluids in microchannels. This is clear from the Figures 6.13-6.15 that at very low Reynolds number, thermal resistance is very high and with increase in Reynolds number, resistance decreases. The same trend was followed by friction factor at low Reynolds number. From these results, it was confirmed that fluid flow at low Reynolds number was not suitable for MCHS (Table 6.4). In addition to this, at high Reynolds number thermal resistance becomes almost same i.e. less than 0.5 for all the nanoparticles and the base fluids.

Table 6.4: Range of Reynolds number not suitable for MCHS

Basefluids used	W	W/EG (90:10)	W/EG (80:20)	W/EG (70:30)	W/EG (60:40)	W/EG (50:50)
Reynolds number (less than or equal)	14	13	9	7	5	4

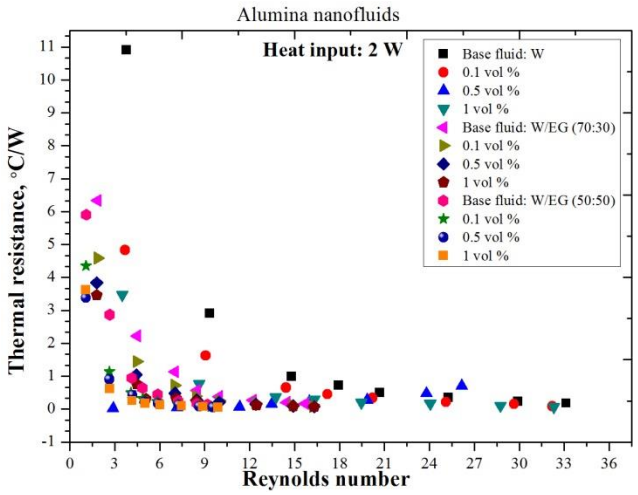

(a)

At heat input of 2 W

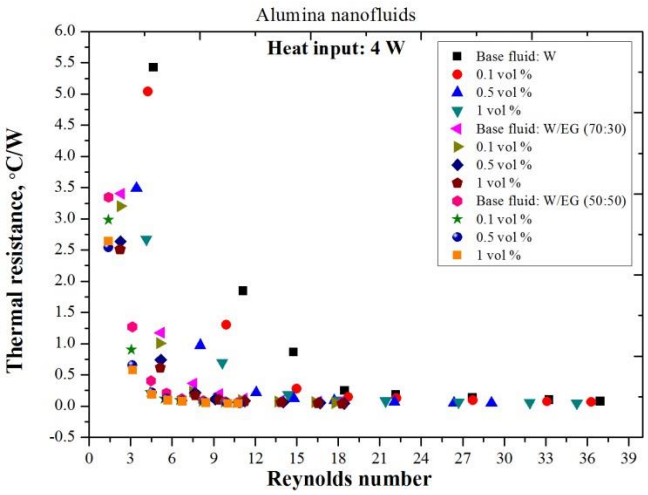

(b)

At heat input of 4 W

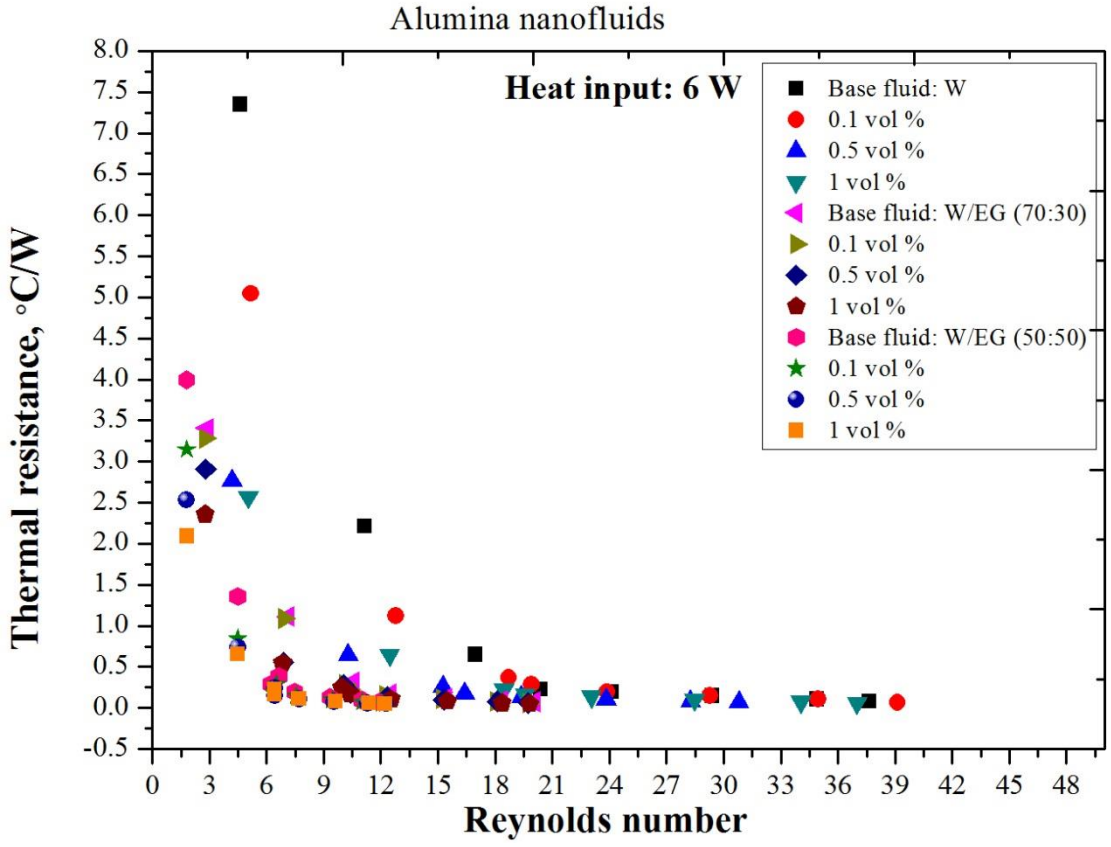

(c)

At heat input of 6 W

Figure 6.13: Thermal resistance with Reynolds number for alumina nanofluids

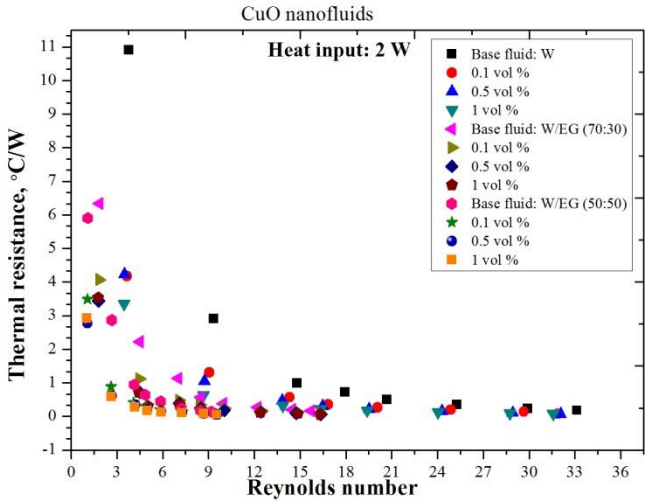

(a)

At heat input of 2 W

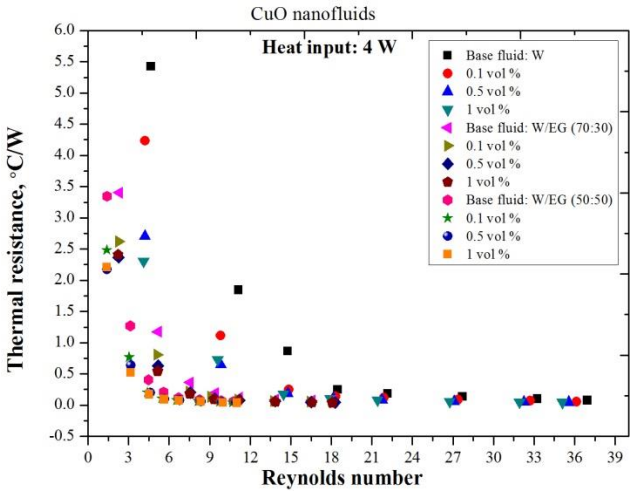

(b)

At heat input of 4 W

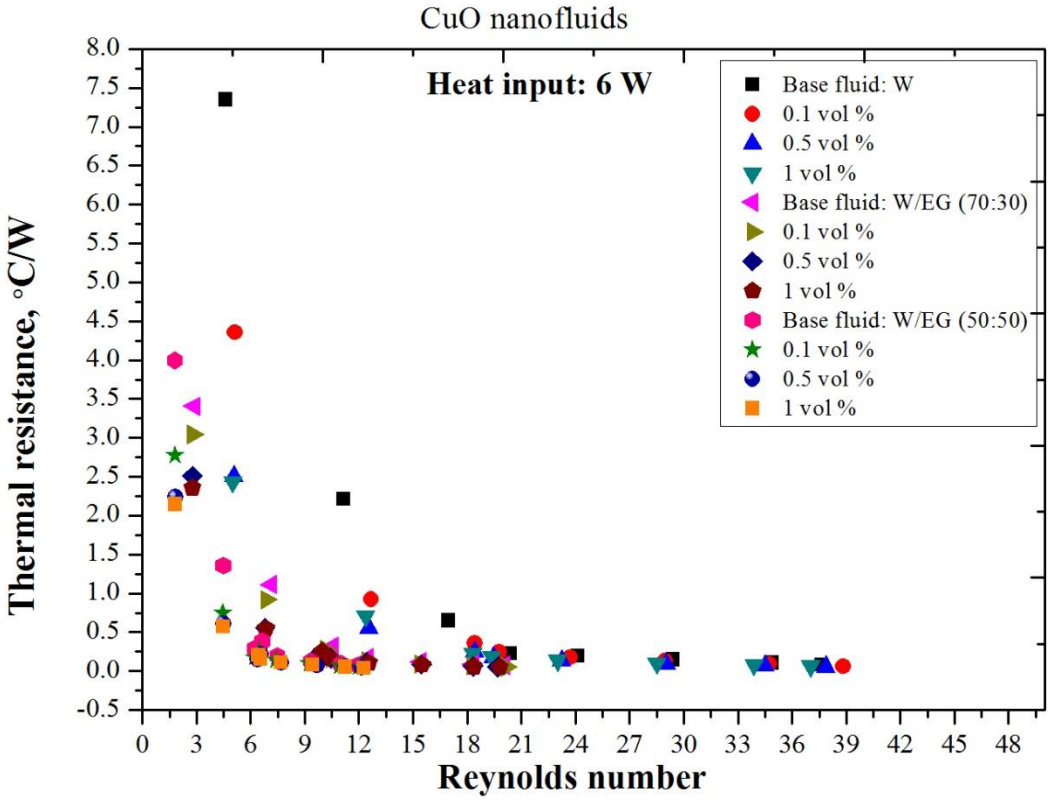

(c)

At heat input of 6 W

Figure 6.14: Thermal resistance with Reynolds number for CuO nanofluids

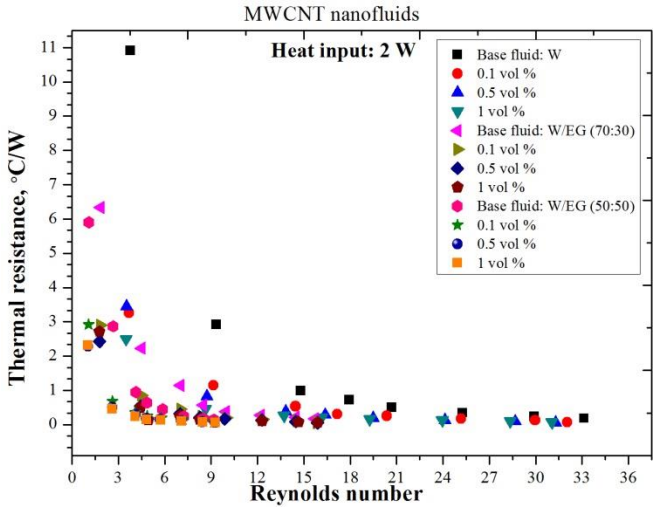

(a)

At heat input of 2 W

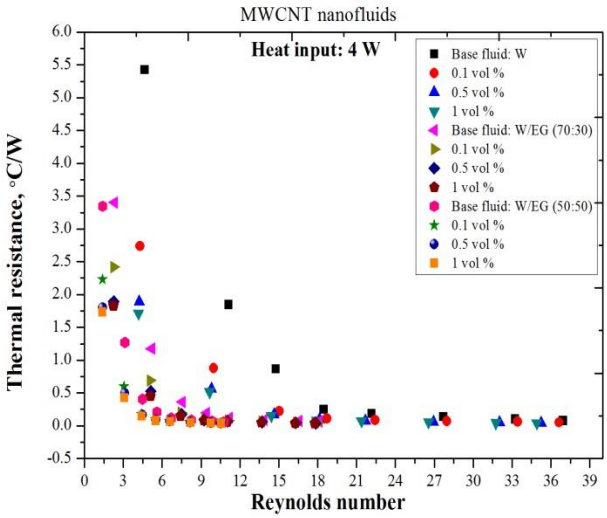

(b)

At heat input of 4 W

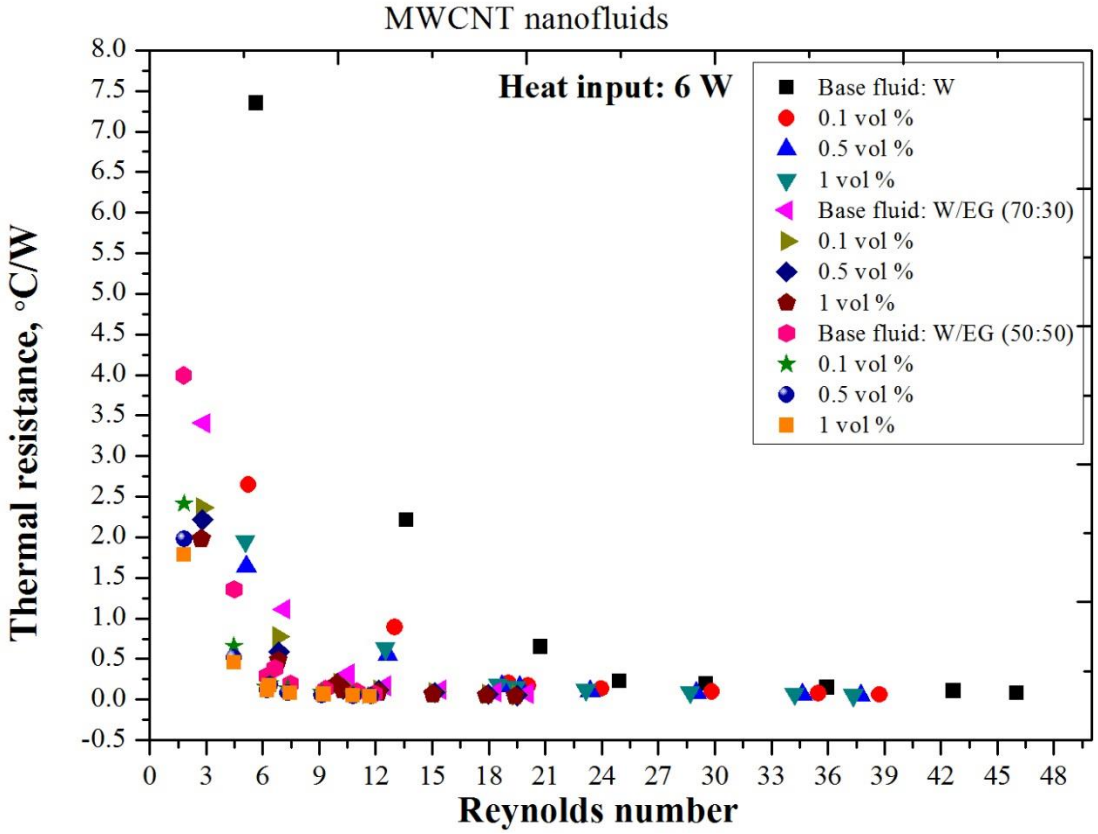

(c)

At heat input of 6 W

Figure 6.15: Thermal resistance with Reynolds number for MWCNT nanofluids

6.3.3 Effect of base fluids

Base fluids such as W with 0.1 vol % nanoparticles concentration have highest thermal resistance in comparison with the other base fluids. Further, W/EG (50:50) base fluid with the nanoparticles had lowest thermal resistance in comparison with other base fluids. From the Figure 6.16, it can be clearly observed that thermal resistance decreases with increase in the ethylene glycol ratio in water.

6.3.4 Effect of nanoparticles and its volume concentration

It can be concluded that with the addition of nanoparticles in the base fluids, sudden deduction in thermal resistance was observed [127] as depicted from the Figures 6.13-6.15. A maximum thermal resistance was reduced with MWCNT in comparison with the alumina and CuO as shown in Figure 6.16. At a fixed flow rate and nanoparticle concentration (2 ml/min and 0.1 vol %), thermal resistance was reduced by 29 % for MWCNT-W nanofluid and maximum reduced upto 56 % for MWCNT-W/EG (50:50) nanofluid. The 18 % reduction in thermal resistance was observed for alumina-W nanofluids and it reaches to 42 % for alumina-W/EG (50:50) nanofluid. Moreover, with CuO nanoparticles thermal resistance reduced by 33 % with water and 48 % with W/EG (50:50) base fluids. Further, thermal resistance was also reduced by increase in nanoparticle concentration. Maximum thermal resistance is decreased by 61 % with MWCNT- W/EG (50:50) nanofluid at 1 vol % nanoparticle concentration.

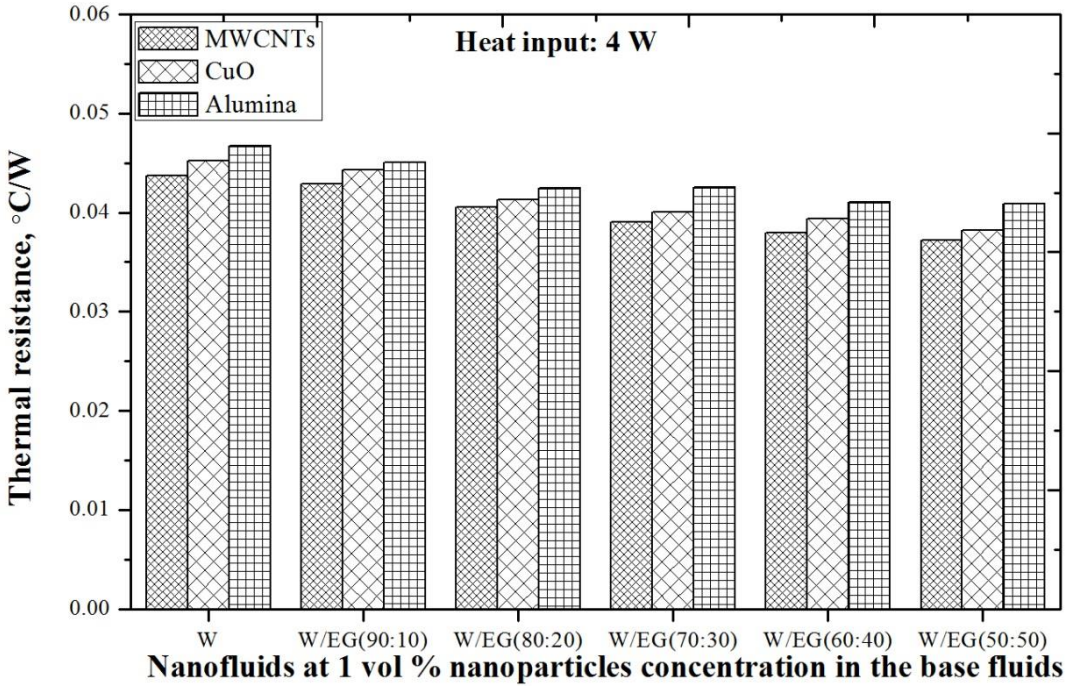

Figure 6.16: Comparison of thermal resistance of Alumina, CuO and MWCNT nanofluids

6.4 HEAT REMOVAL FROM MCHS

Thermal performance or the efficiency of MCHS is important to decide and it depends on the amount of heat removed from MCHS by using nanofluids. At 2 ml/min, maximum 65 % heat is removed by MWCNT-W nanofluids while nanoparticles with W/EG (50:50) base fluids remove less heat in comparison with other fluids as shown in Figure 6.17. But the overall enhancement in heat transfer in comparison with their respective base fluids was more for W/EG (50:50) base fluids either any kind of nanoparticles used. Maximum 22 % enhancement in heat transfer was observed for MWCNT-W/EG (50:50) nanofluids in comparison with their respective base fluids (Figure 6.18).

These results are seemed to be very important for microchannels heat sink and it can be easily implement to the industrial scale project as an efficient amount of heat was removed from the system by using nanofluids.

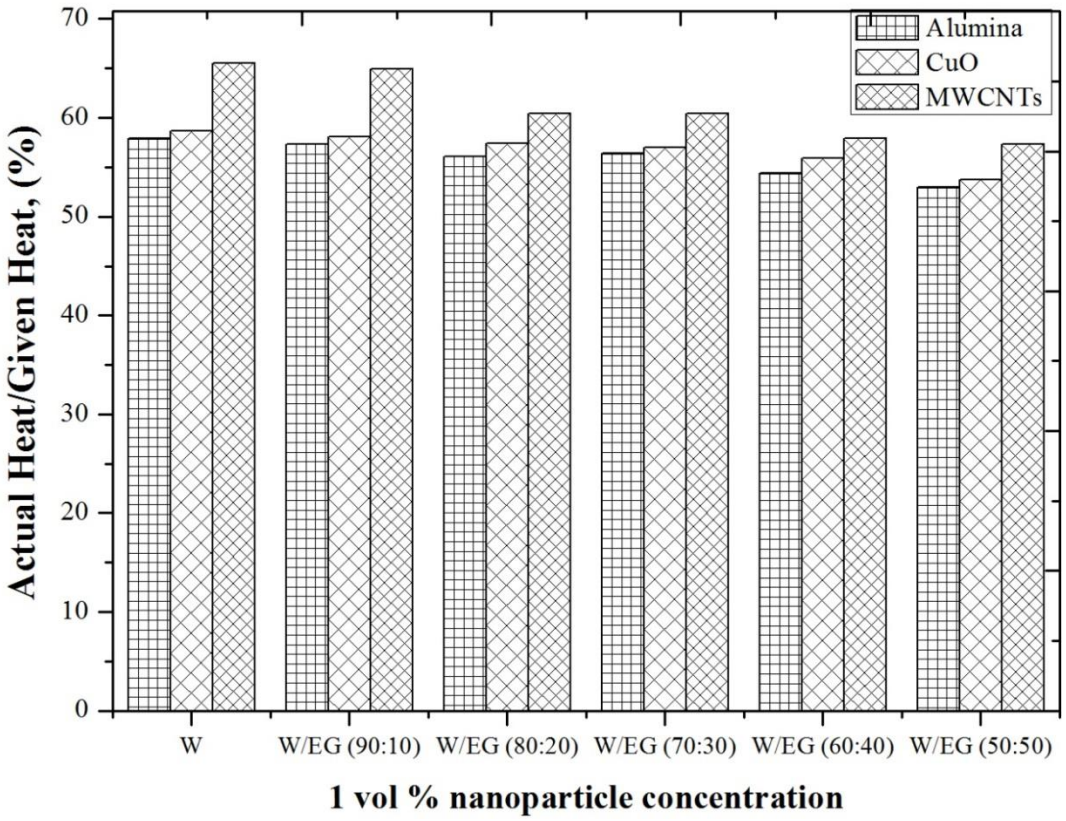

Figure 6.17: Overall heat removal from the MCHS

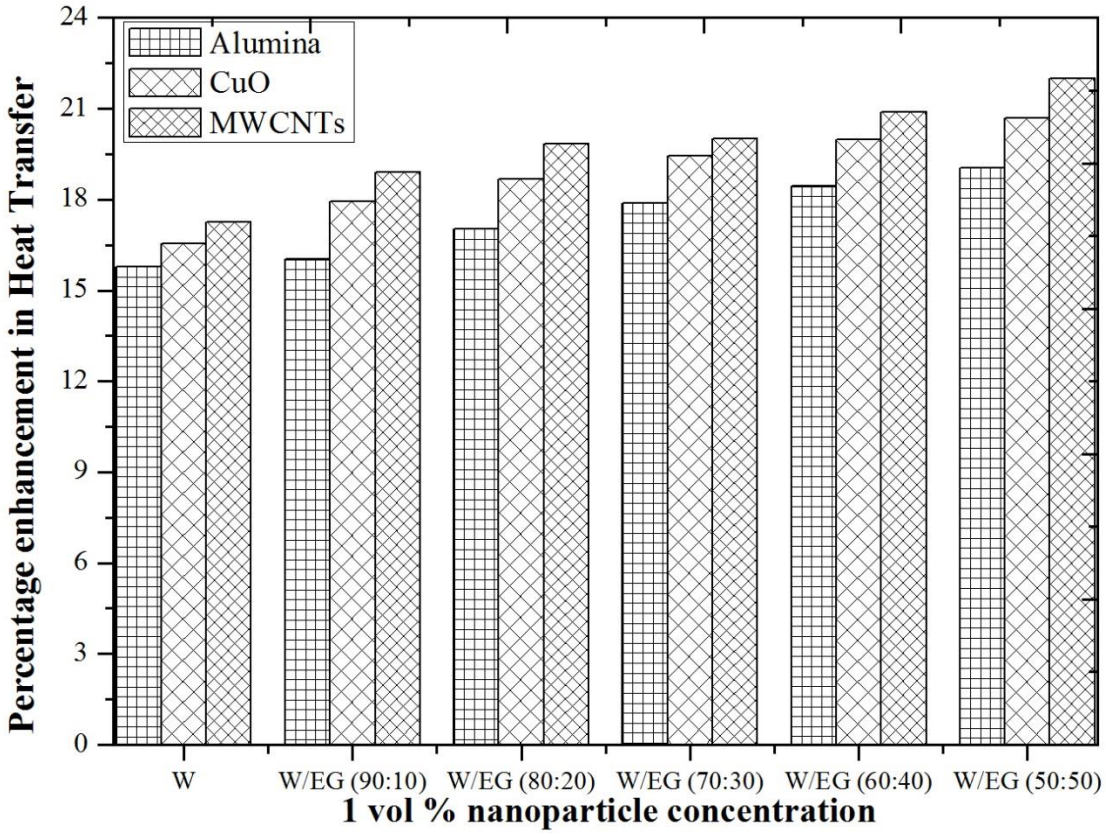

Figure 6.18: Percentage enhancement in heat transfer from the MCHS

6.5 COMPARISON OF EXPEIMENTAL DATA WITH ANALYTICAL MODEL

A computer program was developed from the standard heat transfer equations and empirical correlations obtained from the experimental data. By giving the input of fluid inlet temperature and specifications of microchannels geometry and heater, final outlet temperature of fluid obtained and further at this outlet temperature, Nusselt number, Reynolds number and friction factor calculated. Afterwards, both the experimental data and the data obtained from the analytical model were validated.

From the Figure 6.19, it can be found that experimental observed Nusselt number shows a good agreement with analytical data. The analytically obtained Nusselt number shows ± 15 % deviation with the experimental readings. There was 7.2 % uncertainty associated with Nusselt number calculated experimentally as tabulated in Table 5. So, ± 15 % deviation of analytical data with experimental data is in acceptable range. Both experimentally observed Reynolds number and friction factor deviates in the range of less than ± 10 % with their analytical data as shown from Figure 6.20-6.21. This shows a very good agreement between experimental and analytical data. Hence, both the model and experiments are best fit for each other. Hence, this model is valid for alumina, CuO and MWCNT nanoparticles for 0.1 to

1 vol % concentration with the combination of W or W/EG mixtures (90:10, 80:20, 70:30, 60:40 and 50:50) base fluids.

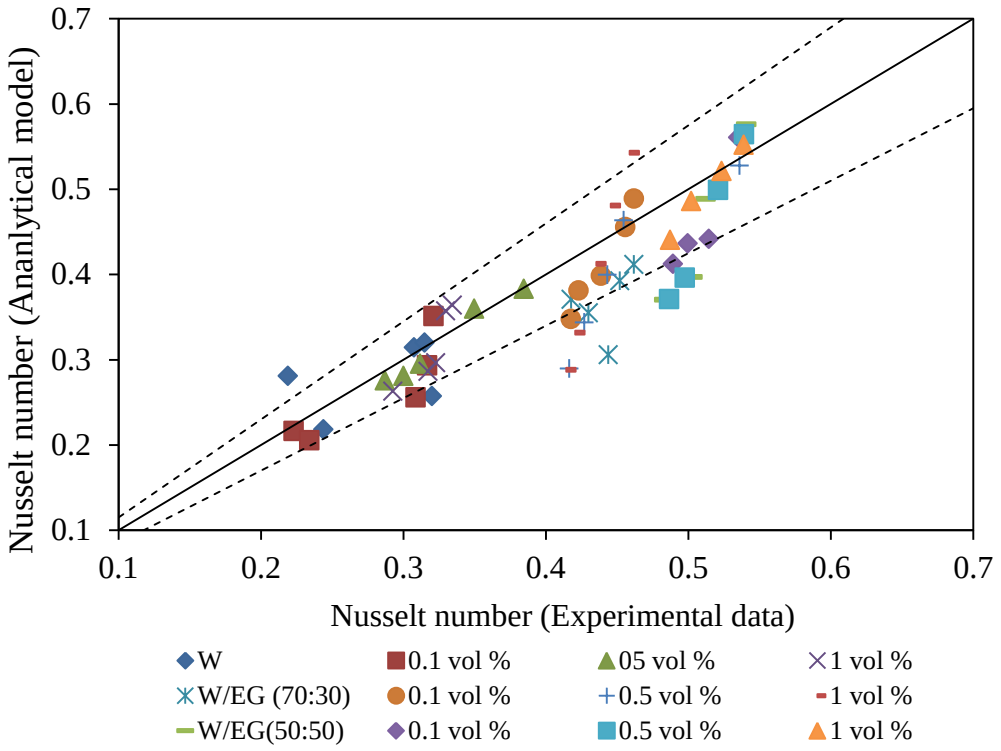

Figure 6.19: Correlation of analytical Nusselt number with experimental data

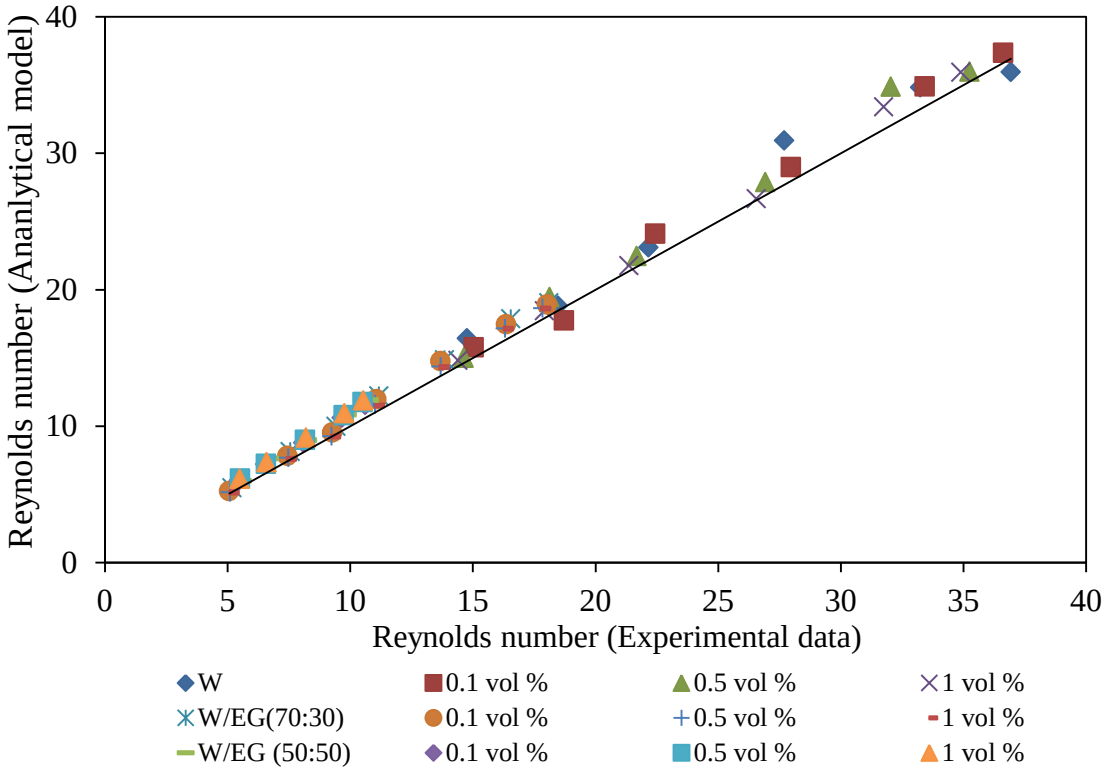

Figure 6.20: Correlation of analytical Reynolds number with experimental data

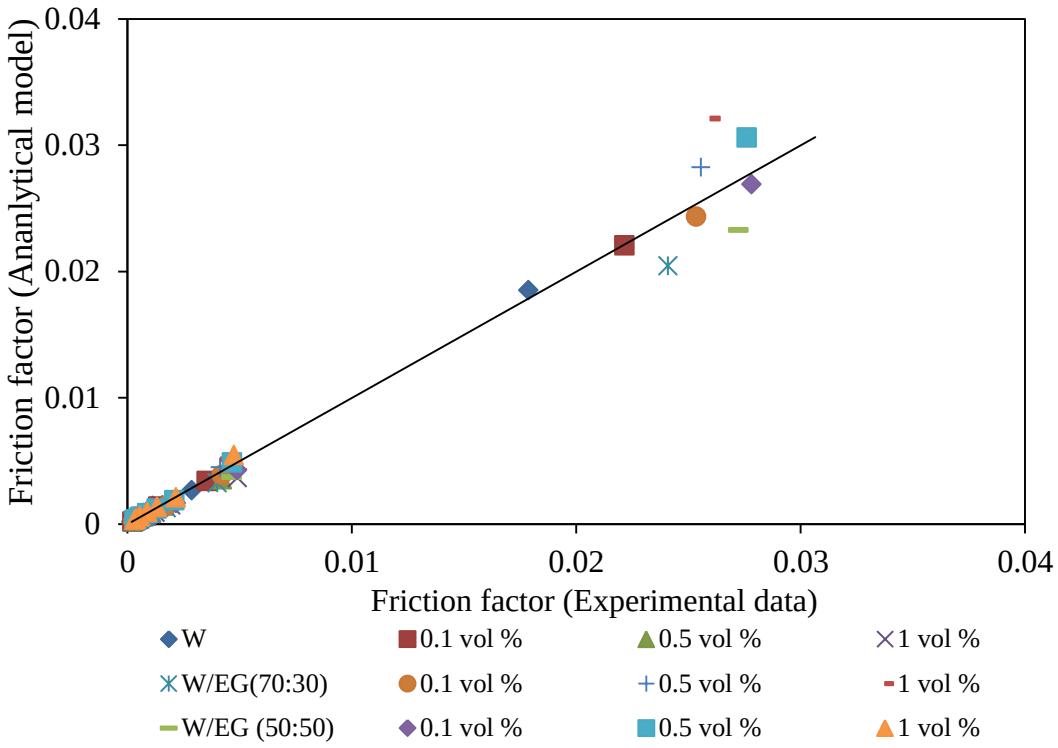

Figure 6.21: Correlation of analytical friction factor with experimental data

6.6 CLOSURE

The present chapter investigates the heat transfer and hydraulic performance of nanofluids flowing through rectangular shaped microchannels. Convective heat transfer is improved by using nanofluids and it increases with nanoparticle concentration and flow rate. In the present work, no appreciable enhancement is observed at very low flow rates such as less than 0.8 ml/min. A significant amount of heat was absorbed by nanofluids in comparison with base fluids. Maximum heat transfer performance was obtained with MWCNT nanofluids with lowest thermal resistance. A very low pressure drop was obtained with lowest friction factor which have no adverse effect during the flow of nanofluids in microchannels. An analytical model was also having good fit with experimental data with a deviation of ± 15 %. Next chapter discuss an MADM-TOPSIS approach to find the suitable nanofluids for the MCHS.

CHAPTER 7
SELECTION OF BEST NANOFLUIDS FOR THERMAL SYSTEMS BY USING MADM-TOPSIS APPROACH

After meeting all the objectives of thesis, an attempt is made to find out the best suitable nanoparticles and base fluids for thermal systems. For this, MADM-TOPSIS approach is implemented which depends on the different attributes. This chapter discusses all the parameters which affect the nanofluids and their performance. This scheme is very user friendly and can be implementing by any researcher to select a suitable nanofluids for enhancing the efficiency of their system.

7.1 IDENTIFICATION OF NANOFLUIDS ATTRIBUTES

The best selection of nanofluid is dependent on different attributes e.g. types of base fluids, nanoparticles and their concentration, thermal properties, etc., which ultimately affect the performance of nanofluids in various applications. Due to these identified attributes, the computer can assess, choose and rank the existing nanofluid on the basis of their appropriateness to the user. The numbers of identified attributes which are taken into consideration are directly proportional to the overall performance of a particular type of a nanofluid. Therefore, 125 pertinent attributes are identified and revealed in Table 7.1 like metallic, non-metallic, carbon nanotubes, etc. under the category of types of nanoparticles (no. 1 to 7) which influence the selection of particular nanofluid for a particular application. After nanoparticles selection, its shape (no. 8 to 20), size (no. 21) and concentration (no. 22) are important attributes to be considered. The properties like thermal conductivity, density, chemical reactivity of nanoparticles are the general attributes (no. 23 to 38). Then, the heat transfer fluids are selected (no. 39 to 48) with some broad attributes (no. 49 to 56) like boiling point, freezing point etc.

Several methodologies are followed for nanofluids preparation (57 to 67) and suitable surfactants and stabilizers (no. 68) are added to enhance their stability. Some attributes listed as 69 to 74 such as magnetic stirrer or high pressure homogenizer is further used for uniform dispersion. The pH of the fluid (no. 75) is also maintained in the specified range. High frequency ultrasonication controls the stability of nanofluids (no. 76 to 81) and further characterizations of nanofluids are carried out by Zeta potential, SEM, TEM, etc. (no. 82 to 93). Thermophysical properties of nanofluids have an important role for selecting the suitable nanofluids. All the methods used for the measurement of thermophysical properties are listed

as 94 to 108. The percentage enhancements in these properties are under no. 109 to 111. Heat transfer and fluid flow properties can also be measured (no. 112 to 117) to determine the thermal performance of any system. In addition to the above discussion, some general attributes are identified as nanofluids properties (no. 118 to 125). Many parameters are considered concurrently for good stability and thermal properties and overall reduction in their development time and cost during the preparation of nanofluids.

7.2 QUANTIFICATION AND MEASUREMENT OF THE ATTRIBUTES

Selection of appropriate nanofluids for a meticulous application is going to influence the total performance of the thermal system. Each value of an attribute affects the quality and efficiency of nanofluids. Some of the attributes of which quantification is not readily available from the manufacturer can be identified by some other way like mathematical modeling, simulation and analysis. To identify, quantify and provide the information of these attributes, manufacturers make a standard practice so that it will be helpful for manufacturer, user, application designer or industrialist etc. During efficient and effective nanofluid preparation, an effort is made for optimum selection of attributes and other parameters for enhancement of stability and thermal properties and reduction in fluid development time and cost (Figure 7.1).

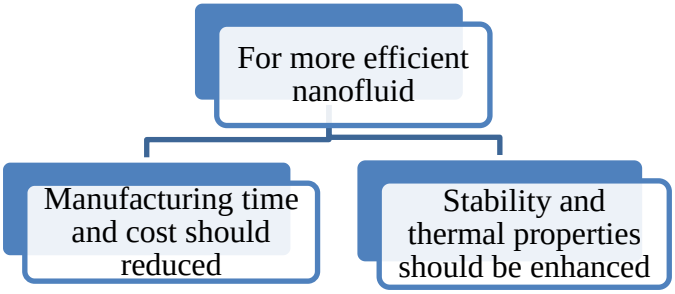

Figure 7.1: Prerequisite for nanofluids preparation

In order to achieve this, all the activities are considered concurrently. These activities are identified and categorized in five subsystems such as nanoparticles subsystem, base fluids subsystem, nanofluids preparation subsystem, characterization and nanofluids subsystem. All the subsystems are overlapping with each other which show that by altering any attribute, it changes the characteristics of nanofluids as shown in Figure 7.2. It shows clearly in Figure 7.3 that if it is not possible to carry out all the activities together, overlapping of activities is permitted. These subsystems are correlated with each other so appropriate change in any attribute can improve the stability and other properties of nanofluids. Nanofluids characterization is carried out after nanofluids preparation by different methods.

Table 7.1: List of nanofluids attributes

Types of nanoparticles		**Shape of**	**25**	Specific heat	**53**	Thermal conductivity
1. Nonmetallic	**8**	Spherical	**26**	Magnetism	**54**	Viscosity
Aluminium oxide	**9**	Rectangular	**27**	Aspect ratio	**55**	pH
Copper oxide	**10**	Cube	**28**	Crystal structure	**56**	Thermal expansion
Iron oxide	**11**	Branched	**29**	Shape factor		**Nanofluids preparation**
Lithium Iron phosphate	**12**	Hexagon	**30**	Sphericity	**57**	Single step direct evaporation method
Zinc oxide	**13**	Star	**31**	Boiling point	**58**	Organic reduction method
Aluminium nitride	**14**	Triangle	**32**	Melting point	**59**	Single step laser ablation method
Cerium oxide	**15**	Prisms	**33**	Brownian motion	**60**	Chemical reduction one step method
Indium Tin Oxide	**16**	Tetrapod	**34**	Wear and erosion	**61**	Chemical vapour deposition method
Titanium oxide	**17**	Spindly	**35**	Chemical reactivity	**62**	Physical vapour deposition method
Silicon oxide	**18**	Rod-shaped	**36**	Thermal expansion	**63**	Arc submerged nanoparticles synthesis
2. Metallic nanoparticles	**19**	Panicle	**37**	Electrical conductivity	**64**	Thermal decomposition of
Aluminium	**20**	Flower shaped	**38**	Specific surface area	**65**	Chemical precipitation method
Iron	**21**	**Nanoparticles size**		**Selection of Base fluids**	**66**	Nanoparticles purchased from suppliers and dispersed in the base fluids
Silicon		1-10 nm	**39**	Water		
Copper		11-20 nm	**40**	Ethylene glycol	**67**	Directly purchased the stable
Gold		21-30 nm	**41**	Water- ethylene glycol	**68**	**Surfactant added**
Si-Al		30-50 nm	**42**	Propylene glycol		Salt
Silver		50-90 nm	**43**	Water-propylene glycol		Cetyltrimethyl-ammonium bromide
3. Carbon nanotubes	**22**	**Nanoparticles fraction**	**44**	Glycerol		Sodium dodecyl sulphate
Multi walled		0.01 -0.1 vol %	**45**	Car engine coolant		Sodium octanoate
Single walled		0.10 – 0.5 vol %	**46**	Transformer oil		Chitosan
4. Quantum dots		0.5 – 1 vol %	**47**	Pump oil		Sodium dodecyl benzene sulphonate
Element Group I-VII		1 – 5 vol %	**48**	Vacuum pump fluid		Oleic acid
Element Group II-VI		5 and above vol %		**Base fluids properties**		Dodecyltrimethyl-ammonium bromide
Element Group III-V		**Nanoparticles properties**	**49**	Freezing point		Gum Arabic
5. Polymeric			**50**	Boiling point		**Uniform dispersion**
6. Fullerenes	**23**	Thermal conductivity	**51**	Specific heat	**69**	Functionalization of nanoparticles
7. Graphene nanoplatelets	**24**	Density	**52**	Density	**70**	Ball milling

71	Magnetic stirrer	**83**	U.V Spectrophotometer	**108**	Theoretical Model	**120**	Color change
72	High pressure homogenizer	**84**	Scanning electron microscope		**Heat transfer and Thermal properties**	**121**	Freezing point
73	Additives	**85**	Transmission electron microscopy	**109**	Thermal conductivity enhancement	**122**	Temperature
74	High shear mixing	**86**	X-ray Diffraction		0-5 %	**123**	Boiling point
75	**pH Range**	**87**	Particle size analyzer		5-10 %	**124**	Critical heat flux
	1-3	**88**	Turbidity		10- 15 %		
	3-5	**89**	3ω and sedimentation balance method		15-20 %	**125**	Electrical conductivity
	5-7	**90**	Thermogravimetric analysis		20 % and above		
	7-9	**91**	Differential scanning calorimtery	**110**	Viscosity		
	9-14	**92**	Photo capturing		Very Highly viscous		
	Sonication parameters	**93**	Photoluminescence spectroscopy		Highly viscous		
76	Water bath		**Thermal conductivity measurement**		Medium viscous		
77	Temperature	**94**	Transient hot wire method		Very Low viscous		
78	Frequency	**95**	Temperature oscillation method		Low viscous		
79	Probe	**96**	KD2 Pro	**111**	Density		
80	Time	**97**	Transient plane source		Very Highly dense		
81	**Sonication time**	**98**	Steady state Method		Highly dense		
	10 - 30 min	**99**	Theoretical Model		Medium dense		
	30 - 90 min		**Viscosity measurement**		Very Low dense		
	90 - 120 min	**100**	Portable viscosimeter		Low dense		
	2 - 5 hrs	**101**	Brookfield Viscometer	**112**	Specific heat		
	5 hrs and above	**102**	U- capillary Viscometer	**113**	Heat transfer coefficient		
	Characterization	**103**	Theoretical Model	**114**	Nusselt number		
82	Zeta potential		**Density measurement**	**115**	Friction factor		
	0-10 mV	**104**	Pycnometer	**116**	Pumping power		
	10-20 mV	**105**	Stabinger Viscometer	**117**	Thermal Resistance		
	20-30 mV	**106**	Theoretical Model		**Nanofluids general properties**		
	30-40 mV		**Specific heat measurement**	**118**	Thermal Diffusivity		
	40 mV and above	**107**	Differential scanning calorimeter	**119**	Tribological Properties		

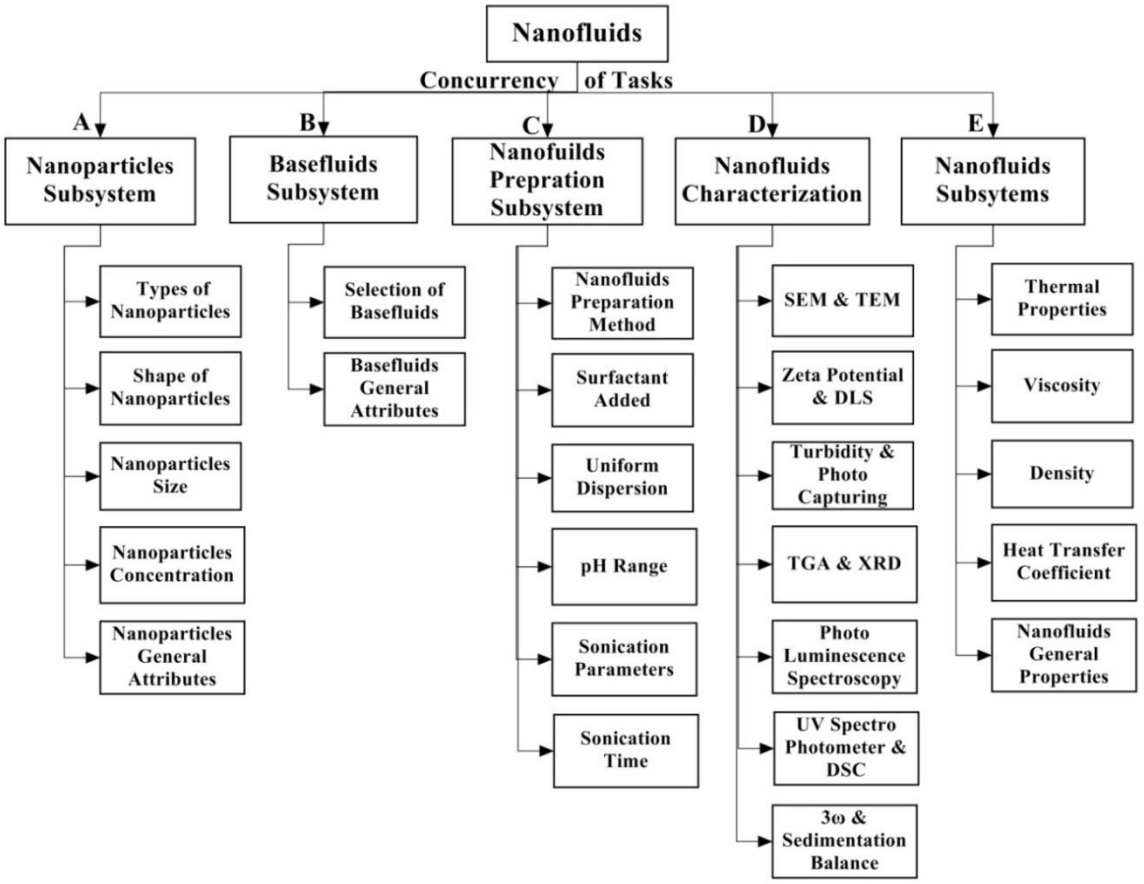

Figure 7.2: Concurrency of nanofluid design and development processes

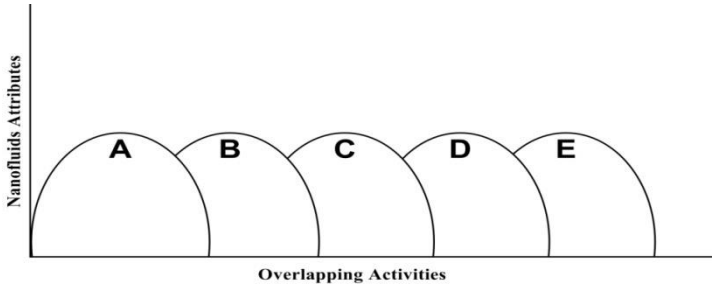

(b)

Figure 7.3: Overlapping of different subsystems of nanofluids

7.3 CODING SCHEME OF NANOFLUIDS ATTRIBUTES

The identified attributes are very important and coded on the basis of their probable values. The n - digit coding scheme will work as a global directory of nanofluids in future and any new findings will added to this directory any time. Proposed coding scheme is illustrated with example based on heat transfer applications. A compact 125-attribute coding scheme (Table 7.2) is developed for identification of suitable nanofluids which can be used to eradicate high heat load in microchannels. In this coding scheme, attributes represent in digits form given in

a box and all the boxes are organized in a particular order no. as in Table 7.1. The coding is done in the format of u_i/v_i, i = 1, 2,...n, where u_i is the order no. of attributes and v_i is the code given to that particular attribute. First, the categorization of the attributes is done either qualitatively or quantitatively. Qualitative attributes which affect the performance of nanofluids are type and shape of nanoparticles, base fluids, preparation method, etc. and coded with alphabets or any short form while the quantitative attributes such as size of nanoparticles, thermal properties of nanofluids, etc. are measurable and having units so coding is given in ascending/descending order. Attributes for nanofluids can be rated on 1-5 scale represents its performance rate. The scale 5 shows the excellent performance while the scale 1 shows the least performance. For example, Low viscous alumina nanofluid (Code-5) having thermal conductivity enhancement upto 5 % (Code-2) with a tendency to enhance heat transfer coefficient of 15.8% (Code-4) is preferred to flow in microchannels. The numerical value of zero (0) represents the attributes with no information. In a related manner, coding was given to remaining attributes according to their importance in this application.

Authors are recommended that the suppliers must supply the complete information for user's benefit so that this information can be used to identify the best suitable nanofluid. There are some informative attributes which tells the information of nanofluids but having no mathematical significance. But still this attribute stored in the database which might be indirectly affects the performance. This coding scheme is used for the visual and faster comparison of nanofluids due to more precise and accurate database storage, retrieval and the selection procedure.

Table 7.2: Coding scheme for alumina nanofluid used in microchannels [127]

Types of nanoparticles	1/Al_2O_3	2/0	3/0	4/0	5/0	6/0	7/0		
Shape of nanoparticles	8/0	9/0	10/0	11/0	12/0	13/0	14/S	15/0	16/0
	17/0	18/0	19/0	20/0					
Nanoparticles size	21/1								
Nanoparticles concentration	22/2								
Nanoparticles general attributes	23/3	24/0	25/3	26/0	27/0	28/0	29/0	30/0	31/0
	32/0	33/0	34/0	35/0	36/0	37/0	38/0		
Selection of base fluids	39/W	40/0	41/0	42/0	43/0	44/0	45/0		
	46/0	47/0	48/0						
Base fluids properties	49/0	50/0	51/3	52/3	53/0	54/3	55/0	56/0	
Nanofluids preparation	57/0	58/0	59/0	60/0	61/0	62/0	63/0	64/0	65/0
	66/DM	67/0							
Type of Surfactant	68/0								
Uniform dispersion	69/0	70/0	71/0	72/0	73/0	74/0			
pH range	75/2								
Sonication parameters	76/0	77/P	78/0	79/T	80/F				
Sonication time	81/2								
Characterization	82/5	83/0	84/TEM	85/0	86/0	87/0	88/0	89/0	90/0
	91/0	92/PCS	93/0						
Measurement of thermal conductivity	94/0	95/0	96/0	97/0	98/0	99/TM			
Viscosity measurement	100/0	101/0	102/0	103/TM					
Specific heat measurement	104/0	105/TM							
Density measurement	106/0	107/0	108/TM						
Heat transfer and Thermal properties	109/1	110/5	111/5	112/3	113/4	114/0	115/4	116/2	117/4
Nanofluids general properties	118/0	119/0	120/0	121/0	122/0	123/0	124/0	125/0	

7.4 THREE-STAGE MADM METHODOLOGY

7.4.1 Elimination search (stage 1)

During the selection of optimal nanofluids for a particular application, time, cost and effort made for nanofluids preparation do not permit to go high. All the identified attributes are not equally important to be considered, so there is no need to use all the attributes concurrently for the better performance of nanofluids in various applications. Since, the attributes which are having direct effect on the evaluation procedure say as pertinent attribute has to be identified for a particular application. Then, the expertise assigned some threshold values to these pertinent attributes for the short listing of alternatives. Therefore, on the basis of the threshold values a large list of nanofluids converged to adaptable list assigned to these pertinent attributes. Thus, a mini database is formed by alternatives with these pertinent attributes under elimination search for a particular application.

7.4.2 TOPSIS approach (stage 2)

i. Decision matrix/Data matrix

After the result of an elimination search of alternatives, further filtration will done to get an optimal nanofluids for a particular system. Each row characterizes particular nanofluid information regarding pertinent attributes present in the database in a form of matrix such as Decision matrix, D. It is a mathematical term which helps the researchers to evaluate and prioritize all of their options when considering solutions to a difficult task.

Matrix D can be expressed as

$$D = [d_{ij}]_{m\times n}, \quad i = 1,.....m;\ j = 1,.....,n \tag{7.1}$$

where ‘m’ is the number of short listed nanofluids and ‘n’ is the number of pertinent attributes. Each element of the matrix, d_{ij}, represents value of j^{th} attribute corresponding to i^{th} alternative. Elements in each column of this matrix have different units and scales. Hence this is a non-normalized form of a matrix.

ii. Normalized matrix

The next step is to normalize the value by converting the elements of matrix D into a particular scale and unit independent quantity. The normalized specification matrix is having magnitudes of all the attributes of nanofluids on the common scale of 0 to 1. Normalized

decision making matrix, N, is obtained from the decision matrix D and each element of this matrix, n_{ij}, is expressed as:

$$n_{ij} = \frac{d_{ij}}{(\sum_{i=1}^{m} d_{ij}^2)^{1/2}} \quad (7.2)$$

where, d_{ij} is an element of the decision matrix, D.

iii. Relative importance matrix

The third step is to acquire all the information from the group of expertise or user on the relative importance of one attribute with respect to another To incorporate the relative importance of attributes for given application a relative importance matrix, A = a_{ij} of size $n \times n$ is defined. An element a_{ij} of matrix A is defined as:

$$a_{ij} = \frac{importance\ of\ ith\ attribute}{importance\ of\ jth\ attribute} \quad (7.3)$$

Matrix, A, gives the information about the pair-wise comparison of attributes for a typical application or physical situation. The symmetric terms of this matrix will be reciprocals of each other while the diagonal will be unity. Normalization is significant, when the weight of each attribute is found and those weights are absolute in values i.e. cumulative sum of the weights of all the attributes is equal to unity.

iv. Eigenvalue formations

There might be inconsistencies in the judgment of relative importance matrix due to the imprecise human judgments for eq. 7.3. Eigenvalue method is employed to prevail over this negative aspect and this helps to find a weight matrix 'W'' where β is the eigenvalue/variable,

$$AW' = \beta W' \quad (7.4)$$

Here, $W' = [w_1, w_2, w_3, ..., w_n]^T$

From eq. 7.4

$$(A - \beta I)W' = 0 \quad (7.5)$$

If $W' = 0$, then this gives a trivial solution with no meaning. Therefore,

$$(A - \beta I) = 0 \quad (7.6)$$

After solving the Eq. (7.6), the user will get a set of n eigenvalues (β_1, β_2,.....β_i,....β_n) and out of those maximum eigenvalue β_{max} is preferred to find the weight matrix such as,

$$(A-\beta_{\max} I)W'=0 \tag{7.7}$$

And Eq. (7.7) gives the weight vector such as

$$W'=[w_1, w_2, w_3, ...w_n]^T$$

Hwang and Yoon [163] considered the real eigenvalues and real eigenvectors as real eigenvalues provide the stable solution while complex eigenvalue predicts unstable process results in oscillating results and has no physical significance in ranking process. So, real eigenvalues and eigenvectors are considered for the optimum selection of nanofluids

v. Weight normalized decision matrix

The weights obtained from the relative importance matrix is incorporated in to the normalized decision matrix, to make this weight matrix more meaningful and further a new weighted normalized decision matrix, Z, is formed. This will provide true comparable values of each attributes. The element of this matrix is defined as

$$Z=[z_{ij}]=[n_{ij}]\times[w_j] \tag{7.8}$$

where i = 1, 2, 3, ..., m; j = 1, 2, 3,....n.

vi. Positive ideal and negative ideal solution

The positive ideal solution *(A*)* and negative ideal solution *(A^-)* are the imaginary solutions which correspond to the optimum attribute values available in the database. These results are resolute by choosing the maximum and minimum values of the attributes from the Z matrix. Therefore,

$$A^* = z_{ij\max} \text{ For benefit attributes; or} \tag{7.9}$$

$$= z_{ij\min} \text{ For cost attributes; and}$$

$$A^- = z_{ij\min} \text{ For benefit attributes; or} \tag{7.10}$$

$$= z_{ij\max} \text{ For cost attributes; and}$$

where i = 1,2,3, . . .,m and j = 1,2,3,. . ., n. Hence,

$$A^*=(Z_1^*, Z_2^*, Z_3^*, ...Z_n^*)$$

$$A^-=(Z_1^-, Z_2^-, Z_3^-, ...Z_n^-)$$

vii. Determination of separation measures

The separation of each alternative, z_i from positive ideal solution is as follows:

$$S_i^* = [\sum_{j=1}^{n} (z_{ij} - z_1^*)^2]^{1/2} \text{ (i = 1, 2,...., m)} \quad (7.11)$$

And separation from the negative ideal solution is as follows:

$$S_i^- = [\sum_{j=1}^{n} (z_{ij} - z_1^-)^2]^{1/2} \text{ (i = 1, 2,....m)} \quad (7.12)$$

viii. Suitability index

After measure the separation from positive and negative ideal solution, calculate the relative closeness to the ideal solution. All these ranked nanofluids satisfy conditions of upper and lower limits required for all attributes. This is defined as suitability index, C*, a single numerical index as an evaluation index of alternative nanofluids

$$C_i^* = \frac{S_i^-}{S_i^- + S_i^*} \text{ where, } 0 \leq C_i^* \leq 1 \quad (7.13)$$

ix. Ranking procedure

Ranking of nanofluids depend upon the value of suitability index, C*. The solution with highest value of C* will be given the highest rank and so on. As a result, arrange the nanofluids preference order in descending order and final list are obtained for the researchers so that they can used the nanofluids according to their need. It ensures that the nanofluid optimally selected is closest to the ideal solution and the farthest from the worst solution.

7.4.3 Final decision making (stage 3)

Assortment of a best nanofluid to a specific application can be done on the basis of preference order in the existence of other attributes and business developed schemes prepared in the earlier section. Proposed approach is computational and user friendly in optimum selection of nanofluids system. All listed nanofluids are acceptable for thermal management systems. With the consideration of both government rules and regulations and cost factor, suitable nanofluid can be opt for that particular application. If a nanofluid with highest rank is not suitable then choose the next option and so on. MADM-TOPSIS, a numerical analysis has empowered to reduce the overall time taken by series of experiments conducted to obtain the better results. The only inputs required for this methodology are relative importance matrix, A, and decision matrix, D, and final ranking can be done. This methodology is useful for the

researchers for the selection of nanofluids with better performance and good stability in less time and effort.

7.4.4 Computer program MATLAB

A matrix program laboratory (MATLAB) is developed for solving the above methodology from steps 1 to 9. The decision matrix and relative important matrix are the two input matrices in MATLAB programming and after completing all the calculations, suitability index can be obtained. Ranking of the nanofluids can be done on the basis of suitability index value. The complete listing of the program is specified in Appendix B.

7.5 SELECTION OF OPTIMAL NANOFLUIDS FOR MCHS

The methodology explained above is used to select optimal nanofluids to enhance the cooling efficiency of microchannel heat sink. To validate this methodology, attributes are taken from the experimentation.

Stage 1. Elimination Search method

There are some minimum decisive factors required for the target nanofluids for their better performance in microchannels. The first stage is the elimination stage in which large list of alternatives gets eliminated to manageable list. Attributes which are very important for this system and having some minimum criteria is considered from Table 3.1, 4.1, 4.2 and 4.3.

The pertinent attributes are identified after the elimination of large list of alternatives which helps in the selection of an optimal nanofluid are listed in Table 7.1.

Stage 2. TOPSIS approach

Step1.Formation of decision matrix

With the help of Table 7.3, decision matrix can be formed which contains all the magnitudes of specifications in which row represents as the nanofluids and their attributes value are listed in columns. Resistance, friction factor, density and viscosity should be of minimum magnitude for better nanofluids so the reciprocal of the values in column used for this type of attributes to form the decision matrix.

$$D_{\exp} = \begin{bmatrix} 6.2 & 4560.671 & 15.1664 & 2 & 1.19047 & 0.123457 & 40 & 19 \\ 25 & 4173.849 & 18.8629 & 5.6 & 2.17391 & 0.30581 & 50 & 25 \\ 36.5 & 3769.247 & 22.0410 & 6.6 & 1.85185 & 0.480769 & 58 & 28 \\ 23.46 & 4567.858 & 17.6342 & 3.8 & 1.08695 & 0.110865 & 40 & 2 \\ 45.5 & 4175.993 & 21.90676 & 9.7 & 1.66666 & 0.274725 & 44 & 3 \\ 47.4 & 3772.247 & 23.7868 & 11.3 & 1.58730 & 0.42735 & 48 & 4 \\ 37.99 & 4555.892 & 19.70638 & 13 & 1.33333 & 0.145349 & 45 & 24 \\ 49.8 & 4157.002 & 22.54537 & 22.7 & 2.63158 & 0.320513 & 52 & 30 \\ 52.8 & 3770.284 & 24.65787 & 28 & 2.27273 & 0.515464 & 58 & 36 \end{bmatrix}$$

Step 2. Normalized matrix

After making a decision matrix, next step is to normalize the matrix, N according to the Eq. 7.2:

$$N = \begin{bmatrix} 0.0532 & 0.3637 & 0.2418 & 0.0474 & 0.2176 & 0.1235 & 0.2735 & 0.2810 \\ 0.2146 & 0.3329 & 0.3008 & 0.1326 & 0.3974 & 0.3058 & 0.3418 & 0.3698 \\ 0.3133 & 0.3006 & 0.3515 & 0.1563 & 0.3386 & 0.4808 & 0.3965 & 0.4141 \\ 0.2014 & 0.3643 & 0.2812 & 0.0900 & 0.1987 & 0.1109 & 0.2735 & 0.0296 \\ 0.3905 & 0.3331 & 0.3493 & 0.2297 & 0.3047 & 0.2747 & 0.3008 & 0.0444 \\ 0.4068 & 0.3009 & 0.3793 & 0.2676 & 0.2902 & 0.4274 & 0.3281 & 0.0592 \\ 0.3261 & 0.3634 & 0.3142 & 0.3078 & 0.2438 & 0.1454 & 0.3076 & 0.3550 \\ 0.4274 & 0.3315 & 0.3595 & 0.5375 & 0.4811 & 0.3205 & 0.3555 & 0.4437 \\ 0.4532 & 0.3007 & 0.3932 & 0.6630 & 0.4155 & 0.5155 & 0.3965 & 0.5325 \end{bmatrix}$$

Step 3.Relative importance matrix

The third step is to construct the relative importance matrix for a particular cooling device such as MCHS which is decided by the team of expertise in the area of nanofluids and microchannels. For this, relative importance matrix, A:

$$A = \begin{bmatrix} 1.00 & 2.00 & 2.00 & 1.30 & 1.00 & 4.00 & 4.00 & 1.30 \\ 0.50 & 1.00 & 1.00 & 2.00 & 2.00 & 1.30 & 1.30 & 4.00 \\ 0.50 & 1.00 & 1.00 & 2.00 & 2.00 & 4.00 & 4.00 & 1.30 \\ 0.75 & 0.50 & 0.50 & 1.00 & 1.00 & 0.25 & 0.50 & 0.75 \\ 1.00 & 0.50 & 0.50 & 1.00 & 1.00 & 0.50 & 0.25 & 0.75 \\ 0.25 & 0.75 & 0.25 & 4.00 & 2.00 & 1.00 & 2.00 & 4.00 \\ 0.25 & 0.75 & 0.25 & 2.00 & 4.00 & 0.50 & 1.00 & 1.30 \\ 0.75 & 0.25 & 0.75 & 1.30 & 1.30 & 0.25 & 0.75 & 1.00 \end{bmatrix}$$

Step 4. Weight vector

Maximum eigenvalue helps to calculate the weight vector.

$$W' = [0.2229 \quad 0.1428 \quad 0.1880 \quad 0.0658 \quad 0.0728 \quad 0.1349 \quad 0.0966 \quad 0.0761]$$

Step 5. Weight normalized decision matrix

By substituting the values of normalized decision matrix, N and weight vectors, W' in eq. 7.8, the weighted normalized decision matrix can be obtained as follows:

$$Z = \begin{bmatrix} 0.0119 & 0.0520 & 0.0455 & 0.0031 & 0.0159 & 0.0167 & 0.0264 & 0.0214 \\ 0.0478 & 0.0475 & 0.0566 & 0.0087 & 0.0289 & 0.0413 & 0.0330 & 0.0282 \\ 0.0698 & 0.0429 & 0.0661 & 0.0103 & 0.0247 & 0.0649 & 0.0383 & 0.0315 \\ 0.0449 & 0.0520 & 0.0529 & 0.0059 & 0.0145 & 0.0150 & 0.0264 & 0.0023 \\ 0.0870 & 0.0476 & 0.0657 & 0.0151 & 0.0222 & 0.0371 & 0.0290 & 0.0034 \\ 0.0907 & 0.0430 & 0.0713 & 0.0176 & 0.0211 & 0.0576 & 0.0317 & 0.0045 \\ 0.0727 & 0.0519 & 0.0591 & 0.0203 & 0.0178 & 0.0196 & 0.0297 & 0.0270 \\ 0.0953 & 0.0474 & 0.0676 & 0.0354 & 0.0350 & 0.0432 & 0.0343 & 0.0338 \\ 0.1010 & 0.0430 & 0.0739 & 0.0436 & 0.0303 & 0.0695 & 0.0383 & 0.0405 \end{bmatrix}$$

Step 6. Positive ideal and negative ideal solution

Positive ideal and negative ideal solution is expressed from eq. 7.9 and 7.10 by choosing the maximum and minimum values of the attribute.

$$A^* = [0.1010 \quad 0.0520 \quad 0.0739 \quad 0.0436 \quad 0.0350 \quad 0.0695 \quad 0.0383 \quad 0.0405]$$

$$A- = [0.0119 \quad 0.0429 \quad 0.0455 \quad 0.0031 \quad 0.0145 \quad 0.0150 \quad 0.0264 \quad 0.0023]$$

Step 7. Determination of separation measures

Separation measures from positive and negative ideal solution are obtained from the expressions 7.11 and 7.12 as follows:

$$S_1^* = 0.1186 \; S_2^* = 0.0734 \; S_3^* = 0.0494 \; S_4^* = 0.1001 \; S_5^* = 0.0615 \; S_6^* = 0.0505 \; S_7^* = 0.0680$$
$$S_8^* = 0.0303 \; S_9^* = 0.0103$$

$$S_1^- = 0.0213 \; S_2^- = 0.0555 \; S_3^- = 0.0862 \; S_4^- = 0.0352 \; S_5^- = 0.0824 \; S_6^- = 0.0948 \; S_7^- = 0.0701$$
$$S_8^- = 0.1039 \; S_9^- = 0.1234$$

Step 8. Suitability index

Relative closeness to the ideal solution or suitability index can be obtained as per expression 7.13.

$C_1^* = 0.1521\ C_2^* = 0.4308\ C_3^* = 0.6357\ C_4^* = 0.2599\ C_5^* = 0.5725\ C_6^* = 0.6525\ C_7^* = 0.5078$
$C_8^* = 0.7743\ C_9^* = 0.9232$

C_i^* closer to 1 is best and closer to zero is worst. On the basis of C_i^* value, ranking of the nanofluids can be done (Table 6).

Stage 3. Final decision making

Ranking is done only for the selected nine types of nanofluids which are prepared experimentally. From this example, MWCNT-W/EG (50:50) are best nanofluid and alumina-W are worst nanofluids for MCHS to remove high heat load. This approach benefits in decreasing the manufacturing cost and time.

As authors determined the stability of nanofluids in terms of days, hence, full batch of nanofluid can be substituted by a freshly prepared nanofluid earlier their stability ended for any kind of continuous application. This is proposed by authors to the industrialist or researchers who are working in this particular area.

7.6 USEFULNESS

Usefulness discussions should be based on exhaustive attributes and other parameters, hierarchical tree, five subsystems and sub- sub systems, overlapping activities, example of coding three-stage procedure, TOPSIS solution procedure, selection of appropriate nanofluid for different solutions and final decision process.

7.7.1 Usefulness to the manufacturer

The main aim of the work is to produce optimal nanofluids with a good stability in the minimum possible time. For this a proper quantification and screening of the attribute magnitudes had done from the database. It will help to find out the market trend and gives the direction to manufacturer so that they control the attributes magnitude according to the future demand of the nanofluids based applications.

7.7.2 Usefulness to the researcher/industrialist

These classifications of the attributes facilitate the user for the data storage and their recovery. This will create the computerized database which can be used in different formats to select the best possible nanofluid for the particular application. This will be very helpful for the different researchers or people working in the different organizations or industries so that they will know the exactly performance and stability of nanofluids before use it any application. It is not essential that user have any knowledge of mathematical tool as some professional trainee can also hired to solve the problem. Otherwise, with the help of program a user can solve the problem easily.

7.7.3 Usefulness for thermal management systems

Nanofluids performance plays a very important role in thermal systems. Identification of various attributes helps to select an optimal nanofluid for particular applications. If any new parameter is identified which is not earlier mentioned in the database then it can also add in this system. By this, nanofluid performance will improve which will further help to enhance the efficiency of thermal system.

Table 7.3: Performance attributes for nanofluids

Samples	HTR	Friction factor	Resistance (°C/W)	Thermal conductivity enhancement (%)	Rise in density (no. of times)	Rise in viscosity (no. of times)	Zeta potential (mV)	Stability (Days)
Al_2O_3-W	6.20	0.0002192	0.065935	2	0.84	8.10	40	19
Al_2O_3-W/EG (70:30)	25	0.0002395	0.053014	5.6	0.46	3.27	50	25
Al_2O_3-W/EG (50:50)	36.5	0.0002653	0.04537	6.6	0.54	2.08	58	28
CuO-W	23.46	0.0002189	0.056708	3.8	0.92	9.02	40	2
CuO-W/EG (70:30)	45.5	0.0002394	0.045648	9.7	0.60	3.64	44	3
CuO-W/EG (50:50)	47.4	0.0002650	0.04204	11.3	0.63	2.34	48	4
MWCNT-W	37.99	0.0002194	0.050745	13	0.75	6.88	45	24
MWCNT-W/EG	49.8	0.0002405	0.044355	22.7	0.38	3.12	52	30
MWCNT-W/EG	52.8	0.0002652	0.040555	28	0.44	1.94	58	36

Table 7.4: Ranking of Nanofluids

Nanofluids	Rank
Al_2O_3- W	9
Al_2O_3- W/EG (70:30)	8
Al_2O_3- W/EG (50:50)	5
CuO- W	7
CuO-W/EG (70:30)	4
CuO-W/EG (50:50)	3
MWCNT- W	6
MWCNT- W/EG (70:30)	2
MWCNT- W/EG (50:50)	1

7.7 CLOSURE

The present work proposed a methodology which is useful for the selection of nanofluids in thermal management systems. The methodology is based on the MADM- TOPSIS technique. A proposed list of 125 attributes characterizing the nanofluids which helps researchers, manufacturers, designer as well as end user to have in depth understanding of the nanofluid in comparison with others. N- attribute coding scheme is developed to store all the available nanofluids globally in the computer and retrieve whenever necessary for comparison and further improvement. MADM-TOPSIS approach considers large number of attributes concurrently and converts into a single characteristic evaluation index for comparison, ranking and optimum selection. Authors recommend that manufacturers of nanofluids must provide information to all the attributes. This will in turn helps them and others to improve the performance of existing nanofluids and select optimum one. This work is providing a support for current research in the area of nanofluids to determine their stability and thermal performance for industrial cooling applications.

CHAPTER 8

CONCLUSIONS AND FUTUTRE SCOPE OF WORK

In previous chapters, detailed study of preparation and stability of nanofluids with their thermophysical properties are discussed. Afterwards, fabrication of microchannels and experimental setup are done and developed the analytical model. Nanofluids flow and heat transfer characteristics are studied and compared with the analytical model. A MADM-TOPSIS approach was introduced for selecting the suitable nanofluids for particular application by considering the various attributes. This chapter discusses the concluding remarks achieved from the thesis work and further provides some suggestions or the future scope of present work.

8.1 CONCLUSIONS

1. Two step dispersion method is opted for the preparation of nanofluids as the nanoparticle concentration are in higher ranges i.e. 0.1 vol % to 5 vol %. Stable alumina nanofluids were prepared without the use of surfactant while stable MWCNT based nanofluids were prepared by using GA as a surfactant and CuO nanofluids were prepared by using SDS surfactant.
2. Optimization of sonication time was done to make nanofluids more stable. The 80 min sonication was obtained by observing the thermal conductivity of nanofluids at different intervals of sonication time i.e. 40 min, 60 min, 80 min, and 100 min. The 80 min sonication is more enough to stabilize the any type of nanofluids as more sonication time reduces the stability by retarding the repulsive forces between the nanoparticles.
3. Stability is an important concern for any nanofluids, so it is determined by measured the thermal conductivity, absorbance and zeta potential of nanofluids with days. Maximum stability was achieved for MWCNT nanofluids i.e. 24 days with water and reaches up to 36 days with W/EG (50:50) base fluid. Alumina nanofluids show stability of 19-28 days with the change in base fluids while CuO nanofluids are least stable nanofluids with 2-4 days stability. Stability of nanofluids is increased with the addition of ethylene glycol in water and W/EG (50:50) base fluids give the maximum stability either any kind of nanoparticles used.
4. Without any stirring and shaking of the samples, nanofluids stability was for some days. If the nanofluids will use in continuous flow then stability will increases

appreciably as the nanoparticles remain in motion during flow. During experiments, no settling of nanoparticles was observed so nanofluids can be used for commercial products for years.

5. Thermophysical properties of nanofluids depend on the type of nanoparticles and its concentration, base fluids and temperature. Thermal conductivity, viscosity and density of nanofluids increase while specific heat decreases with the addition of nanoparticles in base fluids.
6. With increase in temperature, thermal conductivity of nanofluids increases whereas viscosity and density decreases. With increase in ethylene glycol ratio in W/EG mixtures, more enhancement in thermal conductivity was observed with W/EG (50:50) base fluid either any kind of nanoparticles used.
7. Out of alumina, CuO, MWCNT nanofluids, MWCNT nanofluids shows maximum 40.8 % enhancement in thermal conductivity while least enhancement of 13.3 % observed with alumina-W/EG (50:50) nanofluid at 5 vol % concentration. The rise in density and viscosity of nanofluids are quite low when compared with thermal conductivity enhancement which makes the nanofluids more fit to the thermal applications.
8. Rectangular shaped microchannels are fabricated to observe the cooling performance by using nanofluids. Appreciable heat transfer improvement is observed by using nanofluids in comparison with the base fluids when nanofluids flow through the microchannels.
9. Heat transfer increases with increase in flow rate, as well as with increase in nanoparticle concentration. No significant enhancement in heat transfer was observed at low Reynolds number i.e. less than or equal to 14 for water, 13 for W/EG (90:10), 9 for W/EG (80:20), 7 for W/EG (70:30), 4 for W/EG (60:40 and 50:50).
10. At 2 ml/min, MWCNT nanofluids give an heat transfer enhancement of 38 % to 53 % while alumina shows 6 % to 36.5 % and CuO nanofluids have 23 % to 47.4 % enhancement with the change in base fluids from Water to W/EG (50:50) at 0.1 vol % concentration.
11. Out of all the prepared nanofluids, MWCNT nanofluids with W/EG (50:50) base fluids have lowest thermal resistance. Nanofluids with water base fluids absorb more amount of heat from the MCHS but the overall enhancement in heat absorption was maximum for W/EG (50:50) base fluids with any type of nanoparticles used.

12. At low flow rates, friction factor is quite high showing the undeveloped flow while at high flow rates, friction factor of all the nanofluids was almost same with negligible effect on thermal systems.
13. An analytical model was developed to correlate the experimental data of Nusselt number, Reynolds number, friction factor and a good agreement found with a model data within deviation of ± 15 %.
14. Selection of best suitable nanofluids is carried out for thermal systems by using MADM-TOPSIS approach. For this approach, 9 different types of nanofluids are chosen and for the MCHS, MWCNT-W/EG (50:50) proves best nanofluid while Alumina-W proves worst nanofluid.
15. With increase in miniaturization and increasing heat dissipation, the results would be useful to the microelectronics industry. Results for the heat transfer and pressure drop of nanofluids in microchannels are very appreciable in comparison with the existing results. Moreover, analytical model gives the good agreement with experimental results which become useful for the researchers in future. Multiwalled carbon nanotubes based nanofluids absorb the maximum amount of heat from the MCHS becomes the most efficient nanofluid for cooling applications.

8.2 FUTURE RECOMMENDATIONS

While carrying out the present studies, some suggestions for the future work are feeling to pursue this research in more defined form:

1. Detailed study of different type of metallic and nonmetallic nanofluids stability need to be explored by using different base fluids.
2. In the present study, rectangular shape of microchannels is considered. While in future, nanofluids can used in different shape of microchannels and comparison can be made experimentally.
3. Different inlet and outlet arrangements of nanofluids flow through microchannels can also be explored.
4. Two phase boiling phenomenon at high heat input loads can also be studied by using ethylene glycol base fluids with any kind of nanoparticles used.

APPENDIX–A

ANALYTICAL MODEL USING TURBO C++

```
#include<stdio.h>
#include<conio.h>
#include<math.h>

// GLOBAL VARIABLE DECLARATIONS

double channelWidth;  //Width of the Channel
double wfin; //Width of fin
double channelHeight; //Height of Channel
double channelLength; //Length of Channel
double numChannels; //Number of channels

double km; //Thermal Conductivity of Substrate Material
double conc; //Nanoparticle volume concentration
double weg; //Ethylene Glycol Ratio in water
double flowRate; //Volumetric Flow Rate
double tin; //Inlet Temperature of Fluid
double tb; //Heat Sink Base Temperature
double to; //Assumed Initial Outlet Temperature
double tavg; //Initial Average Temperature
double tref;
double reswire;
double wirelen;
double wirediam;
double wiretempcoeff;

int voltage;
double current;

double crossSectionalArea; //Cross-sectional area of microchannels
double wettedSurfaceArea; //Total Wetted Surface Area of microchannels
double dh; //Hydraulic Diameter for Rectangular microchannels
```

```
double velocity; //Fluid Velocity
double conc1;
double specificHeat; //Specific heat of Nano Fluid

double getSpecificHeat(double);
void calculate(int);
double getFrictionFactor(double, double);

void main() {
	int choice;
	clrscr();
	printf("Choose the nano particle\n");
	printf("1. Multi Walled Carbon Nanotubes (MWCNT)\n");
	printf("2. Alumina\n");
	printf("3. Copper Oxide\n");
	printf("Enter your choice: ");

	scanf("%d", &choice);

	if (choice > 3 || choice < 1) {
		printf("Invalid choice\n");
		getch();
		return;
	}

	printf("\nDefine Microchannel Geometry: \n");
	printf("Enter Channel Width (in microm): ");
	scanf("%lf", &channelWidth);
	channelWidth = channelWidth * pow(10, -6);
	printf("Enter Fin Width: (in microm): ");
	scanf("%lf", &wfin);
	wfin = wfin * pow(10, -6);
	printf("Enter Channel Height (in mm): ");
	scanf("%lf", &channelHeight);
	channelHeight = channelHeight * pow(10, -3);
```

```
printf("Enter Channel Length (in mm): ");
scanf("%lf", &channelLength);
channelLength = channelLength * pow(10, -3);
printf("Enter Number of Channels: ");
scanf("%lf", &numChannels);
printf("\n");

printf("Enter diameter of Nano Particle (in nm): ");
scanf("%f", &dp);
dp /= 1000000000;
printf("Enter Nano Particle Volume Concentration (in %): ");
scanf("%lf", &conc);
printf("\n");

printf("Enter thermal conductivity of substrate material (in W/m\xf8%c): ", 'C');
scanf("%lf", &km);
printf("\n");

printf("Define Input Conditions\n");
printf("Enter Inlet Temperature (in \xf8%c): ", 'C');
scanf("%lf", &tin);
printf("Enter Volumetric Flow Rate (in m3/sec): ");
scanf("%lf", &flowRate);

printf("Enter Input Voltage (in V): ");
scanf("%d", &voltage);

printf("Enter Input Current (in A): ");
scanf("%lf", &current);

printf("Enter Reference Temperature of Heater (in \xf8%c): ", 'C');
scanf("%lf", &tref);

printf("Enter Resistivity of Heater Material (in \xea%c): ", 'm');
scanf("%lf", &reswire);
```

```
        printf("Enter Length of Wire (in m): ");
        scanf("%lf", &wirelen);

        printf("Enter Diameter of Wire (in mm): ");
        scanf("%lf", &wirediam);

        wirediam /= 1000;

        printf("Enter Temperature Coefficient of Wire (in /\xf8%c): ", 'C');
        scanf("%lf", &wiretempcoeff);

        printf("Enter Ethylene Glycol Ratio: ");
        scanf("%lf", &weg);

        double rt = voltage / current;
        double r0 = (reswire * wirelen) / (3.14 * (wirediam * wirediam) / 4);

        tb = tref + 1/wiretempcoeff * (rt/r0 - 1);

        to = tb;
        tavg = (tin + to) / 2;

        crossSectionalArea = channelWidth * channelHeight;
        wettedSurfaceArea = channelLength * numChannels * (2 * channelHeight +
channelWidth);
        dh = (2 * channelWidth * channelHeight) / (channelHeight + channelWidth);
        velocity = flowRate / crossSectionalArea;

        calculate(choice);

        getch();
}

void calculate(int choice) {
```

```
int again = 1;
double tout = 0;
double thermalConductivity = 0, n = 0, viscosity = 0, density = 0, reynoldNum = 0;
//Thermophysical Properties to be calculated at average temperature
double specificHeat;
double nusseltNum;
while (again) {
    switch (choice) {
        case 1:

            thermalConductivity = 0.6480765 + (0.00108329 * tavg) +
(0.020423 * conc) - (0.0049797 * weg);
            viscosity = 1.706344 - (0.0262813 * tavg) + (0.010705 * conc)
+ (0.0326505 * weg);
            density = 1013.064313 - (0.412946 * tavg) + (1.736101 * conc)
+ (1.4648252 * weg);

            viscosity *= pow(10, -3);

            break;

        case 2:

            thermalConductivity = 0.6016226 + (0.0008969 * tavg) +
(0.007895 * conc) - (0.0051 * weg);
            viscosity = 1.72275603 - (0.0265935 * tavg) + (0.011464 *
conc) + (0.032778 * weg);
            density = 1014.3351 - (0.42628 * tavg) + (1.78487 * conc) +
(1.467506 * weg);

            viscosity *= pow(10, -3);

            break;

        case 3:
```

```
                    thermalConductivity = 0.60568226 + (0.0008918 * tavg) +
(0.0094104 * conc) - (0.004801 * weg);
                    viscosity = 1.7363124 - (0.0267501 * tavg) + (0.0117586 *
conc) + (0.032747 * weg);
                    density = 1015.10982 - (0.431133 * tavg) + (1.81809 * conc) +
(1.46761 * weg);

                    viscosity *= pow(10, -3);

                    break;

            default:
                    printf("Invalid Choice");
                    return;
        }

        conc1 = conc / 100;

        specificHeat = getSpecificHeat(weg);

        printf("\n");

        reynoldNum = (dh * velocity * density) / viscosity;


        double thermalDiffusivity = thermalConductivity / (density * specificHeat);

        double prandtlNum = (specificHeat * viscosity) / thermalConductivity;

        double pecletNum = (dp * velocity) / thermalDiffusivity;

        nusseltNum = 0.1205 * (1 + (4.285 * pow(conc * pow(10, -2), 0.854) *
pow(pecletNum, 0.118))) * pow(reynoldNum, 0.133) * pow(prandtlNum, 0.4);
```

```
            double htc = (nusseltNum * thermalConductivity) / dh; //htc = Heat Transfer
Coefficient

            double msquare = (2 * htc) / (km * wfin);
                  //
            double m = pow(msquare, 0.5);
                              // Efficiency of Fin
            double efficiency = tanh(m * channelHeight) / (m * channelHeight);
      //

            double tdNum = voltage * current;

                  //
            double tdDen = htc * (2 * channelHeight * efficiency + channelWidth) *
numChannels * channelLength;          // Average Temperature Difference of Surface and
Fluid
            double td = tdNum / tdDen;
                                                                                    //

            tout = (tb - td);                              //Final Outlet Temperature
            double tavg2 = (tin + tout) / 2;          //Average temperature calculated at final
outlet temperature

            if (to - tout > 0.5) {
                  to = tout;
                  tavg = tavg2;
            } else {
                  again = 0;
            }
      }

      double ff = getFrictionFactor(weg, reynoldNum);
      double Q = flowRate * density * specificHeat * (tout - tin);

      printf("Reynold Number: %f\n", reynoldNum);
```

```
        printf("Nusselt Number: %f\n", nusseltNum);
        printf("Friction Factor: %f\n", ff);
        printf("Heat Removal Q: %f\n", Q);

}

double getSpecificHeat(double weg) {
 int weg1 = (int) weg;
 double a, b, c;
 switch(weg1){
  case 0:
   a = 1.00380;
   b = -2.2459 * pow(10, -4);
   c = 2.6257 * pow(10, -6);
   break;
  case 10:
   a = 0.97236;
   b = 1.8001 * pow(10, -4);
   c = 5.7049 * pow(10, -7);
   break;
  case 20:
   a = 0.93576;
   b = 3.9963 * pow(10, -4);
   c = 0;
   break;
  case 30:
   a = 0.89889;
   b = 5.1554 * pow(10, -4);
   c = 0;
   break;
  case 40:
   a = 0.85858;
   b = 6.2639 * pow(10, -4);
   c = 0;
   break;
```

```
  case 50:
   a = 0.81485;
   b = 7.3219 * pow(10, -4);
   c = 0;
  }
  double specHeat = a + (b * tavg) + (c * tavg * tavg);
  return specHeat * 4184;
}

double getFrictionFactor(double weg, double rn){
  int eg = (int) weg;
  double c;
  switch(eg){
   case 0:
    c = 0.560325;
    break;
   case 10:
    c = 0.2439;
    break;
   case 20:
    c = 0.1989835;
    break;
   case 30:
    c = 0.1540667;
    break;
   case 40:
    c = 0.105942;
    break;
   case 50:
    c = 0.05781667;
  }
  return c / (pow(rn, 2.21966667));
}
```

APPENDIX-B

MATLAB PROGRAM FOR MADM TOPSIS APPROACH

```
RIM=csvread('relative_importance_matrix.csv');
DM=csvread('decision_matrix.csv');
[EVB,EDB]=eig(RIM,'balance');
W=bsxfun(@rdivide,EVB,sum(EVB));
W=W(:,1);
R=normc(DM);
V=bsxfun(@times,R,W');
Vp=max(V);
Vm=min(V);
Sp=sqrt(sum(power(bsxfun(@minus,V,Vp),2),2));
Sm=sqrt(sum(power(bsxfun(@minus,V,Vm),2),2));
Cp=Sp./(Sp+Sm);
Cm=Sm./(Sp+Sm);
printf('    Weight Vector \r\n')
disp(W')
fprintf('    Normalized Decsion Matrix "R" \r\n')
disp(R)
fprintf('    "V" Matrix \r\n')
disp(V)
fprintf('    V+ \t')
disp(Vp)
fprintf('    V- \t')
disp(Vm)
fprintf('    S+ \t')
disp(Sp')
fprintf('    S- \t')
disp(Sm')
fprintf('    C+ \t')
disp(Cp')
fprintf('    C- \t')
disp(Cm')
```

REFERENCES

1. Moore, G.E., 1965. "Cramming more components onto integrated circuits", *Electronics*, pp. 114-117.
2. Sohel, M.R., Khaleduzzaman, S.S., Saidur, R., Hepbasli, A., Sabri, M.F.M. and Mahbubul I.M., 2014. "An experimental investigation of heat transfer enhancement of a minichannel heat sink using Al_2O_3 - H_2O nanofluid", *International Journal of Heat and Mass Transfer*, 74, pp. 164–172.
3. Tuckerman, D.B .and Pease, R.F.W., 1981. "High-performance heat sinking for VLSI", *IEEE Electron Device Lett*er, 2, pp. 126–129.
4. Kandlikar, S.G. and Grande, W.J., 2003. "Evolution of microchannel flow passages thermohydraulic performance and fabrication technology", *Heat Transfer Engineering*, 24 (1), pp. 3–17.
5. Kandlikar, S.G. and Grande, W.J., 2004. "Evaluation of single phase flow in microchannels for high heat flux chip cooling thermohydraulic performance enhancement and fabrication technology", *Heat Transfer Engineering,* 24 (1), pp. 5–16.
6. Halelfadl, S., Adhamb, A.M., Ghazali, N.M., Mare, T., Estelle, P. and Ahmadd, R., 2014. "Optimization of thermal performances and pressure drop of rectangular microchannel heat sink using aqueous carbon nanotubes based nanofluid", *Applied Thermal Engineering*, 62 (2), pp. 492-499.
7. Ahuja, A.S., 1975. "Augmentation of heat transport in laminar flow of polystyrene suspensions. II. Analysis of the data", *Journal of Applied Physics*, 46 (8), pp. 3417 – 3425.
8. Choi, S.U.S., 1995. "Enhancing thermal conductivity of fluid with nanoparticles", *ASME International Mechanical Engineering Congress & Exposition*, pp. 99–105.
9. Choi, S.U.S., Zhang, Z.G., Yu, W., Lockwood, F.E. and Grulke, E.A., 2001. "Anomalous thermal conductivity enhancement in nano-tube suspensions", *Applied Physics Letters,* 79, pp. 2252–2254.
10. Xuan, Y. and Li, Q., 2000. "Heat transfer enhancement of nanofluids", *International Journal of Heat and Fluid Transfer,* 21, pp. 58-64.
11. Xuan, Y. and Roetzel, W., 2000. "Conceptions for heat transfer correlation of nanofluids", *International Journal of Heat and Mass Transfer,* 43, pp. 3701-3707.
12. Wong, K.V. and Leon, O.D., 2010. "Applications of Nanofluids: Current and Future", Advances in Mechanical Engineering, Article ID 519659, pp. 1-11.

13. Singh, P.K., 2010. “Hydrodynamic and thermal transport in nanofluids inside microchannels, *Ph.D. thesis*, Indian institute of technology Madras, India.
14. Akoh, H., Tsukasaki, Y., Yatsuya, S. and Tasaki, A., 1978. “Magnetic properties of ferromagnetic ultrafine particles prepared by vacuum evaporation on running oil substrate”, *Journal of Crystal Growth*, 45, pp. 495-500.
15. Lo, C.H., Tsung T.T. and Chen, L.C., 2005. “Shaped-controlled synthesis of cu-based nanofluid using submerged arc nanoparticle synthesis system (SANSS)”, *Journal of Crystal Growth*, 277, pp. 636-642.
16. Lo, C.H., Tsung, T.T., Chen, L.C., Su, C.H. and Lin, H.M., 2005. “Fabrication of copper oxide nanofluid using submerged arc nanoparticles synthesis system (SANSS)”, *Journal of Nanoparticle Research*, 7, pp. 313–320.
17. Chang, H., Tsung, T.T., Chen, L.C., Yang, Y.C., Lin, H.M., Lin, C.K. and Jwo, C.S, 2005. “Nanoparticle Suspension Preparation Using the Arc Spray Nanoparticle Synthesis System Combined with Ultrasonic Vibration and Rotating Electrode”, *The International Journal of Advanced Manufacturing Technology*, 26, pp. 552-558.
18. Phuoc, T.X., Soong, Y. and Chyu, M.K., 2007. “Synthesis of Ag-deionized water nanofluids using multi-beam laser ablation in liquids”, *Opt Lasers Engineering*, 45, pp. 1099-1106
19. Anoop, K. B., 2009. “Study on thermo-physical transport in nanofluids”, *Ph.D. thesis*, Indian institute of technology Madras, India.
20. Patel, H.E., Das, S.K., Sundararajan, T., Sreekumaran, N.A., Georgeand, B. and Pradeep, T., 2003. “Thermal conductivities of naked and monolayer protected metal nanoparticle based nanofluids: manifestation of anomalous enhancement and chemical effects”, *Applied Physics Letters*, 83, pp. 2931-2933.
21. Liu M.S., Lin, M.C., Tsai, C.Y. and Wang, C., 2006. “Enhancement of thermal conductivity with Cu for nanofluids using chemical reduction method”, *International Journal of Heat and Mass Transfer*, 49, pp. 3028–3033.
22. Chen, H., Yang, W., He, Y., Ding, Y., Zhang, L., Tan, C., Lapkin, A. and Bavykin, D.V., 2008. “Heat transfer and flow behaviour of aqueous suspensions of titanate nanotubes (nanofluids), *Powder Technology*, 183, pp. 63-72.
23. Kumaresan, V. and Velraj, R., 2012. “Experimental investigation of the thermo-physical properties of water-ethylene glycol mixture based CNT nanofluids”, *Thermochimica Acta*, 545, pp. 180-186.

24. Li, Q., Xuan, Y., Jiang J. and Xu, J.W., 2005. “Experimental investigation on flow and convective heat transfer feature of a nanofluid for aerospace thermal management, *Journal of Astronautics*, 26, pp. 391-394.

25. Chung, S.J., Leonard, J.P., Nettleship, I., Lee, J.K., Soong, Y., Martello, D.V. and Chyu, M.K., 2009. “Characterization of ZnO nanoparticle suspension in water: Effectiveness of ultrasonic dispersion”, *Powder Technology*, 194 (1–2), pp.75-80.

26. Buhrman, R.A. and Granqvistt, C.G., 1976. “Log-normal size distributions from magnetization measurements on small superconducting AI particles”, *Journal of Applied Physics*, 47 (5).

27. Das, S.K., Putra, N., Thiesen, P. and Roetzel W., 2003. “Temperature dependence of thermal conductivity enhancement for nanofluids”, *Journal of Heat Transfer*, 125, pp. 567–574.

28. Kole, M. and Dey, T.K., 2012. “Thermophysical and pool boiling characteristics of ZnO - ethylene glycol nanofluids”, *International Journal of Thermal science*, 62, pp. 61-70.

29. Suresh, S., Chandrasekar, M. and Sekhar, S.C., 2011. “Experimental studies on heat transfer and friction factor characteristics of CuO/water nanofluid under turbulent flow in a helically dimpled tube”, *Experimental Thermal and Fluid Science*, 35, pp. 542-549.

30. Yang, X.F. and Liu, Z.H., 2012. “Flow boiling heat transfer in the evaporator of a loop thermosyphon operating with CuO based aqueous nanofluid”, *International Journal of Heat and Mass Transfer*, 55, pp.7375-7384.

31. Kannadasan, N., Ramanathan, K. and Suresh, S., 2012. “Comparison of heat transfer and pressure drop in horizontal and vertical helically coiled heat exchanger with CuO/water based nanofluids”, *Experimental Thermal and Fluid Science*, 42, pp. 64-70.

32. Matthew, D.B., Robert A.H. and Alexandre K.D.S., 2012. “Experimental thermal-hydraulic evaluation of CuO nanofluids in microchannels at various concentrations with and without suspension enhancers”, *International Journal of Heat and Mass Transfer*, 55, pp. 2684-2691.

33. Namburu, P.K., Kulkarni, D.P., Misra, D. and Das, D.K., 2007. Viscosity of copper oxide nanoparticles dispersed in ethylene glycol and water mixture”, *Experimental Thermal and Fluid Science*, 32, pp.397-402.

34. Heris, S.Z., 2011. “Experimental investigation of pool boiling characteristics of low-concentrated CuO/ethylene glycol-water nanofluids”, *International Communications in Heat and Mass transfer,* 38, pp.1470-1473.

35. Suresh, S., Selvakumara, P., Chandrasekar, M. and Raman, V.S., 2012. “Experimental studies on heat transfer and friction factor characteristics of Al_2O_3/water nanofluid under turbulent flow with spiraled rod inserts”, *Chemical Engineering and Processing,* 53, pp. 24-30.

36. Gharagozloo, P.E. and Goodson, K.E. (2011). “Temperature-dependent aggregation and diffusion in nanofluids”, *International Journal of Heat and Mass Transfer,* 54, pp. 797-806.

37. Raveshi, M.R., Keshavarz, A., Mojarrad, M.S. and Amiri, S., 2013. “Experimental investigation of pool boiling heat transfer enhancement of alumina/water-ethylene glycol nanofluids”, *Experimental Thermal and Fluid Science,* 44, pp. 805-814.

38. Hung, Y.H., Teng, T.P. and Lin, B.G., 2013.” Evaluation of the thermal performance of a heat pipe using alumina nanofluids”, *Experimental Thermal and Fluid Science,* 44, pp. 504-511.

39. Heyhat, M.M., Kowsary, F., Rashidi, A.M., Momenpour, M.H. and Amrollahi, A., 2013. “Experimental investigation of laminar convective heat transfer and pressure drop of water-based Al_2O_3 nanofluids in fully developed flow regime”, *Experimental Thermal and Fluid Science,* 44, pp. 483-489.

40. Lee, J.H., Hwang, K.S., Jang, S.P., Lee, B.H., Kim, J.H., Choi, S.U.S. and Choi, C.J., 2008. “Effective viscosities and thermal conductivities of aqueous nanofluids containing low volume concentrations of Al_2O_3 nanoparticles”, *International Journal of Heat and Mass Transfer,* 51, pp. 2651-2656.

41. Sundar, L.S., Ramana, E.V., Singh, M.K., and Sousa, A.C.M., 2014. “Thermal conductivity and viscosity of stabilized ethylene glycol and water mixture Al_2O_3 nanofluids for heat transfer applications: An experimental study”, *International Communications in Heat and Mass Transfer,* 56, pp. 86-95.

42. Lamas, B., Abreu, B., Fonseca, A., Martins, N. and Oliveira, M., 2012. “Assessing colloidal stability of long term MWCNTs based nanofluids”, *Journal of Colloid Interface Science,* 381, pp. 17-23.

43. Yousefi, T., Shojaeizadeh, E., Veysi, F. and Zinadini, S., 2012. “An experimental investigation on the effect of pH variation of MWCNT-H_2O nanofluid on the efficiency of a flat-plate solar collector”, *Solar Energy,* 86, pp. 771-779.

44. Phuoc, T.X., Massoudi, M. and Chen, R.H., 2011. "Viscosity and thermal conductivity of nanofluids containing multi-walled carbon nanotubes stabilized by chitosan, *International Journal of Thermal science* 50, pp. 12-18.

45. Xie, H., Wang, J., Xi, T., Liu, Y., Ai, F. and Wu, Q., 2002. "Thermal conductivity enhancement of suspensions containing nano-sized alumina particles", *Journal of Applied Physics,* 91 (7), pp. 4568-4572.

46. Lee, D., Kim, J.W. and Kim, B.G., 2006. "A new parameter to control heat transport in nanofluids: Surface charge state of the particle in suspension", *Journal of Physical Chemistry B,* 110 (9), pp. 4323-4328.

47. Sundar, L.S., Farooky, M.H., Sarada, S.N. and Singh, M.K., 2013. "Experimental thermal conductivity of ethylene glycol and water mixture based low volume concentration of Al_2O_3 and CuO nanofluids", *International Communications in Heat and Mass Transfer,* 41, pp. 41-46.

48. Fedele, L., Colla, L., Bobbo, S., Barison, S. and Agresti, F., 2011. "Experimental stability analysis of different water based nanofluids", *Nanoscale Research Letters,*6, pp. 300.

49. Gowda, R., Sun, H., Wang, P., Charmchi, M., Gao, F., Gu, Z. and Budhlall, B., 2010. "Effects of particle surface charge, species, concentration, and dispersion method on the thermal conductivity of nanofluids", Hindawi Publishing Corporation, *Advances in Mechanical Engineering,* Article ID 807610, pp. 1-10. doi:10.1155/2010/807610

50. Mondragon, R., Segarra, C., Cuenca, R.M., Julia, J.E. and Jarque, J.C., 2013. "Experimental characterization and modeling of thermophysical properties of nanofluids at high temperature conditions for heat transfer applications", *Powder Technology*, 249, pp. 516-529.

51. Ghadimi, A., Saidur, R. and Metselaar, H.S.C., 2011. "A review of nanofluid stability properties and characterization in stationary conditions", *International Journal of Heat and Mass Transfer,* 54, pp. 4051-4068

52. Naraki, M., Peyghambarzadeh, S.M., Hashemabadi, S.H. and Vermahmoudi, Y., 2013. "Parametric study of overall heat transfer coefficient of CuO/water nanofluids in a car radiator," *International Journal of Thermal Sciences,* 66, pp. 82-90.

53. Wen, D. and Ding, Y., 2004. Experimental investigation into convective heat transfer of nanofluid at the entrance region under laminar flow conditions, *International Journal of Heat and Mass Transfer,* 47, pp. 5181-5188.

54. Singh, N., Chand, G. and Kanagaraj, S., 2012. "Investigation of thermal conductivity and viscosity of carbon nanotubes-ethylene glycol nanofluids", *Heat Transfer Engineering*, 33 (9), pp. 821–827.

55. Hwang, Y., Lee, J.K. and Lee, C.H., "Stability and thermal conductivity characteristics of nanofluids," *Thermochimica Acta*, 455 (1-2), pp. 70–74.

56. Yu, Q., Kim, Y.J. and Ma, H., 2008. "Nanofluids with plasma treated diamond nanoparticles," *Applied Physics Letters*, 92 (10), Article ID 103111.

57. Yu, W. and Xie, H., 2012. Review article: A review on nanofluids: Preparation, stability mechanisms, and applications", Hindawi Publishing Corporation, *Journal of Nanomaterials*, Article ID 435873, pp. 1-17.

58. Maxwell, J. C., 1881. "A Treatise on electricity and magnetism", 2nd ed., *Clarendon Press*, Oxford, U.K.

59. Hamilton, R.L., and Crosser, O.K., 1962. "Thermal conductivity of heterogeneous two component systems", *Industrial & Engineering Chemistry Fundamentals*, 1, pp. 187-191.

60. Eastman, J.A., Choi, S.U.S., Li, S., Thompson, L.J. and Lee, S., 1997. "Enhanced thermal conductivity through the development of nanofluids", *Materials Research Society Symposium -Proceedings*, 457, pp. 3–11.

61. Lee, S., Choi, S.U.S., Li, S. and Eastman, J.A., 1999. "Measuring thermal conductivity of fluids containing oxide nanoparticles", *Journal of Heat Transfer*, 121, pp. 280-289.

62. Wang, X., Xu, X. and Choi, S.U.S., 1999. "Thermal conductivity of nanoparticle-fluid mixture", *Journal of Thermophysics and Heat Transfer*, 13 (4), pp. 474–480.

63. Li, C.H. and Peterson, G.P., 2006. "Experimental investigation of temperature and volume fraction variations on the effective thermal conductivity of nanoparticles suspensions (nanofluids)", *Journal of Applied Physics*, 99 (8), pp. 084314.

64. Wen, D. and Ding, Y., 2004. "Effective thermal conductivity of aqueous suspensions of carbon nanotubes (carbon nanotube nanofluids)", *Journal of Thermophysics and Heat Transfer*, 18 (4), pp. 481–485.

65. Assael, M.J., Chen, C.F., Metaxa, I.N. and Wakeham, W.A., 2003. "Thermal conductivity of suspensions of carbon nanotubes in water, in: 15th Symposium on Thermophysical Properties, National Institute of Standards, University of Colorado, Boulder, USA, 2003.

66. Assael, M.J., Chen, C.F., Metaxa, I.N. and Wakeham, W.A., 2004. "Thermal conductivity of suspensions of carbon nanotubes in water", *International Journal of Thermophysics*, 25 (4), pp. 971-985.

67. Assael, M.J., Metaxa, I.N., Arvanitidis, J., Christofilos, D. and Lioutas, C., 2005. "Thermal conductivity enhancement in aqueous suspensions of carbon multiwalled and double-walled nanotubes in the presence of two different dispersants", *International Journal of Thermophysics*, 26 (3), pp. 647-664.

68. Masuda, H., Ebata, A., Teramae, K. and Hishinuma, N., 1993. "Alteration of thermal conductivity and viscosity of liquid by dispersing ultra-fine particles (dispersion of Al_2O_3, SiO_2, and TiO_2 ultra-fine particles)", *Netsu Bus-sei (Japan)*, 7, pp. 227.

69. Zhou, L.P. and Wang, B.X., 2002. "Experimental researches on the thermophysical properties of nanoparticle suspensions using the quasi-steady state method", *Annual Proc. Chinese Engineering Thermophysics (in Chinese)*, pp. 889.

70. Zhu, H.T., Zhang, C.Y., Tang, Y.M. and Wang, J.X., 2007. "Novel synthesis and thermal conductivity of CuO nanofluid", *The Journal of Physical Chemistry C, 111*, pp. 1646.

71. Xie, H., Lee, H., Youn, W. and Choi, M. 2003. "Nanofluids containing multiwalled carbon nanotubes and their enhanced thermal conductivities", *Journal of Applied Physics*, 94, pp. 4967.

72. Liu, M.S., Lin, M.C.C., Huang, I.T. and Wang, C.C., 2005. "Enhancement of thermal conductivity with carbon nanotube for nanofluids", *International Communications of Heat and Mass Transfer*, 32, 1202.

73. Beck, M., Yuan, Y., Warrier, P., and Teja, A.S. 2009. "The effect of particle size on the thermal conductivity of alumina nanofluids", *Journal of Nanoparticle Research*, 11, pp. 1129-1136.

74. Mintsa, H.A., Roy, G., Nguyen, C.T. and Doucet, D., 2009. "New temperature dependent thermal conductivity data for water-based nanofluids", *International Journal of Thermal Science*, 48, pp. 363-371.

75. Teng, T.P, Hung, Y.H., Teng, T.C., Mo, H.E. and Hsu, H.G., 2010. "The effect of alumina/water nanofluid particle size on thermal conductivity", Applied Thermal Science, 30, pp. 2213-2218.

76. Gallego, M.J.P., Lugo, L., Legido, J.L. and Pineiro, M.M., 2011. "Thermal conductivity and viscosity measurements of ethylene glycol-based Al_2O_3 nanofluids", Nanoscale Research Letters, 6, pp. 221.

77. Kim, N.J., Park, S.S., Lim, S.H. and Chun, W., 2011. "A study on the characteristics of carbon nanofluids at the room temperature (25 °C)", *International Communications of Heat and Mass Transfer*, 38, pp. 313-318.

78. Shima, P.D., Philip, J. and Raj, B., 2010. “Influence of aggregation on thermal conductivity instable and unstable nanofluids”, *Applied Physics Letters*, 97, pp. 153113.

79. Ding, Y., Alias, H., Wen, D. and Williams, R.A., 2006. “Heat transfer of aqueous suspensions of carbon nanotubes (CNT nanofluids)”, *International Journal of Heat and Mass Transfer*, 49, pp. 240-250.

80. Gallego, M.J.P., Casanova, C., Paramo, R., Barbes, B., Legido, J.L. and Pineiro, M.M., 2009. “A study on stability and thermophysical properties (density and viscosity) of Al_2O_3 in water nanofluid”, *Journal of Applied Physics*, 106, pp. 064301.

81. Yu, W., Xie, H., Chen, L. and Li, Y., 2011. “Investigation on the thermal transport properties of ethylene glycol-based nanofluids containing copper nanoparticles, *Powder Technology*, 197, pp. 218-221.

82. Heris, S.Z., Etemad, S.G. and Esfahany, M.N., 2006. “Experimental investigation of oxide nanofluids laminar flow convective heat transfer”, *International Communications of Heat and Mass Transfer,* 33, pp. 529-535.

83. Yu, W., Xie, H., Li, Y., Chen, L. and Wang, Q., 2012. “Experimental investigation on the heat transfer properties of Al_2O_3 nanofluids using the mixture of ethylene glycol and water as base fluid”, *Powder Technology*, 230, pp. 14-19.

84. Einstein, A., 1911. “A new determination of molecular dimensions”, *Annual Physics*, 34, pp. 591.

85. Durlofsky, L. and Brady, J.F., 1987. “Analysis of the Brinkman equation as a model for flow in porous media”, *Physics of fluid*, 30 (1), pp. 3329-3341.

86. *Liu*, M.S., *Lin*, M.C.C., *Huang*, I.T. and *Wang, C.C., 2006. “*Enhancement of thermal conductivity with CuO for nanofluids”, *Chemical Engineering Technology*, *29* (1), pp. 72-77.

87. Chen, L., Xie, H., Li, Y. and Yu, W., 2008. “Nanofluids containing carbon nanotubes treated by mechanochemical reaction”, *Thermochimica Acta*, 477, pp. 21-24

88. Garg, P., Alvarado, J.L., Marsh, C., Carlson, T.A., Kessler, D.A. and Annamalai, K., 2009. “An experimental study on the effect of ultrasonication on viscosity and heat transfer performance of multi-wall carbon nanotube-based aqueous nanofluids”, *International Journal of Heat and Mass Transfer,* 52, pp. 5090-5101.

89. Sridhara, V. and Satapathy, L.N., 2011. “Al_2O_3-based nanofluids: A review”, *Nanoscale Research Letters*, 6, pp. 456.

90. Liu, M.S., Lin, M.C.C. and Wang, C.C., 2011. “Enhancements of thermal conductivities with Cu, CuO, and carbon nanotube nanofluids and application of

MWNT/water nanofluid on a water chiller system", *Nanoscale Research Letters*, 6, pp. 297.

91. Khedkar, R.S., Sonawane, S.S. and Wasewar, K.L., 2012. "Influence of CuO nanoparticles in enhancing the thermal conductivity of water and monoethylene glycol based nanofluids", *International Communications in Heat and Mass Transfer*, 39, 665-669

92. Vajjha, R.S., Das, D.K. and Mahagaonkar, B.M., 2009. "Density measurement of different nanofluids and their comparison with theory", *Petroleum Science and Technology*, 27 (6), pp. 612-624.

93. Harkirat and Gangacharyulu, D., 2010. "Preparation and characterization of nanofluids and some investigation in biological applications", *M.Tech Thesis*, Thapar University, Patiala.

94. Shoghl, S.N., Jamali, J. and Moraveji, M.K., 2016. "Electrical conductivity, viscosity, and density of different nanofluids: An experimental study", *Experimental Thermal and Fluid Science*, 74, pp. 339-346

95. Pak, B. and Cho, Y.I., 1998. "Hydrodynamic and heat transfer study of dispersed fluids with submicron metallic oxide particle", *Experimental Heat Transfer*, 11, pp. 151-170.

96. Maiga, S.E.B., Nguyen, C.T., Galanis N. and Roy G., 2004. "Heat transfer behaviours of nanofluids in a uniformly heated tube", *Super lattices and Microstructures*, 35 (3-6), pp. 543-57.

97. Jang, S.P. and Choi, S.U.S., 2004. "Role of Brownian motion in the enhanced thermal conductivity of nanofluids", *Applied Physics Letter*, 84, pp. 4316.

98. Namburu, P.K., Kulkarni, D.P., Dandekar, A. and Das, D. K., 2007. "Experimental investigation of viscosity and specific heat of silicon dioxide nanofluids", *Micro & Nano Letters*, 2(3), pp. 67-71.

99. Bergman, T.L., 2009. "Effect of reduced specific heats of nanofluids on single phase, laminar internal forced convection, *International Journal of Heat and Mass Transfer*, 52 (5-6), pp. 1240-4.

100. Zhou, S.Q. and Ni, R., 2008. "Measurement of the specific heat capacity of water-based Al_2O_3 nanofluid", *Applied Physics Letters*, 92, pp. 093123.

101. Vajjha, R.S., and Das, D.K., 2012. "A review and analysis on influence of temperature and concentration of nanofluids on thermophysical properties, heat transfer and pumping power", *International Journal of Heat and Mass Transfer*, 55, pp. 4063–4078.

102. Esfe, M.H., Saedodin, S., Mahian, O. and Wongwises, S., 2014. "Thermophysical properties, heat transfer and pressure drop of COOH-functionalized multi walled carbon nanotubes/water nanofluids", *International Communications in Heat and Mass Transfer*, 58, pp. 176-183.

103. Xuan, Y. and Li, Q., 2003. "Investigation on convective heat transfer and flow features of nanofluids, *Journal of Heat Transfer*, 125, pp. 151-156.

104. Nguyen, C.T., Roy, G., Gauthier, C. and Galanis, N., 2007. "Heat transfer enhancement using Al_2O_3- water nanofluid for electronic liquid cooling system", *Applied Thermal Engineering*, 28, pp. 1501.

105. Rea, U., McKrell, T., Hu, L. and Buongiorno, J., 2009. "Laminar convective heat transfer and viscous pressure loss of alumina-water and zirconia-water nanofluids", *International Journal of Heat and Mass Transfer*, 52(7-8), pp. 2042-8.

106. Williams, W., Buongiorno, J. and Hu, L., 2008. "Experimental investigation of turbulent convective heat transfer and pressure loss of alumina/water and zirconia/water nanoparticle colloids (nanofluids) in horizontal tubes", *Journal of Heat Transfer*, 130, pp. 042412-1.

107. Ho, C.J. and Chen, W.C., 2013. "An experimental study on thermal performance of Al_2O_3/water nanofluid in a minichannel heat sink", *Applied Thermal Engineering*, 50, pp. 516-522.

108. Ijam, A., Saidur, R. and Ganesan, P., 2012. "Cooling of minichannel heat sink using nanofluids, *International Communications in Heat and Mass Transfer*, 39, pp. 1188-1194.

109. Ijam, A. and Saidur, R., 2012. "Nanofluid as a coolant for electronic devices (cooling of electronic devices)", *Applied Thermal Engineering*, 32, pp. 76-82.

110. Naphon, P. and Nakharintr, L., 2013. "Heat transfer of nanofluids in the mini-rectangular fin heat sinks", *International Communications in Heat and Mass Transfer*, 40, pp. 25-31.

111. Sohel, M.R., Khaleduzzaman, S.S., Saidur, R., Hepbasli, A., Sabri, M.F.M. and Mahbubul, I.M., 2014. "An experimental investigation of heat transfer enhancement of a minichannel heat sink using Al_2O_3-H_2O nanofluid, *International Journal of Heat and Mass Transfer*, 74, pp. 164-172.

112. Aliabadi, M.K. and Sahamiyan, M., 2016. "Performance of nanofluid flow in corrugated minichannels heat sink (CMCHS)", *Energy Conversion and Management*, 108, pp. 297-308.

113. Moraveji, M.K. and Ardehali, R.M., 2013. “CFD modeling (comparing single and two-phase approaches) on thermal performance of Al_2O_3/water nanofluid in minichannel heat sink”, *International Communications in Heat and Mass Transfer*, 44, pp. 157–64.

114. Aliabadi, M.K., Hormozi, F. and Zamzamian, A., 2014. “Effects of geometrical parameters on performance of plate-fin heat exchanger: vortex-generator as core surface and nanofluid as working media*”, Applied Thermal Engineering*, 70, pp. 565-79.

115. Koo, J. and Kleinstreuer, C., 2005. “Laminar nanofluid flow in microheat-sinks”, *International Journal of Heat and Mass Transfer*, 48(13), pp. 2652-2661.

116. Chein, R. and Huang, G., 2005. “Analysis of microchannel heat sink performance using nanofluids, *Applied Thermal Engineering*, 25(17-18), pp. 3104-3114.

117. Jang, S.P. and Choi, S.U.S., 2006. “Cooling performance of a microchannel heat sink with nanofluids”, *Applied Thermal Engineering*, 26, pp. 2457-2463.

118. Abbassi, H. and Aghanajafi, C., 2006. “Evaluation of heat transfer augmentation in a nanofluid-cooled microchannel heat sink”, *Journal of Fusion Energy*, 25(3-4), pp. 187-96.

119. Lajvardi, M., Sabbaghzadeh, J., Ebrahimi, S. and Hadi, I., 2007. “Analysis of microchannel heat sink performance using spherical nanofluids”, *Proceedings of the 7th IEEE International Conference on Nanotechnology*, August 2 - 5, 2007, Hong Kong.

120. Chein, R. and Chung, H., 2007. “Experimental microchannel heat sink performance studies using nanofluids”, *International Journal of Thermal Sciences*, 46(1), pp. 57-66.

121. Tsai, T.H. and Chein, R., 2007. “Performance analysis of nanofluid-cooled microchannel heat sinks”, *International Journal of Heat and Mass Transfer*, 28(5), pp. 1013-1026.

122. Lu, X. and Nnanna, A.G.A., 2008. “Experimental study of fluid flow in microchannel”, *Proceedings of IMEC 2008 ASME International Mechanical Engineering Congress and Exposition*, October 31-November 6, 2008, Boston, Massachusetts, USAIMECE2008-67932.

123. Li, J. and Kleinstreuer, C., 2008. “Thermal performance of nanofluid flow in microchannels”, *International Journal of Heat and Fluid Flow*, 29, pp. 1221–1232.

124. Shokouhmand, H., Ghazvini, M. and Shabanian, J., 2008. “Performance Analysis of Using Nanofluids in Microchannel Heat Sink in different Flow Regimes and its

simulation using Artificial Neural Network", *Proceedings of the World Congress on Engineering*, Vol III WCE 2008, July 2 - 4, 2008, London, U.K.

125. Jung, Y., Oh, H.S. and Kwak, H.Y., 2009. "Forced convective heat transfer of nanofluids in microchannels", *International Journal of Heat and Mass Transfer*, 52, pp.466–472.
126. Bhattacharya, P., Samanta, A.N. and Chakraborty, S., 2009. "Numerical study of conjugate heat transfer in rectangular microchannel heat sink with Al_2O_3/H_2O nanofluid", *Heat Mass Transfer*, 45, pp. 1323–1333.
127. Wu, X., Wu, H. and Cheng, P., 2009. "Pressure drop and heat transfer of Al_2O_3-H_2O nanofluids through silicon microchannels", *Journal of Micromechanics and Microengineering*, 19, pp. 105020-1-11.
128. Harirchian, T. and Garimella, S.V., 2009. "The critical role of channel cross-sectional area in microchannel flow boiling heat transfer", *International Journal of Multiphase Flow*, 35, pp. 904-913.
129. Chein, R. and Chen, J., 2009. "Numerical study of the inlet/outlet arrangement effect on microchannel heat sink performance", *International Journal of Thermal Sciences*, 48, pp. 1627-1638.
130. Gunnasegaran, P., Mohammed, H. and Shuaib, N.H., 2009. "Pressure drop and friction factor for different shapes of microchannels", *Proceedings of ICEE 2009 3rd International Conference on Energy and Environment*, 7-8 December 2009, Malacca, Malaysia IEEE 418.
131. Mohammed, H.A., Gunnasegaran, P. and Shuaib, N.H., 2010. "Heat transfer in rectangular microchannels heat sink using nanofluid", *International Communications in Heat and Mass Transfer*, 37, pp. 1496–1503.
132. Escher, W., Brunschwiler, T., Shalkevich, N., Shalkevich, A., Burgi, T., Michel, B. and Poulikakos, D., 2011. "On the cooling of electronics with nanofluids," *Journal of Heat Transfer*, 133, pp. 0514011-11.
133. Mohammed, H.A., Gunnasegaran, P. and Shuaib, N.H., 2011. "The impact of various nanofluid types on triangular microchannels heat sink cooling performance," *International Communications in Heat and Mass Transfer*, 38 (6), pp. 767–773.
134. Solovitz, S.A. and Mainka, J., 2011. "Manifold design for micro-channel cooling with uniform flow distribution", *Journal of Fluids Engineering*, 133, pp. 051103-1-11.
135. Seyf, H.R. and Mohammadian, S.K., 2011. "Thermal and hydraulic performance of counter flow microchannel heat exchangers with and without nanofluids", *Journal of Heat Transfer*, 133, pp. 081801-1-9.

136. Farsad, E., Abbasi, S. P., Zabihi, M. S. and Sabbaghzadeh, J., 2011. "Numerical simulation of heat transfer in a micro channel heat sinks using nanofluids", *Heat Mass Transfer,* 47, pp. 479–490.

137. Singh, P.K., Harikrishna, P.V., Sundararajan, T. and Das, S.K., 2011. "Experimental and numerical investigation into the heat transfer study of nanofluids in microchannel", *Journal of Heat Transfer,* 133, pp. 121701-1-9.

138. Anoop, K., Sadr, R., Yu, J., Kang, S., Jeon, S. and Banerjee, D., 2012. "Experimental study of forced convective heat transfer of nanofluids in a microchannel", *International Communications in Heat and Mass Transfer*, 39, pp. 1325-1330.

139. Hung, T.C., Yan, W.M., Wang, X.D. and Chang, C.Y., 2012. "Heat transfer enhancement in microchannel heat sinks using nanofluids", *International Journal of Heat and Mass Transfer*, 55, pp. 2559–2570.

140. Kamali, R., Jalali, Y. and Binesh, A.R., 2013. "Investigation of multiwall carbon nanotube-based nanofluid advantages in microchannel heat sinks", *Micro & Nano Letters*, 8 (6), pp. 319–323.

141. Mirzaei, M. and Dehghan, M., 2013. "Investigation of flow and heat transfer of nanofluid in microchannel with variable property approach", *Heat Mass Transfer*, 49, pp. 1803–1811.

142. Ramiar, A. and Ranjbar, A.A., 2013. "Two-Dimensional variable property conjugate heat transfer simulation of nanofluids in microchannels", *Journal of Nanoscience*, Article ID 217382, pp. 1-9.

143. Rimbault, B., Nguyen, C.T. and Galanis, N., 2014. "Experimental investigation of CuO-water nanofluid flow and heat transfer inside a microchannel heat sink", *International Journal of Thermal Sciences*, 84, pp. 275-292.

144. Duursma, G., Sefiane, K., Dehaene, A., Harmand, S. and Wang, Y., 2015. "Flow and heat transfer of single and two-phase boiling of nanofluids in microchannels", *Heat Transfer Engineering*, 36, pp. 1252–1265.

145. Yang, X.F. and Liu, Z.H., 2011. "Pool boiling heat transfer of functionalized nanofluid under sub-atmospheric pressures", *International Journal of Thermal Science,* 50, pp. 2402-2412.

146. Qu, J. and Wu, H., 2011. Thermal performance comparison of oscillating heat pipes with SiO_2/water and Al_2O_3/water nanofluids", *International Journal of Thermal Science,* 50, pp. 1954-1962.

147. Haddad, Z., Abi, C., Oztop, H.F. and Mataoui, A., 2014. "A review on how the researchers prepare their nanofluids", *International Journal of Thermal Science,* 76, pp. 168-189.

148. Ashby, M.F., 2000. "Multi-objective optimization in material design and selection", *Materials & Design,* 48, pp. 359-69.

149. Khabbaz, S.R., Manshadi, B.D., Abedian, A. and Mahmudi, R., 2009. A simplified fuzzy logic approach for materials selection in mechanical engineering design", *Materials* & *design,* 30, pp. 687-97.

150. Kiran, C.P., Clement, S. and Agrawal, V.P., 2011. "Coding, evaluation and optimal selection of a mechatronic system", *Expert Systems with Applications,* 38, pp. 9704-9712.

151. Yang, T., and Hung, C.C., 2007. "Multiple-attribute decision making methods for plant layout design problem", *Robotics and Computer-Integrated Manufacturing,* 23, pp. 126-137.

152. Bhangale, P.P., Agrawal, V.P. and Saha, S.K., 2004. "Attribute based specification, comparison and selection of a robot", *Mechanism and Machine Theory,* 39, pp. 1345-1366.

153. Li, G.D., Yamaguchi, D. and Nagai, M., 2007. "A grey-based decision making approach to the supplier selection problem", *Mathematical and Computer modeling,* 46, pp. 573-581.

154. Masipa, P. M., Magadzu, T. and Mkhondo, B., 2013. "Decoration of multi-walled carbon nanotubes by metal nanoparticles and metal oxides using chemical evaporation method", *South African Journal of Chemistry,* 66, pp. 173–78.

155. Bandyopadhyaya, R., Nativ-Roth, E., Regev, O. and Rozen, R.Y., 2002. "Stabilization of individual carbon nanotubes in aqueous solutions", *Nano Letters,* 2 (1), pp. 25–28.

156. Wang, X., Li, X. and Yang, S., 2009. "Influence of pH and SDBS on the stability and thermal conductivity of nanofluids", *Energy Fuels,* 23, pp. 2684-2689.

157. Mahbubul, I.M., Chong, T.H., Khaleduzzaman, S.S., Shahrul, I.M., Saidur, R., Long, B.D. and Amalina, M.A., 2014. "Effect of ultrasonication duration on colloidal structure and viscosity of alumina-water nanofluid", *Industrial and Engineering Chemistry Research,* 53, pp. 6677-6684.

158. Kumar, J.G., Kathirkaman, M.D., Raja, K., Kumaresan, V. and Velraj, R., 2015. "Experimental study on density, thermal conductivity, specific heat and viscosity of

water-ethylene glycol mixture dispersed with carbon nanotubes", *Thermal science* 10.2298/TSCI141015028G.

159. Kandlikar, S.G., Garimella, S., Li, D., Colin, S. and King, M.R., 2006. "Heat transfer and fluid Flow in minichannels and microchannels", First edition, Elsevier Limited, Oxford, OX5 1GB, UK.

160. Sehgal, S.S., Murugesan, K. and Mohapatra, S.K., 2011. "Experimental investigation of the effect of flow arrangements on the performance of a micro-channel heat sink", *Experimental Heat Transfer*, 24, pp. 215–233.

161. Gangacharyulu, D., 1997. "Heat transfer and pressure drop characteristics of some compact heat exchangers for turbo-charged diesel engines", *Ph.D. Thesis*, Department of Mechanical and Industrial Engineering, Thapar Institute of Engineering and Technology, Patiala, Punjab, India.

162. Giraldo, M., Ding, Y. and Williams, R. A., 2008. "Boundary integral study of nanoparticle flow behaviour in the proximity of a solid wall", *Journal of Physics D: Applied Physics*, 41, 085503.

163. Hwang, C. L. and Yoon, K., 1981. "Multiple attribute decision making- a state of the art survey", *In lecture notes in Economics & Mathematics* (Berlin: Springer – Verlag), 186 (5), pp.191.

PUBLICATIONS BASED ON THE RESEARCH WORK

SCI Indexed Journals

1. Sandhu, H. and Gangacharyulu, D., 2016, "An Experimental study on stability and some thermophysical properties of multiwalled carbon nanotubes with water-ethylene glycol mixtures", *Journal of Particulate Science and Technology*, DOI: 10.1080/02726351.2016.1180335.

2. Sandhu, H., Gangacharyulu, D. and Agrawal, V.P., 2016, "Coding, Evaluation, Comparison, Ranking and Optimal Selection of Nanoparticles with Heat Transfer Fluids for Thermal Systems", *Journal of Particulate Science and Technology*, DOI: 10.1080/02726351.2016.1208695.

International/National Conferences

1. Kaur, H. and Gangacharyulu, D., " Enhancement of Thermal Conductivities among Al_2O_3, CNT and CuO Nanoparticles with Different Base Fluids, *International ISHMT-ASTFE Heat and Mass Transfer Conference*, 17-20 December, 2015, ISRO, Thiruvananthapuram, India.

2. Sandhu, H. and Gangacharyulu, D., "Studies on Some Transport Properties of Nanofluids and its Biological Applications, *NCONAD-2013*, 3-5 Oct., 2013, NIT Srinagar, India.

3. Sandhu, H. and Gangacharyulu, D., "Heat Transfer and Fluid Flow Study of CuO-W/EG (50:50) Nanofluids through Aluminium Microchannels", *International ISHMT-ASTFE Heat and Mass Transfer Conference*, 27-30 December, 2017, BITS Pilani, Hyderabad Campus, Telangana, India.